

ISSN 1088-3800

# Evaluation of Seismic Retrofit Methods for Reinforced Concrete Bridge Columns

by

T.J. Wipf, F.W. Klaiber and F.M. Russo

Technical Report NCEER-97-0016

December 28, 1997

This research was conducted at Iowa State University and was supported by the Federal Highway Administration under contract number DTFH61-92-C-00106.

## NOTICE

This report was prepared by Iowa State University as a result of research sponsored by the National Center for Earthquake Engineering Research (NCEER) through a contract from the Federal Highway Administration. Neither NCEER, associates of NCEER, its sponsors, Iowa State University nor any person acting on their behalf:

- a. makes any warranty, express or implied, with respect to the use of any information, apparatus, method, or process disclosed in this report or that such use may not infringe upon privately owned rights; or
- b. assumes any liabilities of whatsoever kind with respect to the use of, or the damage resulting from the use of, any information, apparatus, method, or process disclosed in this report.

Any opinions, findings, and conclusions or recommendations expressed in this publication are those of the author(s) and do not necessarily reflect the views of NCEER or the Federal Highway Administration.



NATIONAL  
CENTER FOR  
EARTHQUAKE  
ENGINEERING  
RESEARCH

*Headquartered at the State University of New York at Buffalo*

---

## **Evaluation of Seismic Retrofit Methods for Reinforced Concrete Bridge Columns**

by

T.J. Wipf<sup>1</sup>, F.W. Klaiber<sup>1</sup> and F.M. Russo<sup>2</sup>

Publication Date: December 28, 1997

Submittal Date: February 3, 1997

Technical Report NCEER-97-0016

NCEER Task Number 106-F-2.2

FHWA Contract Number DTFH61-92-C-00106

- 1 Professor, Department of Civil and Construction Engineering, Iowa State University
- 2 Ph.D. Graduate Student, Department of Civil and Construction Engineering, Iowa State University

NATIONAL CENTER FOR EARTHQUAKE ENGINEERING RESEARCH  
State University of New York at Buffalo  
Red Jacket Quadrangle, Buffalo, NY 14261

---

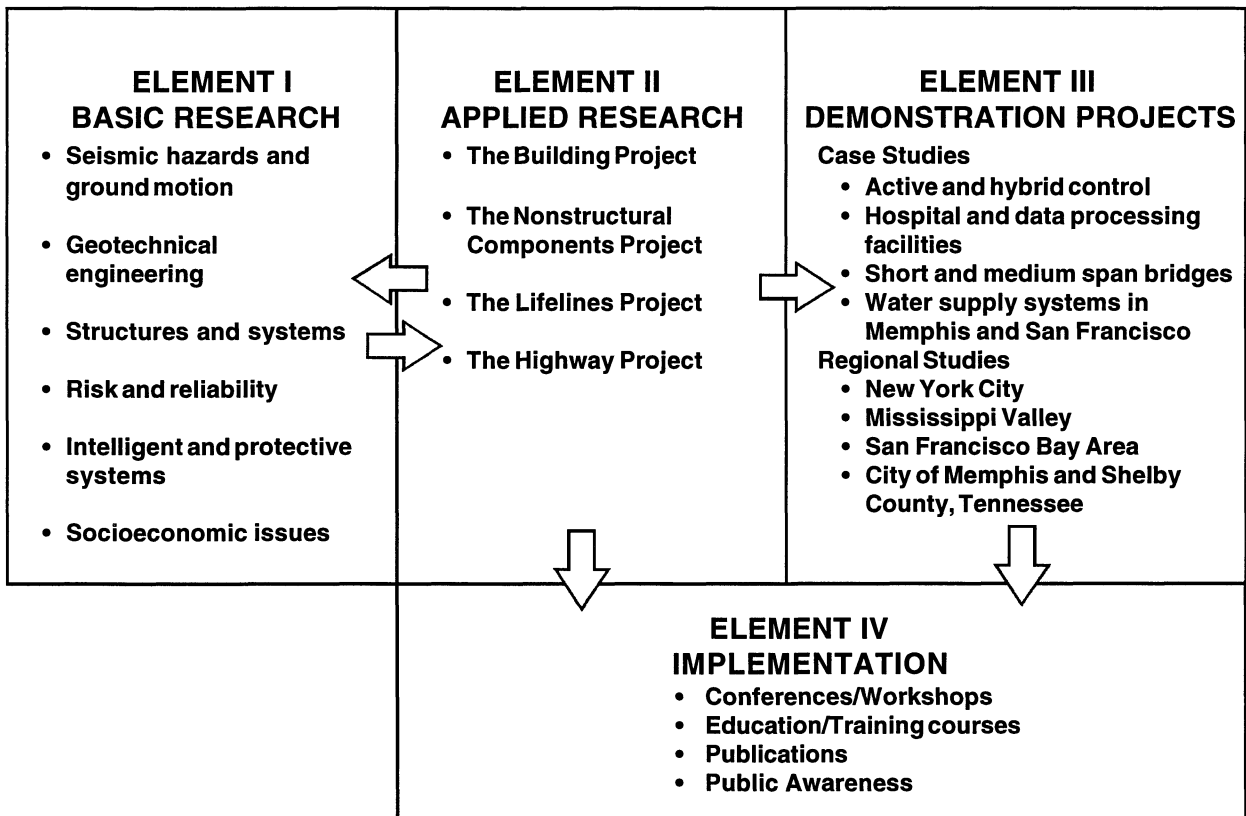


## PREFACE

The National Center for Earthquake Engineering Research (NCEER) was established in 1986 to develop and disseminate new knowledge about earthquakes, earthquake-resistant design and seismic hazard mitigation procedures to minimize loss of life and property. The emphasis of the Center is on eastern and central United States *structures*, and *lifelines* throughout the country that may be exposed to any level of earthquake hazard.

NCEER's research is conducted under one of four Projects: the Building Project, the Nonstructural Components Project, and the Lifelines Project, all three of which are principally supported by the National Science Foundation, and the Highway Project which is primarily sponsored by the Federal Highway Administration.

The research and implementation plan in years six through ten (1991-1996) for the Building, Nonstructural Components, and Lifelines Projects comprises four interdependent elements, as shown in the figure below. Element I, Basic Research, is carried out to support projects in the Applied Research area. Element II, Applied Research, is the major focus of work for years six through ten for these three projects. Demonstration Projects under Element III have been planned to support the Applied Research projects and include individual case studies and regional studies. Element IV, Implementation, will result from activity in the Applied Research projects, and from Demonstration Projects.



Research under the **Highway Project** develops retrofit and evaluation methodologies for existing bridges and other highway structures (including tunnels, retaining structures, slopes, culverts, and pavements), and develops improved seismic design criteria and procedures for bridges and other highway structures. Specifically, tasks are being conducted to: (1) assess the vulnerability of highway systems and structures; (2) develop concepts for retrofitting vulnerable highway structures and components; (3) develop improved design and analysis methodologies for bridges, tunnels, and retaining structures, with particular emphasis on soil-structure interaction mechanisms and their influence on structural response; and (4) review and improve seismic design and performance criteria for new highway systems and structures.

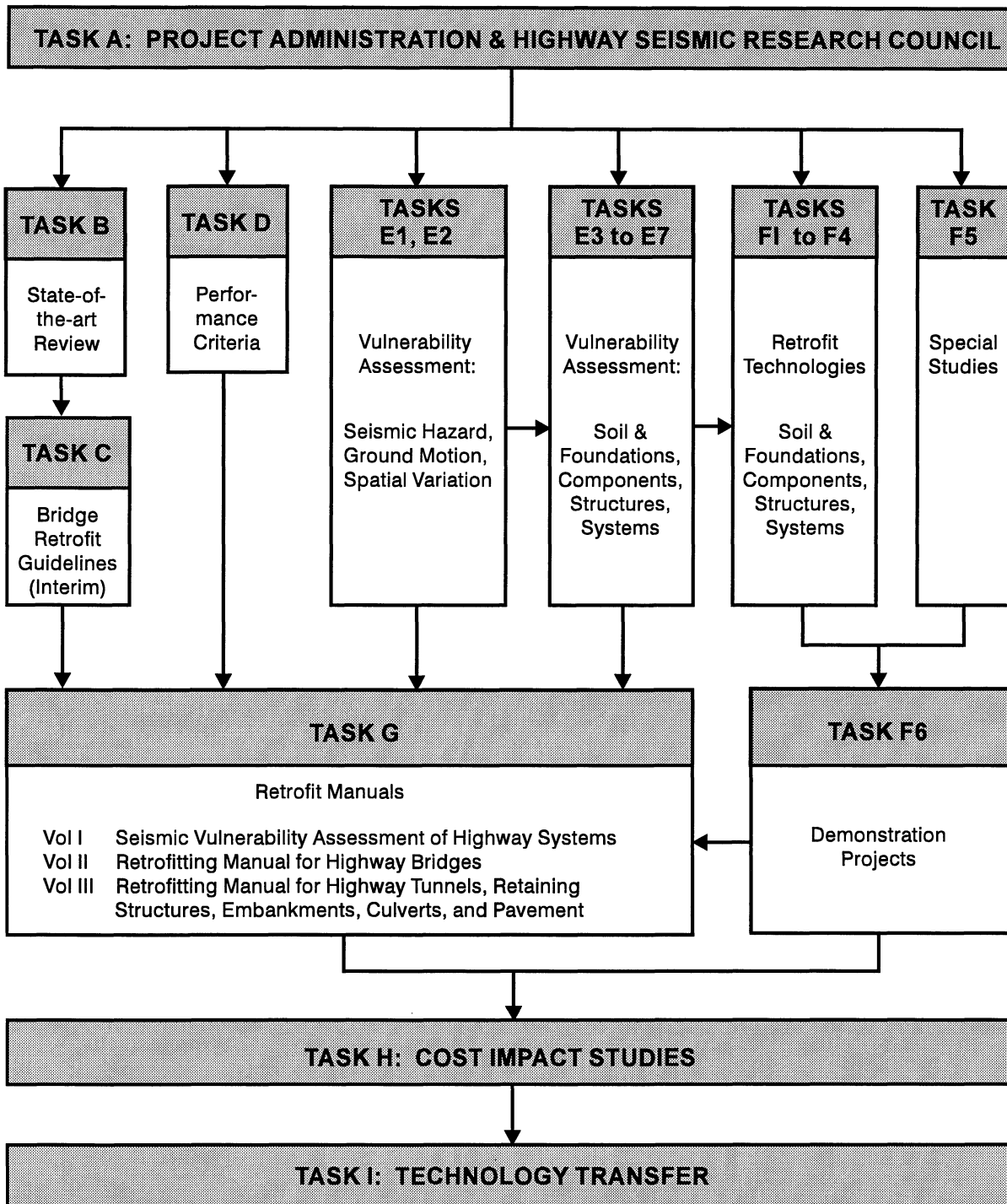
**Highway Project** research focuses on one of two distinct areas: the development of improved design criteria and philosophies for new or future highway construction, and the development of improved analysis and retrofitting methodologies for existing highway systems and structures. The research discussed in this report is a result of work conducted under the existing highway construction project, and was performed within Task 106-F-2.2, “Evaluation of Seismic Retrofit Methods for Reinforced Concrete Bridge Columns” of the project as shown in the flowchart on the following page.

*The overall objective of this task was to collect and review information on the current state of practice for upgrading seismically vulnerable concrete bridge columns. Bridge columns designed before the development of modern seismic codes are known to be deficient in a number of details. Failures occur due to inadequate transverse reinforcement for both flexure and shear, and insufficient splice and anchorage lengths for the longitudinal steel. A number of methods for retrofitting these vulnerable columns have been developed in recent years which include column jacketing (using steel shells and wire wraps, composite fiber wraps and concrete jackets) and column modifications using fuse-like hinges and hinge shifting techniques. In addition, seismic isolation has been used to reduce the demand on vulnerable columns as an alternative to these conventional retrofit measures.*

*Despite this activity, column retrofitting is still an immature science, with conflicting information as to the applicability and reliability of the various methods. Some methods have now been widely used in the field whereas others are still only promising laboratory concepts.*

*This report consolidates the various literature on concrete column retrofitting into a single source and summarizes the strengths and limitations of the various approaches as identified in the literature and reported by end-users. Future research needs for retrofitting bridge columns were also identified.*

**SEISMIC VULNERABILITY OF EXISTING HIGHWAY CONSTRUCTION**  
**FHWA Contract DTFH61-92-C-00106**





## ABSTRACT

The objective of this task was to collect and review information on the current state-of-the-art for seismically upgrading vulnerable concrete bridge columns. Over 200 (national and international) references were collected. A questionnaire was developed and disseminated to obtain information on the column retrofit activities of the various states (and Canadian provinces). The survey had a response rate of over 77%.

The majority of published information is one the two most commonly used column retrofit techniques: steel jacketing and composite fiber jacketing. Several other techniques such as infilled walls in multi-column piers, external prestressing using high strength bars, and internal column strengthening, among others, were examined.

The majority of research completed to date has been on reduced-scale laboratory specimens subjected to lateral loads. These tests have shown that column jacketing can substantially improve the ultimate ductility and lateral load capacity of reinforced concrete columns. Jacketing can arrest the two common column failure modes: loss of confinement with subsequent slip in column lap splices, and premature brittle shear failure of columns with inadequate shear capacity. The structural performance of steel and composite jacketed specimens is similar.

An evaluation technique for assessing the relative merits of dissimilar was developed. Included in this technique are the following four parameters: structural performance, cost, environmental performance, and design process. To date, there is insufficient data available to use the technique developed. Areas requiring further investigation have been presented in the final chapter of the report.

A classification chart which assists the reader in determining the type of information a particular reference contains is presented in an appendix. Also included is a cross-reference list which assists the reader in locating where a specific reference is cited in the report.



## **ACKNOWLEDGMENT**

The study presented in this report was conducted by the Bridge Engineering Center under the auspices of the Engineering Research Institute of Iowa State University. The research was sponsored by the National Center for Earthquake Engineering Research in Buffalo, NY.

The authors wish to extend sincere appreciation to the numerous engineers who responded to our questionnaire as well as to other researchers, manufacturers, etc. who responded to our request for column retrofitting information. Special thanks are accorded to the following individuals for their assistance and cooperation in various aspects of the project: Ian G. Buckle, Ian M. Friedland, and Dorothy S. Tao - National Center for Earthquake Engineering Research and John B. Mander - State University of New York at Buffalo.



## TABLE OF CONTENTS

SECTION	TITLE	PAGE
<b>1</b>	<b>INTRODUCTION</b> .....	<b>1</b>
1.1	Project History and Need for the Study .....	1
1.2	Current Design Philosophy for Column Retrofit .....	8
1.3	Report Format .....	11
<b>2</b>	<b>STEEL JACKET COLUMN RETROFITS</b> .....	<b>13</b>
2.1	Introduction .....	13
2.2	Laboratory Testing of Steel-Jacketed Specimens .....	14
2.2.1	Steel Jacket Retrofit of Flexurally Deficient Bridge Columns .....	14
2.2.1.1	Circular Flexural Columns .....	14
2.2.1.2	Rectangular Flexural Columns .....	21
2.2.2	Steel Jacket Retrofit of Shear Deficient Bridge Columns .....	34
2.2.2.1	Circular Shear Columns .....	34
2.2.2.2	Rectangular Shear Columns .....	40
2.3	Field Installations .....	49
2.4	Analytical Models and Design Guidelines .....	52
<b>3</b>	<b>COMPOSITE JACKETING</b> .....	<b>59</b>
3.1	Introduction .....	59
3.2	Material Types and Strengths .....	59
3.2.1	Fiber Properties .....	59
3.2.2	Matrix Properties .....	60
3.2.3	Composite Properties .....	60
3.2.4	Effect of Fiber Orientation on Expected Performance .....	61
3.2.5	Methods of Construction .....	63
3.3	Laboratory Test Results .....	64
3.3.1	Composite Jacket Retrofit of Flexurally Deficient Bridge Columns .....	65
3.3.1.1	Circular Flexural Columns .....	65
3.3.1.2	Rectangular Flexural Columns .....	77
3.3.2	Composite Jacket Retrofit of Shear Deficient Bridge Columns .....	84
3.3.2.1	Circular Shear Columns .....	84
3.3.2.2	Rectangular Shear Columns .....	90
3.3.3	Environmental Testing and Effects on Composite Performance .....	95
3.4	Field Installations .....	98
3.5	Analytical Models and Design Considerations .....	105
3.5.1	Analytical Models for Composite Retrofit Column Behavior .....	106
3.5.2	Design Considerations and Recommendations .....	115
<b>4</b>	<b>OTHER COLUMN RETROFIT METHODS</b> .....	<b>119</b>
4.1	Concrete Jacketing and Infill Shear Walls .....	119
4.2	External Post-Tensioning and Mild Reinforcing Retrofits .....	124
4.3	External Angle and Bar Retrofit .....	130
4.4	Internal Reinforcing Methods .....	131

## TABLE OF CONTENTS (Cont'd)

SECTION	TITLE	PAGE
<b>5</b>	<b>COLUMN PERFORMANCE EVALUATION METHODS</b> .....	133
5.1	Introduction .....	133
5.2	Minimum Acceptable Performance Criteria .....	134
5.3	Numerical Assessment and Ranking of Alternatives .....	136
5.3.1	Structural Performance .....	137
5.3.1.1	Capacity Increase, CI .....	137
5.3.1.2	Displacement Ductility Increase, DDI .....	137
5.3.1.3	Number of Cycles to Failure, NC .....	137
5.3.1.4	Hysteretic Energy Absorption, HEA .....	138
5.3.1.5	Response Degradation, RD .....	139
5.3.1.6	Comparison to Modern Designs, CMD .....	140
5.3.1.7	Post-Earthquake Assessment, PEA .....	140
5.3.2	System Cost, SC .....	140
5.3.2.1	Material Cost, MC .....	140
5.3.2.2	Labor and Equipment Cost, LEC .....	141
5.3.2.3	Long-Term Maintenance and Inspection Costs, MIC .....	141
5.3.2.4	Life-Cycle Cost, LCC .....	141
5.3.3	Environmental Performance, EP .....	141
5.3.3.1	Ultraviolet Effect, UE .....	141
5.3.3.2	Salt-Air Effect, SAE .....	142
5.3.3.3	Freeze and Thaw Effect, FTE .....	142
5.3.3.4	Pollution Effect, PE .....	142
5.3.3.5	Alkali Effect, AE .....	142
5.3.4	Design Process, DP .....	142
5.3.4.1	Process Knowledge, PK .....	142
5.3.4.2	Quality of Information, QI .....	143
5.3.5	Overall Rating .....	143
5.4	Analytical Hierarchy Process Evaluation Technique .....	143
<b>6</b>	<b>SUMMARY AND ISSUES FOR FURTHER STUDY</b> .....	147
6.1	Task Summary .....	147
6.2	Issues for Further Study .....	147
6.2.1	Scale Effects .....	147
6.2.2	Dynamic Effects .....	148
6.2.3	Standardized Testing .....	148
6.2.4	Standardized Reporting .....	148
6.2.5	Definition of Critical Parameters and Limit States .....	149
	<b>BIBLIOGRAPHY</b> .....	151
	<b>APPENDIX A REFERENCE CLASSIFICATION CHART AND CROSS-REFERENCE LIST</b> .....	169

**TABLE OF CONTENTS (Cont'd)**

<b>SECTION</b>	<b>TITLE</b>	<b>PAGE</b>
<b>APPENDIX B</b>	<b>INDUSTRY SURVEY .....</b>	<b>181</b>



## LIST OF ILLUSTRATIONS

FIGURE	TITLE	PAGE
FIGURE 1-1	Column Retrofit Details Incorporating Steel or Composite Jackets . . . . .	5
FIGURE 1-2	Steel Jacket Pier Wall Retrofit . . . . .	6
FIGURE 1-3	Carbon Fiber Sheet / Strand Retrofit . . . . .	6
FIGURE 1-4	Composite Strap Retrofit . . . . .	7
FIGURE 1-5	In-Fill Wall Retrofit . . . . .	7
FIGURE 1-6	Retrofit for Columns with Premature Longitudinal Steel Termination . . . . .	8
FIGURE 2-1	Schematic of an Oval Steel Jacket (Sun, Seible, and Priestley, 1993b) . . . . .	22
FIGURE 2-2	Built-Up Channel and Stiffened Plate Retrofits . . . . .	26
FIGURE 3-1	Circular Column with Lap Splice, CF2 (Seible, Hegemier, et al., 1995d) . . . . .	76
FIGURE 3-2	Rectangular Flexural Column with Lap Splice, RFLS (Seible, Hegemier, et al., 1995e) . . . . .	80
FIGURE 3-3	Continuous Reinforcing Specimen RF5 (Seible, Hegemier, et al., 1995a) . . . . .	81
FIGURE 3-4	Circular Shear Column with 2.5% Reinforcing, CS2.5 (Seible, Hegemier, et al., 1994b) . . . . .	87
FIGURE 3-5	Circular Shear Deficient Column with 1% Reinforcing (Seible, Hegemier, et al., 1994a) . . . . .	89
FIGURE 3-6	Rectangular Shear Deficient Column RS2.5 (Seible, Hegemier, et al., 1995c) . . . . .	93
FIGURE 3-7	Confined and Unconfined Concrete Stress-Strain Diagram . . . . .	107



## LIST OF TABLES

<b>TABLE</b>	<b>TITLE</b>	<b>PAGE</b>
TABLE 2-1	Flexurally Deficient Circular Columns (Chai, Priestley, and Seible, 1991b) . . . . .	15
TABLE 2-2	Steel Jacket Retrofit of Flexurally Deficient Columns (Sun, Seible, and Priestley, 1993b) . . . . .	25
TABLE 2-3	Circular Shear Columns (Verma, Priestley, and Seible, 1993) . . . . .	35
TABLE 2-4	Rectangular Shear Deficient Columns (Xiao, Priestley, and Seible, 1993). . . . .	41
TABLE 3-1	University of Arizona Composite Retrofit Column Specimens . . . . .	69
TABLE 3-2	I-70 Bridge Retrofit Test Columns . . . . .	101
TABLE A-1	Reference Classification Chart . . . . .	170
TABLE A-2	Cross-Reference List . . . . .	175
TABLE B-1	Industry Survey Response Summary . . . . .	183



## **SECTION 1 INTRODUCTION**

The goal of this project is to review the state-of-the-art in the field of column retrofitting for enhanced earthquake performance. A number of tasks were undertaken.

The vast majority of the work has centered around the collection and review of all relevant information on column retrofit for earthquakes from information solicited worldwide. The final bibliography, while not entirely comprehensive of all relevant information, nears 200 references. The actual number of independent pieces of information number somewhat less because of some multiple citations of essentially the same information appearing in multiple sources, e.g., conference proceedings, journal papers, research reports. However, duplication aside, thousands of pages of technical reports, graphs, photographs, and equations were examined for their relative contribution to the field of column jacketing.

Ancillary activities consisted of the preparation of a comprehensive table detailing the contents of every reference with respect to the author, date of publication, column geometry, deficiency type, retrofit technique, type of research, number of specimens, and specimen scale. This table appears in Appendix A of this report. Also in Appendix A, accompanying the classification table, is a cross-reference list indicating where in this report citations to a particular reference are made.

In addition, an industry questionnaire was developed and circulated to gain input from those practitioners responsible for implementing retrofit designs. Information requested included design techniques, retrofit methods, research activities and retrofit suppliers. A copy of the questionnaire as well as a summary table of the responses is presented in Appendix B of this report.

The results of this research is a document that accurately portrays the many options currently available for column retrofit construction and highlights the advantages and disadvantages of each system when necessary, appropriate, and possible.

### **1.1 Project History and Need for the Study**

The history of column retrofitting in the United States can be directly tied to the efforts of Caltrans. A brief history of the evolution of the current seismic retrofit programs will be presented as a prelude to understanding the various projects that have been undertaken in the past decade. These facts are primarily derived from California Department of Transportation (1995a, 1996b).

In February, 1971, the San Fernando (Sylmar) Earthquake resulted in major damage of a number of Caltrans bridges in southern California. Based on their damage assessment, the Caltrans Post Earthquake Investigation Team (PEQIT) presented the following findings.

- 1.) Unrestrained bridge deck joints at hinges and abutments separated due to large horizontal movements.
- 2.) Narrow hinge and abutment seats were inadequate for expected movements.
- 3.) Reinforcing steel extending from the foundations was not sufficiently lap spliced to main column reinforcing.
- 4.) Seismic lateral force requirements were inadequate for the large accelerations expected in the San Fernando earthquake.

A memo to designers was issued in order to effect the following immediate changes in seismic design policy:

- 1.) Existing lateral force requirements were increased by a factor of 2.5.
- 2.) The use of lap splices at column bases was discontinued. Only welded or mechanical splices would be allowed in lieu of continuous reinforcing.
- 3.) Hinge seat widths were significantly increased and more attention was to be given to the anticipated movements for a particular design.
- 4.) Positive connection between adjacent elements at thermal expansion joints was mandated. This was the beginning of Phase I of the Caltrans retrofit program.

The Phase I retrofit program was instituted to install hinge restrainers and seat extensions because these were deemed more critical than the column retrofits. This program, completed in 1989, cost \$54 million and retrofit 1,262 bridges.

When the Phase I project was nearing completion in the Spring of 1987, Caltrans began the single column retrofit research program at the University of California at San Diego (UCSD) which began Phase II. The Whittier Earthquake of October 1987 provided further confirmation of the need to address the column deficiencies present in pre-1971 designs, and the UCSD research program was accelerated. By 1988, tests on steel-jacketed round columns had been completed with excellent results, and the first contract was begun in April 1990 in Los Angeles County, shortly after the 1989 Loma Prieta Earthquake in the San Francisco area. By the Northridge Earthquake on January 17, 1994, 122 bridges in the Los Angeles area had been retrofitted and performed extremely well. Of the seven bridges that collapsed, five were scheduled for retrofitting.

The current Caltrans seismic retrofit program is divided into Phases 1 and 2. Phase 1 includes 1,039 bridges identified as needing retrofitting after the Loma Prieta Earthquake at a cost of \$760 million. By November 1995, 1,026 of these bridges were either completed or under construction. Phase 2 includes an additional 1,364 bridges identified after the Northridge Earthquake. This number has since been revised to 1,208. As of November 1995, 181 bridges were complete or under construction. The Phase 2 bridges are estimated to cost \$1.05 billion and should be completed by the end of 1997. In addition, 998 city and county bridges have been identified as candidates for retrofit, with 61 completed or under construction by November 1995. In all, the earthquake strengthening program will involve 2,200 structures and cost approximately \$2.5 billion, with funding coming from motor vehicle fuel taxes. The performance of these retrofit bridges in recent earthquakes has been very positive.

The Concrete Reinforcing Steel Institute (1994) reports on the general performance of concrete bridges in the January 1994 Northridge Earthquake near Los Angeles. The document reports that of the 120 bridges that had column retrofits installed prior to the earthquake, 24 were in the 0.5g acceleration zone. The retrofit of the columns was seen to be extremely effective as demonstrated by the failure of the Fairfax and La Cienega undercrossings while the adjacent Cadillac offramp suffered no visible damage. Only minor spalling of the column between the top of the jacket and the bridge soffit was noted.

Yashinsky and Hipley (1996) and Yashinsky, Hipley, and Nguyen (1995) describe the performance of retrofitted bridges in the Los Angeles area during the 1994 Northridge Earthquake. The Northridge Earthquake was a 6.7 magnitude earthquake centered in Los Angeles. Many bridges in the area had been retrofitted with hinge restrainers, seat extensions, catcher blocks, and bearing replacements as part of the

Phase 1 retrofit program. Approximately 1,600 Caltrans-owned bridges were in an area of 0.25g acceleration or greater. Of these bridges, 79 bridges were retrofitted as part of Phase 2 and experienced no serious damage. The most common column retrofit in the area was the use of partial or full height steel jackets. Special retrofit types such as the addition of new columns and outrigger cap beams at the Wicks Street Pedestrian Overcrossing, Olinda Street, and Sharp Avenue, concrete jacketing at Tuxford Ramp, and composite fiberglass jacketing at the Route 2/5 Separation, and Griffith Park also performed very well. Yashinsky, Hipley, and Nguyen (1995) caution that one should not be overly optimistic about the retrofit performance because the earthquake had a short duration, 20 seconds of strong shaking, and a moderate magnitude of 6.7. The maximum credible earthquake in the Los Angeles area will be of higher magnitude and will consist of approximately 40 seconds of strong shaking.

Dokken (1995) presents an overview of 65 seismic bridge retrofits in California. These structures constitute a combined deck area of 241,550 m<sup>2</sup> (2.6 million ft<sup>2</sup>). Retrofit on nine of the structures was deemed inappropriate; one was condemned; and the other 55 are being retrofit at a cost of \$33 million. With the exception of one bridge, all of the retrofitted bridges were constructed prior to the 1971 San Fernando Earthquake. The typical problems found in the columns were the presence of inadequate lap splices at the footing and also cap beam intersections as well as insufficient transverse reinforcement. Over 60% of the structures in this contract will have column retrofits, including the removal and complete replacement of some columns. In addition to typical Caltrans steel jacket retrofits, another method was also employed where the existing column was converted into a super bent. This super bent, constructed at the Guadalupe River Bridge, transformed 2.13 m x 1.52 m (7 ft x 5 ft) oblong flared columns into 7 m x 2.13 m (23 ft x 7 ft) prismatic columns. The purpose of this retrofit was to draw load away from columns located near a river and a light rail line to a location where it could be accommodated. Additionally, at the Patton Street undercrossing, the use of infill walls was chosen as the retrofit because the tall slender columns at this site lacked sufficient transverse rigidity. This method was accompanied by footing enhancement via additional reinforcing and tie down anchors.

Kawashima (1990, 1991), Kawashima and Unjoh (1992), and Kawashima, Unjoh, and Iida (1991, 1992), detail a number of issues related to the design, construction, and retrofit of bridges in Japan with consideration to earthquake performance in particular. The references provide a detailed history of the evolution of the Japanese bridge design codes and correlate deficiencies in previous versions of the code with the failures observed in past earthquakes. Of particular interest in the references is the description of a vulnerability assessment procedure for bridges and the correlation of this assessment to subsequent retrofit types. In addition, a number of feasible retrofits are presented for seismically deficient columns. Among these retrofit types are infill walls, full-height anchored steel jackets where anchor bolts secure the jacket to the existing column, full-height concrete jackets, and partial-height concrete and anchored steel jackets centrally located in the vicinity of premature longitudinal steel termination. A description of the successful implementation of the retrofits mentioned above via case studies accompanies Kawashima, Unjoh, and Iida (1992).

A number of retrofit techniques exist for bridges with concrete substructures. These techniques include, but are not limited to, steel, composite, and concrete jacketing; wrapping with prestressed strand and mild reinforcing; construction of infill shear walls; and construction of auxiliary columns, known as outrigger bents, to help support the deficient substructure. Other alternatives to retrofit exist.

One alternative is the "do-nothing" option. This option may be selected due the type of road the bridge carries, e.g., a low-volume road may be selected because of the difficulties associated with retrofit or because higher priority structures are yet to be retrofit.

Another alternative that warrants consideration is the use of seismic isolation. In some instances it may be a more cost-effective and structurally sound decision to employ seismic isolation bearings at the column tops than to retrofit with jackets or infill walls, the substructure. The use of these bearings is not the focus of this report, but should be considered in some instances as a viable alternative to structural retrofit.

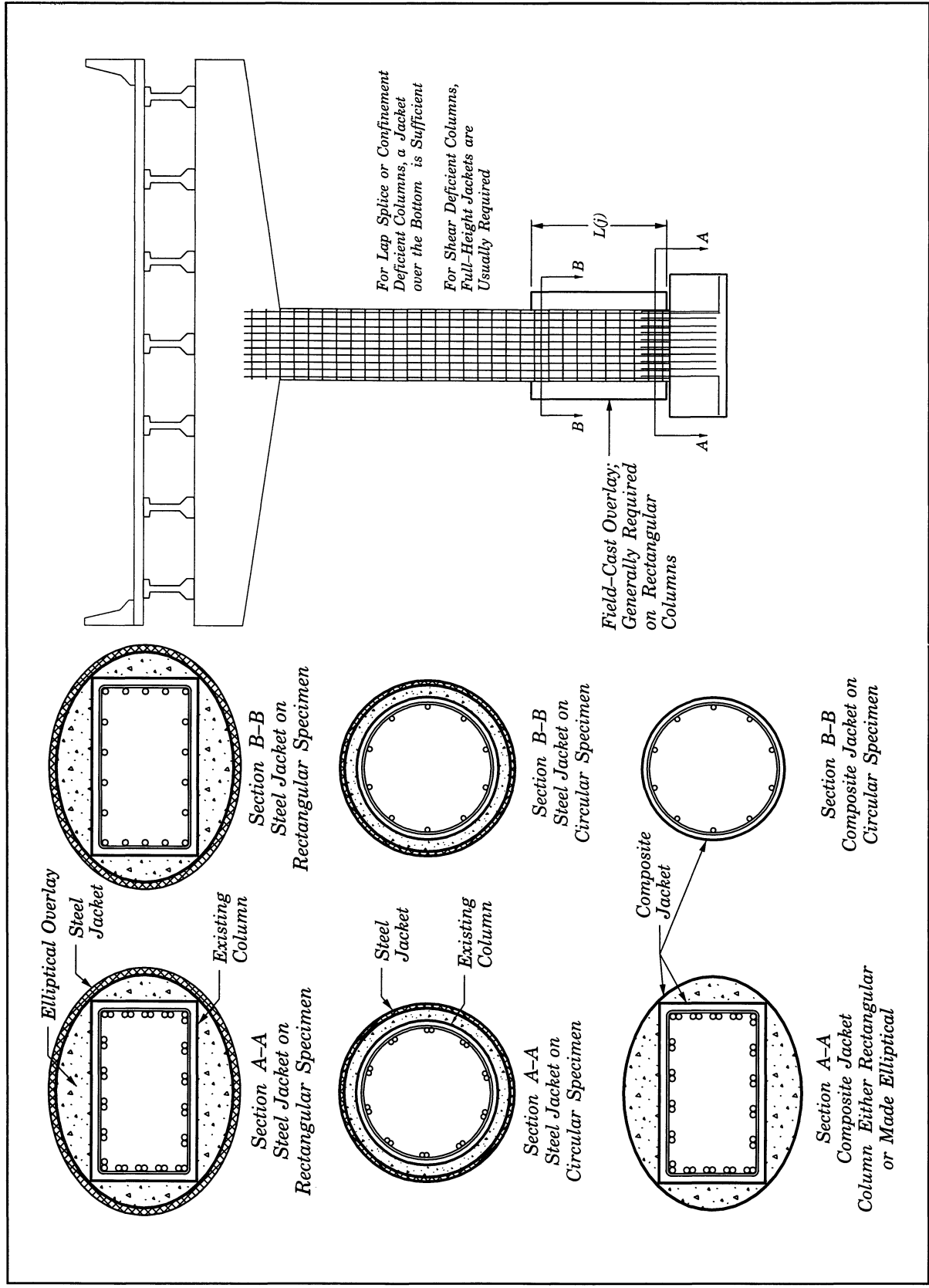
A series of retrofit diagrams is presented on the following pages showing a variety of retrofit types explored in this document. In addition, one should consult Imbsen and Associates (1994) for detailed retrofit type graphics and standard details.

Figure 1-1 illustrates the general configuration of many of the retrofits described in this report. The figure presents section and elevation views of steel and composite jacketed columns. The length of the jacket,  $L(j)$ , is presented as a variable because, depending on the type of retrofit required, i.e., shear or lap splice confinement, the jacket will need to extend over different portions of the column. The composite jacket may be applied directly to the surface of a rectangular column or as commonly done on steel jacket retrofits of rectangular columns, over a concrete overlay. The composite jacket details illustrate this possibility.

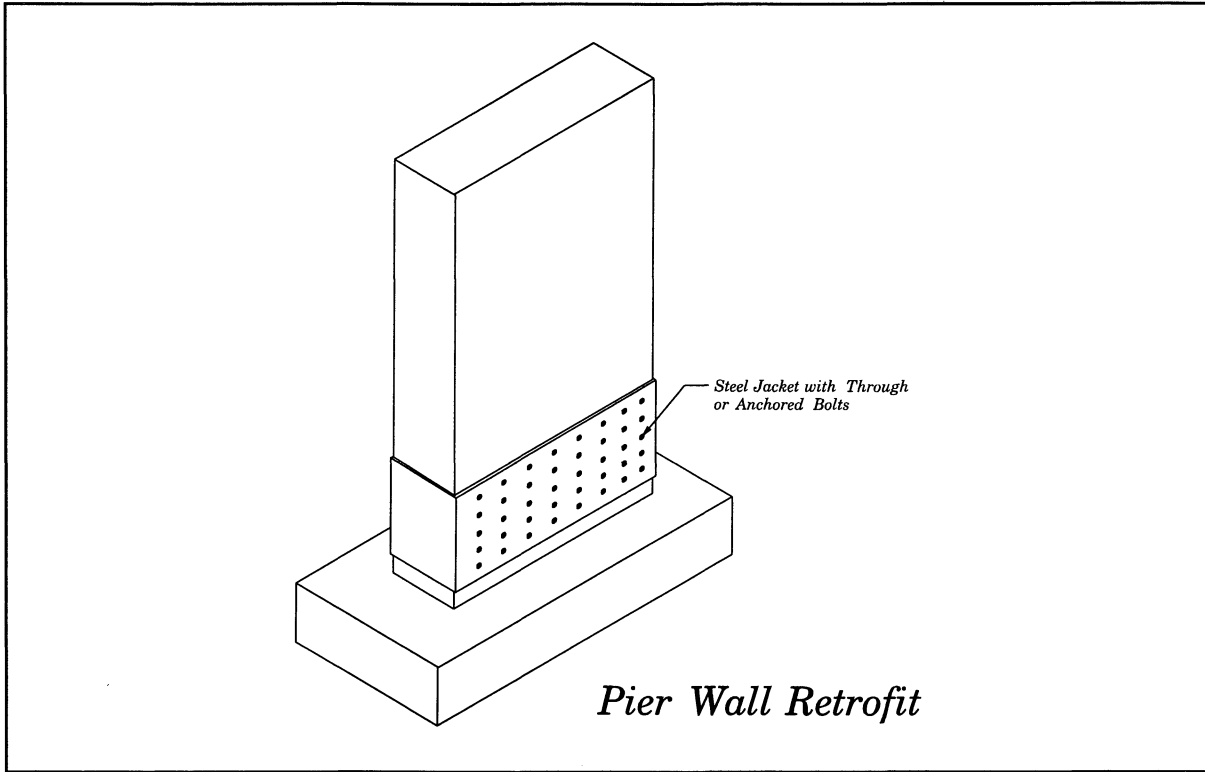
Figure 1-2 illustrates the use of bolted steel jackets on pier walls. In this scenario, a steel jacket is bolted directly to the faces of a deficient pier wall structure in order to enhance the member strength and survivability. These retrofits are used when additional lap splice confinement and plastic hinge region ductility are required.

Figure 1-3 depicts the use of carbon fiber sheets and/or strand in the retrofit of deficient concrete columns. In columns where an increase in shear capacity or flexural ductility is required, the sheets and/or strand are oriented with the fibers in the horizontal direction. In columns where a flexural strength increase is desired due to premature termination of the longitudinal steel, the fibers are oriented vertically so as to lap over the deficient region. A combination of the vertical and horizontal orientations is applied in certain occasions. This composite fiber retrofit has been presented in several Japanese references, (Ogata et al, 1993) and (Matsuda et al, 1990), among others, as a means of enhancing the flexural and shear strength of columns with premature longitudinal steel termination. These references are described in this document on pages 83 and 82 respectively.

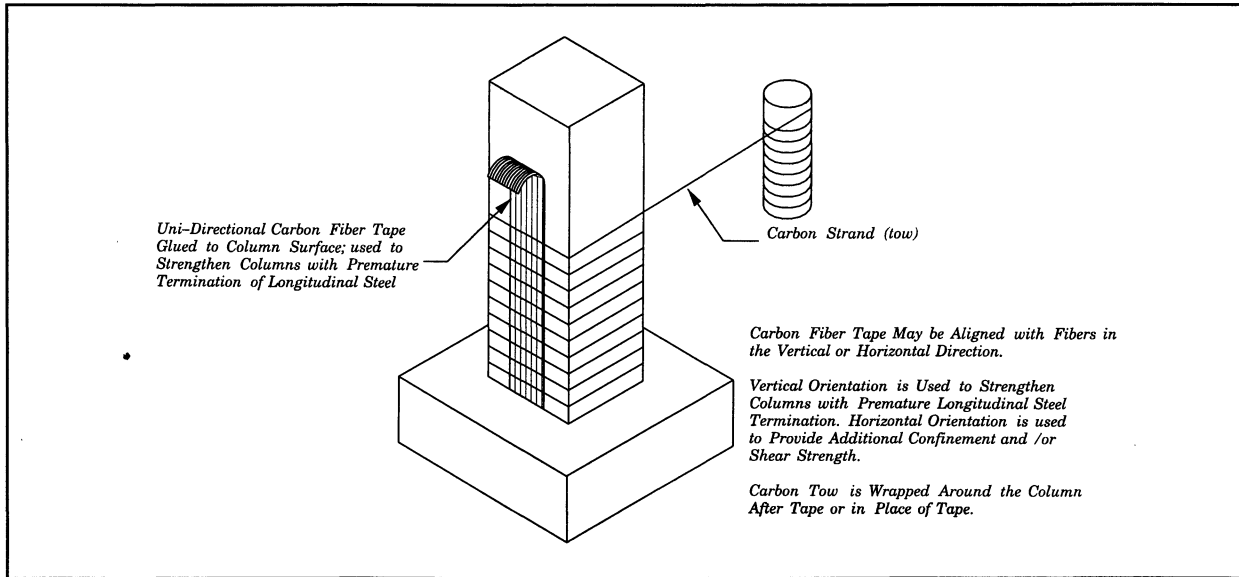
Figure 1-4 depicts the use of glass or carbon fiber tapes in columns requiring an increase in flexural capacity and plastic hinge region confinement. This retrofit was developed and tested at The University of Arizona and is referred to in Jin, Saadatmanesh, and Ehsani (1994), Li, Saadatmanesh, and Ehsani (1992), Saadatmanesh (1994), Saadatmanesh, Ehsani, and Jin (n.d., 1996a, 1996b), and Saadatmanesh, Ehsani, and Li (1992, 1994).



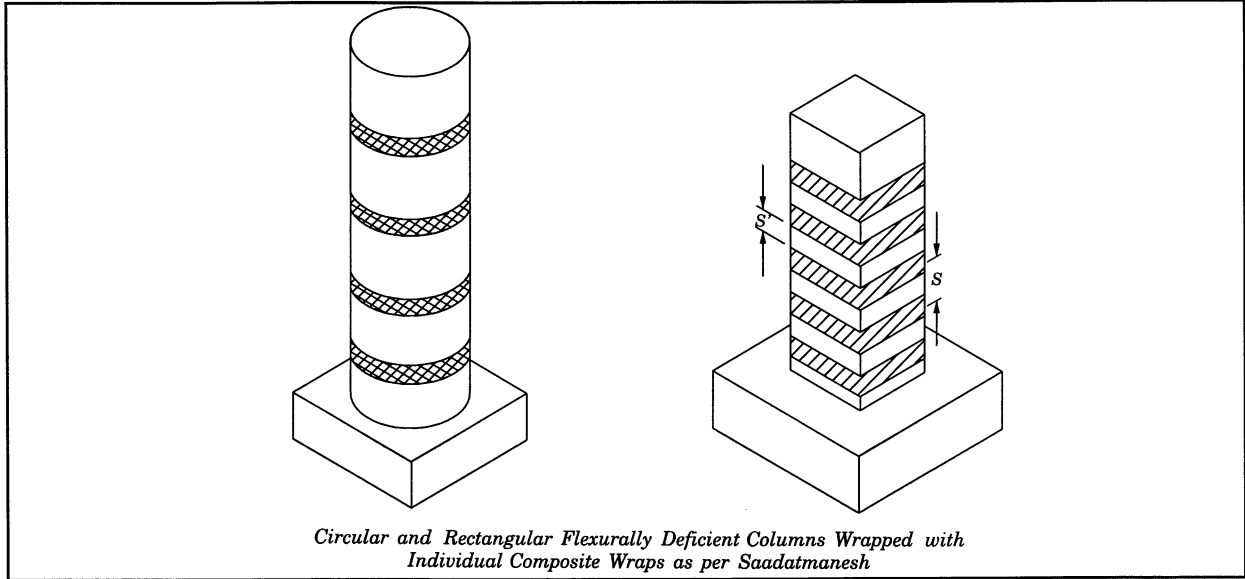
**FIGURE 1-1 Column Retrofit Details Incorporating Steel or Composite Jackets**



**FIGURE 1-2 Steel Jacket Pier Wall Retrofit**

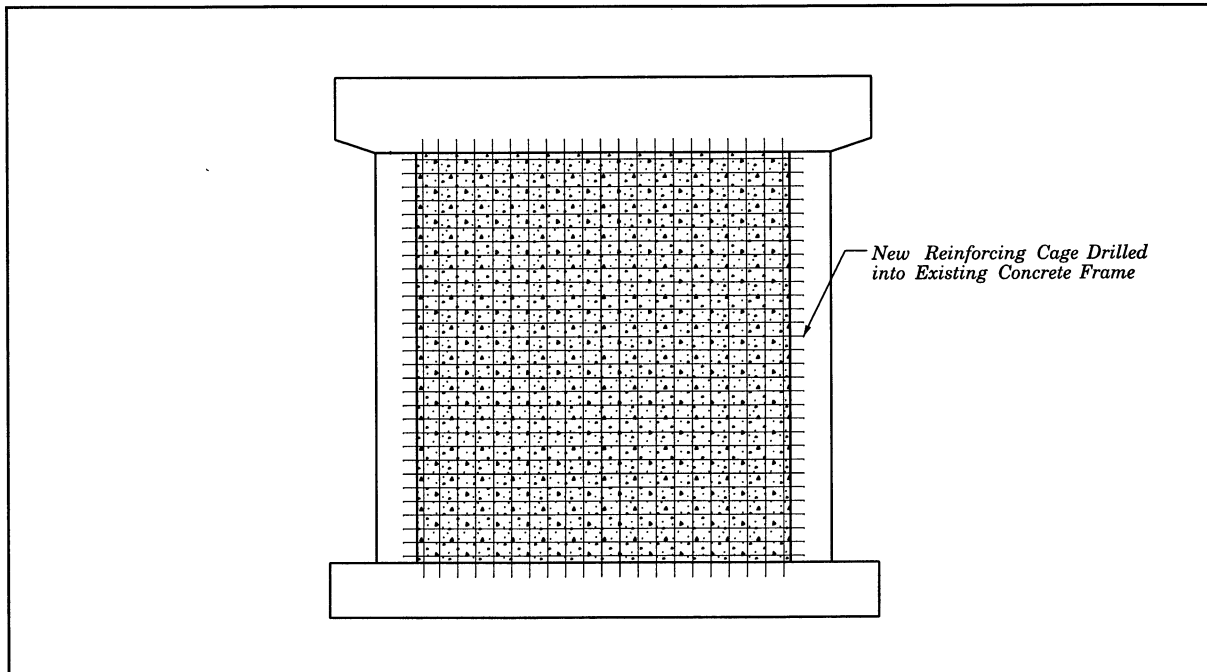


**FIGURE 1-3 Carbon Fiber Sheet / Strand Retrofit**



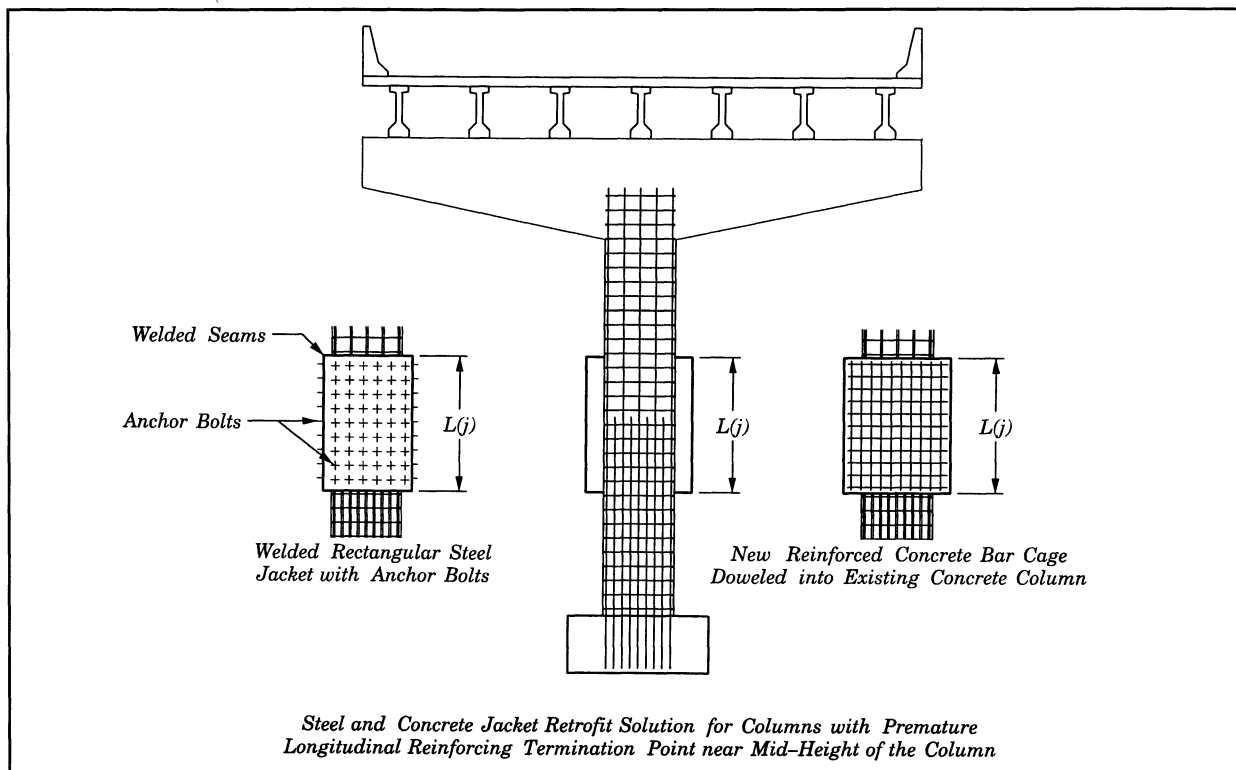
**FIGURE 1-4 Composite Strap Retrofit**

Figure 1-5 depicts the use of an infill shear wall as a retrofit option. The use of these walls is described in Section 4.1 of this report. The primary use of these walls is to increase the transverse response of multi-column rigid frame bridge piers. Their effect on the longitudinal response of such frames has been shown to be negligible.



**FIGURE 1-5 In-Fill Wall Retrofit**

Figure 1-6 depicts retrofit types commonly cited in a number of references that discuss deficient columns in Japan. A common deficiency in Japanese construction is the premature termination of the column longitudinal steel. The flexural cracks that develop in this area of premature termination degrade the section to the point that an eventual shear failure occurs at the cutoff point. Steel or concrete jackets can be applied over the termination point to confine the section and provide for greater strength.



**FIGURE 1-6 Retrofit for Columns with Premature Longitudinal Steel Termination**

Figures 1-1 through 1-6 are representative of some of the strengthening solutions employed by researchers engaged in concrete column retrofitting. Other figures indicative of steel and composite retrofits can be found in Section 2 and Section 3 (Refer to the List of Illustrations on page xiii). There are numerous variations of the figures presented as well as other retrofit types not shown. It was decided that the figures presented in this document, though not indicative of all possible retrofit variations, would be sufficient to represent the general types of retrofits encountered in this literature review.

## 1.2 Current Design Philosophy for Column Retrofit

The California Department of Transportation's Memo to Designers 20-4, "Earthquake Retrofit Guidelines for Bridges" (California Department of Transportation, 1995c), is the latest major revision to the design and retrofit guidelines established for bridge columns. Originally published in 1990 as Memo to Designers 20-4, "Earthquake Retrofit Analysis for Single Column Bridges" (California Department of Transportation, 1990), this memo has been periodically revised through the years. The evolution of the design philosophy from the first recommendations to current form is presented below.

The 1990 edition of the Memo to Designers, 20-4, mentioned in the previous paragraph, describes for the first time the analysis procedures and rules for retrofitting single column bridge bents. Column retrofit recommendations at that time were based solely on the use of steel jackets as retrofit solutions. The California Department of Transportation (1990) defined the procedure by which the need for a column retrofit would be established. Following an initial elastic analysis of the column and comparison to column capacities, retrofit would be required on lap splice columns when the ratio of  $M_{EQ}/M_n$  exceeded 1.5, where  $M_{EQ}$  is the seismic moment demand based on response spectrum analysis, and  $M_n$  is the nominal capacity of the column. The limit state of 1.5 was established by the research performed at the University of California, San Diego, where it was determined that "as-built" columns would sufficiently degrade to a pinned base condition at a moment ratio of 1.5. If at the end of a bridge analysis, one or more of the columns exceeds the 1.5 ratio, the original elastic computer model must be revised to account for the hinged condition at these locations.

If it is necessary to retrofit a column, Memo 20-4 clearly indicates that the Class P retrofit should be the desired option if feasible. Class P retrofits are intended to confine the poorly detailed plastic hinge regions of flexurally deficient columns. These retrofits, (1) allow for the formation of hinges and lap splice slippage in a stable fashion while maintaining sufficient column integrity so that the axial load capacity is not compromised, and (2) allow for lap splice debonding by providing a polystyrene layer over the column prior to jacket installation and grouting. The compressible material allows for limited dilation of the concrete to occur under seismic loads, thus allowing for lap splice slippage. On the other hand, the use of Class F retrofits, which extend the full height of the column and generally require footing retrofits so that the footing can sustain the forces transmitted by the retrofit column, is strongly discouraged except in select circumstances. Class F retrofits do not allow for the column to pin because they provide much greater confinement in lap splice regions due to the lack of the compressible polystyrene material. The Class P retrofit is expected to cost a few thousand dollars per column while the Class F retrofit can cost up to one hundred thousand dollars per column with only one column per frame being retrofit in multi-column bents. In shear-deficient columns, full height jackets, with the column end condition being selected as hinged or fixed depending on the connection between the column and footing, are usually required.

Examination of the current Memo 20-4, (California Department of Transportation, 1995c) renamed from "Earthquake Retrofit Analysis for Single Column Bridges" to "Earthquake Retrofit Guidelines for Bridges" in order to reflect a substantial change in content through the years, appears below. A discussion of differences in the original and current memos follows.

The original form of the ductility demand on bridge columns was in the form of the moment ratio,  $M_{EQ}/M_n$ . The general form of the equation has been modified to  $(M_{EQ}+M_D)/M_n$  in order to reflect the influence of dead load moment. This more detailed equation reduces to the original form when for single column bents, transverse loads govern the response. In this scenario,  $M_D$  is set equal to zero. In either scenario, a plastic hinge is still assumed to have formed when the moment ratio exceeds 1.5. In these cases, the columns must either have continuous longitudinal reinforcing in the hinge area or be retrofit with a jacket. Columns can only be assumed to have capacity to develop plastic hinges if the reinforcing development length is reasonably close to that required by Attachment B of the California Department of Transportation (1995c) 20-4 Memo. If this reasonable closeness does not exist, the column base should not be considered fixed in a computer analysis.

The retrofit strategy for multi-column bents is to retrofit one bent per frame. If the bent contains more than two columns, it may not be necessary to retrofit all columns. If the column is allowed to pin at the base, column casings are not required as long as the column is not a shear deficient column. In columns where the reinforcing is continuous from the footing, the plastic hinge may form in the footing and this scenario warrants additional consideration. Multi-column retrofits will generally have an allowable ductility of 6, and with special approval, 8.

The retrofit strategy for single column bents is to apply a Class F retrofit to one column per frame. In keeping with the original Memo to Designers (California Department of Transportation, 1990), a single column bent assumed to yield at the base has two possible retrofit options. The class P retrofit can be employed and the base assumed to yield in subsequent analysis. However, shear deficient columns will be retrofit with full height jackets. Alternately, Class F retrofits can be applied and the column assumed to have fixed ends in subsequent analyses. The Class F retrofit will in general require footing modifications. Single column retrofits will generally have an allowable ductility of 4.0, with ductilities as high as 6.0 pending special approval.

The major revision to the 1995 edition of the 20-4 Memo is the inclusion of significant attachments to the memo.

Attachment A contains STRUDL modeling guidelines for conducting computer seismic analysis of bridges. STRUDL provides an elastic analysis of bridge structures and is used as a diagnostic tool when performing analysis on the need for and location of column retrofits. Caltrans is moving away from the elastic analysis procedures used in determining displacement and ductility demands and towards a procedure that provides a more rational prediction of curvature and displacement ductility as shown in their Attachment C, "Special Considerations". Attachment C also contains guidelines for when and how seismic isolation may be considered as an alternative to substructure retrofit. Caltrans recognizes that for some bridges, such as those on steel rocker bearings, the forces transmitted to the substructure may require extensive retrofit in order to assure adequate strength and ductility. The use of seismic isolation is an accepted alternative but only after careful consideration and a great deal of caution as outlined by the Caltrans Seismic Advisory Board in Attachment C of California Department of Transportation (1995c).

Attachment B of the 1995, 20-4 memo, contains standard design details and guidelines for bridge retrofits and also for new designs.

In the section on steel jacketing, a third retrofit type, the type P/F shell, is described. The type P/F shell is a full height shell that provides a fixed condition, Type F, at the column top, while allowing the lap splice to slip at the bottom of the column through installation of the Type P retrofit.

In Section 2 of Attachment B, the potential use of composite jackets is discussed. In particular, reference is made to the system developed at the University of California, San Diego, consisting of a glass and polyester resin composite wrapped in sheets around a column. The attachment states that the use of composite retrofits requires special evaluation and should proceed only on a case by case basis. The design constraints on composite casings currently limit their use to columns whose ductility demand is four or less or when moderate increases in shear capacity are required. The use of composite retrofits was limited by the 20-4 memo to circular columns of 1,220 mm (48 in.) diameter or less and rectangular columns whose long side does not exceed 915mm (36 in.). The standard drawing for "Composite Column Casing Seismic Retrofit" is supplied in Attachment B and indicates that the proposed casing is a

passive retrofit design wrapped directly onto the column surface. Unlike the steel jackets and other composite jackets that actively exert pressure on the column, the Caltrans standard composite casing does not sustain hoop stresses until the cover concrete begins to dilate. Further amendment to this attachment can be found in Hipley (1996) where design equations and criteria are established for composite jackets of carbon and glass as well as traditional steel jackets.

This summary has briefly presented some of the key seismic assessment and retrofit concerns as delineated by Caltrans. Other agencies and countries have somewhat different approaches but the same general goals. The use of different methods and materials was discussed in preparation for the more detailed chapters to follow which extensively report on the theoretical and laboratory development of the column seismic retrofit guidelines.

### **1.3 Report Format**

The following three Sections, Section 2, 3, and 4, deal with the primary focus of the report, the description of the retrofits. Sections 2 and 3 are divided into many sub-sections that specifically address the type of testing described, i.e., laboratory tests, field tests, analytical models, etc. in the context of deficiency type, i.e., flexure or shear, and column type, i.e. circular or rectangular. Section 4 has a slightly different presentation because it contains a number of retrofit types all with special characteristics. Section 5 presents the different methods of evaluation considered in trying to objectively evaluate the various retrofit options. Section 6 presents the conclusions and identifies areas for further research. A comprehensive reference list follows Section 6. The two Appendixes mentioned previously, Appendix A, which contains the reference classification chart, and Appendix B, which contains the industry survey results, conclude the report.



## SECTION 2 STEEL JACKET COLUMN RETROFITS

### 2.1 Introduction

The use of steel jackets is the most common retrofit technique for the strengthening of reinforced concrete bridge columns. They are not only the most commonly used but also have a recognized design procedure that is generally easy to understand and implement. The design procedures and retrofit method are based on the ability of the jacket, usually oval or circular in shape, to provide sufficient confinement to the column so that a predetermined response level can be achieved. Steel jackets can be used to strengthen a seismically "weak" column, to confine the plastic hinge and lap splice regions of seismically deficient columns, and to enhance the shear strength of columns predisposed to brittle shear failure.

Much of the information in this document relating to steel jacketing, whether for shear or flexurally deficient columns, circular or rectangular, single or multi-column bents, relates to the research work conducted at the University of California at San Diego primarily by M. J. Nigel Priestley and Frieder Seible. They have established the ground rules by which steel jacket seismic retrofits are designed and constructed in the State of California.

The use of steel jackets in the United States generally revolves around the construction of partial or full height steel shells, constructed in halves and field welded. They are usually circular or elliptical in shape. The use of flat steel jackets is not well received in the United States because of the relative efficiency of a steel jacket in a state of hoop tension as compared to bending stiffness. The axial stiffness of the thin plate is many times larger than the bending stiffness of the same plate. However, the use of flat steel jackets seems to be much more of an acceptable retrofit in Japan. Japanese construction, like construction in the United States, has a number of deficiencies due to a lack of understanding of earthquakes and earthquake design when many of the structures were constructed. The most commonly cited problem with Japanese columns is premature termination of a percentage of the flexural reinforcement near mid-height. In an earthquake, these termination zones are not adequate to resist the imposed flexural demands. As a consequence, they degrade rapidly with extensive spalling and buckling of terminated and continuing reinforcing. A common failure mode is a shear failure in the termination zone due to extensive flexural degradation of the mid-height region of the column. Several references pertaining to this type of deficiency are reviewed here so as to illustrate the differences in deficiencies and design philosophies.

The nature of seismic deficiencies in bridge column is that they can generally be characterized as either flexurally deficient or shear deficient. A flexurally deficient column is one that is unable to reach and/or sustain its flexural capacity in an earthquake, usually because of the existence of base region lap splices and/or inadequate base confinement. A shear deficient column, generally a short and stocky column, is one in which the shear capacity is exceeded before the member has the opportunity to function in a ductile flexural mode. These failures are characterized by extensive and sometimes catastrophic damage. Because these two types of behavior are easy to delineate and because specific retrofit strategies have been developed to address the different scenarios, the presentation of material in this section and in Section 3 dealing with composite jackets will be divided into flexure and shear deficient concrete bridge columns.

## 2.2 Laboratory Testing of Steel-Jacketed Specimens

This section on laboratory testing constitutes the vast majority of information on steel jacketing and also the other jacketing techniques to be presented in subsequent discussions. A typical laboratory experiment consists of the construction of a reduced-scale column specimen. These specimens are tested under a constant axial load and variable cyclic loading. The cyclic load is applied and column displacement monitored during testing so that the onset of longitudinal column steel yield can be determined. Having yielded the extreme tension reinforcing steel in the column, the column is loaded through prescribed displacement levels. In general, a pattern of cycles are imposed with several cycles per ductility level and ever-increasing levels of ductility until either the column fails or it is determined that satisfactory performance has been demonstrated. Several references also report that the retrofit response was stable all the way up to the capacity of the test equipment indicating that the true capacity of the retrofit is not known in these specimens. The nomenclature adopted for the commonly reported displacement ductility in this report is  $\mu_{\Delta}$ . This term represents the ratio of the actual displacement to the yield displacements at the point of lateral load application. A much less frequently cited term is  $\mu_{\phi}$ , the curvature ductility of the plastic hinge. This term is the ratio of the measured curvature to the yield curvature in the plastic hinge region.

### 2.2.1 Steel Jacket Retrofit of Flexurally Deficient Bridge Columns

In order to identify the type of column one desires information on more easily, the retrofits will be further divided into sub-sections that deal exclusively with the results of tests on circular and rectangular columns. Section 2.2.1.1 pertains to circular columns and Section 2.2.1.2 is dedicated to rectangular or otherwise non-circular bridge column as well as pier walls.

#### 2.2.1.1 Circular Flexural Columns

Results of a study (Chai, Priestley, and Seible, 1991b) conducted at the University of California at San Diego on the steel jacketing of flexurally deficient, circular, reinforced concrete, bridge columns, are presented below. These results are also presented in part in a number of secondary sources. These sources are Chai, Priestley, and Seible (1991c, 1991d), University of California (1991), Priestley and Seible (1991, 1992), Priestley, Seible, and Chai (1992b), and Priestley, Seible, Chai, and Sun (1991). A companion theoretical study was also conducted and these results can be found in Chai, Priestley, and Seible (1991a, 1994). In addition, other researchers have used the results originally presented by the University of California researchers as the benchmarks against which adequate performance of other retrofit techniques can be measured.

The use of steel jackets as external confinement is based on an extension of the confined concrete model developed in Mander, Priestley, and Park (1988b). In the original model developed by Mander, Priestley, and Park, the increase in compressive strength of the confined concrete core was due to the effects of internal steel reinforcing assumed to be acting at its yield stress level. Internal confinement not only enhanced the compressive strength of the concrete substantially but also increased significantly the strain to failure/ultimate strain,  $\epsilon_{cu}$ . Failure of the confined specimen was at the occurrence of first hoop fracture, which would constitute the point where adequate confinement was no longer present and the core would fail. In order to develop this ultimate confined strain in the concrete, a corresponding increase in the tension steel strain into the strain-hardening region is required. The limit state of low-

cycle fatigue fracture of longitudinal bars may control the performance of the confined specimen. This scenario results in an unattainable value of  $\epsilon_{cu}$  and a correspondingly smaller amount of ductility.

In addition to providing external confinement so that stable plastic hinge mechanisms can develop, the external steel jacket can also be thought of as external shear reinforcing, although that is not the primary focus of this particular set of experiments and will not be elaborated upon at this point.

In the research described, six columns of a 40%-dimensional scale were constructed and tested under axial load and reversed cyclic loading. The columns were typical of pre-1971 prototype columns with details as described in table 2-1. Typical pre-1971 column designs in California possess inadequate longitudinal steel lap splices at the base of generally 20 bar diameters ( $d_b$ ). These lap splices have proven to be a main source of concern as evidenced by poor performance of these columns in the San Fernando (1971), Whittier Narrows (1987), Loma Prieta (1989) and Northridge (1994) earthquakes. In order to study the effect of the lap splice and performance of continuous longitudinal steel, columns of both types were constructed in the "as-built" and retrofit condition.

**TABLE 2-1 Flexurally Deficient Circular Columns (Chai, Priestley, and Seible, 1991b)**

Test Units	Column Details	Footing Details	Remarks
1	20 $d_b$ Lap Splice	Weak Footing	Reference
2	20 $d_b$ Lap Splice, Steel Jacket	Weak Footing	Full Retrofit
3	Continuous Bars	Strong Footing	Reference
4	Continuous Bars with Steel Jacket	Strong Footing	Full Retrofit
5	20 $d_b$ Lap Splice, Steel Jacket and Styrofoam	Strong Footing	Partial Retrofit
6	20 $d_b$ Lap Splice, Steel Jacket	Strong Footing	Full Retrofit
1-R	20 $d_b$ Lap Splice, Repaired with Steel Jacket	Weak Footing with 1,334 kN (300 kip) Prestress	Full Retrofit

The footing strength criteria refers to the fact that in addition to poor column detailing and design prior to 1971, the footing designs were also inadequate. The first two columns tested were constructed with a pre-1971 type footing and the enhanced strength due to the retrofit of column specimen 2 precipitated failure in the footing during testing. Subsequent footings were redesigned so as to preclude footing failure and are referred to as the "strong footing."

Partial retrofitting is a scenario whereby a compressible material, in this set of experiments, Styrofoam®, is placed on the column surface prior to installation of the steel jacket. This compressible layer allows for concrete dilation and subsequent lap splice slip at high lateral displacements or hinge rotations. The

retrofit confines the concrete so as to maintain axial load capacity and provide stable inelastic response but is not intended as a means of increasing lateral load capacity. A full retrofit is one where the objective is not only to confine the concrete but maintain lap splice confinement so that the flexural strength will be enhanced. In both scenarios, the steel jacket had a thickness of 5 mm (3/16 in.) with a 6 mm (1/4 in.) grout infill.

The repair test column, specimen 1-R, involved repair of previously tested specimen 1 and retesting with the same loads and displacement as previously applied. Repair consisted of chipping away the loose concrete before installation of the grouted steel jacket. The steel jacket installation for this specimen was atypical in that the jacket was allowed to extend down to, and bear on, the top of the footing. This was to assure a good seal under the grouting pressure. The weak footing was externally post-tensioned in the direction of lateral load with a force of 1334 kN (300 kips) at the mid-height of the footing.

The columns were designed so that flexural failure would precede brittle shear failure. This was accomplished by making the columns six times as high as the diameter. The column diameter was 610 mm (24 in.), and its height from top of the footing to point of lateral load application was 3,660 mm (12 ft). Longitudinal reinforcing consisted of twenty six, 19 mm (#6) reinforcing bars (2.53% reinforcing ratio) and the transverse steel was 6 mm (#2) bars spaced vertically at 125 mm (5 in.) on center (0.174% reinforcing ratio). The axial load was  $0.177f'_cA_g$ , 1,779 kN (400 kips); the flexural capacity based on ACI equations and an extreme compression strain of 0.003 was 754 kN-m (6671 kip-in.); and the nominal shear stress,  $V_u/0.8A_g$ , was 883 kPa (128 psi). Specified material strengths were 34.5 MPa (5 ksi) for the concrete and 276 MPa (40 ksi) for the reinforcing steel.

The transverse steel ratio was slightly different than that in the prototype, 0.118%. If the dimensional scale factor of 0.4 times the prototype stirrup spacing of 305 mm (12 in.) was used, i.e., 120 mm (4.8 in.), a smaller bar than the 6 mm (#2) bar would have been required. In order to use these bars, the smallest available, spacing was slightly increased to a practical number of 125 mm (5 in.) so as to closely approximate the prototype volumetric confining ratio.

The axial load of  $0.177f'_cA_g$  was a reasonable estimate of  $0.18f'_cA_g$ , a likely upper bound of the axial load that can be expected in single-column bridge piers. This high axial load would impact the overall column response by most dramatically decreasing ultimate ductility since the maximum ductility is inversely related to axial load level.

The required height of the steel jacket in a column requiring flexural retrofit is usually considerably less than the full height of the column. The jacket height used in this series of experiments was made long enough that it would extend up the column to the point where the moment in the original column was less than 75% of the original flexural capacity of the column. It was extended above the point where it was technically required in the unretrofit column because of the increase in moment capacity of the retrofit specimen due to strain hardening of the longitudinal steel. For the columns tested in this set of experiments, the required jacket height was determined to be 1,150 mm (45.2 in.) but was rounded to a practical length of 1,220 mm (48 in.).

The load tests consisted of first applying the axial load to the column via two high-strength steel bars post-tensioned to the laboratory floor with center hole jacks. The horizontal force was applied with a double acting actuator having a push capacity of 667 kN (150 kips), a pull capacity of 578 kN (130 kips), and a maximum stroke of 455 mm (18 in.). The bending moment was corrected to account for the

horizontal component of the axial load due to rotation of the load stub. The corrected bending moment at the base,  $M_b$ , is as shown in the equation below.

$$M_b = (V - P \sin \theta_t) L' + P \Delta \cos \theta_t \quad (2-1)$$

where

V	=	Applied lateral load
P	=	Axial load
L'	=	Height of column from top of footing to load point, 3.66 m (12 ft)
$\theta_t$	=	Rotation of load stub
$\Delta$	=	Horizontal displacement of the lateral load point

This corrected formula takes into account the modified lateral load due to the horizontal component of the axial load induced by column rotation and also the reduction in the  $P\Delta$  effect due to inclination of the axial load. The equation shown above can be modified into the following form.

$$M_b = R_f V L' \quad (2-2)$$

where

$$R_f = 1 - \frac{P}{V} \left( \sin \theta_t - \frac{\Delta}{L'} \cos \theta_t \right) \quad (2-3)$$

The quantity  $R_f$  is a reduction factor which has very little overall impact. Chai, Priestley, and Seible (1991b) state that for the maximum extension of the hydraulic cylinder, 230 mm (9 in.),  $\theta = 4$  degrees,  $P = 1,779$  kN (400 kips), and  $V = 245$  kN (55 kips), the value for  $R_f = 0.946$ . Note that the value for  $P$  is not constant during the test and varies as the displacement of the column because the neutral axis does not coincide with the column centerline. Cracks in the column will tend to extend the column and henceforth increase the axial load. During the tests the column axial force was reduced after  $\mu_\Delta = 3$  so that the capacity of the axial load bars was not exceeded. The axial force varied in the test of column 4 from a maximum of 2,019 kN (454 kips) in some of the initial cycles to a minimum of 1,379 kN (310 kips) during maximum ductility cycling.

In addition to measuring displacement ductility, linear potentiometers were mounted in the plastic hinge region on opposite sides of the column so that an average curvature could be calculated through knowledge of the vertical displacement of the opposite gages and the horizontal distance between them.

All columns were tested under the following load pattern. Two cycles to  $\pm 36$  kN (8 kips) and one cycle to  $\pm 67$  kN (15 kips) were imposed in order to verify operation of the data acquisition system and to look for cracks that may develop before this load level. Five cycles to  $\pm 122$  kN (27.5 kips), approximately 50% of the lateral load corresponding to the nominal flexural strength, were imposed to check for premature lap splice bond failure. One cycle to  $\pm 178$  kN (40 kips), the lateral load which approximately corresponds to that required to cause first yield, was carried out to define the experimental yield displacement. The average of the displacements under the push and pull cycles was defined as the yield

displacement. The behavior of the lap-spliced columns is presented below while the performance of columns with continuous reinforcing is presented afterwards.

"As-built" column 1 experienced flexural cracking during the first cycle to 67 kN (15 kips) and spread to half of the column height when the force was increased to 122 kN (27.5 kips). Cracks outside the lap splice region were wider and grew faster than those in the lap splice region. Vertical cracks developed near the base at 178 kN (40 kips), indicating the beginnings of bond failure. Spalling began at  $\mu_{\Delta} = 1$  and became extensive at  $\mu_{\Delta} = 1.5$ . A peak lateral load of 218 kN (49 kips), approximately 94% of the ideal lateral strength,  $V_i$ , was recorded at  $\mu_{\Delta} = 1.5$ , with a corresponding drift ratio of 1.4%. The ideal lateral strength,  $V_i$ , is the shear force corresponding to the flexural strength of an unconfined column. The first signs of footing failure were also noted at this ductility level with a significant crack on top of the footing propagating in the direction of load. The crack stabilized due to bond failure and subsequent lack of force transfer. The second and third cycles to  $\mu_{\Delta} = 1.5$  had significant reductions from the maximum capacity of 18% and 12%, respectively. Severely pinched hysteresis loops were characteristic of the remaining response with lateral load capacity degradation to approximately 89 kN (20 kips). This capacity is due to the load resisted by the horizontal component of the inclined vertical load. Final failure was due to loss of confinement of the lap splice region caused by extensive spalling and stirrup fracture at  $\mu_{\Delta} = 4$ . The fact that the stirrup fractured is indicative of a significant amount of force transfer in the stirrup lap splice which was located in the cover concrete, a much less than ideal location.

Retrofit column 2 presented some difficulties in observing crack formation because an epoxy resin seal at the top and bottom of the jacket, in addition to the jacket itself, obscured much of the critical areas. A crack in the epoxy seal was noted at the base at a lateral load level of 111 kN (25 kips) with cracking above the jacket being noticed at 122 kN (27.5 kips). Slightly inclined flexural cracks were noted above the jacket at a load level of 178 kN (40 kips) indicating the influence of shear on the crack formation. Separation between the epoxy seal and column as well as jacket and column was noticed at this stage. Top cracks in the footing were growing with increasing ductility. A maximum lateral load of 260 kN (58.5 kips) was noted on the first push cycle to  $\mu_{\Delta} = 3$  before brittle failure of the footing occurred in the third cycle to this ductility level.

Column 6, constructed with the strong footing, had similar initial behavior as column 2. Minor flexural cracking and epoxy seal separation at the top of the jacket were noted in the 89 kN (20 kip) to 111 kN (25 kip) range. The flexural cracks were essentially spaced with the transverse hoops, indicating that the stirrups were initiating the cracking. At 178 kN (40 kips) flexural cracks extended about 2/3 of the column height.

At the bottom of the column, epoxy seal separation occurred at  $\mu_{\Delta} = 1.5$  and minor crushing was noted at  $\mu_{\Delta} = 2$ . Cracks on the top of the footing fanned out radially from the column beginning at  $\mu_{\Delta} = 3$ . Large inelastic strains in the longitudinal steel and penetration of the strain into the footing were noted at  $\mu_{\Delta} = 5$ , with corresponding spalling of the cover concrete at the column base between the bottom of the jacket and top of the footing. Failure was due to low-cycle fatigue of the longitudinal steel at  $\mu_{\Delta} = 8$ . The maximum lateral load of 343 kN (77 kips) was noted on the first push cycle to  $\mu_{\Delta} = 7$  at a drift ratio of 5.3%. This lateral force was 39% above the plastic lateral force. The plastic lateral force,  $V_p$ , is the lateral load which corresponds to the development of the plastic moment in the confined section using a compressive strain of 0.005 in the confined core. Excellent hysteretic response was observed with very little pinching of the loops at even high ductilities.

The test results of column 5, constructed with the partial retrofit, follow. Because of the soft foam wrap on the surface of the column, early separation of the epoxy seal from the column occurred at a load of 68 kN (15 kips). Flexural cracks first appeared above the jacket at a load of 89 kN (20 kips). A maximum lateral force of 209 kN (47 kips) was recorded on the first push cycle to  $\mu_{\Delta} = 1.5$  after which bond slip progressively diminished the lateral force resistance. The peak force was slightly less than the "as-built" column 1 due to a lower actual measured concrete strength in column 5. Even though bond slip was occurring, the peak strength of this column at a ductility of  $\mu_{\Delta} = 7$  was still greater than that of the "as-built" specimen at  $\mu_{\Delta} = 4$ . This indicates that some bond strength must still be present since the strength of column 4 was due to the resistance presented by the inclined axial load. The retrofit column 5 was still able to maintain its axial load capacity after testing was complete and validates that the objectives of this test were attained. Additionally, the strong footing used in this test performed well, exhibiting no measurable damage due primarily to degradation of the force transfer mechanism in the column.

The results of the repaired lap splice specimen, column 1-R, are presented below. The first two columns constructed, C-1 and C-2, were purposely constructed as weak footings and with internal conduit which would allow for subsequent post-tensioning if necessary. After tests were carried out on C-1, the footing was strengthened via post-tensioning by four Dywidag bars carrying a total prestress of 1,334 kN (300 kips) applied parallel to the direction of load.

The initial loss of cover at the base presented a problem when trying to contain the grout at the column base. Consequently, the jacket was allowed to bear on the top of the footing as previously mentioned. The jacket was seen to bear significantly on the footing even at low load levels. High hoop strains and vertical bearing caused the jacket to bell out significantly over the lower 150 mm (6 in.) of the column jacket.

Behavior of this specimen was very stable. No extension of previously developed cracks was noticed for forces below 178 kN (40 kips). The maximum lateral force of 254 kN (57 kips) was observed at  $\mu_{\Delta} = 3$  and was in excess of the peak resistance of the "as-built" column of 218 kN (49 kips) which occurred at  $\mu_{\Delta} = 1.5$ . The peak lateral load also exceeded the theoretical "as-built" flexural strength. The column did not perform as well as column 6 but exhibited stable response with only a slight decrease in lateral resistance up to  $\mu_{\Delta} = 6$ . At this level, the lateral resistance was still approximately 85% of the ideal resistance,  $V_i$ . Removal of the jacket following the test indicates that bond failure had indeed occurred.

For columns with continuous reinforcing, "as-built" column 3 and retrofit column 4, two tests were conducted. Cracking in the "as-built" column 3 did not begin until a load of 80 kN (18 kips), slightly higher than in column 1. First cracking at the base was noted at 93 kN (21 kips). Cracking covered half of the column at a load of 122 kN (27.5 kips). First crushing of the concrete base was noted at  $\mu_{\Delta} = 1.5$  with crushing on the pull side delayed until  $\mu_{\Delta} = 2$ . The ideal capacity of the column was first exceeded at  $\mu_{\Delta} = 2$ . Spalling of the cover concrete at the base on both column sides occurred at  $\mu_{\Delta} = 3$ . The maximum lateral force of 245 kN (55 kips), approximately 11% higher than  $V_i$ , was noted at this ductility level. Buckling of the longitudinal steel was noted at  $\mu_{\Delta} = 4$ . The second hoop above the base fractured at  $\mu_{\Delta} = 5$ . The first, third, and fourth hoops did not fracture but exhibited some slip in their lap splices. However, until the column failed due to a confinement failure at the second cycle to  $\mu_{\Delta} = 5$ , no real drop in lateral load resistance was noted. Chai, Priestley, and Seible (1991b) indicate that the reliable capacity of this column be taken as 3 due to the onset of spalling at this level.

The retrofit column with continuous longitudinal reinforcing is column 4. The response of this column is very similar to column 6. The plastic lateral force was first exceeded during cycling at  $\mu_{\Delta} = 3$ . There was a minor drop in lateral force during repeat cycling to the same ductility level. The maximum lateral force was measured at the maximum ductility level,  $\mu_{\Delta} = 8$ . This load was 325 kN (73 kips). Failure due to low cycle fatigue occurred after two cycles to this ductility level with a corresponding drift ratio of 6%. The response of this column was corrected due to the effects of inclination of the axial load as previously described. This correction factor resulted in a slight reduction in the lateral force at large displacements and a reduction in energy from the measured dissipated energy of 884 kJ (7,823 kip-in.) to a corrected energy of 867 kJ (7,678 kip-in.), an approximate 2% difference.

The summary of these tests indicates that for "as-built" columns with widely spaced transverse reinforcing and short lap splices typical of pre-1971 designs, the columns are unlikely to reach their nominal flexural capacity and will degrade rapidly. "As-built" columns with continuous reinforcing can attain their nominal flexural strength and have a dependable ductility of approximately  $\mu_{\Delta} = 3$ . Degradation of response is slower than with the lap splice detail columns. Failure of column 2 indicates that the footings in pre-1971 designs may be susceptible to failure if the column is retrofit and the footing left unchanged.

The retrofit columns with a volumetric confinement ratio of 3.1% demonstrated stable response up to  $\mu_{\Delta} = 7$  with final failure being through low cycle fatigue of the reinforcing steel. The use of a foam wrap over the column surface effectively eliminated the strengthening capabilities of the steel jacket but allowed for stable hinge formation. It also allowed the column to maintain its vertical capacity after completion of the testing. The fully grouted jackets were seen to increase the lateral stiffness of the columns by 10% to 15%.

The tests also showed that the steel jacket technique is effective as a repair method for damaged columns. The strength of the retrofit column was greater than the original undamaged column but hysteretic energy absorption capacity was slightly compromised.

The results of the curvature measurement on the columns supports use of the following formula for determination of the plastic hinge length in "as-built" columns with continuous reinforcement.

$$L_p = 0.08L' + 6d_b \quad (2-4)$$

In the retrofit columns, the curvature occurs in a smaller region defined below.

$$L_p = 12d_b + v_g \quad (2-5)$$

where  $v_g$  is the gap height between the top of the footing and the bottom of the column.

Finally, validation of the proposed jacket height criteria which establishes that the jacket height extend to the point where the moment is less than 75% of the capacity of the original unretrofit specimen was completed. This criteria was shown to be sufficient in ensuring that a plastic hinge mechanism could develop at the base and would be contained in the jacketed region.

The results of this summary clearly illustrate the effectiveness of steel jackets in providing confinement and strength enhancement to circular reinforced concrete bridge columns.

Jaradat, McLean, and Marsh (1996) primarily emphasize the testing of a variety of seismically deficient "as-built" bridge columns but also include test results from steel-jacketed specimens. The document presents the results from a work in progress and as a consequence provides only a small amount of information. The results of 1/3.6 scale model tests on 8 reinforced concrete columns are presented. The columns incorporate deficiencies common in pre-1971 concrete bridge columns, namely short lap splices and inadequate confinement. The columns were rotationally fixed at both ends so that the shear behavior of the degrading plastic hinge regions could be assessed during testing. Of the eight specimens tested, six were in the "as-built" condition, one column was retrofit at the base with a typical Caltrans Type P retrofit, and the final column was retrofit using a Caltrans Type F retrofit. The columns were tested under constant axial load and increasing inelastic displacement levels. The specimen variables consisted of column height, longitudinal reinforcing ratio, lap splice length, and base retrofit method.

The performance of the specimens was evaluated based on flexural and shear capacity, displacement ductility, strength degradation and hysteretic energy absorption. The results of the test were compared to the predicted results from procedures established by Priestley and Seible at the University of California at San Diego (1991), FHWA recommendations (Federal Highway Administration, 1995), and newly proposed models from the University of California at San Diego (Priestley, Verma, and Xiao, 1993). The results will be used to characterize the behavior of concrete bridge columns under seismic loading. The ability of the yielded hinge region to continue transferring shear and axial forces will be evaluated and the effect of retrofits will be considered.

Preliminary results indicate that flexural failures occurred in five of the eight specimens. The poor confinement and insufficient lap splice length led to rapid strength degradation. The column tops, which did not contain a lap splice region, did not suffer similar degradation until higher ductility levels, with eventual degradation attributable to longitudinal bar buckling.

Shear failures were noted in three of the eight specimens. The two types of shear failures observed were shear failure with little or no flexural yielding in the middle of the columns and shear failure after extensive yielding occurring at the column ends. The second failure type is caused by primary flexural degradation in the hinge region and occurred at lower shear levels than the first failure type.

The Caltrans Type F retrofit was also shown to be effective in maintaining the full flexural capacity of the column base in the presence of large ductility demands. The Type P alternative did not provide as significant an enhancement in specimen strength and the results were considered to be intermediate to the "as-built" and Type F retrofits.

Work continues on this project with evaluation of the test results and comparison to current and proposed assessment models.

#### **2.2.1.2 Rectangular Flexural Columns**

The retrofit of rectangular flexurally deficient bridge columns using steel jacketing techniques is described in Sun, Seible, and Priestley (1993b) as well as in a number of summary documents (Priestley and Seible, 1991, 1992), (Priestley, Seible, and Chai, 1992a, 1992b), (Priestley, Seible, Chai, and Sun, 1991), and (University of California, 1991). The information from these documents has been incorporated into the seismic retrofit guidelines published by the Federal Highway Administration (1995).

The primary retrofit type studied in Sun, Seible, and Priestley (1993b) is the use of an oval steel jacket employed around a rectangular concrete column. Refer to figure 1-1 for a sketch of this type of retrofit. The purpose of this oval jacket is to enhance the strength of bridge columns by providing a much higher ultimate concrete compressive strain due to confinement, confine the lap splice region of flexurally deficient columns in order to promote force transfer, and enhance the shear strength of the specimen due to the action of the steel shell as external shear stirrups. The basis for the confined concrete approach is the model for confined concrete developed in Mander, Priestley, and Park (1988b). Mander, Priestley, and Park's model was originally developed for concrete columns with the confinement provided internally due to closely spaced lateral ties. However, the steel jacket can be converted into what is essentially, a continuous external tie providing a constant volumetric confining ratio. The core concrete is then restrained by the lateral confining stress imposed by the stirrups and jacket while the cover is only restrained by the steel jacket. Testing of stiffened rectangular retrofits was carried out in a separate research program at the University of California at San Diego (1991), (Priestley, Seible, and Chai, 1992a), and these results will serve as a means of comparison for the oval jacket specimens. It was anticipated that the oval jackets would be more effective because the resisting mechanism is hoop tension in the plates as opposed to lateral bending stiffness, a significantly less efficient means of confinement, in the stiffened flat plate options.

The hoop tension in a curved surface can be found from thin-shell equilibrium equations to be  $pr/t$ , where  $p$  = internal radial pressure,  $r$  = shell radius, and  $t$  = shell thickness. In an ellipse, this indicates that for a given lateral stress, the hoop tension is constantly changing due to the variation in radius. Conversely, for a constant state of hoop tension, the radial stress is variable over the surface of the column. Implementation of this variable stress concept into Mander, Priestley, and Park's model, which assumes a constant radial stress and stress in the confining elements, is difficult. As a compromise, a uniform lateral pressure concept was adopted on the basis of an average confining stress on the compression side of a column cross-section. The average radius was defined as the average of the jacket radius at the column corner point, point 2 in figure 2-1, with the jacket radius measured along the principal axis for the compression side under consideration. Therefore, for the x-axis, the average radius,  $R_x$ , was defined as the average of the radii of points 1 and 2 in figure 2-1. For the y axis, the average radius was defined as the average of the radii to points 2 and 3.

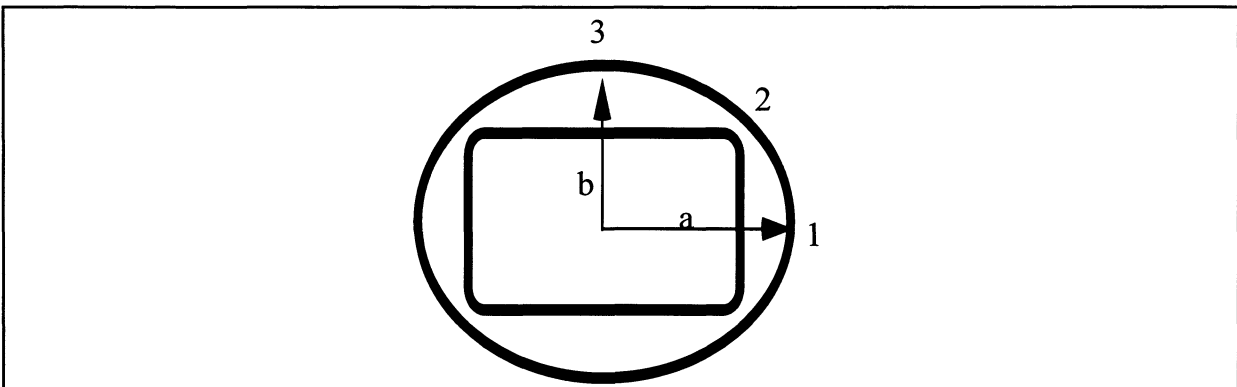


**FIGURE 2-1 Schematic of an Oval Steel Jacket (Sun, Seible, and Priestley, 1993b)**

If one is to assume that the jacket yielded, the equivalent lateral confining stress can be defined using thin shell equilibrium as given by equation (2-6).

$$f_{jl} = \frac{f_{jys}t}{R_o} \quad (2-6)$$

where

$f_{jl}$	=	Equivalent lateral confining stress
$f_{jys}$	=	Yield strength of the steel jacket
$t$	=	Thickness of the jacket
$R_o$	=	Average radii based on the criteria described previously

The effective confining pressure will be less in the weak direction because the quantity  $R_o$  will be larger due to the larger radius of the jacket along the long face of the column. In very narrow piers, it will be very difficult to attain adequate confinement on the long faces due to the very flat jacket that will be placed adjacent to these surfaces. In many cases, a realistic assessment of the displacement demand in the weak direction does not necessitate retrofit. In most cases the strong direction retrofit requirements will drive the design.

In order to test the effectiveness of oval steel jackets on flexurally deficient columns, six models, 40% of the size of a prototypical column constructed prior to 1971, were constructed. The objective of the testing was to investigate the performance of both "as-built" and retrofit columns. Two type of columns were investigated, columns with a lap splice at the base, and columns with continuous longitudinal reinforcing.

The columns were 730 mm x 490 mm (28.75 in. x 19.25 in.) in plan and stood a height of 3.66 m (12 ft) from the top of the footing to the point of lateral load application. The imposed axial load was 1,779 kN (400 kips) and corresponded to an axial load ratio of  $0.145A_g f'_{co}$ . The design material strengths for the test specimens were 34.5 MPa (5 ksi) for the concrete and a yield of 276 MPa (40 ksi) for the reinforcing steel. Transverse reinforcing consisted of 6 mm (#2) reinforcing bars spaced vertically on 125 mm (5 in.) centers. This constituted a transverse confining ratio of 0.17%.

In columns constructed with a lap splice, the longitudinal reinforcing consisted of thirty-two 19mm (#6) reinforcing bars for a longitudinal steel ratio of 2.55%. For the columns constructed with continuous reinforcing, the longitudinal steel was a combination of fourteen, 25 mm (#8) reinforcing bars and twenty-eight, 22 mm (#7) reinforcing bars for a longitudinal steel ratio of 5.03%.

The design of the oval steel jacket shape, thickness, and height is based on the following criteria.

The major criteria for determining the design of an oval jacket involve (a) provision of a sufficient lateral confining stress at the yield of the jacket so a desired ductility can be achieved and (b) minimization of the dimensions of the steel jacket based on the sum of the major and minor axis lengths of the oval shape.

The design of the shape of the steel jacket is based on the fact that the jacket must pass through point 2 as shown in figure 2-1 whose coordinates are  $(a_2, b_2)$  which are the dimensions to the corner of the column and any adjustments for the corner chamfer and required gap between the column and jacket. Therefore, the equation for the ellipse is defined by equation (2-7).

$$\frac{a_2^2}{a^2} + \frac{b_2^2}{b^2} = 1 \quad (2-7)$$

Minimization of the sum of dimensions a and b leads to the results presented in equation (2-8).

$$a = bk \quad b = \sqrt{\left(\frac{a_2}{k}\right)^2 + b_2^2} \quad k = \left(\frac{a_2}{b_2}\right)^{2/3} \quad (2-8)$$

The parameters,  $a_2$  and  $b_2$ , are user specified and can be substituted into the above equation to determine the shape of the jacket.

The jacket height in a flexurally deficient column is usually confined to an area near the lap splice region and does not necessarily have to extend the entire height of the column. In order to provide an adequate jacket height, one must consider that the jacket must be long enough to encase the plastic hinge region and must also eliminate the possibility of shear failure above the termination of the jacket.

The length of the jacket is chosen so that the moment demand in the retrofit column adjacent to the termination of the jacket is smaller than the moment capacity of the original column, taking into account a safety factor for unexpected moment shift or member understrength. The following expression, based on a linear variation of the moment in the column, is used for proportioning the length of the column jacket.

$$L_j > \left(1 - \alpha \frac{M_u}{M_r}\right) L - H_g \quad (2-9)$$

where

$L_j$	=	Jacket height
$M_u$	=	Moment capacity of the "as-built" section
$M_r$	=	Moment capacity of the retrofit section
$L$	=	Column height
$H_g$	=	Height of the gap between the top of footing and bottom of jacket
$\alpha$	=	Safety factor, taken in this research to be 0.85

If the original column is found to be shear deficient above the jacket, then a full height jacket is required.

Design of the jacket thickness can proceed using equation (2-6) once the shape of the jacket has been found. As a prerequisite to determining the jacket thickness, the required lateral confining stress must be established for the particular column in question through use of moment-curvature analysis incorporating different confining stresses until a satisfactory solution is found.

These guidelines were used in determining the jacket sizes used in the experimental tests described in the following text.

The test procedure employed in this research was nearly identical to that used in Chai, Priestley, and Seible (1991c) presented previously in this chapter. Because the axial load varies along with the column displacement due to cracking of the specimen and shifting of the neutral axis during testing, the load was adjusted periodically so that the capacity of the vertical bars used to provide the axial load was not exceeded. As the test progressed, the axial load at zero displacement progressively decreased to the point where on cycling to the maximum displacement level, the load was as low as 1,246 kN (280 kips). The axial load was highest in a given cycle at the maximum displacement and reached as high as 2,002 kN (450 kips). A description of the test specimens can be found in table 2-2.

**TABLE 2-2 Steel Jacket Retrofit of Flexurally Deficient Columns  
(Sun, Seible, and Priestley, 1993b)**

Test #	Test Specimen	Design Details	Reinforcing Ratio	Test Orientation	Remarks
1	R-1	20 d <sub>b</sub> lap splice	2.55%	Strong	Reference
2	R-2	20 d <sub>b</sub> lap splice	2.55%	Strong	Retrofit
3	SF-1	20 d <sub>b</sub> lap splice	2.55%	Strong	Built-up Channel Retrofit
4	SF-2	20 d <sub>b</sub> lap splice	2.55%	Strong	Stiffened Plate Retrofit
5	R-3	20 d <sub>b</sub> lap splice	2.55%	Weak	Reference
6	R-4	20 d <sub>b</sub> lap splice	2.55%	Weak	Retrofit
7	R-5	Continuous Reinforcing	5.03%	Strong	Reference
8	R-6	Continuous Reinforcing	5.03%	Strong	Retrofit

Sun, Seible, and Priestley (1993b) present the results of specimens SF-1 and SF-2 as a comparison to the oval steel jacket retrofit method. However, the only presentation is a load-displacement envelope comparing the SF retrofits to the oval jacket retrofits. The results presented for these retrofits below have been taken from Section 3.4.1.4 of Priestley, Seible, and Chai (1992a). The two specimens in question were originally designed as temporary retrofit methods for the double deck viaducts in San Francisco.

The built-up channel system retrofit consists of steel channels placed flange inward along the vertical axis of the column. Behind these channels, on all four faces of the column, are wide flange beams whose ends are tied across the column corners using high strength rods. The height of the steel channel retrofit is 715 mm (28.2 in.). Refer to figure 2-2 for a description of this retrofit.

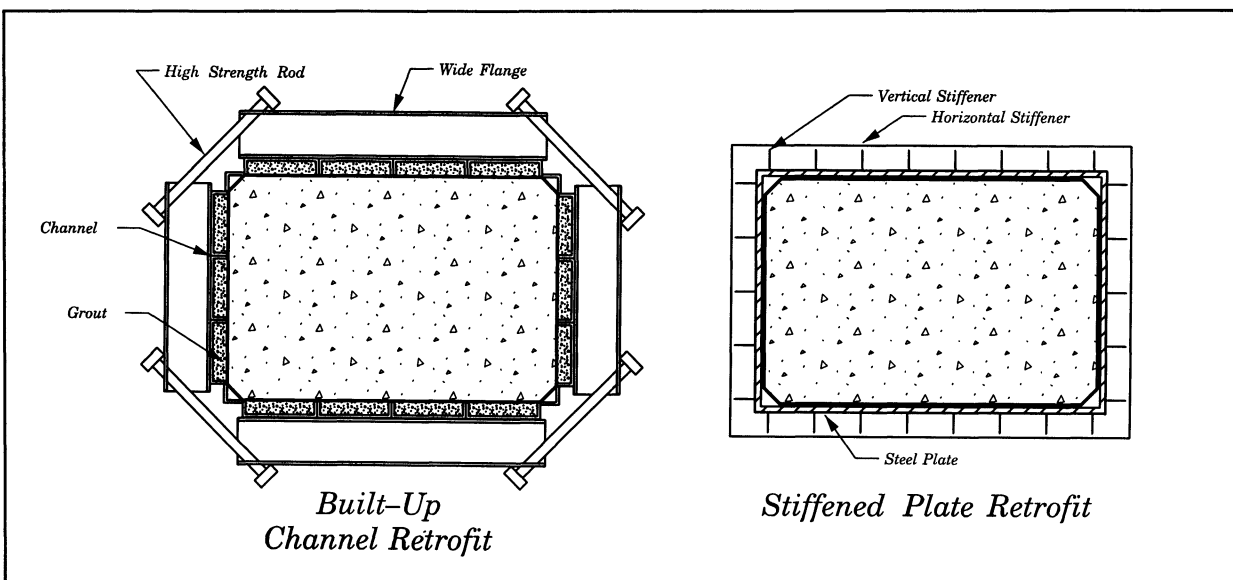


**FIGURE 2-2 Built-Up Channel and Stiffened Plate Retrofits**

The load-displacement response of this retrofit illustrated stable response up to  $\mu_{\Delta} = 4$  with only slight degradation during cycles to  $\mu_{\Delta} = 5$  and 6. A significant drop in lateral capacity was observed during cycling to  $\mu_{\Delta} = 7$  and 8. Both the yield and ideal capacities were exceeded and resistance maintained in excess of these values until  $\mu_{\Delta} = 7$ . The maximum load recorded for this test is only 9% lower than for the comparable oval jacket results. The maximum usable drift ratio for this retrofit was 2.7%, much less than the oval jacket results.

The stiffened plate system, as the name implies, involves the placement of a rectangular steel plate box around the existing column. This set of four plates is stiffened in the vertical and horizontal direction with steel plates and the space between the jacket and column is grouted. Refer to figure 2-2 for a description of this retrofit.

There was no difficulty in this retrofit's ability to exceed the ideal capacity of the column, but ductility enhancement was limited. The peak lateral load was reached on the first push cycle to  $\mu_{\Delta} = 4$ , but dramatic drops in stiffness and load capacity were noted thereafter.

In testing the "as-built" and retrofit specimens R-1 through R-6 in Sun, Seible, and Priestley (1993b), from the oval steel jacket tests, both displacements and curvatures were measured. Horizontal displacement was measured at approximately mid-height and at the top of the steel jacketed region, mid-height of the unretrofit region, and at the level of horizontal load. Rotation measurements were made at the top of the column via four linear potentiometers. Seven pairs of linear potentiometers were used near

the base of the column. The displacement of each pair of opposite face potentiometers was used in conjunction with the vertical and horizontal distances between potentiometers in order to compute the curvature.

The load-displacement input consists of a load control phase followed by a displacement control phase. The first cycle was to the cracking lateral load,  $V_{cr}$ . The second cycle was to twice this load. Several more cycles were used to transition to a lateral load of  $0.5V_{iu}$ , where  $V_{iu}$  is the lateral load corresponding to the ideal ultimate moment capacity of the section defined as the moment acting simultaneously with five times the yield curvature. After five cycles to this level, one cycle was imposed at average lateral load of  $0.5V_{iu}$  and  $V_y$ , where  $V_y$  is the lateral load required to produce first yield in the longitudinal steel at the base of the column. Following three cycles to  $V_y$ , displacement control began with three cycles each at increasing levels of ductility. The results from Chai, Priestley, and Seible (1991c) demonstrated that the  $P\Delta$  effects on this test setup were negligible and were therefore neglected in this research.

In the test results from the lap splice columns the "as-built" column 1 tested in the strong direction demonstrated predictably poor performance. The first flexural cracks developed at the bottom of the column during the first push cycle to 89 kN (20 kips) and increased as the load was increased. At the theoretical yield load of 267 kN (60 kips), initial vertical cracks were noticed on the tension side of the column. These cracks spread over the entire lap length at  $\mu_\Delta = 1$  and the peak lateral load of 302 kN (68 kips) was recorded at this level. As cycling progressed to  $\mu_\Delta = 1.5$ , the cover concrete spalled at the top of the splice and the lateral load capacity dropped 28%. As testing continued, the lateral capacity progressively decreased to the point where at  $\mu_\Delta = 3$ , the entire cover concrete in the lap splice region fell off and the lateral load resistance was reduced to 133 kN (30 kips). This resistance was due to the effect of the inclined vertical load. In this test, the ideal load,  $V_{iu}$ , 347 kN (78 kips) was never reached.

Retrofit column R-2 demonstrated significantly improved performance. The first flexural cracks were observed above the jacket at 178 kN (40 kips). The spacing of the cracks was essentially the same as the stirrup spacing indicating that the horizontal cracking was due to the presence of the stirrups. These cracks extended up to 2/3 of the column height by  $\mu_\Delta = 2$ . The ideal flexural capacity of the column,  $V_{iu}$ , of 347 kN (78 kips) was observed at  $\mu_\Delta = 1.5$ . Yield penetration into the footing resulted in a spall on the top of the footing at the compression toe at  $\mu_\Delta = 5$ . The maximum lateral load of 472 kN (106 kips) was applied at this ductility level. No degradation in response was noted up to  $\mu_\Delta = 7$ . At  $\mu_\Delta = 8$ , a noticeable slip of the tension side lap splice occurred and the lateral load capacity dropped 24%. Although this eventual slip resulted in termination of the test, excellent results as compared to the "as-built" column and the SF-1 and SF-2 retrofits were obtained. This test produced hysteresis loops that were wide and demonstrated only minor pinching at high ductility levels. Excellent energy dissipation, lateral load resistance, and ultimate ductility results were obtained.

"As-built" column R-3, typical of "as-built" specimens with lap-spliced reinforcing, performed poorly. At a lateral load level of 89 kN (20 kips), approximately twice the cracking load, the first horizontal cracks were noticed. These cracks spread uniformly over the column spaced approximately with the stirrups. Vertical cracks along the lap splice were noticed at  $\mu_\Delta = 1.5$  at the column corners and spread to the entire tension face at  $\mu_\Delta = 2$ . The maximum lateral load of 262 kN (59 kips), slightly greater than the ideal,  $V_{iu}$ , of 252 kN (56.6 kips), was noted at this ductility on the first cycle. However, a 50% drop in resistance occurred following the third cycle at this ductility level. The cover concrete began to spall at the column base at  $\mu_\Delta = 3$ , and a separation between the cover and bars was noted during subsequent

cycling at this level. A bond failure at  $\mu_{\Delta} = 6$  resulted in capacity being reduced to 89 kN (20 kips). This capacity was due entirely to the inclined axial load contribution.

Column R-4 demonstrated much improved performance. First flexural cracks above the jacket were noticed at 156 kN (35 kips) and spread to within 900 mm (approximately 3 ft) of the top of the column during testing. Stable hysteretic response with almost no pinching was observed up to the first cycle to  $\mu_{\Delta} = 8$  where the maximum lateral load capacity was attained. The column exceeded its ideal capacity at  $\mu_{\Delta} = 1.5$  and sustained this capacity until the second cycle to  $\mu_{\Delta} = 8$  where a 14% drop from the maximum resistance was noted due to bond slip at the base of the column. This retrofit once again demonstrates the excellent performance of the oval steel jacket.

In the results of the continuous reinforcing column tests, the response of "as-built" R-5 was significantly better than column R-1, an "as-built" column with a lap splice, as would be expected. The first flexural cracks were observed at a load twice the theoretical cracking load. At a load level of 445 kN (100 kips), the angle of inclination of the cracks approached 45 degrees and the cracks propagated downward toward the compression toe. The ideal capacity of the column was attained at  $\mu_{\Delta} = 1.5$  and crushing of the cover began. At a displacement of  $\mu_{\Delta} = 3$ , large inclined shear cracks formed and reinforcing on the compression side buckled suddenly. This buckling occurred over a region of 635 mm (25 in.) from the top of the footing. This buckled reinforcing straightened and buckled again during load reversal up to  $\mu_{\Delta} = 4$ . At this point, the reinforcement ties started to open at the corner laps and a major shear crack developed in the plastic hinge region with a dramatic drop in lateral load capacity.

Finally, the response of retrofit column R-6 is presented. The yield moment strength of the retrofit column was essentially the same as the "as-built" column R-5. As the displacement approached  $\mu_{\Delta} = 1$ , flexural cracks above the steel jacket began to incline due to shear. The flexural shear cracks extended as the ductility increased to  $\mu_{\Delta} = 3$ . At  $\mu_{\Delta} = 4$ , shear cracks developed below the load stub at the top of the column. The top of the footing spalled at  $\mu_{\Delta} = 4$  in the load direction. As the ductility increased to  $\mu_{\Delta} = 6$ , a large shear crack formed at the first load peak and began immediately under the load stub on one side of the column and reached almost as low as the top of the jacket on the other side of the column. The lateral load remained near a maximum of 712 kN (160 kips) until a ductility of  $\mu_{\Delta} = 7.7$ . At this point, the concrete compressive struts between the inclined cracks began to crush and the cover at the ends of the struts was pushed out. Brittle shear failure of the column above the jacket finally halted the test at this ductility level.

Further commentary on the test results is presented in the research report reviewed here and modifications of the design procedure for oval steel jackets are proposed. These modifications depend on whether the column has a lap splice or continuous reinforcing and for the case of lap-spliced reinforcing are also based on displacement ductility requirements and the bond strength of the lap-spliced reinforcing. A procedure is also presented to identify whether a retrofit column is subject to brittle shear failure above the jacket.

A highly detailed analytical study (Sun, Seible, and Priestley, 1993a) was also prepared in conjunction with this experimental research. This analytical investigation contains most of the information found in Sun, Seible, and Priestley (1993b) as well as extensive derivation of material constitutive relationships and bond-slip models to be used in a nonlinear finite element analysis of jacketed columns using fiber elements.

The experimental investigation described in Amari et al. (1994), had as its focus the development of strengthening techniques for reinforced concrete columns. The experimental performance of steel jacket, concrete jacket, and combined steel and concrete jacketing techniques was examined. The description of the steel jacket retrofit techniques is described below while the concrete jacket and mixed jacket retrofits are described in Section 4.1, which deals with concrete jacketing.

For flexural testing of the steel-jacketed specimens, an "as-built" specimen, column F1, and two retrofit specimens, F3 and F5, were constructed. The cross-sectional dimensions of all of the columns were the same prior to jacketing. The columns measured 500 mm x 500 mm (19.7 in. x 19.7 in.) and were 2,300 mm (7.55 ft) tall above the top of footing. The column reinforcing consisted of twenty longitudinal bars, 19 mm (0.75 in.) in diameter, and 10 mm (0.39 in.) diameter transverse bars spaced 90 mm (3.54 in.) on center. The jacketed columns, numbers F3 and F5, were retrofit with 6 mm (0.24 in.) thick and 750 mm (29.5 in.) high steel plate jackets placed directly on the column surfaces. The difference in the specimens is that the jacket in column F3 was mechanically attached to the footing via dowels and the jacket in column F5 was not.

Tests on the column were carried out using a constant axial stress of 1.96 MPa (20 kgf/cm<sup>2</sup>, 284 psi) so as to simulate the effects of dead load. The lateral load was progressively statically applied until yield of the longitudinal steel was noted. Further cycling at  $\mu_{\Delta} = 2, 3, 4,$  and 5 was carried out by applying one static cycle and ten dynamic cycles followed by a change to the next ductility level if warranted.

The "as-built" specimen was able to achieve a displacement ductility of  $\mu_{\Delta} = 4$ . This was accompanied by concrete spalling, hoop tie loosening, and longitudinal bar buckling. Specimens F3 and F5 were able to achieve ductilities of  $\mu_{\Delta} = 7$  and 6 respectively. The maximum load predictions for these retrofit columns was very accurate but the calculated values of displacement under maximum load were 50% lower than those observed during testing.

The seismic retrofit of bridge columns in the Reno/Sparks area of Nevada is discussed in Darwish, Saiidi, and Sanders (1995a, 1995b, 1996). In this experimental program, four 0.4 scale columns were constructed and tested at the University of Nevada, Reno. Two of the columns were tested in the "as-built" condition, while two columns were retrofit with steel jackets. The prototype columns all have very short lap splices and dowel bars at the bottom of the column. They are highly rectangular in shape, 610 mm x 2,135 mm (2 ft x 7 ft), are tapered in width, and are inadequately confined. The narrowest part of the column is at the base and tapers linearly towards the top. The columns are typical of very thin tapered columns in the area.

For purposes of conducting the experimental tests, the "as-built" specimens tested include one column with a fixed base and one which incorporates a one-way hinge at the base. The one-way hinge is intended to preclude moment transfer at the column base in the weak direction and is common in bridges on I-80 in the Reno/Sparks area. The fixed base was intended to transfer moment in both directions. Similar specimens were constructed for the retrofit tests. The columns were tested under a constant axial load intended to simulate the bridge dead load and in combined shear and flexure in the strong direction. The specimens were intended to represent the prototype column geometry from the top of the footing to the inflection point.

The one-way hinge test specimen is as described below. Total height from the load point to the top of footing was 1,475 mm (58 in.). The one-way hinge is formed by casting a 635 mm x 150 mm x 32 mm

(25 in. x 6 in. x 1.25 in.) keyway in the footing and lining the keyway with expansion material. Dowel reinforcing consists of nine, 16 mm (#5) reinforcing bars of a specified 276 MPa (40 ksi) yield. The bars were straight and had development lengths of 140 mm (5.5 in.) above the hinge and 150 mm (6 in.) below the hinge, which corresponds to 8.8 and 9.6  $d_b$ , respectively. The column section contains sixteen bars of the size described above. The bars are laterally tied with 9.5 mm (#3) bars spaced at 127 mm (5 in.) on center. The combination of bars described above almost exactly duplicates the reinforcing percentages in the prototype column.

The fixed-base specimen has a height to the load point of 1,220 mm (48 in.). In order to simulate the dowels in the prototype column, sixteen 19 mm (#6) reinforcing bars of 276 MPa (40 ksi) yield were used. The column longitudinal reinforcing consisted of sixteen 19 mm (#6) bars and the tie reinforcing was the same as previously described for the hinged specimen.

The retrofit specimens were identical to the "as-built" specimens except for column height and footing details. The footing details were changed to prevent premature footing failure and the column height reduced in order to simulate the footing overlay that is expected to be constructed. The height of the column from load point to the top of footing in the hinge specimen is 1,420 mm (56 in.). The steel jacket consists of two parts; an oblong jacket that has the same tapered shape as the column and a rectangular jacket to confine the pedestal. The jacket provides a volumetric confinement ratio of 0.087 in the column strong direction. A 13 mm (0.5 in.) gap is provided between the column and jacket for grouting. In order to ensure adequate moment transfer, the jacket is bolted to the footing with a 38 mm (1.5 in.) thick A36 base plate placed only in the direction of moment transfer in the one-way hinge specimen. The base plate was placed on a leveling grout layer and bolted to the footing with single rows of three ASTM A307 bolts, 19 mm (0.75 in.) in diameter, anchored 355 mm (14 in.) into the footing. The plate thickness was chosen so as to preclude yielding in the hinged specimen. Additionally, 19 mm (0.75 in.) thick A36 stiffeners were used to limit the size of the weld between the jacket and base plate.

For the fixed base specimen, the base plate was made thinner and its yielding during testing was used as a means of dissipating energy. The column height was the same as for the "as-built" specimen except for a 50 mm (2 in.) reduction in height for a footing overlay as previously mentioned. The dowels connecting the column to the base were eliminated except for six dowels whose purpose was to ensure proper connection of the column and footing during handling. The jacket provided the same degree of confinement as the one installed on the hinged specimen. The base plate for this specimen was anchored by two rows of three bolts on each side of the column's strong direction with the first (outer) row having four equally spaced bolts and the second (inner) row having three equally spaced bolts. The jacket also had 16 mm (5/8 in.) A36 stiffeners at the base to reduce the size of the weld between the jacket and base plate.

Test results on the "as-built" hinged specimen included sixteen cycles of load reversal at seven different amplitudes. Minor cracks were observed above the pedestal at a load of 91 kN (20.5 kips) corresponding to a drift ratio of 0.13%. One vertical splitting crack was also noticed on the narrow face, throat side, of the specimen. Significant strength degradation of 43% and 21% in the positive and negative direction was noted at a drift level of 1%, approximately  $\mu_\Delta = 1.5$ . The first cycle to  $\mu_\Delta = 1.5$  represented the maximum lateral load resistance of approximately 133 kN (30 kips). In the test, only two of the nine dowels were able to reach yield, and the two that did, were not able to hold for one complete cycle. Failure was due to extensive loss of concrete at the base.

The retrofit for the hinged column performed in a much more desirable fashion with stable behavior until  $\mu_{\Delta} = 4.5$  after which the anchor bolts fractured. The steel base plate did not yield and the welded connections remained intact. Minor cracking of the tapered side of the column was noted at drift levels in excess of 4% and higher. A displacement ductility of 1 was achieved with a lateral load of 257 kN (57.7 kips). Significant pinching of the hysteresis loops was noted because of the elongation of the anchor bolts. The anchor bolts were not effective in unloading and reloading cycles until the gap that existed due to bolt elongation was closed due to base rotation. Ultimate strength degradation was extrapolated to be 48% with relatively small energy absorption. The displacement ductility of  $\mu_{\Delta} = 4.5$  represents a significant improvement over the "as-built" ductility of  $\mu_{\Delta} = 1.5$ .

Results for the "as-built" fixed-base specimen were similarly poor with significant stiffness and strength degradation during the test. Shear and flexural cracks were observed. Eventual bond failure and lap splice slippage led to a 255 mm (10 in.) long spall on the straight side of the column. Concrete spalling was not observed on the tapered side of the column. The lap splice bars on the tapered side were not as efficient as on the straight side, leading to smaller force transfer and subsequently less damage. Strength degradation of nearly 50% was noted at a drift ratio of approximately 3%. The maximum lateral load capacity of approximately 334 kN (75 kips) was noted on the first pull cycle to a drift ratio of approximately 2.5%. Significant pinching of the response was noted in examination of the hysteresis loops.

In contrast to the poor performance of the "as-built" fixed-base specimen, the retrofit specimen provided excellent response. The redesign of the base plate area assured that the base plate would yield before the anchor bolts so that a stable hysteretic dissipation of energy could occur. The outer row of anchor bolts on each side of the column remained totally elastic, while the inner row demonstrated minor strain hardening but did not fracture. Weld failure was noted between the stiffeners and base plate and allowed for base plate deformation to extend to the area under the stiffeners. The load and displacement corresponding to  $\mu_{\Delta} = 1.0$  were 338 kN (76 kips) and 11.7 mm (0.46 in.). Ultimate load and displacement of the column were 474 kN (106.56 kips) at a displacement of 97 mm (3.8 in.) corresponding to a displacement ductility of  $\mu_{\Delta} = 8.0$ . No real degradation of response was noted on subsequent cycles to the same ductility levels. The steel jacket was not observed to have yielded because of the removal of the dowels from this specimen. Removal of the dowels precluded significant expansion of the column because of tensile splitting. Removing the jacket at the end of the test, showed that the column had become separated from the footing due to fracturing of the small bars used for anchorage of the column to the footing during construction and movement of the specimen.

Results for this specimen indicate that the "as-built" details are inadequate to provide stable performance under reversed cyclic and constant axial loading because of significant slippage in the lap splice region. The columns were seen to behave differently in push and pull cycles due to the difficulty of attaining adequate lap splices of the inclined vertical bars on the tapered side of the column. The steel jacket retrofits proved to be an effective retrofit for flexural as well as shear capacity and provided sufficient enhancements in ductility. Base plate yield as opposed to bolt yield was shown to be the desired retrofit option as it allows for a stable dissipation of hysteretic energy. Primary bolt yield led to bolt fracture, significant pinching of the load-displacement response and poor energy dissipation.

The 1/6-scale test results of an "as-built" and retrofit two-column bent are presented in Macrae, Priestley, and Seible (1994). The test specimen was a model of the bents on the Route 5/405 bridge which

collapsed in the 1971 San Fernando Earthquake. This test is one of only a few that incorporates dynamic input into the test through use of a shake table.

The "as-built" bent column was detailed to have a similar strength and spacing as the prototype column considering the scale effects. The footing only had a bottom mat of steel. The footing was not tied to the test table so that footing uplift could occur. Lateral restraints were placed on the footing so as to allow for shear force transfer. The cap beam and joint between the cap and column were designed and detailed so as to resist the maximum force generated from the development of plastic hinges at the top and bottom of the columns. The 1/6 scale model comprises columns standing 1,105 mm (43.5 in.) tall and octagonal in shape. The overall plan dimensions of the column were 255 mm x 205 mm (10 in. x 8 in.) with 50 mm x 38 mm (2 in. x 1.5 in.) chamfers at each corner to provide the octagonal shape. The longitudinal reinforcing consists of a total of twenty-eight, 9.5 mm (#3) reinforcing bars and the transverse reinforcing of 12 gage wire (2.7 mm) diameter wire spaced vertically at 50 mm (2 in.) centers.

The retrofit bent was identical in construction to the "as-built" bent except that a 1.6 mm (1/16 in.) oval steel jacket was installed on each column in order to prevent shear failure and provide confinement. The gap was filled with grout. A 13 mm (1/2 in.) gap was left at the top and bottom of the jacket so as to prevent bearing of the jacket against the footing or cap beam during column rotation. The footing was strengthened with a mat of top steel and shear reinforcing and was made 25% thicker than in the "as-built" specimen.

The shake table test required the addition of dynamic mass to the specimen. A mass block of 9,070 kg (20 kips) was added to the column and cap assembly to provide inertial mass and axial load. An additional 249 kN (56 kips) was added via tiedown rods to provide the required axial load of 169 kN (38 kips) per column, and also for stability of the mass block. The shape of the mass block was chosen so that the center of mass was located at the vertical center of the cap beam. The total participatory mass was 9,750 kg (21.5 kips). Column steel was strain gaged and a  $\pm 5g$  accelerometer was placed on the beam and  $\pm 2g$  and  $\pm 5g$  accelerometers were mounted on the shake table. A pulse input was applied to the specimen so that the natural frequency could be obtained. Subsequent testing consisted of an input record of the north-south component of the 1940 El Centro Earthquake. A time scale,  $T_s$ , of 0.216 was used. Very small acceleration scale factors were initially used but were made increasingly larger until failure occurred. Each time the record was applied, the sign of the input was changed from the previous run.

The "as-built" strength was calculated from a computer model which could accurately model the lift-off from the shake table and was based on moment-curvature analysis with an extreme fiber compression strain of 0.005. The ideal lateral strength was computed to be 249 kN (56 kips). Considering axial load effects on bent strength, the calculated strength of the bent was 173 kN (39 kips), which relates to a failure acceleration of  $(39 \text{ kips}/21.5 \text{ kips}) = 1.81g$  in the model. The acceleration scale was the ratio of the dimensional scale divided by the square of the time scale,  $0.1667/(0.216)^2$ , and equals 3.57. This scale indicates that the failure acceleration of the prototype is  $1.81g/3.57$ , or, 0.507 g.

The predicted capacity of the retrofit bent of 350 kN (78.6 kips) was based on assumed hinging at the top and bottom of the bent. The estimated lateral strength of 449 kN (101 kips) was attained through moment-curvature analysis.

Observed performance of the "as-built" bent indicated that on run #29, at a table acceleration of 0.98 g corresponding to a prototype acceleration of 0.27 g, lift-off of the footings was apparent. This was accompanied by extensive shear cracking at the top of the columns. During run #31, with a table acceleration of 1.06 g, prototype of 0.30 g, the peak inertial force was obtained. The south column spalled at the top and large shear cracks occurred. Both columns collapsed in the following run. The main longitudinal reinforcing buckled similar to the original bridge which failed in 1971.

The peak inertia forces were +165 kN (+37 kips) and -135 kN (-30.3 kips), and peak displacements were +19.6 mm (+0.77 in.) and -28.7 mm (-1.13 in.). The bent strength was 162 kN (36.5 kips), 94% of the predicted value.

The retrofit bent was nominally elastic until run #20 which had an unexpectedly large acceleration due to operator error. The peak table acceleration reached  $\pm 6$  g several times during the cycling. It was believed that the actual input may have easily reached 7.14 g, corresponding to a base acceleration of 2 g in the prototype. Significant yielding occurred at this time and spalling of cap beam concrete adjacent to the columns as well as column concrete in the gap between the jacket and cap beam was noticed. It was concluded that the bent reached its damage limit state and subsequent low intensity shaking indicated that the stiffness and strength were much less than that observed during run #20. Most of the total displacement contribution occurred at the top of the column between the beam longitudinal bars and the steel jacket. The region acted as a quasi isolation pad. The column longitudinal bars were bent in double curvature and eventually fractured on retesting to the response displacement obtained during run #20.

The peak inertia forces were +450 kN (+101 kips) and -401 kN (-90 kips), and peak displacements were -54.6 mm (-2.15 in.) and +69.6 mm (+2.75 in.). The peak strength of the retrofit was 2.73 times greater and the peak displacement 4.7 times greater than the "as-built" two column bent.

The test results reported herein demonstrate through actual dynamic input, the ability of steel jacket retrofits to change the failure mode of a deficient bent from shear to flexure. The results also illustrate the dramatic ability of the retrofit in increasing lateral load capacity and ultimate displacement.

A study which compared the calculated and observed performance of bridge pier walls primarily loaded in the weak direction, and also developed steel jacket retrofit schemes, is detailed in Haroun, Pardoen, and Shepherd (1994). Haroun, Pardoen, and Shepherd state that like reinforced concrete columns, pier walls also suffer from many "as-built" deficiencies. They are typically reinforced with lateral steel reinforcing less than the ratio of 0.25% required to prevent premature diagonal tension cracking. The lap length of the footing dowels is a Class A splice of  $16 d_b$  rather than a Class C splice of  $28 d_b$ . This insufficient lap may lead to brittle bond failure of the reinforcing under cyclic lateral loading. In addition, the inadequate lateral steel may allow the longitudinal steel to buckle due to lack of confinement under combined loading.

The experimental testing was carried out in two phases. The first phase involved testing half-scale model piers to evaluate the strength, ductility, and failure mechanisms. Eight different specimens with two different lap splices were constructed. Six of these specimens were tested in the weak direction. The specimens were loaded vertically to simulate the dead load of the supported structure as well as laterally with alternating push-pull loading. The second phase included five specimens with four of the specimens employing different retrofit schemes.

The Phase I piers measured 3,225 mm (127 in.) tall, 255 mm (10 in.) thick, and were 965 mm (38 in.) wide. The Phase II walls were of similar dimensions except that they were 2,490 mm (98 in.) wide. Vertical reinforcing consisted of 276 MPa (40 ksi) bars at a ratio of 0.56% with transverse reinforcing of the same material at 0.15%. Half of the specimens had Class A splices, the others, Class C splices.

The retrofit piers in the second phase had four different retrofit types. All of the different retrofit types employed flat steel plates bolted through the thickness of the wall to each other. Type R1 was encased in a 5 mm (3/16 in.) thick, 1,525 mm (5 ft) high plate with a gap between the wall and plates of 19 mm (3/4 in.). The gap was filled with grout. Bolts measuring 16 mm (5/8 in.) in diameter were passed through the column and spaced vertically and horizontally at 610 mm (24 in.) on center. Retrofit R2 was similar to R1 except that the bottom row bolt spacing was reduced by 50% and 13 mm (1/2 in.) diameter washers were placed on the bolts. R3 consisted of a small 205 mm (8 in.) high and 13 mm (1/2 in.) thick plate at the base of the column with bolts and washers as described previously placed horizontally at 185 mm (7.25 in.) on center. The height of the plate is approximately that of the length of lap splice "A". R4 is similar to R3 except that the height of the plate is doubled to 405 mm (16 in.). A single row of bolts was employed in both R3 and R4 and the bolts were spaced so as to clear the existing longitudinal bars.

Loading consists of a vertical load of approximately 5% of the axial strength of the specimen as well as increasing lateral loads and displacements. General observations on the test results show that the first crack was a horizontal crack which usually occurred near the end of the splice. These cracks became more numerous with the largest cracks being observed at the base. Substantial spalling occurred with the Class A splice walls late in the test cycle while the Class C walls required higher ductility levels in order to produce the same loss of cover. Several longitudinal bars buckled in the Class C walls while no buckling was observed in the Class A walls. This is indicative of a lack of force transfer in the Class A walls due to loss of confinement. In the retrofit walls, buckling was noticed at the base of specimens R1 and R2 after removing the jackets. In R3 and R4, large horizontal cracks occurred near the end of the splice length.

Specimens with the Class C splice had improved ductility and strength over Class A construction. In addition, the Class A columns had a dramatic drop in stiffness during testing due to lack of confinement. Phase I specimens exhibited almost identical initial stiffness while retrofit column R2 demonstrated the highest stiffness of the retrofit specimens. Phase I walls with no retrofit demonstrated a minimum  $\mu_A = 6$  with no loss in lateral load capacity. Ductility is most significantly enhanced in the Class A column by providing a jacket height equal to twice the length of the lap splice. Ductility enhancement of Class C walls is substantially improved through the use of jackets equal in height to the lap splice. Specimen W12, a Class C splice wall retrofit per the R3 method, had an ultimate  $\mu_A = 10$  with no discernable drop in lateral load-resisting capacity.

## **2.2.2 Steel Jacket Retrofit of Shear Deficient Bridge Columns**

Similar to the flexural column research summary, the results of shear deficient column tests will be divided into circular and rectangular columns.

### **2.2.2.1 Circular Shear Columns**

The "as-built" and retrofit behavior of circular columns subject to shear failure is documented in Verma, Priestley, and Seible (1993). The results of this study are also presented in a number of summary

documents: (Priestley and Seible, 1991), (Priestley, Seible, and Chai, 1992a, 1992b), (Priestley, Seible, Xiao, and Verma, 1991, 1994a, 1994b), (University of California, 1991), and (Verma, Priestley, and Seible, 1994). In addition, guidelines developed in Verma, Priestley, and Seible (1993) can be found in the seismic retrofit manual (Federal Highway Administration, 1995).

In this research, a dimensional scale of 0.40 was adopted. This resulted in test columns having a diameter of 610 mm (24 in.) and a height of either 2,440 mm (8 ft) or 1,830 mm (6 ft) from the top of the footing to the bottom of the load stub. These different heights lead to shear span aspect ratios,  $M/VD$ , of 2 and 1.5 respectively. The columns were reinforced with twenty-six continuous 19 mm (#6) longitudinal reinforcing bars for a longitudinal steel ratio of 2.53%. Transverse reinforcing consisted of 6 mm (#2) reinforcing bars spaced vertically at 125 mm (5 in.). The transverse bars are lapped in the cover concrete with a lap splice of  $48 d_b$ . The transverse confining ratio is 0.174%. The axial load was either 1,779 kN (400 kips) or 592 kN (133 kips). This constitutes an axial load ratio of  $0.177f'_cA_g$  and  $0.059f'_cA_g$ , respectively. The longitudinal steel used had a specified yield of either 276 MPa (40 ksi) or 414 MPa (60 ksi) depending on the test specimen. The transverse steel had a specified yield of 276 MPa (40 ksi) in all specimens. A concrete compressive strength of 34.5 MPa (5 ksi) was selected to represent the in-situ concrete strength of older columns. All columns were tested under uniaxial load and cyclic horizontal load until failure. The circular steel jackets were either 5 mm (3/16 in.) or 3 mm (1/8 in.) thick. The 5 mm (3/16 in.) steel jackets were designed to be A36 steel but actually tested to a yield strength of 347 MPa (50.4 ksi). These jackets were used early in the test program and were deemed to be excessive strengthening. Subsequent jackets were sized to be 3 mm (1/8 in.) thick and were made of ASTM A569 steel with a yield point of 286 MPa (41.5 ksi). Table 2-3 is presented to document the various aspects of the test program.

**TABLE 2-3 Circular Shear Columns (Verma, Priestley, and Seible, 1993)**

Test Column	Longitudinal Steel Grade	Axial Load	Aspect Ratio, $M/VD$	Comments
1	276 MPa (40 ksi)	592 kN (133 kips)	2	"as-built"
2				5 mm (3/16 in.) jacket
3		1,779 kN (400 kips)		"as-built"
4				5 mm (3/16 in.) jacket
5	414 MPa (60 ksi)	592 kN (133 kips)	2	"as-built"
6				3 mm (1/8 in.) jacket
7			1.5	"as-built"
8				3 mm (1/8 in.) jacket

Measured material properties for the test columns yielded an average compressive strength for the column concrete of 34 MPa (4.94 ksi), an average longitudinal steel yield strength of 324 MPa (47 ksi) for the Grade 40 reinforcing bars and 469 MPa (68 ksi) for the Grade 60 reinforcing bars. Except for

columns 1 and 2 where the lateral reinforcing had a yield strength of 359 MPa (52 ksi), all other columns had a transverse reinforcing yield strength of 324 MPa (47 ksi).

The test columns were extensively instrumented with each column containing over 200 strain gages. Displacement transducers were mounted to measure flexural displacements and shear displacements. Estimation of the flexural deformation is made by multiplying the measured curvature at five locations along the vertical axis by the distance from the top of the columns to these theoretical concentrated curvature locations. The summation of the product of curvature and distance gives a rough estimate of the flexural contribution to the overall load stub displacement. A procedure is used to predict the shear displacements that measures relative diagonal and horizontal displacements in the column. Ideally, the extrapolated shear and flexural components would add up to the measured displacement, but unknowns such as bar slip and footing rotation will introduce experimental errors into the process.

The loading procedure consisted of a number of load control cycles leading up to 50% of the ideal lateral load,  $V_{if}$ , the lateral load which corresponds to the theoretical flexural capacity of the specimen using a maximum concrete strain  $\epsilon_{cu}$  of 0.005. Following five cycles at this level, the load was increased until the onset of first yield at which point, one cycle was applied. The test was changed to displacement control from this point and consisted of three cycles at the following ductility levels,  $\mu_{\Delta} = 1, 1.5, 2, 3, 4, 5, 6, 8, 10$ , or until the specimen failed.

For column 1, the initial response at low load levels was a stable flexural response. At a lateral load of approximately 67 kN (15 kips), the first flexural cracks developed at the top and bottom of the column. These cracks grew and became more numerous during the increasingly more demanding load cycles leading to first longitudinal yield. At the lateral load corresponding to first yield, 378 kN (85 kips), the flexure shear cracks became more inclined to the vertical with the inclination measuring 68 degrees to the vertical. At  $\mu_{\Delta} = 1$ , very pronounced flexure-shear cracks were observed as well as independent web shear cracks in the central region of the column. At  $\mu_{\Delta} = 1.5$ , the ideal capacity of 529 kN (119 kips) was obtained. Clear signs of pending failure were noticeable at this time. However, very little degradation in stiffness or strength were apparent. The column lost its entire load carrying capacity while being pushed for the first time past  $\mu_{\Delta} = 2.5$  due to the opening up of a wide diagonal shear crack starting at the column top and extending to mid-height.

Examination of the displacement components for this column after testing illustrated that most of the shear displacements were concentrated at the top and bottom of the column and that the vast majority of displacements were due to the flexural components.

Retrofit column 2, like all of the retrofit specimens in this test program, was shielded from examination by the presence of the full-height steel jacket. This column demonstrated an initial stiffness some 30% greater than the "as-built" column. Column 2 exceeded its ideal lateral capacity,  $V_{if}$ , at  $\mu_{\Delta} = 2$  and was able to demonstrate increasing lateral strength through subsequent ductility levels up to  $\mu_{\Delta} = 10$ . Testing was discontinued at this point due to limitations in the capacity of the test set-up. Very little degradation of response is noted on subsequent cycles to the same ductility level and no pinching of the hysteresis loops is evident. The column demonstrated very ductile flexural response and was able to dissipate 149 times more hysteretic energy than the comparable "as-built" specimen 1. Shear deformation contributed only 10% to 20% of the total displacement in this column with the higher contributions occurring at larger ductility levels.

"As-built" column 3 was tested at a higher axial load level than either column 1 or 2. This column behaved similar to "as-built" column 1 at low load levels but had a higher yield and ideal strength due to the effect of the higher lateral load. These increases were from 378 kN (85 kips) to 525 kN (118 kips) for yield capacity and 529 kN (119 kips) to 672 kN (151 kips) for ideal capacity.

At a displacement ductility level of  $\mu_{\Delta} = 1$ , a large number of flexural cracks had already developed during the initial load stages and began to grow steeply inclined. At a ductility level,  $\mu_{\Delta} = 1.5$ , the ideal capacity of the column was exceeded and significant independent web shear cracks extended from the central region of the column to the ends. At  $\mu_{\Delta} = 2$ , the maximum lateral load on the column, 738 kN (166 kips), was attained, but no sign of degradation was apparent. During the first cycle to  $\mu_{\Delta} = 3$ , a minor drop was noticed and on subsequent cycles to  $\mu_{\Delta} = 3$ , a drop of over 40% in lateral capacity was noted. Failure was a limited flexure, brittle shear failure mode but was less sudden than in column 1. The initial shear failure seemed to be a shear-bond failure. The flexural component of deformation is nearly 80% at first yield but drops to approximately 58% by the time cycling to  $\mu_{\Delta} = 2$  is complete. This high degree of shear displacement is attributed to the widening and extension of existing cracks and the formation of new cracks at this displacement level.

Column 4 is similar in all respects to column 3 but is retrofit with a circular steel jacket. Column 4 was able to maintain a ductile flexural response up to  $\mu_{\Delta} = 10$ , a drift ratio of 4.37%, without a significant reduction in capacity or stiffness. The initial stiffness was 28% higher than the "as-built" specimen 3. The ideal flexural capacity of 734 kN (165 kips) was exceeded at  $\mu_{\Delta} = 2$  and continued to be exceeded through all subsequent cycling. After three cycles to  $\mu_{\Delta} = 10$ , the only signs of distress were shallow cracks in the load stub and footing as well as spalling of the concrete in the gap between the end of the jacket and the top and bottom of the column. The dominant mode of deformation for this column is a flexural mode with maximum shear components of 25% being observed at the maximum ductility level of  $\mu_{\Delta} = 10$ . Column 4 was able to dissipate 121 more times the hysteretic energy as its counterpart column 3.

Column 5 was the first of a second set of tests with higher yield point steels that would tend to exacerbate the shear deficiencies in the columns by increasing the ratio of flexural strength to shear strength. This column was barely able to reach its first yield lateral load capacity of 534 kN (120 kips) during which time, extensive cracking had already occurred. At a ductility of  $\mu_{\Delta} = 1$ , the maximum lateral load of 614 kN (138 kips) was attained immediately followed by the formation of very wide diagonal shear cracks and significant spalling in the upper region of the column. Following formation of these cracks, an immediate drop in capacity of 42% was observed with no corresponding increase in load stub displacement. A second cycle to  $\mu_{\Delta} = 1$  resulted in a further 25% drop in capacity and a third cycle seemed to stabilize the response following another drop of 14%. Several hoops in the upper portion of the column fractured on the way to  $\mu_{\Delta} = 2$  and cracking was so extensive that it was possible to see completely through the column by looking through some of the wide diagonal shear cracks. The appearance of this column following testing was very similar to columns observed following the San Fernando Earthquake of 1971, with extensive shear cracking, twisted rebar, fractured hoops, dilated core, and extensive destruction of the column in general. The shear deformations were seen to vary from 27% prior to yield to as much as 70% at  $\mu_{\Delta} = 1$  after the occurrence of brittle shear failure.

Retrofit column 6, was constructed with a thinner jacket than previously used in column 2 and 4 as it was thought these columns were "over-strengthened". The response of this column was extremely stable to  $\mu_{\Delta} = 10$ , similar to columns 2 and 4, with little or no degradation in strength and stiffness. The column

exceeded its theoretical ideal flexural capacity at  $\mu_{\Delta} = 2$  and maintained at least this resistance throughout the entire test. At  $\mu_{\Delta} = 8$ , the jacket was seen to bulge and to lose its ability to confine the very top and bottom of the plastic hinge regions at the top and bottom of the column. The column was however still able to maintain stable load carrying capacity to  $\mu_{\Delta} = 10$  but degradation of the response was noted on subsequent cycles to 8 and 10. Flexural deformations dominated the total deflection of the column, even at high ductility levels.

"As-built" column 7 demonstrated extensive cracking at a load level of  $0.5V_{if}$ , 467 kN (105 kips). At the lateral load corresponding to first yield, 734 kN (165 kips), vertical bond splitting cracks were noticed as was shear cracking in the central region of the column. The column was able to reach a maximum lateral force of 792 kN (178 kips) at  $\mu_{\Delta} = 1$  at which point steep diagonal cracks began to appear in the central region of the column. Previously developed flexure-shear cracks in the central region propagated toward the column ends. A 20% drop in capacity was noted at the second cycle to  $\mu_{\Delta} = 2$ , the onset of shear failure. A total drop in capacity of 40% was noted over the three cycles to  $\mu_{\Delta} = 2$ . Several wide and short web shear cracks in the central region of the column were seen to cause loss of a large patch of cover concrete. At ductility levels  $\mu_{\Delta} = 2$  and 3, the peak load resisted on the first cycle was higher than the peak load recorded at the third cycle to the previous ductility level. A total drop in capacity of 47% was seen from the first to third cycles at  $\mu_{\Delta} = 3$  with the lateral force capacity after the third cycle being less than 267 kN (60 kips). Several wide and short web shear cracks in the central region of the column were seen to cause loss of a large patch of cover concrete. The shear deformation component ranged from 33% before first yield to 79% following shear failure at  $\mu_{\Delta} = 2$ .

Retrofit column 8 performed extremely well, exceeding its ideal flexural capacity of 1,005 kN (226 kips) at  $\mu_{\Delta} = 2$  and demonstrating ever increasing lateral load resistance until the first push cycle to  $\mu_{\Delta} = 8$  at which point low cycle fatigue fracture of the longitudinal steel began. The fracture of the first two bars resulted in a drop in capacity of 10%. On the first pull cycle, another bar fractured. During the next push cycle, two more bars fractured resulting in a further degradation of resistance of 20%. The test was discontinued after three cycles to  $\mu_{\Delta} = 8$ . The portion of total displacement attributable to flexure ranged from 75% at  $\mu_{\Delta} = 1$  to 70% at  $\mu_{\Delta} = 8$ . The retrofit column was able to dissipate 172 times the amount of hysteretic energy as the counterpart "as-built" column 7.

Attention now shifts to a series of theoretical models presented in Verma, Priestley, and Seible (1993) for predicting the various contributions to shear strength as well as comparison of the numerous analytical approaches to observed specimen behavior. In addition, theoretical bilinear load-displacement envelopes were constructed and compared to the experimental results. This comparison shows that the theoretical results were significantly over-predicting the response of the "as-built" column because of the brittle nature of their performance. The theoretical response of the retrofit columns was, however, in excellent agreement with the measured values.

The research presented in Verma, Priestley, and Seible (1993) demonstrates the ability of full-height steel jackets to modify the response of shear-dominated columns from brittle shear failure to ductile flexural failure. Very significant gains in maximum ductility and load resistance were noted as well as very substantial gains in hysteretic energy dissipation capabilities. The use of very thin jackets was even demonstrated to provide very stable behavior up to such high ductility levels such as  $\mu_{\Delta} = 8$  or 10.

Jaradat, McLean, and Marsh (1996) emphasize the testing of a variety of seismically deficient as-built bridge columns but also include test results from steel-jacketed specimens. The document presents the

results from a work in progress and as a consequence provides only a small amount of information. The results of 1/3.6 scale model tests on eight reinforced concrete columns are presented. The columns incorporate deficiencies common in pre-1971 concrete bridge columns, namely, short lap splices and inadequate confinement. The columns were rotationally fixed at both ends so that the shear behavior of the degrading plastic hinge regions could be assessed during testing. Of the eight specimens tested, six were in the "as-built" condition, one column was retrofit at the base with a typical Caltrans Type P retrofit, and the final column was retrofit using a Caltrans Type F retrofit. The columns were tested under constant axial load and increasing inelastic displacement levels. The specimen variables consisted of column height, longitudinal reinforcing ratio, lap splice length, and base retrofit method.

The performance of the specimens was evaluated on the basis of flexural and shear capacity, displacement ductility, strength degradation and hysteretic energy absorption. The results of the test were compared to the predicted results from procedures established by Priestley and Seible at the University of California at San Diego, FHWA recommendations, and newly proposed models from the University of California at Berkeley. The results will be used to characterize the behavior of concrete bridge columns under seismic loading. The ability of the yielded hinge region to continue transferring shear and axial forces will be evaluated and the effect of retrofits will be considered.

Preliminary results indicate that flexural failures occurred in five of the eight specimens. The poor confinement and insufficient lap splice length led to rapid strength degradation. The column tops, which did not contain a lap splice region, did not exhibit similar degradation until higher ductility levels with eventual degradation attributable to longitudinal bar buckling.

Shear failures were noted in three of the eight specimens. Two types of shear failures were observed: shear failure with little or no flexural yielding in the middle of the columns and shear failure after extensive yielding occurring at the column ends. The second failure type is due to primary flexural degradation in the hinge region and occurred at lower shear levels than the first failure type.

Jaradat, McLean, and Marsh also showed that the Caltrans Type F retrofit was effective in maintaining the full flexural capacity of the column base in the presence of large ductility demands. The Type P alternative, however, did not provide as significant an enhancement in specimen strength, and the results were considered to be intermediate to the "as-built" and Type F retrofits. Work continues on this project with evaluation of the test results and comparison to current and proposed assessment models.

Akimoto, Hakajima, and Kogure (1990) describe the retrofit of single column piers on Route 6 of the Metropolitan Expressway in Tokyo. These columns were judged in need of retrofit following the third stage of a three stage seismic safety inspection, which showed that these columns would likely suffer shear failures following shear strength degradation from flexural cracks near the mid-height longitudinal steel termination point. In all, 36 of 156 columns were judged to be deficient. Of these 36 columns, 16 were solid round piers, 9 were circular hollow piers, and 11 were rectangular solid piers.

Retrofit tests were carried out by the Metropolitan Expressway Public Corporation on four specimens with hollow circular cross sections: (a) "as-built" specimen, (b) specimen with a steel jacket height of 1.0 D and epoxy grouting, (c) retrofit specimen with jacket height of 1.5 D, and (d) steel jacket of height 1.5 D without the epoxy grouting, where D is the column diameter. In all cases where jackets were used, the jacket extended 0.5 D below the termination of longitudinal steel, and the balance of the jacket height was placed above the termination point.

Test results indicate that the most effective retrofit was the 1.5 D jacket with epoxy grouting. This retrofit type was able to change the failure location from the termination point to flexural failure at the base of the column. The steel jacket of 1.5 D without the grout suffered from steel jacket buckling in the termination region. The successful grouted steel jacket was able to increase the columns lateral load capacity by 30%. Similar results were obtained by the Hanshin Expressway Public Corporation on tests conducted with rectangular specimens.

The successful field retrofit of the deficient columns is also reported. The steel jacket was assumed to act compositely with the column in resisting bending and lateral loads, and its thickness was sized accordingly to be a minimum of 4.5 mm (0.18 in.). An actual thickness of 6 mm (0.24 in.) is used in the field for enhanced handling stiffness and resistance to deformation during grouting. Additionally, because the steel plate is several meters high and relatively thin, the steel plate is anchored to the concrete column with anchor bolts to prevent excessive deformation and overstress during the pressure-grouting operations. These anchor bolts were designed to resist the pull-out forces due to pressure grouting and are spaced at 1 m (3.28 ft) intervals in circular jackets and 0.5 m (1.64 ft) in rectangular jackets. The smaller pitch in the rectangular plate anchors is due to the out-of-plane bending mode of the rectangular plates as opposed to the membrane stress induced in the circular plate. The jackets were actually installed over the full height of the columns for aesthetics and to alleviate public concerns about the safety of the structural, although previous experimentation showed it is only necessary to jacket the 1.5 D high region surrounding the termination point.

#### **2.2.2.2 Rectangular Shear Columns**

The steel jacket retrofit of rectangular bridge columns prone to premature failure by shear is detailed in Xiao, Priestley, and Seible (1993). Results from this research have also been summarized and excerpted in a number of other references, including: (Priestley and Seible, 1991, 1992), (Priestley, Seible, and Chai, 1992a, 1992b), (Priestley, Seible, Chai, and Sun, 1991), (Priestley, Verma, and Xiao, 1993), (Priestley, Seible, Xiao, and Verma, 1994a, 1994b) and (University of California, 1991). The results of this study have also been incorporated into the seismic retrofit recommendations presented in Federal Highway Administration (1995).

In this experimental research project, six columns were constructed as 0.35 scale models of column construction common prior to 1971. All test columns had cross-sectional dimensions of 610 mm x 405 mm (24 in. x 16 in.). The test columns were tested in reverse curvature bending, simulating a fixed-fixed condition at the top and bottom of the columns. Four of the columns had a clear height of 2,440 mm (8 ft), and two of the columns had a shorter height of 1,830 mm (6 ft). These two scenarios resulted in M/VD ratio of 2 and 1.5 respectively for testing about the strong axis. A matrix of test parameters is presented in table 2-4 for the six column specimens. The specimens with higher longitudinal steel strengths and the columns with the smaller shear span ratios are more likely to suffer shear failures before the flexural capacity of the columns can be realized.

**TABLE 2-4 Rectangular Shear Deficient Columns (Xiao, Priestley, and Seible, 1993)**

Test Specimen	Longitudinal Steel	Axial Load	M/(VD)	Retrofit
R-1	2.5%, 276 MPa (40 ksi)	507 kN (114 kips)	2	"as-built"
R-2				5 mm (3/16 in.) steel jacket
R-3				"as-built"
R-4				5 mm (3/16 in.) steel jacket
R-5	2.5%, 414 MPa (60 ksi)		1.5	"as-built"
R-6				3 mm (1/8 in.) steel jacket

The design concrete strength of all specimens is 34.5 MPa (5 ksi), although actual concrete strengths varied from 32.8 MPa (4.75 ksi) to 38.3 MPa (5.56 ksi). The longitudinal reinforcing used in specimens R-1 and R-2 had a measured yield of 317 MPa (46 ksi) and an ultimate tensile strength of 453 MPa (65.7 ksi). The longitudinal steel used in specimens R-3 through R-6 had a yield of 470 MPa (68.1 ksi) and an ultimate strength of 747 MPa (108.3 ksi). The hoop yield was 361 MPa (52.3 ksi) in specimens R-1 and R-2 and 324 MPa (47.0 ksi) in R-3 through R-6. The jacket used on specimen R-2 had a yield of 355 MPa (51.5 ksi) and that used on R-4 and R-6 had a yield of 292 MPa (42.3 ksi).

The elliptical jacket mentioned in table 2-4 is sized as follows. In order to fit around the rectangular column and to be of a minimum length, the elliptical jacket measured 810 mm (32 in.) along the major axis and 610 mm (24 in.) along the minor axis. The jacket was also made shorter than the column by a total of 51 mm (2 in.) so that the jacket does not bear on the footing or the load stub at the top of the column. The gap between the column and jacket was filled with normal concrete.

In testing the columns, rotation of the substantial loading arm was controlled by use of a load follower controlled by pressure valves. The axial load was imposed via high-strength post-tensioning bars.

Instrumentation of the columns consisted of vertically oriented potentiometers for flexural deformation measurements as well as horizontal and diagonal potentiometers for measurement of shear deformation. The deformation was decomposed into four modes: pure flexural deformation, pure shear deformation, horizontal expansion, and vertical extension. A large number of strain gages were also mounted on the jacket and reinforcing bars before testing. Conversion of the measured strains into stresses was based on a plane stress assumption in the jacket.

Loading was the same in all columns. A number of load control cycles were imposed, increasing the load by 67 kN (15 kips) per cycle, until the lateral load reached  $0.5V_{if}$  where  $V_{if}$  is the shear corresponding to the ideal flexural strength of the specimen. Following five cycles at this load level, the lateral load was once again incremented until the load corresponded to  $V_y$ , the lateral load corresponding to first yield. At this point, the load was changed to displacement control with three cycles at each of the following

ductilities,  $\mu_{\Delta} = 1, 1.5, 2, 3, 4, 5, 6, 8$ , or until failure occurred. Results of the column testing are presented below.

Column R-1, an "as-built" column, initially developed flexural cracks at the top and bottom of the column. These cracks became inclined at a force level of 400 kN (90 kips), the predicted first yield load. During loading at  $\mu_{\Delta} = 1$  and 1.5, inclined shear cracks independent of the original flexural cracks developed and became wide spread. The column developed its ideal flexural strength at  $\mu_{\Delta} = 1.5$  with stable hysteresis loops until  $\mu_{\Delta} = 2$ . The maximum lateral load of 566 kN (127.2 kips) was recorded on the first cycle to  $\mu_{\Delta} = 3$  at a drift ratio of 1.4%. A significant drop in lateral resistance occurred during the three cycles to  $\mu_{\Delta} = 3$  when a major diagonal crack penetrated the lower half of the column following the crushing of concrete in the bottom compression zone. The failure mode was characterized as a flexural shear failure since the column failed in shear after attaining its flexural strength.

Decomposition of the total deflection into shear and flexure components was performed as previously described. It was found that the lateral force-flexural deformation response was stable until  $\mu_{\Delta} = 2$  with little strength degradation. During cycling to  $\mu_{\Delta} = 3$ , the flexural loops shrank with an increasing number of cycles.

The lateral force-shear deflection loops were stable until  $\mu_{\Delta} = 2.0$ . With cycling to  $\mu_{\Delta} = 3.0$ , the shear loops expanded significantly and the shear displacement was the dominant component of total deflection by the time of failure.

Column R-3 was able to develop some flexural cracking before the onset of shear cracking but shear cracks were observed early in the testing. At a lateral load of  $V_y$ , a major inclined shear crack had already developed in the upper half of the column. At  $\mu_{\Delta} = 1.0$ , more shear cracks developed and covered a significant portion of the column. A peak ductility of  $\mu_{\Delta} = 1.5$  was developed under the maximum lateral load of 627 kN (141 kips). At this point, a brittle shear failure occurred. The ideal flexural strength was not obtained. During further displacement to  $\mu_{\Delta} = 2.2$ , the resistance dropped to 138 kN (31.0 kips) and 80 kN (18.0 kips) on the push and pull cycles, respectively, which is less than the calculated contribution from the transverse shear reinforcing alone, 155 kN (34.9 kips).

"As-built" column R-5 having a high longitudinal yield strength and the shortest shear span of "as-built" specimens could be predicted to have the poorest performance, which is borne out in examination of the performance of this column. Inclined cracks were developed at a load of 334 kN (75 kips), less than half of the predicted yield capacity,  $V_y$ , 734 kN (165 kips). At a load of 667 kN (150 kips), vertical splitting cracks developed along the extreme tensile reinforcing. At  $V_y$ , extensive cracking had propagated over the column surface. No warning of failure was apparent when brittle shear failure occurred under a load of 747 kN (168 kips) at  $\mu_{\Delta} = 1$ . Negligible strength and stiffness existed after failure with the lateral strength of 129 kN (29 kips) during the third pull cycle to  $\mu_{\Delta} = 2$  being less than the strength attributable to the stirrups, 181 kN (40.7 kips).

For both column R-3 and R-5, the flexural deformation was greater than the shear deformation prior to shear failure. After shear failure, however, the shear deformation became the dominant mode of deflection.

Results for retrofit columns R-2, R-4, and R-6 are described below. In general, full height elliptical steel jackets prevented brittle shear failure in all columns. Very little comment was made in the research

report on these column, primarily because of the fact that the entire column is obscured from view by the jacket. The only portion of the column that could be viewed is the portion between the ends of the column and the load stub/footing.

Column R-2 demonstrated excellent response under reversed cyclic loading until  $\mu_{\Delta} = 12.0$  when the longitudinal steel fractured due to low cycle fatigue. The column exceeded its ideal lateral strength,  $V_{if}$ , of 545 kN (122.5 kips) at  $\mu_{\Delta} = 2$  and continued to demonstrate ever higher lateral strength until failure. The maximum lateral load was 665 kN (149.6 kips), 21% higher than  $V_{if}$ , at a ductility  $\mu_{\Delta} = 10$ . The drift ratio at this load was 3.3%. Upon low cycle fatigue fracture at  $\mu_{\Delta} = 12$ , the drift ratio had exceeded 3.3% in the push direction and 4.0% in the pull direction.

Retrofit column R-4 also exhibited a demonstrative increase in performance as compared to its "as-built" counterpart, R-3. The column exceeded its ideal flexural capacity of 752 kN (169 kips) at a ductility of  $\mu_{\Delta} = 2$  and continued to demonstrate increased capacity until  $\mu_{\Delta} = 8$  at which point the test was discontinued due to limitations in the test equipment. At this point, no signs of failure were evident. No real drop in lateral load resistance was evident in subsequent cycling to the same ductility level. This is typical of all of the retrofit tests.

Retrofit column R-6 was affected by limitations in the tensile force capacity of the actuator, resulting in reduced displacement in the pull direction. The calculated ideal flexural strength of 1,005 kN (226 kips) was realized at  $\mu_{\Delta} = 1.5$ . All successive peak forces were higher than this value. A maximum lateral force of 1,308 kN (294.1 kips), which exceeded  $V_{if}$  by nearly 30%, was realized at  $\mu_{\Delta} = 7.0$  at a drift ratio of 3.7%. The standard loading pattern was applied to this column up to  $\mu_{\Delta} = 3.0$  after which the standard loading was only continued in the push direction because of the limitations in the actuator. The maximum lateral load in the pull direction was 1,425 kN (280 kips) at  $\mu_{\Delta} = -3.5$  and corresponded to a drift ratio of 1.8%. The push direction load was stable until  $\mu_{\Delta} = 7.0$  when low-cycle fatigue fracture of the reinforcing steel occurred. Pinching due to the use of a thinner jacket than on the other specimens is noted in this column.

Relative contributions to total column displacement were similar for all retrofit specimens with the shear deformation component ranging from 1/4 to 1/3 of the flexural displacements. For column R-6, the total displacement is greater than the sum of the flexural and shear components due to the effects of bond slip which can be significant in retrofit columns.

Theoretical force-deflection envelopes prepared in conjunction with the experimental results were based on the recommendations found in University of California (1991) as well as Mander, Priestley, and Park (1988b) and were found to be in very good agreement with the experimental values.

The energy absorbed per cycle was plotted for each pair of "as-built" and retrofit specimens and showed that for low levels of load, due to the highly linear elastic response of the member at these levels, very little energy is absorbed. All of the retrofit columns demonstrated stable energy absorption capability with the energy per cycle growing as the number of cycles increased. The results for column R-6 are not as well defined as for R-2 and R-4 due to the problems encountered in loading the column, yet this column demonstrates a dramatic increase in capacity over "as-built" R-5.

The energy per cycle was compared to an ideal elasto-plastic hysteretic response parallelogram. The energy absorbed per cycle in this elasto-perfectly plastic parallelogram is given by:

$$\Delta E_i = 4(\mu - 1)\Delta_y V_{if} \quad (2-10)$$

where both  $\Delta_y$  and  $V_{if}$  are calculated by using Mander, Priestley, and Park's (1988b) confined concrete model and an ultimate compressive strain of 0.005. The energy absorption ratio is defined as the area in the actual loop divided by the area in the ideal loop. For "as-built" R-1, this ratio was 0.38 at  $\mu_A = 3$  while the ratio for R-2 was slightly higher at this ductility level and continued to increase to 0.48 at  $\mu_A = 10.0$ . The ratios for R-3 and R-5 were unstable due to the brittle shear failure of these specimens. These ratios dropped to as low as 0.1. R-4 demonstrated excellent behavior with a ratio of 0.42 at  $\mu_A = 8.0$ . Compared to the very poor response of R-5, R-6 dissipated significantly more energy but the plot of the dissipation ratio as a function of the ductility factor was somewhat erratic due to complications encountered in loading this specimen.

Results of this series of tests are very promising. They not only confirm the poor performance of pre-1971 shear-dominated designs but also illustrate the effectiveness of full-height elliptical steel jackets in converting a brittle shear failure mode into a very ductile flexural response. The following approach is recommended by Xiao, Priestley, and Seible (1993) for determining the required strength of a steel jacket for purposes of implementing a shear retrofit. The required strength of the jacket should be based on:

$$V_{sj} = \frac{V_{fu}}{\phi} - (V_c + V_{sh} + V_p) \quad (2-11)$$

where

$V_{sj}$	=	Required shear strength of the jacket
$V_{fu}$	=	Ultimate capacity based on flexural overstrength
$V_c$	=	Shear strength provided by concrete
$V_{sh}$	=	Shear strength provided by original transverse reinforcement
$V_p$	=	Shear strength provided by axial load
$\phi$	=	Strength reduction factor, taken as 0.85

The terms  $V_{sj}$ ,  $V_{fu}$ , and  $V_p$  are as defined below and are based on a shear model presented in Priestley, Seible, Verma, and Xiao (1993) and Priestley, Verma, and Xiao (1993).

$$V_c = k \sqrt{f'_c} A_e \quad (2-12)$$

where

$k$  varies from 0.29 (3.5 for English units) for  $\mu \leq 2$  to 0.1 (1.2 English units) for  $\mu \geq 4$

$A_e = 0.8 A_g$  for circular and rectangular columns.

$$V_{sh} = \frac{A_v f_{yh} D'}{s} \cot \theta \quad (2-13)$$

where

$A_v$  = Total area of transverse steel within spacing  $s$

$f_{yh}$  = Yield stress of transverse steel

$D'$  = Distance between the centers of the hoop periphery measured in the plane of the hoop and in the direction of lateral loading

$s$  = Vertical spacing of hoops

$\phi$  = Angle between compression strut and the column axis, can be taken as 30 degrees

$$V_p = \frac{D-a}{2D \left( \frac{M}{VD} \right)} P_u \quad (2-14)$$

where

$a$  = Depth of the compression zone

Finally, having obtained the required shear strength of the jacket, its thickness can be determined by the following two equations for the strong and weak direction respectively.

$$t_j = \frac{V_{sj}}{2f_{yj} D_j \cot\theta \left[ 1 - \left( 1 - \frac{\pi}{4} \right) \frac{B_j}{D_j} \right]} \quad \text{for strong direction}$$

$$t_j = \frac{V_{sj}}{2f_{yj} D_j \cot\theta \left[ 1 - \left( 1 - \frac{\pi}{4} \right) \frac{D_j}{B_j} \right]} \quad \text{for weak direction}$$

(2-15)

where

$B_j$  = Minor jacket diameter

$D_j$  = Major jacket diameter

Because of the interdependency of  $V_{sj}$ ,  $V_{fu}$ , and jacket thickness,  $t_j$ , an iterative procedure must be employed in order to arrive at a governing jacket thickness. If it is determined that a column is in need of flexural and shear enhancement, the requirements for thickness of the jacket will generally be based on the flexural requirements and a design can reasonably start with that assumption.

Research concerning the retrofit of shear deficient rectangular bridge columns via steel jackets and external steel angles placed at column corners is described in McLean and Bernards (1992) and in summary fashion in Bernards, McLean, and Henley (1992). The portion of the project that employed steel jackets will be presented below, while the steel angle retrofits will be discussed in Section 4.3.

Washington State Transportation Center of Washington State University carried out this study for the Washington State Department of Transportation. They selected columns typical of those constructed in the Puget Sound region of Washington as the prototype column. Specimens of a 2/5 scale were then

constructed, employing the shear deficient details common in the prototype columns. The prototype columns measured 510 mm x 760 mm (20 in. x 30 in.) and had a longitudinal reinforcing ratio of 2.6% with the reinforcing concentrated on the short faces. A lap splice was not present at the base of the columns. Transverse reinforcing consisted of 9.5 mm (#3) bars spaced at 305 mm (12 in.) with 100 mm (4 in.) hook extensions lapped in the cover concrete. All column reinforcing had a yield strength of 276 MPa (40 ksi), that was typical for the columns under investigation. The test specimens were rectangular, 205 mm x 305 mm (8 in. x 12 in.) in plan, and were 915 mm (36 in.) high measured from the top of the footing. Test specimens were vertical cantilevers tested in single curvature bending.

All specimens were tested using the same procedure. An axial load was applied to the specimen approximately equal to  $0.09f'_cA_g$ . This load varied by approximately  $\pm 12\%$  during the test. The cyclic lateral load was applied at 760 mm (30 in.) above the footing and consisted of two cycles at  $\mu_\Delta = 1, 2, 4, 6,$  and  $8$ , unless failure occurred before this cycling was completed. The yield displacement,  $\Delta_y$ , was initially computed to be 2.8 mm (0.11 in.) but was modified during testing after researchers realized this value was too low. The refined value of 6.6 mm (0.26 in.) was adopted as  $\Delta_y$ .

The first two columns tested were control columns. Both columns exhibited classic shear failure as demonstrated by pronounced x-cracking. Column 1 was originally tested with the low estimation of yield displacement, and consequently its results could not be used in computing ductility. Upon assessment of the response of this column, the refined estimate of yield displacement was made and column 2 was tested using the modified yield displacement of 6.6 mm (0.26 in.). Specimen 2 exhibited shear cracking and tie yielding at  $\mu_\Delta = 1$ . There was a significant drop in load carrying capacity at  $\mu_\Delta = 2$  after which very little lateral load could be sustained. The reliable ductility of this column was judged to be  $\mu_\Delta = 1$ .

The steel jacket technique employed plates welded on four longitudinal seams. The jacket was slightly oversized and the gap between the jacket and column filled with high strength, non-shrink grout. The jacket had a 13 mm (1/2 in.) gap between the bottom of the jacket and footing so that the plate would not bear on the top of the footing during rotation of the column. The plates were 585 mm (23 in.) in length, covering approximately the lower 2/3 of the column height. There were a number of steel plate variations studied. The effect of plate thickness was studied; two thicknesses, 12-gage (2.67mm, 0.105 in.) and 16-gage (1.6 mm, 0.063 in.) were used. As an alternate to cement grout, commercially available epoxy grout used in anchor bolting was used. In a third variation, steel dowels were anchored into the column core near the footing to improve confinement and prevent longitudinal bar buckling. Dowels were 6 mm (1/4 in.) in diameter and were set into 100 mm (4 in.) deep pre-drilled holes and anchored with epoxy. The dowels had end threads and were bolted to the jacket at 25 mm (1 in.) and 100 mm (4 in.) above the bottom of the jacket on each short face of the column. Columns 4, 6, 7, and 8 were constructed by using the various steel jacketing techniques previously described.

Column 4, retrofit using the 16-gage jacket and the nonshrink cement grout alternative, demonstrated a lateral load capacity increase of 16% over the "as-built" specimen with little decrease in lateral capacity at  $\mu_\Delta = 8$ . During the  $\mu_\Delta = 4$  cycle, longitudinal bar buckling occurred near the base of the column but was confined by the jacket. As a result of confinement, cracks penetrated into the footing. Neither internal tie yielding nor shear cracking were evident after removal of the jacket.

Column 6, which was retrofit using a 12-gage steel jacket and cement grout, exhibited stable load-carrying capacity until  $\mu_\Delta = 8$ . Although the steel jacket in this specimen was significantly thicker than the one used on column 4, the capacities were the same. Somewhat wider hysteresis response loops were

noted in this test indicating a somewhat greater energy dissipation. Longitudinal bar buckling also began in this test at  $\mu_{\Delta} = 4$  but was of a lesser degree than column 4 due to the thicker jacket. Once again neither tie yielding nor shear cracking was observed.

Column 7 with a 16-gage jacket, cement grout, four dowels into the core, and performed well until  $\mu_{\Delta} = 8$ . This column exhibited a 19% increase in lateral load capacity over the control specimen, the largest noted in any specimen, due to the enhanced confinement provided by the grouted anchors. The anchors increased the width of the hysteresis loops. Longitudinal bar buckling was all but eliminated except on one side of the column where drilling of the anchor holes severed one of the internal ties. No shear cracking was observed after removal of the jacket, but cracking of the footing was observed due to hinge penetration into the footing.

Column 8, retrofit with a 16-gage steel jacket and epoxy grout, demonstrated acceptable performance until  $\mu_{\Delta} = 8$ . The lateral load capacity increased by 18% over the control. Once again tie yielding and shear cracking were prevented. The load displacement curve is very similar to that of column 6 which employed a thicker jacket. The epoxy filler improved the performance of this column when compared to column 4, which used cement grout. The significant extra cost of the epoxy filler was not seen as warranted because of the modest increase in performance over cement grout. The epoxy grout was able to significantly delay the onset of longitudinal bar buckling, but buckling did eventually occur to the same extent as in the other specimens.

The load capacity increase for these four specimens ranged from 16% to 19% with all columns successfully attaining  $\mu_{\Delta} = 8$ . The specimen which incorporated the dowels most significantly improved the lateral load capacity and hysteretic capacity. However, all specimens had significant improvements in hysteretic energy dissipation capacity over the control specimen, column 2. The increase in jacket thickness and use of epoxy grout slightly improved the column performance. In all columns, buckling of the longitudinal steel as well as yielding and buckling of the jacket occurred. The jackets were still able to maintain confinement in this region but in the scenario where a lap splice would have been present at the base, these buckled jackets would not have provided sufficient lateral clamping pressure for longitudinal force transfer in the lap splice.

The use of steel jackets in the strengthening of reinforced concrete bridge columns is also described in Unjoh and Kawashima (1992). In this study, a total of 24 columns were constructed - 13 specimens to examine the vulnerability of columns with differing geometries and reinforcing characteristics, and 11 specimens with steel jacket retrofits. Results of only 4 of the jacketed specimens, columns 9 through 12, were presented in the paper because they were deemed to be representative of the entire set of columns. All columns were subjected to the same loading pattern, increasing load until yield, and then ten cycles at each ductility level thereafter.

The four retrofit columns presented in the paper were 500 mm square (19.7 in.), measured 2.6 m (8.53 ft) from the top of the footing to the lateral load point, and had a shear span ratio of 5.6. The longitudinal reinforcing ratio at the base was 1.31% and the lateral tie reinforcing ratio was 0.05%. Above the termination point, located 900 mm (35 in.) above the top of footing, the longitudinal reinforcing ratio decreased to 0.63%. This column geometry and bar arrangement was a 1/5 scale representation of typical Japanese bridge columns. Columns of this construction type are liable to shear failure in the region of the longitudinal steel termination due to excessive primary flexural degradation of this region. Though initial

damage is of a flexural nature, final failure is by shear and these columns are therefore described along with other shear-deficient columns.

Columns 9 and 10 were retrofit with 1 mm (0.04 in.) thick steel jackets of length 1 D, placed D/2 above and below the termination point, where D is the lateral dimension of the column. Concrete mortar was injected between the jacket and column for specimen 9 and epoxy resin was used for column 10. These two specimens, under loads described previously, failed in flexure at  $\mu_{\Delta} = 7$  at the base and developed diagonal shear cracks in the region of the termination point. The epoxy resin provided a better bond between the column and jacket because separation of the jacket from the column occurred with the mortar. Overall, the 1 D jacket was deemed to exhibit unacceptable performance and the jacket was lengthened to 1.5 D for column 11. This jacket was placed so that it extended D above and D/2 below the termination point.

Column 11, retrofit as described above, suffered a flexural failure at  $\mu_{\Delta} = 8$  at the base. No damage was observed near the termination point thus validating the effectiveness of the longer jacket.

In contrast to the three retrofits described above, column 12, an "as-built" specimen, first developed extensive flexural cracking in the termination zone and subsequently failed in shear at this location at  $\mu_{\Delta} = 7$ .

The author concluded from the results of the 24 columns, both "as-built" and retrofit tested as described, that shear failures at the termination point could be prevented by providing a development length of the longitudinal reinforcing of 1.0 D and that a reasonable minimum jacket length would be 1.5 D to 2 D in length.

In Matsuura, Nakamura, and Sekimoto (1990), the use of steel jackets by the Hanshin Expressway Public Corporation is explored as a means of strengthening columns prone to shear failure due to flexural degradation of the column in the area of mid-height longitudinal steel termination. This reference presents laboratory test results and a description of full-scale field implementation of the steel jacket retrofit.

In the test program conducted in conjunction with the Public Works Research Institute and Metropolitan Expressway Public Corporation, a variety of column and reinforcing geometries were examined in the "as-built" and retrofit state. This reference deals with square test sections. Test columns measured 500 mm x 500 mm (19.7 in. x 19.7 in.), had a shear span ratio of 5.3 and were 2.6 m (8.53 ft) tall from the top of the footing to point of lateral load application. Partial longitudinal steel termination occurred at 900 mm (35 in.) above the footing. The columns were intended to be 1/6 scale representations of actual bridge columns. Similar to the testing carried out by the Metropolitan Expressway Public Corporation (Akimoto, 1990) previously presented on page 39, four specimens were constructed. The first specimen was an "as-built" specimen, the second had a 1.0 D steel jacket and non-shrink mortar, the third had a 1.0 D jacket with epoxy resin, and the fourth was constructed with a 1.5 D jacket with epoxy resin where D represents the lateral dimension of the column. The steel jacket is 1 mm (0.04 in.) thick and is consistently placed over the termination point so that it extends 0.5 D below and 0.5 D or 1.0 D above the termination point.

Loading consisted of an axial load of 282 kN (28.8 tf, 63.5 kips) and a gradually increasing static lateral load, 10 full cycles in all, until the yield displacement of 15mm (0.6 in.) occurred. The dynamic test was

displacement controlled and applied integer increments of the yield displacement to the top of the column with 10 fully reversed cycles per ductility increment. Test results indicate that the "as-built" specimen failed before termination of the static portion of the load test, indicating failure before yield displacement occurred. All three of the retrofitted columns showed a relocation of the failure location to the column base and an accompanying increase in lateral load capacity of 30%. The columns with the non-shrink grout were compared to tests performed by the Metropolitan Expressway Public Corporation (Akimoto, Hakajima, and Kogure, 1990) and found to be very similar although the "as-built" specimens were significantly different, thus indicating that the retrofit system is applicable to a variety of situations.

Field installations consisted of 6 mm (0.24 in.) thick plates selected thicker than the required 4.5 mm (0.18 in.) in order to provide enhanced handling stiffness. The installation reported in Matsuura, Nakamura, and Sekimoto (1990) is on a single column on the Airport Line of the Hanshin Expressway. This single column pier of 3 m x 3 m (9.84 ft x 9.84 ft) cross-section was successfully jacketed with a 6 m (19.69 ft) tall steel jacket. This jacket, similar to those constructed in Tokyo for the Metropolitan Expressway (Akimoto, Hakajima, and Kogure, 1990) is an anchored steel jacket where the anchors are intended to keep the flat rectangular plate jacket in reasonable condition during the grouting operations. Due to the flexibility of thin plates in bending, an anchor pattern of 500 mm x 500 mm (19.7 in. x 19.7 in.) was established so as to limit out-of plane displacement of the jacket plates to 3 mm (0.12 in.) during grouting. This test showed that different clearances of 4 mm (0.16 in.) and 10 mm (0.39 in.) are required between the column and jacket for epoxy and non-shrink mortar injection respectively. Moreover, the epoxy grout method only involves anchor bolts while the mortar injection requires anchor bolts and pour staging. The results of the demonstration test indicated that steel jacketing of rectangular columns through anchored steel jackets was a feasible option for the Hanshin Expressway Public Corporation.

### **2.3 Field Installations**

The description of several field installations of steel jacket retrofits is described below. Also included in some of the reviews is information on how the retrofit alternatives were selected and what circumstances led to the selection of the steel jacket.

Serroels (1993) describes the evaluation of four retrofit alternatives for the Sutterville Road Overhead in Sacramento, California. The bridge is a low priority structure carrying local traffic over two surface streets and five rail lines. The structure is 110 m (360 ft) long and is supported by three, two-column bents. Each of the columns is approximately 8.5 m (28 ft) high and measures 1.22 m x 1.22 m (4 ft x 4 ft). Transverse reinforcing is inadequate with 13 mm (#4) transverse bars spaced vertically at 305 mm (12 in.). The connection between the column and the footing was designed so as to provide for no moment transfer. The structure in its "as-built" condition was analyzed by using the GTSTRUDL program for an estimate of the ratio of the elastic force demand to the nominal capacity as well as maximum longitudinal and transverse displacements.

Retrofit Strategy 1 involved the placement of shear walls between the columns of two of the three bents with the assumption that the columns in the third bent would pin at the top. For analysis, the walls were assumed for analysis to be at bents 2 and 3 so as to minimize the eccentricity between the center of transverse stiffness and the center of mass. This reduces the contribution of torsionally induced forces in the structure. The wall was intended to resist shear forces, and the existing columns, the overturning axial forces. Also included was a tie at the base of the columns to prevent them from relative movement and possible separation from the wall boundary. This retrofit was one which primarily resists transverse

displacements and does very little in the longitudinal direction due to the negligible out-of-plane stiffness of the wall as compared to its transverse shearing stiffness. The wall was therefore assumed to be pinned at the top and bottom. Computer analysis of this retrofit alternative indicated significant transverse displacement reduction along with forces at the base of the wall strong enough to disconnect it from the footing. This scenario was deemed desirable because decoupling the wall from the excitation point, i.e., the footing, would effectively result in partial isolation of the structure.

Retrofit Strategy 2 employed steel jackets as a means of increasing ductility but not strength. The jacket thickness was chosen so that it would be capable of developing 2.1 MPa (300 psi) of lateral confining pressure. The jacket was a circular jacket placed around a square column and filled with grout, with no connection between the grout, jacket, and existing column. This detail will provide a negligible change in stiffness to the column and henceforth little additional load. Due to the negligible effect on stiffness, the torsional excitation will not be an issue as with the shear walls; and the jackets can be placed on the structure without concern for this issue. In this scenario, jackets were placed on bents 3 and 4 but not on 2 so as to avoid construction near the adjoining railroad tracks. The columns of bent 2 were assumed to pin at the top. Analysis of this retrofit assumed no change in column section properties for the jacket because of the assumption of no increase in stiffness, and results showed that the two retrofit jacket columns would be expected to see flexural demands on the order of 4.0 - 4.5, which is well within the ductility capacity of steel-jacketed columns.

Retrofit Strategies 3 and 4 did not involve any modifications to the columns and are not presented here though they do include modifications at the abutment areas intended to draw load away from the columns or in other ways modify the bridge response.

Serroels concludes that options 1, 2 and 4 would be feasible but would require the consideration of factors other than those that are purely structural. The issue of cost, construction impacts on the road and rail lines below, and other factors pertaining to expected damage would all need to be considered in determining the feasible retrofit scenario.

Shirolé and Halik (1993) discuss two bridges in New York, where as part of a general structural retrofit program, seismic retrofit details have also been incorporated. Only one of the two bridges involved a column retrofit, where steel shells were installed along the column in order to account for the lack of transverse confinement in the column end regions. An elastic packing material was placed between the column and the steel shell to inhibit composite action between the jacket and column, so that the column would not have an increased stiffness and would not force the failure location into the cap beam or footing.

Turkington, Wilson, and Kennedy (1991) describe the retrofit of the Oak Street Bridge in Vancouver, British Columbia, Canada. The bridge is 1,840 m (6034 ft) long and is supported by 83 reinforced concrete piers. The bridge has three main steel spans over the Fraser River, five steel approach spans on the south side, and concrete approach spans. The approach spans are supported on two column piers, while the main river spans are supported on a solid wall pier to above the high water line and twin columns upward to the bridge seat. A seismic analysis indicated that the short approach span piers were shear deficient and that there was inadequate confinement and lap splice length at the column base. Numerous other deficiencies in the structure were also found, such as a shear deficient cap beam and inadequate bridge beam seats.

As part of a bridge widening project, the cap beam was extended and widened so as to accommodate the additional loads and to provide sufficient seismic capacity. This cap beam was then strong enough to force plastic hinges to develop in the columns. The concern was inadequate shear capacity in the plastic hinge regions following degradation in an earthquake. The remedy was to place full-height steel jackets on all approach span columns less than approximately 10.5 m (35 ft) in height, although partial-height jackets would have been sufficient. The main river spans were expected to develop plastic hinges at the location where the twin columns tie into the wall pier and where the wall pier is connected to the unreinforced footings. A rocking response was also expected under longitudinal seismic load. Two of the piers were to be retrofit by providing an infill wall above the termination of the existing wall pier and vertically post-tensioning through the infill and existing pier shaft, a combined height of approximately 19.2 m (63 ft), with a 3.66 m (12 ft) anchorage length in the footing.

Casey et al. (1994) discuss the retrofit of the China Basin Viaduct in San Francisco, California, following damage suffered during the 1989 Loma Prieta Earthquake. Based on the design spectrum used by the consulting firm CH2M Hill for the retrofit design for 169 columns and piers on the project, 118 would need retrofit to carry lateral load, 8 columns would need to be replaced, 18 columns would require confinement jacketing, 6 piers required upgrading, and space constraints would not allow some of the deficient columns to be retrofit. This assessment is based on analysis which indicated that in many of the columns, plastic hinges were expected to form at the top and bottom in columns that had inadequate transverse confinement and lap splice lengths of only  $25 d_b$ .

In order to retrofit these columns, the steel shell retrofits developed at the University of California, San Diego, were employed. Jackets ranging from 10 mm (3/8 in.) to 16 mm (5/8 in.) were employed with design capacities of  $\mu_\Delta = 4$  to 6 for single column bents and  $\mu_\Delta = 6$  to 8 for multi-column bents. Where required, additional longitudinal reinforcing was placed between the jacket and the column and bonded into the existing footing. The steel casing was designed to provide a radial confining stress of 2.1 MPa (300 psi) at a radial dilation strain of 0.1 percent so as to provide for lap splice confinement and force transfer.

The retrofit of the Route 242-Route 680 Separation near San Francisco, California, is described in Fish and Rowe (1994). This structure is composed of two distinct bridge types. The South structure is a three-span prestressed concrete box girder bridge supported by steel bearings at abutment 1 and bent 4. Bents 2 and 3 support the structure with fixed steel bearings and are composed of five columns each. The bridge is on a 69 degree skew. The North structure is a continuous box girder with bent 4 on a 69 degree skew and bent 5 through abutment 13 on a 54 degree skew. Bents 5 through 12 are two column bents with caps cast monolithically with the superstructure. The bridge spans Walnut Creek between bents 9 and 10. The bridge has debris walls at bents 7 through 11 to protect the columns when the channel is at flood stage. The bridge was previously retrofit with hinge restrainers and catcher blocks during the Caltrans Phase I retrofit program.

The North structure was retrofit with steel casings 10 mm (3/8 in.) thick so as to provide ductility in the plastic hinge region due to inadequate transverse confinement. Footing modifications were also made because the footing was deemed inadequate to resist the moment demands at the column/footing interface. Additional columns were retrofit using steel jackets so as to increase shear strength. A connection was also designed between the column and the previously described debris wall so as to prevent impact of the column against the wall and thus eliminate plastic hinge formation at the top of the wall.

For the South structure, four retrofit solutions were examined - two requiring strength enhancement modifications and two requiring seismic isolation. The final solution was (1) an isolation retrofit with lead core rubber bearings installed at abutment 1 and bent 4 and (2) PTFE-spherical bearings at bents 2 and 3. The decision to employ an isolation retrofit was based on the increased damping provided by the bearings and also on the reduction of the overall structural stiffness from the soft stiffness of the bearings that shifted the structural response to a lower region of the response spectrum. The increase in damping was from 5% to nearly 20%.

On the other hand, the PTFE-spherical bearings installed at the two intermediate bents reduced the frictional forces to 10% of the "as-built" lateral forces. The lead core rubber bearings allowed for a predictable structural displacement and aided in the design of the seat extensions required at parts of the bridge.

The isolation alternative was estimated to cost 1.97 million dollars contrasted with the strengthening alternatives for this South part of the structure estimated to cost 3.5 million dollars. The combination of economic and structural feasibility issues delineated above led to the selection of this mixed retrofit type for the Route 242 and 680 Separation.

#### **2.4 Analytical Models and Design Guidelines**

Much of the information that could be included in this portion of the document has been previously presented when discussing the flexural and shear deficient columns in the earlier parts of this section. Information that was not retrofit type specific but pertains to the analysis, design, or both of steel jackets is presented in this subsection.

The analytical model used as a predictor of both "as-built" and retrofit columns developed in conjunction with the experimental work presented in Chai, Priestley, and Seible (1991b) can be found in Chai, Priestley, and Seible (1991a, 1994). All of the nuances and assumptions made in developing the comprehensive program COLRET are too great too elaborate on in this document and will be presented in summary fashion only. The purpose of the program is to provide a tool for engineers that can be used to assess the capacity of "as-built" specimens and allows them to try a variety of different retrofit schemes, finally settling on one that fulfills the design objectives of the particular project. The results from the program are compared to the experimental results from Chai, Priestley, and Seible (1991b) and other sources referenced by Chai, Priestley, and Seible (1991b) for purposes of demonstrating the effectiveness of the model.

In defining all of the variables that affect the performance of the column, the constitutive properties of the materials are of key concern. The confined concrete model defined in Mander, Priestley, and Park (1988b) has been selected as the model for the concrete columns in this research. This model predicts the increase in confined versus unconfined concrete strengths as a function of the lateral confining stress imposed by the internal reinforcing of the specimen. The external steel jacket was treated as additional transverse hoops in this research and in most other similar analytical and experimental research programs.

In addition to defining the stress-strain characteristics of the confined concrete, a model for the stress-strain properties of steel reinforcing was also employed. This model was divided into three phases; a linear portion up to yield, a yield plateau region, and a strain-hardening region. Different model parameters were used for the two most common reinforcing steel grades, 276 MPa (40 ksi) and 414 MPa

(60 ksi), because of the different strain-hardening characteristics of these two steels. With substitution of appropriate values for the strain and tangent modulus corresponding to the onset of strain hardening, the analytical stress-strain curve for the jacket steel can also be derived.

The analytical model assumes that a cement-based grout is used as the infill material. The degree of composite action between the jacket and column depends on the available bond strength at the steel-grout interface.

The column is analyzed by using a laminar analysis procedure where the column is divided into 100 slices, 5 each in the top and bottom cover and 90 in the column core region. Each strip of the column is divided so that the area in the core and area in the cover region are separated. The program assumes that the longitudinal steel bars are uniformly distributed around the column and subsequently converts these bars into a continuous steel ring around the column. The amount of reinforcing tributary to each slice is computed and assumed to act at the mid-height of the slice.

The assumption that plane sections remain plane is made so that the assumption of a linear strain variation across the column section can be made. The strain in each layer is computed and henceforth the stress and force resultants in each layer can be computed.

The equilibrium of internal forces is assured through use of a convergence criteria. Axial force convergence allows the moment resultant on the column to be computed. The energy balance method proposed by Mander, Priestley, and Park (1988b) is employed in finding the ultimate compressive strain in the confined concrete sample due to the steel jacket used.

The displacement and curvature calculations for an "as-built" column are based on the following assumptions. The computer program assumes an elasto-plastic relationship for the moment-curvature response of the section. In the "as-built" columns the elasto-plastic yield curvature is defined as:

$$\phi_y = \phi'_y \frac{M_u}{M_y} \quad (2-16)$$

where

$$\begin{aligned} M_u &= \text{Ultimate moment capacity of the "as-built" column} \\ M_y &= \text{Yield moment capacity of the "as-built" section} \\ \phi'_y &= \text{Curvature at first yield of the longitudinal steel} \end{aligned}$$

Because strain penetration of the longitudinal steel occurs in the footing, an effective column height is defined as  $L$  and is equal to the original height of the column  $L'$  plus  $6 d_b$ . Considering the inelastic rotations to be concentrated at the midheight of a plastic hinge whose length is given by  $L_p = 0.08L' + 6 d_b$ , the ultimate displacement ductility can be predicted as:

$$\mu = 1 + \frac{3L_p}{L'} \left( \frac{\phi_u}{\phi_y} - 1 \right) \left( \frac{L}{L'} - 0.5 \frac{L_p}{L'} \right) \quad (2-17)$$

where  $\mu$  is equivalent to the term  $\mu_{\Delta}$  used throughout this document and all other terms have been previously defined.

For retrofitted columns, the procedure and equations are slightly different. Depending on the length of the jacket and bond strength between the jacket, grout, and concrete, two possibilities may exist. First, for a long jacket, sufficient length exists for the bond stress to create a region of full composite action. In this scenario, a trapezoidal distribution of bending stiffness exists. The stiffness is assumed to be equal to the stiffness of the bare column at the top and bottom of the jacket and increases linearly to the full composite stiffness over a distance defined as the bond transfer length. In the second scenario, a short jacket would involve the scenario where full composite action could not be attained at any location in the jacket height. In this situation, the bending stiffness varies linearly from the bare stiffness of the column at both ends to the maximum partially composite stiffness at mid-height of the jacket. Because the bending stiffness and bending moment vary within the jacketed region, the computation of the yield displacements and curvatures is not a simple procedure. The displacement of the lateral load point in a retrofit column at first yield of the longitudinal steel can be found by taking the first moment of the curvature distribution about the center of mass as follows:

$$\Delta'_{yr} = \int_0^{L'} \frac{M(y)}{EI(y)} (L' - y) dy \quad (2-18)$$

where  $y$  denotes the vertical distance from the top of the footing. Integration of this equation is described in Appendix A of Chai, Priestley, and Seible (1991a). The integration limits are divided into regions of constant bending stiffness and areas of varying bending stiffness. Areas of constant bending stiffness are those above and below the steel jacket as well as the central fully composite regions of jackets able to attain full composite action. Areas of varying lateral stiffness are the transfer lengths of jackets able to become fully composite as well as the full-jacketed height short jackets which are not fully composite anywhere. The bending moment in either scenario is a linear function of the height from the applied lateral load.

Having obtained the term  $\Delta'_{yr}$ , the equivalent elasto-plastic displacement  $\Delta$  can be calculated similar to an "as-built" column as shown below:

$$\Delta_{yr} = \Delta'_{yr} \frac{M_p}{M_{yr}} \quad (2-19)$$

where

$M_p$  = Plastic moment capacity of the retrofit column  
 $M_{yr}$  = Yield moment at the base of the retrofit specimen

Having established this yield displacement, the displacement ductility factor,  $\mu_{\Delta}$ , can be determined once the maximum displacement is established.

Note that the model describes failure either as the concrete reaching its ultimate confined strain,  $\epsilon_{cu}$ , or the longitudinal steel reinforcing bars reaching their ultimate strain capacity,  $\epsilon_{su}$ , whichever corresponds

to the smaller displacement ductility factor. There is no reasonable means of assessing the other possible controlling limit state, that of low-cycle fatigue failure, due to the dependence of this phenomenon on a displacement history. Chai, Priestley, and Seible (1991a) proposed a reduction in the predicted column ductility of 25% in order to account for this phenomenon.

The computer model also considers the possibility that a column may have inadequate shear strength to obtain the desired column flexural strength. The column is checked to assure that the shear strength is 1.15 times the shear corresponding to the moment  $M_u$  predicted by COLRET in order to account for higher flexural strengths due to material overstrength considerations. A model is employed in the shear capacity provisions of the program to account for the reduction in shear capacity of plastic hinge regions at high ductilities. For ductilities less than two, the column is assumed to have no reduction in plastic hinge region shear capacity, and its capacity is denoted as  $V_i$ . For ductilities greater than six, the shear which can be resisted is a function of the degraded concrete core and transverse reinforcing and is known as  $V_F$ . For intermediate ductilities, the capacity varies linearly between  $V_i$  and  $V_F$ . Full flexural response, unimpeded by shear considerations, is assumed if the design shear force is less than  $V_F$ . If this is not the case, modifications are made in the ductility factor consistent with the models illustrated in Chai, Priestley, and Seible (1991a). The response of retrofit columns is similarly addressed where jacket thickness recommendations can be made in order to attain adequate shear performance and guarantee ductile flexural behavior.

In addition, the program is capable of identifying the failure mode of the column, i.e., flexure or shear, indicating whether ultimate concrete or steel strains govern the ultimate displacement and curvature, and indicating if a jacket is of an inadequate size.

Results from the experimental tests results reported previously in this chapter (Chai, Priestley, and Seible, 1991b), were compared to the computer output and are presented below.

Comparison of the experimental and analytical results for column 3, a reinforced concrete column with continuous reinforcing, shows that the yield displacements in the analytical and experimental models were the same and that the program predicted a peak lateral strength approximately 10% less than experimentally determined. The program under predicted the ultimate displacement by 32%, likely because the equations used in the program, based on Mander, Priestley, and Park's (1988b) energy balance approach, were developed for predicting the ultimate strain in the concrete in axially loaded columns. A procedure was incorporated into the program to account for the strain gradient effect due to bending and the resulting new prediction was within 3% of the experimentally determined value.

Comparisons to column 4, a retrofit column with continuous reinforcing, illustrate that the maximum strength predicted by the program was approximately 6% greater than the experimental results and the yield displacement 3.5% less than experimentally determined. The ultimate displacement predicted by the program was 248 mm (9.764 in.) while bar fracture in the prototype occurred at 220 mm (8.672 in.). The moment curvature analysis carried out by the program identified the concrete strain rather than the strain in the longitudinal steel as the controlling limit state. This result is the justification for reducing the ultimate ductilities by 25% so as to provide an adequate safety margin against low-cycle fatigue fracture. The envelope of the load-displacement response of the experimental and analytical results overlay each other almost perfectly.

Finally, comparison of the results of column 6, a lap splice column, indicates that the program overestimated by slightly less than 5% the shear force corresponding to the development of the plastic moment. The equivalent elasto-plastic yield displacement generated by the program is 26.6 mm (1.047 in.), slightly lower than the experimental displacement of 27.7 mm (1.090 in.). The ultimate displacement predicted by the program, 279.7 mm (11.01 in.), was analytically controlled by the ultimate strain in the concrete. The actual ultimate displacement, controlled by low cycle fatigue fracture of the longitudinal steel, was 221 mm (8.70 in.). Even if the analytical results are reduced by 25% to 210 mm (8.26 in.), this is only 5% less than the experimental value and once again lends credence to a 25% reduction in the ultimate displacement output from the program.

A comprehensive and very detailed analytical model, (Chai, Priestley, and Seible, 1991a), has been highlighted. Far more information than could be properly summarized here is available in the original report (Chai, Priestley, and Seible, 1991a) and in a journal paper (Chai, Priestley, and Seible, 1994). The model takes into account the constitutive properties of the confined concrete in "as-built" and retrofit columns, unconfined cover concrete in "as-built" columns, steel reinforcing properties in "as-built" and retrofit columns, and jacket steel properties in the retrofit specimens. It employs a laminar analysis procedure to compute force and moment resultants on the section. The program can account for shear degradation of plastic hinge regions and modify the expected performance of the column if necessary. Results from the program were in reasonable agreement with "as-built" and retrofit specimens constructed with both continuous and lap splice reinforcing.

The determination of steel jacket thickness as a function of hysteretic failure and cumulative damage is presented in Taylor and Stone (1993). In this reference, the use of an integrated seismic design procedure (ISDP) is presented in summary fashion. The ISDP involves the use of an inelastic time history analysis and empirical relationships in order to define the hysteretic characteristics of the model and the damage threshold levels.

A damage index (DI) is a dimensionless quantity used to describe the results of an inelastic dynamic analysis. A DI is generally tied to measurable quantities that describe the overall state of an element. The formulation used by Taylor and Stone is based on moment and curvature as opposed to a more common formulation of load and deflection. The equation is shown below for reference.

$$DI = \frac{\Phi_m - \Phi_r}{\Phi_u - \Phi_r} + \beta \left( \frac{A_t}{\Phi_u M_y} \right) \quad (2-20)$$

where

$\Phi_m$	=	Maximum curvature attained during seismic loading
$\Phi_u$	=	Ultimate curvature capacity of a section
$\Phi_r$	=	Recoverable curvature at unloading
$M_y$	=	Yield moment
$A_t$	=	Total area contained in M- $\Phi$ loops
$\beta$	=	Strength deterioration parameter

This equation can be evaluated at any discrete time step. The first terms of the equation are a measure of curvature ductility while the second is a damage term related to the cumulative normalized energy

absorbed in the specimen. The fact that the damage equation is non-dimensional allows a comparison between columns of various geometries and load histories.

Taylor and Stone developed three damage thresholds: yield, ultimate, and failure. The yield damage threshold is at first yield of the longitudinal steel, ultimate corresponds to the point where maximum lateral load or moment occurs, and failure is defined as the point where column resistance drops to below 80% of the maximum observed value. A total of 82 spiral-reinforced bridge piers were analyzed using the IDARC program so as to determine an acceptable definition of the damage indices for the three damage states. By analyzing the columns three times each, (1) exploring the cumulative damage until first yield, (2) starting from the virgin state until ultimate load, and (3) starting from the virgin state until failure, and statistically analyzing the data via histograms, acceptable damage indices were derived. The acceptable damage index for yield was found to be 0.11, for ultimate, 0.40, and for failure, 0.77. In addition, three-dimensional damage surfaces for highly important and moderately important bridges were prepared which describe the interaction of earthquake moment magnitude, epicentral distance, and damage index. These surfaces would be compared to the results of inelastic analysis described below to examine the effectiveness of a given retrofit.

To determine the effect of column jacketing on the alteration of structural performance, a parametric study was conducted. The parametric study examined columns under earthquake moment magnitudes,  $M$ , of 5.0, 6.0, 7.0 and 8.0; epicentral distances of 10 km, 20 km, 30 km, 40 km (6.2 mi, 12.4 mi, 18.6 mi, 24.9 mi); height/diameter ( $L/D$ ) ratios of 3, 6, and 9; diameters of 610 mm, 920 mm, 1,220 mm, and 1,520 mm (24 in., 36 in., 48 in., 60 in.); and jacket thickness of 0 mm, 2 mm, 4 mm, 6 mm, 8 mm, 10 mm (0 in., 0.08 in., 0.16 in., 0.24 in., 0.31 in., 0.39 in.). This matrix of tests comprises a total of 1,152 simulations. The base time history for this simulation is the 1971 San Fernando Record recorded at 410 South Grand. This time history was chosen because when scaled for epicentral distance, it closely matched empirically derived response spectrums proposed for the West coast. Additionally, the columns had the following properties. The cylinder strength was selected to be 24 MPa (3.5 ksi); reinforcing yield strength was 276 MPa (40 ksi); ultimate reinforcing tensile strength is 386 MPa (56 ksi); longitudinal reinforcing ratio equals 1%; spiral bars were 16 mm (#5) diameter with variable pitch with an "as-built" pitch of 92 mm (3.6 in.); and cover is 50 mm (2 in.). The effect of the steel jacket was accounted for by converting the steel jacket into an equivalent spiral pitch so as to provide the same volumetric confining ratio. The jacket is assumed to not affect the longitudinal steel ratio.

As a by-product of the simulations, a family of curves was developed that shows the maximum acceptable damage for moderately important and highly important bridges as well as the damage index predicted as a result of the inelastic time history analysis as a function of earthquake magnitude. Results presented in Taylor and Stone (1993) indicate the following. For a 610 mm (24 in.) diameter column with an  $L/D$  ratio of 6, epicentral distance of 10 km and  $M > 7$ , jacketing is ineffective regardless of thickness in preventing damage due to the effects of resonance; reduction in damage is proportional to the epicentral distance; and for situations where resonance will not occur, i.e., epicentral distance  $> 20$  km (12.4 miles), steel jackets as thin as 2 mm (0.08 in.) have a dramatic effect in decreasing the damage index. Furthermore, the change in damage index is less than directly proportional to change in jacket thickness especially at greater epicentral distances. Some situations occur where the jacket is unable to provide a dramatic enough reduction in damage index so that the structure will meet the interaction surface requirements established for highly important bridges. For tests where  $L/D$  equals 9 and the only variable that changed was column diameter, damage is proportional to column diameter with large diameter columns suffering the most damage. Retrofitting has a more pronounced effect on large

diameter columns. Similar trends in diminishing effects of jacket thickness can be seen except for the 1,520 mm (60 in.) column where the thicker jackets eliminate resonance effects. Taylor and Stone use this example to justify conducting site specific analysis and not relying on blanket retrofit techniques or design philosophies.

Retrofit by steel jacketing also has a more significant effect on squat columns (low  $L/D$ ) that are shear dominated. For these columns there was an immediate 50% drop in D.I. with the application of a 2-mm (0.08-in.) jacket, and thicker jackets do provide significant effects. The allowable D.I. was exceeded in these retrofit columns when  $M > 7.5$ . In general for  $L/D > 6$ , the study in question illustrated that a 2-mm (0.08 in.) jacket was sufficient to provide acceptable damage levels for important structures.

Taylor and Stone caution that in light of the column retrofit, the effects of the retrofit on forcing failure into other locations of the structure should be investigated.

## SECTION 3 COMPOSITE JACKETING

### 3.1 Introduction

Although research in the use of composite materials for seismic retrofit is the dominant area of publication and research in concrete column strengthening at this time, it is a relatively new area. The earliest paper presented in the bibliography accompanying this report pertaining to composites is by Katsumata, Kobatake, and Takeda (1988). The majority of information in this area has been presented in the past five years. Research in the United States has primarily been concentrated in California because of the vast infrastructure in that area that is earthquake prone. However, field installations of composites as a means of addressing potential earthquake damage are not limited to that state alone. Other states such as Nevada, Illinois, Pennsylvania, and New York have successfully installed composite retrofits as pilot projects or as standard seismic retrofit solutions. This chapter addresses laboratory test results, field test results, analytical investigations, earthquake and structural performance of composite retrofits, environmental performance, and economic issues. In addition, discrepancies in design processes and philosophy because composites are much newer materials in the civil engineering field than steel, concrete, masonry, timber, etc., will be highlighted when appropriate and possible.

To assist in the understanding of composite strengthening, a brief introduction of the types of materials, material strengths, and means of construction is presented.

### 3.2 Material Types and Strengths

The field of composites comprises literally hundreds of different material types. However, only a few of these materials are common in civil engineering applications: glass fibers, carbon fibers, and aramid fibers in descending order. Composite materials are almost universally linearly elastic until failure and derive their overall properties from the volume fractions and material properties of the constituent materials, the fibers, and matrix. Unless otherwise indicated, the information in Section 3.2 is derived from Agarwal and Broutman (1990).

#### 3.2.1 Fiber Properties

Glass fibers are the most commonly used composite fiber in the civil engineering industry. The most commonly used glass fiber is an E-glass fiber, which in continuous form have material strengths as follows: density, 2.54 g/cm<sup>3</sup> (0.58 oz/in.<sup>3</sup>); tensile strength, 3,447 MPa (500 ksi); elastic modulus, 72.4 GPa (10,500 ksi); and range of diameters, 3-20  $\mu$ m (1.2x10<sup>-4</sup> in. to 7.87x10<sup>-4</sup> in.). The usable value for tensile strength may only be 50% to 75% of these values in a finished product. Note that fibers in and of themselves have no transverse strength and stiffness properties. It is only when combined with a matrix (binder) material that transverse properties are developed.

Glass fibers are available in a number of forms in this research, e.g., glass sheets and prefabricated glass column jackets made from continuous rovings. A roving is a series of continuous fibers aligned and twisted together in specified number so that a certain length per unit weight is achieved. Rovings may be woven together to form fiberglass sheets or may be used in the filament winding of large, generally cylindrical, pieces.

Carbon fibers are produced through a burning process that uses organic precursors whereby all organic material except the carbon is burned off during manufacturing. The three most common organics used as precursors are polyacrylonitrile (PAN), rayon, and pitch with the pitch fibers being the least expensive followed by PAN, and finally, rayon fibers, which are very expensive. The material properties of pitch-based carbon fibers are tensile strength, 1,550 MPa (225 ksi); tensile modulus, 380 GPa (55,114 ksi); and fiber diameter, 10-11  $\mu\text{m}$  ( $3.94 \times 10^{-4}$  in. to  $4.33 \times 10^{-4}$  in.). Carbon fiber, like glass, is available in a number of forms. The most common forms are tows, yarns, rovings, and tape.

A tow is a series of straight-laid fibers and is designated by the number of fibers per tow, i.e., a 12k tow has 12,000 filaments per tow. A yarn is a twisted tow. A tape is a number of tows or yarns, i.e., 300, laid side-by-side on a backing material or stitched together.

Aramid fibers, commonly known by the trademark name, Kevlar, are a very high-strength fiber but with relatively low modulus. Common properties of Kevlar 29 are tensile strength, 2,760 MPa (400 ksi); tensile modulus, 62 GPa (8,992 ksi); and fiber diameter of 12  $\mu\text{m}$  ( $4.72 \times 10^{-4}$  in.).

Information presented in Wallenberger (1994), which discusses the past, present, and future uses of composite materials in the infrastructure, includes economic and material comparisons between several composite materials. Wallenberger states that the most commonly used composites in the area of infrastructure rehabilitation are glass fibers, such as E-glass, and carbon fibers. E-glass fibers are characterized by a cost of \$2/kg. Carbon fibers, such as Thornel 300, are an intermediate cost product at \$18/kg. Aramid fibers are the most expensive, \$35/kg. In addition to these common composite fibers, Wallenberger presents information on a new class of glass-ceramic fibers intended to be price-competitive with traditional glass fibers while possessing a modulus closer to that traditionally attributed to carbon fibers. Wallenberger believes that these new fibers, with a modulus of 170 GPa, 2.4 times that of glass and 75% that of carbon fibers, coupled with a cost of \$4.4/kg, only 2.0 times that of glass and 1/4 that of carbon, will represent a viable alternative in the field of infrastructure rehabilitation.

Brown (1992) indicates that based on Caltrans cost data available at the time the reference was published in 1992, composite fiber-epoxy jackets cost approximately 10% less than a comparable steel jacket.

### **3.2.2 Matrix Properties**

As mentioned previously in the discussion on glass fibers, the fiber only becomes useful as a structural component when combined with a matrix material. The matrix material is in general very compliant and will significantly influence the overall strength of the composite, tempering to a large degree, the extremely high-strength values of the fibers alone. Typical values for a polyester resin, a common matrix material are presented below. The tensile strength can vary from 34.5 MPa to 103 MPa (5,000 psi to 15,000 psi) and tensile modulus from 2 GPa to 4.4 GPa (290 ksi to 638 ksi). Another common matrix material, an epoxy resin, has a tensile strength of 55 MPa to 130 MPa (7,980 psi to 18,855 psi) and a tensile modulus of 2.75 GPa to 4.10 GPa (400 ksi to 595 ksi).

### **3.2.3 Composite Properties**

Composites, in general, are materials with different material strengths and stiffness depending on the direction of load, i.e., longitudinal or transverse. Depending on the orientation of multiple layers of materials, composites can be considered nearly isotropic (known as quasi isotropic), orthotropic, or

anisotropic. With the knowledge of the directional dependence of material properties and the influence of the properties of the fiber and matrix material on overall composite strength and stiffness, the following results are presented as typical of commonly encountered fiber-reinforced composites.

For a unidirectional composite composed of E-glass fibers and an epoxy matrix, where the volume fraction of fibers is 45% of the total volume of the composite, the following strengths and stiffnesses can be obtained: longitudinal modulus,  $E_L$ , 38.6 GPa (5,600 ksi); transverse modulus,  $E_T$ , 8.27 GPa (1,200 ksi); major Poisson's ratio relating transverse strain to longitudinal stress,  $\nu_{LT}$ , 0.26; shear modulus,  $G_{LT}$ , 4.14 GPa (600 ksi); ultimate longitudinal strength,  $\sigma_{LU}$ , 1,061 MPa (154 ksi); ultimate transverse strength,  $\sigma_{TU}$ , 31 MPa (4.5 ksi); and ultimate shear strength,  $\tau_{LTU}$ , 72 MPa (10.4 ksi).

For the carbon-epoxy composite with a fiber fraction of 60%, the following properties can be considered representative of commercially available products:  $E_L$ , 148 GPa (21,467 ksi);  $E_T$ , 9.65 GPa (1,400 ksi);  $\nu_{LT}$ , 0.30;  $G_{LT}$ , 4.55 GPa (660 ksi);  $\sigma_{LU}$ , 1,314 MPa (191 ksi);  $\sigma_{TU}$ , 43 MPa (6.7 ksi);  $\tau_{LTU}$ , 48 MPa (7 ksi).

Comparison of the composite values to the original fiber values clearly illustrates the dramatic decrease in strength and stiffness of the overall composite as a function of the volume fraction occupied by the matrix material.

A general categorization of the influence of the fibers and matrix on the strength and stiffness of composites is that the property of the fibers dominates longitudinal strength and stiffness while the matrix properties dominate the transverse strength and stiffness. The in-plane shear modulus and shear strength are also heavily dominated by the properties of the matrix material.

### 3.2.4 Effect of Fiber Orientation on Expected Performance

The information presented in Section 3.2.3 clearly indicates that a unidirectional fiber composite, one in which all fibers are aligned, has a dramatic difference in strength if the load is applied parallel to the fibers as opposed to perpendicular to the fibers. To counteract these poor transverse properties, a stacking sequence can be adopted where alternate layers are rotated to a prescribed orientation with the axis of the load. Certain combinations of layer orientation and stacking sequence generate quasi isotropic materials, while the same layer orientations simply rearranged or of variable thickness generate anisotropic results. Therefore, the orientation of fibers and the sequence of layer construction is a critical parameter in assessing the possible benefits of a given laminate. In general, fiber composite jackets for concrete columns will have most or all of their fibers aligned in the circumferential direction. This scenario provides the greatest concentration of fibers in the hoop direction so as to constrain column dilation under bending and axial effects and also for the purpose of enhancing shear strength.

The results of several studies describing the general performance of concrete confined with composites of differing properties is described below as a prelude to the column retrofit results.

The effect of composite fiber alignment on the efficiency of the wrap is presented in Howie and Karbhari (1994). Two types of specimens were studied. First, tensile specimens were constructed using the fiber orientations chosen for application to standard test cylinders. Secondly, unreinforced concrete test cylinders were tested in order to investigate wrap orientation efficiency and failure modes. Nine different wrap orientations were studied consisting of the following orientations:  $[0]$ ,  $[0]_2$ ,  $[0]_3$ ,  $[0]_4$ ,  $[90/0]$ ,  $[0/90/0]$ ,  $[+45/-45]$ ,  $[90,+45/-45/0]$ , and  $[+45/-45]_2$ . This standard laminate orientation indicates wraps of

1, 2, 3, and 4 layers of 0 degree oriented fibers, a wrap with a 90 and 0 degree layer, a wrap with fibers oriented at  $\pm 45$  degrees to the specimen axis, a wrap with one 90, 45, -45, and 0 degree layer and finally a wrap with four total layers of alternating  $\pm 45$  degree orientation. The 0 degree axis was defined as the circumferential axis of the cylinder. In specimens where a mixture of orientations was applied, the 0 degree layer was the outermost layer. Each wrap type was applied to three cylinders for a total of 27 tests. Four 0/90 strain gages were used on each cylinder and three on control cylinders. One gage was placed on the cylinder just above the end of the wrap, another immediately below the first on the wrap, a third below these two on the central region of the cylinder and a fourth located 90 degrees around the cylinder from gage 3 and rotated 45 degrees. The first three gages were used for measuring axial and hoop strains while the fourth was used to collect shear strain data.

Analysis of the load displacement curves of the cylinders shows them to be bilinear with the first linear portion having essentially the same slope as an unwrapped specimen and the second part of the bilinear curve having a much flatter slope than the first. The intersection of these two lines is termed the kink point. The second linear portion of the curve terminates at failure of the specimen. Results of the study indicate that the best possible orientation for the composite wrap is one where the largest amount of fiber is placed in the hoop direction. For instance, the maximum increase in strength of a wrapped cylinder to an unwrapped control specimen was the  $[0]_4$  specimen which exhibited an increase in strength of 140%. The lowest amount of strength gain was from the wraps with only  $\pm 45$  degree orientations.

An experimental and analytical examination of the effect of composite materials on the strengthening of standard concrete cylinders was conducted by Bavarian et al. (1996). Concrete cylinders were constructed in the following sizes; 75 mm x 150 mm (3 in. x 6 in.), 100 mm x 205 mm (4 in. x 8 in.), and 150 mm x 305 mm (6 in. x 12 in.), and tested after 28 days in a lime cure tank. Similar cylinders were cast and wrapped with an S-glass and isophthalic polyester resin combination as well as a Kevlar-29 and epoxy resin combination. Both the S-glass and Kevlar were 51 mm (2 in.) wide and  $7.87 \times 10^4$  mm (0.02 in.) thick woven tapes with fiber orientations of 0 and 90 degrees. There was a 10% overlay wrapped 15 degrees to the cylinder axis. Each cylinder was wrapped with either two, three, or four layers of tape.

A number of different test types were conducted. Standard uniaxial load tests were conducted so as to acquire load-displacement information as well as longitudinal and circumferential strains. Cyclic loading tests were conducted with a load ratio of 0.3 and the maximum stress set above the unconfined compressive strength of the concrete cylinder. Maximum and minimum displacements were recorded during the controlled loading of the cylinder. Salt spray tests were conducted at elevated temperatures in order to detect environmental effects on the system. In addition, finite element analysis using the I-DEAS program was carried out on a series of S-Glass retrofit specimens.

Compression tests on the virgin specimens showed ultimate stress values of 25 MPa to 29 MPa (3.6 to 4.2 ksi) with an ultimate strain of 0.5% - 0.6%. The effect of S-glass reinforcing is significant with an increase in strength and ductility of approximately 100% with four layers of tape. It was noted that as cylinder size increases, the ultimate strength decreases with a drop of 15% being noted between the smallest and largest cylinder sizes. Although the authors were concerned about the problems that would be encountered when these results were extrapolated to full-size specimens, they indicate that this problem could be compensated for by applying a greater number of layers to the larger specimens. The Kevlar-wrapped specimens showed an increase in ultimate strength of a factor of three, up to 83 MPa (12 ksi), and an increase in ductility of five to six. The size effect mentioned previously was present with the largest cylinders having a strength increase some 12% less than the smallest cylinders. In addition, a

sample with two layers of Kevlar was tested to failure and then retested. This specimen exhibited strength and ductility approximately twice that of a virgin unreinforced specimen and thus demonstrated the significant reserve capacity against collapse even after first failure.

The fatigue tests were performed on a 100 mm x 205 mm (4 in. x 8 in.) specimen wrapped with two layers of Kevlar-29. The maximum load applied was 80% of the maximum strength of the specimen and the minimum load was 89 kN (20 kips). No failure was observed after 10,000 cycles but a subsequent compression test to failure resulted in an ultimate compressive stress of 41 MPa (6 ksi) and an ultimate strain of 1%. These values, less than those observed in pure compression testing, are possibly attributable to micro-cracking of the core, debonding of the layers, or resin softening due to the temperature increase which accompanies the cyclic loading.

The salt spray tests on Kevlar and S-glass wrapped specimens were conducted with a 5% NaCl solution at a temperature of 48.9° C (120° F) applied continuously in a salt spray chamber for 28 days per ASTM B117. Compression tests on these samples did not demonstrate a degradation in strength, which indicates that composite materials can not only be used as a means of strengthening columns but also protecting them in an aggressive environment.

Finite-element analysis of concrete samples wrapped with S-glass was carried out using the same 445 kN (100 kip) load applied in the cylinder tests, which is above the load that corresponds to the unconfined strength of the cylinders. Use of a linear model showed that the maximum concrete stress, maximum concrete strain, maximum fiberglass stress, and maximum fiberglass strain all decreased with an increase in the number of layers from zero to three. The cone-type failure observed in the experimental portion of the study was also observed in the analytical portion of the study after an examination of the von Mises stress contours.

Results of this experimentation showed that both S-glass and Kevlar-29 were effective in enhancing the ultimate stress and strain of concrete specimens and that the finite element model was adequate in illustrating the failure mode and interaction of the concrete and composite material.

### **3.2.5 Methods of Construction**

A common procedure for construction of large fiber composite pieces involves the hand placement of composite sheets or tape over the designated surface. Prior to placement the sheets are saturated with the resin material which forms the matrix of the laminate. This procedure is known as a wet hand lay-up procedure because the wet resin is applied to the fiber before application and is commonly used in the glass fiber retrofits described in this document. This process can be semi-automated with the aid of machines that will wrap the saturated material around the column.

Carbon fibers are commonly supplied in what is known as prepreg (pre-impregnated) form. Prepreg consists of carbon fiber sheet, tape, or tow, preimpregnated with an excess amount of resin. This resin sufficiently binds the material together during construction so that it maintains its original shape. These materials are then subjected to a period of elevated temperature so that the resin can soften, bleed through the entire composite, and bind the material together. An example of prepreg tow application is cited later in this section when the results of tests on the XXsys Co. Robo-Wrapper automated column winding technique are presented. In short, this technique consists of a machine that when set up around a column,

wraps the column to predetermined thickness and height with prepreg carbon tows. The use of carbon fibers is not however restricted to prepreg forms. Wet lay-up procedures also exist.

Depending on the type of retrofit required, the construction of composite jackets usually takes one of two general forms: active or passive retrofitting. Active retrofit, analogous to the grouted steel jacket retrofits discussed in Section 2, consists of the installation of a slightly oversized composite jacket; and upon cure of the jacket, injection of the void between the jacket and column with a grout. A procedure cited in this document for accomplishing this active pressurization requires installation of a deflated elastomeric bladder around the column prior to composite wrapping. Following jacket cure, grout is injected into ports in the bladder so as to induce radial pressure on the column and jacket along with hoop stresses in the jacket. The active jacket is intended to be used when radial pressure is required at the column base to promote lap splice force transfer.

A passive retrofit, as the name implies, is one that does not undergo a prestressing operation. The composite is simply placed snug around the surface of the column and does not possess a significant degree of circumferential stress until the column's concrete begins to dilate.

The use of a modified construction process for composite material wrapping is introduced in Karbhari, Eckel, and Tunis (1993). This reference describes the use of a resin infusion process and the results of a series of tests on concrete cylinders indicating the effectiveness of various wrap materials and architectures.

Most other composite retrofit techniques employ some variation of a hand lay-up procedure whereby the composite is wet coated with a resin material prior to its being wrapped onto the surface to be repaired. Karbhari, Eckel, and Tunis assert that a major disadvantage of this approach is that it does not provide adequate nor uniform compaction of the composite wrap on the column surface. The resin infusion process is one in which the (1) composite material is first placed on the part to be retrofit or manufactured, (2) a vacuum bag is placed around the part and a vacuum created, and (3) the composite is coated with resin. The resin, introduced into the vacuum bag via injection ports and drawn through the entire part via vacuum pressure, allows for the infiltration of very large parts in a short period of time, provides very uniform wetting and fiber compaction, and is virtually emission free in contrast to many other composite manufacturing processes.

Having tested five cylinders constructed with the resin-infusion process, Karbhari, Eckel, and Tunis concluded that the process was superior to traditional wet lay-up processes in that the wrap was more consolidated, provided a higher degree of confinement, possessed more uniformity in quality and appearance, and was environmentally superior because it was a closed process.

### **3.3 Laboratory Test Results**

This section on laboratory testing, similar to the presentation in Section 2.2 on steel jacket test results, constitutes the vast majority of information on composite jacketing. A typical laboratory experiment consists of the construction of a reduced-scale column specimen, which is tested under a constant axial load and variable cyclic loading. The cyclic load is applied and column displacement monitored during testing so that the onset of longitudinal column steel yield can be determined. Once yield is achieved, the applied loads are introduced by means of the imposition of prescribed displacement levels. In general, a pattern of cycles is imposed, with several cycles per ductility level and ever increasing levels of ductility

until either the column fails or satisfactory performance has been demonstrated. Several references also report that the retrofit response was stable all the way up to the capacity of the test equipment indicating that the true strength of the retrofit is not known in these samples. The nomenclature adopted for the commonly reported displacement ductility in this report is  $\mu_{\Delta}$ . This term represents the ratio of the actual to yield displacements at the level of lateral loading. A much less frequently cited term is  $\mu_{\phi}$ , the curvature ductility of the plastic hinge. This term is the ratio of the measured curvature to the yield curvature in the plastic hinge region.

### **3.3.1 Composite Jacket Retrofit of Flexurally Deficient Bridge Columns**

Results of numerous studies pertaining to the retrofit of flexurally deficient bridge columns are presented. Retrofits will be further divided into sub-sections that deal exclusively with the results of tests on circular and rectangular columns to facilitate locating the desired information more easily.

#### **3.3.1.1 Circular Flexural Columns**

The first retrofit solution for circular flexural columns presents information from numerous references pertaining to the use of hybrid glass fiber and aramid fiber sheets in the retrofit of concrete bridge columns for enhanced seismic performance. These references include: (Brown, 1992), (Civil Engineering, 1994), (Daily Journal of Commerce, 1995), (Fyfe and Kuruvilla, 1993), (Fyfe, 1994a, 1994b, 1995), (Fyfe, Watson, and Watson, 1996), (Hawkins, Patel, and Steckel, 1995, 1996), (Hexcel Fyfe, 1995), (McConnell, 1993), (Priestley, Fyfe, and Seible, 1991), (Priestley, Seible, and Chai, 1992a), (Priestley, Seible, and Fyfe, 1994), (Priestley and Seible, 1995), (Priestley, Seible, and Calvi, 1996), (Seible, 1993a), (Seqad Consulting Engineers, 1992, 1993), and (University of California, 1991) and pertain to the TYFO S Fibrwrap System as designed and installed by the Hexcel Fyfe Co. The information presented in these reports is also contained in the form of design recommendations in Federal Highway Administration (1995). Not all of these references are specifically cited because of the duplication of information in original reports, subsequent conference papers, journal proceedings, etc. or because some are not pertinent to the discussion on circular, flexurally deficient bridge columns.

In the early 1990s, the Hexcel Fyfe Co. endeavored to develop a retrofit system for concrete columns that would provide the desirable features of steel jacketing, namely, an extremely stable response with high levels of displacement ductility. The outgrowth of this research was the TYFO S Fibrwrap system for retrofitting concrete columns.

The Fibrwrap system is based on application of a woven fabric composed of glass fiber and aramid fibers. This fabric is known as SEH51. The epoxy, TYFO S, is a two-part ambient cure epoxy composed of constituents known as TYFO A and TYFO B. The fabrics are generally supplied to a job site in rolls that are 1.37 m (4.5 ft) in width and 47.72 m (150 ft) long (McConnell, 1993). The fabric is passed through an epoxy resin saturator and can be placed by hand or by means of mechanical aids on the surface of the column. The wrap consists of fibers which are 85% glass and 15% aramid (Kevlar) oriented so that approximately 95% of the fibers are aligned with the column circumference. The total thickness of the wraps ranges anywhere from 13 mm (1/2 in.) to 100 mm (4 in.). The wrap is placed in either an active or passive state.

An active wrap is constructed with its main fiber strength circumferentially oriented around the column over an elastomeric bladder. Once the fibers are allowed to cure at room temperature, the elastomeric

bladder is filled with grout to an internal pressure of 690-1380 kPa (100-200 psi). This places the composite in a state of hoop tension which preconfines the concrete column. After the grout hardens, the active wrap is overlaid with additional layers of composite in a passive state.

Professors M. J. N. Priestley and Frieder Seible as well as other investigators tested this system extensively at the University of California, San Diego. Priestley, Seible, and Fyfe (1994) discuss the use of a fiberglass/epoxy jacketing system for use in the retrofit of circular columns. These columns were constructed with lap splices of insufficient length,  $20 d_s$ , at the bottom of the column. This is typical of column construction in the time period of 1950-1970. The results from Priestley, Seible, and Fyfe (1994) are also reported in a number of other references, including: (Brown, 1992), (Fyfe and Kuruvilla, 1993), (Fyfe, 1994a, 1994b, 1995), (Priestley, Fyfe, and Seible, 1991), (Priestley, Seible, and Chai, 1992a), (Priestley and Seible, 1995), (Priestley, Seible, and Calvi, 1996), and (University of California, 1991).

In Priestley, Seible, and Fyfe (1994), three columns were constructed with diameters of 610 mm (24 in.), and clear height to the load point of 3.66 m (12 ft). Reinforcing consisted of twenty-six, 19 mm diameter (#6) reinforcing bars lap spliced at the base. Transverse reinforcement consisted of 6 mm (#2) hoops lap spliced in the cover concrete and spaced vertically at 125 mm (4.9 in.). The reinforcing steel had a yield strength of 315 MPa (45.7 ksi). The nominal concrete strength was 34.5 MPa (5 ksi). The columns were 0.4 scale models of prototype construction. Information regarding the axial load used in these tests is found in a description of the "as-built" specimen in Priestley, Seible, and Chai (1992a). The load consisted of a constant axial load of 1,779 kN (400 kips). The columns were constructed as vertical cantilevers subject to single bending.

For the retrofit, a combination of active and passive fiberglass wraps was applied to the columns. The active wrap consisted of an elastomeric bladder placed over the region to be retrofit prior to the placement of the wrap. The wrap was placed so that the fiber orientation was in the circumferential direction. Upon initial cure of the "active" layers, the elastomeric bladder was injected with grout, which induced radial pressure on the wrap and column and strains in the jacket fibers. These radial pressures are required to preserve the integrity of the force transfer mechanism of the lap splice. Excessive dilation of the cover concrete prohibits the lap splice from transferring load. The passive layers are placed after the pressure grouting is complete and will only be strained as the concrete dilates under load.

For column 1, eight layers of E-glass wrap having an active thickness,  $t_a=2.44$  mm (0.096 in.), along a height of 1,220 mm (4 ft), 33% of the column height, were pressure grouted with an epoxy grout in order to achieve a confinement stress of 1.7 MPa (250 psi). The passive wrap had a thickness of  $t_p=3.25$  mm (0.128 in.), and was placed over the bottom 305 mm (1 ft) of the column.

Column 2 was similar to column 1 in that an active wrap extended over the lower 33% of the column height. However, the active thickness was reduced to 4 layers,  $t_a=1.22$  mm (0.048 in.), and the epoxy grout pressure to 0.69 MPa (100 psi). The passive wrap was the same as for column 1.

For column 3, the grout type was changed from epoxy to cement. During grouting, the jacket fractured at a grout pressure of 1.4 MPa (203 psi). The authors believed this was a procedural problem due to high pumping speeds and was not an inherent weakness of using cement grout. To avoid recurrence in the test column, researchers changed the active thickness to six circumferential layers providing  $t_a=1.83$  mm (0.072 in.) with an additional two layers of vertically oriented fibers. The active pressure was 1.38 MPa (200 psi). Earlier tests on columns 1 and 2 did not show problems at the upper end of the jacket.

Consequently, the passive jacket was reduced from 1,220 mm (4 ft) to 915 mm (3 ft) in height with the wrap thickness remaining the same.

Column 1 testing indicated stable hysteretic response up to  $\mu_{\Delta} = +8, -6$ . Behavior was similar to that of a steel jacket retrofit reported in Chai, Priestley, and Seible (1991d) and in Section 2.2.1.1 of this report. Structural degradation did not occur in the fiberglass/epoxy retrofit until significantly higher ductility levels than in an equivalent steel-jacketed column, probably because of more effective confinement at the column base and a spread of plasticity in the column due to a lesser degree of stiffness enhancement in this retrofit scheme, according to the authors.

The column 2 test results were similar to column 1 until a lateral displacement of 150 mm (5.9 in.),  $\mu_{\Delta} = \pm 6$ , when the peak lateral loads per cycle began to degrade due to bond failure. Although degradation was apparently stabilizing at  $\mu_{\Delta} = \pm 7$  due to clamping pressure on the lap splice, pinching of the hysteresis loops was noted, which resulted in a lesser amount of dissipated energy per cycle.

The behavior of column 3 was similar to that of column 2 despite the increased confining stress except that degradation was more gradual and stabilized at a higher force level. Column 3 was tested to a higher displacement level than column 2.

The load displacement curves for these three columns were plotted along with a theoretical load deflection curve for the 34.5 MPa (5 ksi) nominal strength concrete used in these experiments. The ideal lateral strength based on  $f'_c = 34.5$  MPa (5 ksi),  $f_y = 315$  MPa (45.7 ksi), and ultimate strain of 0.006, was also plotted on the graphs based on a confined concrete model by Mander, Priestley, and Park (1988b). In all three cases, the columns exceeded the ideal lateral strength, even at large displacement levels, and closely followed the theoretical load deflection curve.

The results of experimental tests conducted at the University of Arizona are presented in the following paragraphs. The investigation was a combined analytical and experimental testing program established to determine the performance of circular and rectangular columns under cyclic loading. The experimental results (Jin, Saadatmanesh, and Ehsani, 1994) as well as (Saadatmanesh, Ehsani, and Jin, n.d., 1996a and 1996b), are presented in the following text while the analytical results (Saadatmanesh, Ehsani, and Li, 1992, 1994), and (Saadatmanesh, 1994) are presented in Section 3.5.1 of this report. Because the experimental and analytical tests were on a variety of specimen types, the results are presented in various parts of this Section. As a consequence, a general introduction will be provided for all test types in the following text so that the information does not need to be repeated.

In the experimental program, fourteen columns with a 20% scale factor, seven rectangular and seven circular, were tested under inelastic cyclic load with a constant axial load. Ten specimens were actually constructed, four of which would be tested in an "as-built" and in a repaired condition in order to constitute the total of fourteen tests. The retrofit material chosen was an E-glass composite. E-glass straps of three different fiber volume fractions: 25.4%, 50.2% and 74.0%, were constructed. The properties of the straps are as follows.

The 25.4% fiber volume strap had a tensile strength of 281 MPa (40.8 ksi), a tensile modulus of 9.07 GPa (1,316 ksi), and an ultimate strain of 0.031. The 50.2% fiber volume strap had an ultimate tensile strength of 532 MPa (77.2 ksi), an tensile modulus of 17.75 GPa (2,575 ksi), and an ultimate strain of 0.030. Finally, the 74.0% fiber volume strap had a tensile strength of 814 MPa (118 ksi), tensile modulus

of 29.05 GPa (4,214 ksi) and an ultimate tensile strain of 0.028. These results are characteristic of composite materials in that the volume fraction of the stiffer and stronger fibers dominates the overall tensile strength and modulus of the composite. It is also true that the fibers have a lower failure strain than the matrix and increasing fiber volume fractions will produce lower ultimate strains.

The research program tested columns which were either flexurally deficient or shear deficient. Both passive and active retrofitting schemes were used for flexural enhancement. The passive retrofit involves directly wrapping the column with a series of composite straps. The active retrofit scenario involves circumferentially wrapping the concrete columns with slightly oversized straps and subsequently pressure injecting the gap with an epoxy resin so as to induce active hoop stresses in the straps and radial confinement to the column.

For the retrofit of shear deficient columns, a passive option was selected for tests on rectangular columns with an axial reinforcing ratio of 5.45%. The fiber straps were wrapped directly onto the face of the column.

As part of the research, data were also collected on the ability of composite straps to be used as a means of post-earthquake repair. In the repair testing, columns were first tested and then pushed back to their original positions. Following the chipping out of loose concrete and straightening of buckled bars if possible, new concrete was placed and the active retrofit scheme previously described applied.

For the five circular columns constructed, the diameter was 305 mm (12 in.) and the column height was 1,830 mm (6 ft) from the top of footing to the point of lateral load application. The longitudinal steel ratio was 2.48%. The column slenderness,  $kl/r$ , was 26.0. The transverse steel ratio was 0.1704%. The axial load was  $0.177f'_cA_g$ . Flexural capacity based on ACI equations was computed to be 101 kN-m (891 kip-in.).

The five rectangular columns were constructed as follows. The column cross section measured 370 mm x 240 mm (14.5 in. x 9.5 in.) and had a transverse steel ratio of 0.133%. The axial load was a constant  $0.145f'_cA_g$  and the flexural capacity computed to be 146 kN-m (1,291 kip-in.). Rectangular columns R-1 and R-2 had lap-splice column base details, a longitudinal reinforcing ratio of 2.70%, and a slenderness,  $kl/r$ , of 26. Columns R-3 through R-5 had continuous longitudinal bars, a longitudinal reinforcing ratio of 5.45%, and a slenderness,  $kl/r$ , of 24. For both circular and rectangular columns, the design concrete strength was 34.5 MPa (5 ksi) to account for the expected overstrength of older concrete columns, and the steel was selected to be 276 MPa (40 ksi) yield.

The various parameters which differentiate the ten columns from each other are presented in table 3-1. Columns in which starter bars were used included a  $20 d_b$  lap splice.

For both the active and passive retrofit scenarios, circular columns were wrapped with 6-layer straps with a total thickness of 5 mm (0.2 in.) and rectangular columns with 8-layer straps having a total thickness of 6.8 mm (0.267 in.) in the plastic hinge region. The plastic hinge region is a 635 mm (25 in.) region adjacent to the bottom of the column.

**TABLE 3-1 University of Arizona Composite Retrofit Column Specimens**

Cross Section	Test #	Type	Design Detail	Steel Ratio	Retrofit Type
Circular	C-1	Reference	Starter Bars	2.48%	N/A
	C-2	Retrofit 1	Starter Bars	2.48%	Passive
	C-3	Retrofit 2	Starter Bars	2.48%	Active
	C-4	Reference	Continuous Bars	2.48%	N/A
	C-5	Retrofit	Continuous Bars	2.48%	Passive
Rectangular	R-1	Reference	Starter Bars	2.70%	N/A
	R-2	Retrofit	Starter Bars	2.70%	Active
	R-3	Reference	Continuous Bars	5.45%	N/A
	R-4	Retrofit 1	Continuous Bars	5.45%	Passive
	R-5	Retrofit 2	Continuous Bars	5.45%	Passive

In carrying out the actual column tests, cylinders cast along with the columns at the time of construction were compression tested to determine the column concrete compressive strength. The columns were anywhere from 165 days to 445 days old at the time of testing and compressive strength varied from a low of 33.3 MPa (4,834 psi) in the youngest specimen to 38.5 MPa (5,580 psi) in the oldest. The mean strength was 36.2 MPa (5,251 psi) and the standard deviation, 1.5 MPa (218 psi). For the longitudinal steel, the average yield stress and strain were 358.5 MPa (52 ksi) and 0.0026. The average elastic modulus was measured to be 169 GPa (24,523 ksi) for the 13 mm (#4) reinforcing bars and 139.3 GPa (20,200 ksi) for the 16 mm (#5) reinforcing bars used in the model columns. The average ultimate stress varied from 524 MPa (76 ksi) for the 13 mm (#4) reinforcing bars to 556 MPa (80.6 ksi) for the 16 mm (#5) reinforcing bars.

Load testing was typical of most column retrofit test procedures. A series of low magnitude loads were applied until the onset of longitudinal steel yielding. Thereafter, the loading pattern was displacement controlled with fully reversed cyclic loads being applied. In general, two cycles at each displacement ductility level served as the applied displacement during the inelastic cycling. Results of the cyclic tests indicate the following.

Specimen C-1 began to degrade after the first cycle to  $\mu_{\Delta} = 1.5$  and a drop in axial load was noted at  $\mu_{\Delta} = 3.0$ . The maximum lateral load of 58 kN (13.1 kips) was on the first push cycle to  $\mu_{\Delta} = 1.5$ . Columns C-2 and C-3, with passive and active retrofits, respectively, showed stable response to  $\mu_{\Delta} = 6$ . The maximum lateral strength of 82 kN (18.5 kips) for C-2 represents a 41% increase over the "as-built" specimen. The increase in capacity was even greater for the active retrofit than for the passive retrofit. The overall strength increase provided by the retrofits shows that C-2 and C-3 exhibited an increased lateral capacity of 41% and 53% over "as-built" C-1.

In addition to assessment of strength deterioration over the life of the test, stiffness deterioration was examined by comparing the stiffness at each cycle to the initial stiffness. All of the circular and rectangular columns saw their stiffness at the initial cycle reduced considerably through subsequent inelastic displacement cycles as would be expected. However, the retrofit specimens had a slower rate of stiffness deterioration than did the "as-built" specimens.

Moment curvature loops were plotted for the columns. For retrofit columns C-2 and C-3, the curvature increased significantly after longitudinal steel yield, but the bending moment remained nearly constant. Conversely, the moment curvature response for the "as-built" specimens is characterized by poor performance due to concrete crushing before the onset of steel yield.

Examination of the hysteresis loops of all test specimens showed varying degrees of pinching, which was amplified in columns with lap-spliced bars where the narrowing near the origin is due to longitudinal lap splice slippage.

During the initial test program, a number of columns were selected for repair testing. The repaired columns were subjected to the same loading as the original specimens. The load-displacement envelope of the repaired column was plotted simultaneously with the original test results for comparison. The average stiffness per cycle was also computed for comparison purposes. Results of the test of column C-1/R demonstrated a lateral load strength increase of 24% over the original C-1. However, results of lateral load comparisons are not in and of themselves representative of the overall effects of the repair.

For instance, column C-1, when originally tested, was only able to attain a stable response to  $\mu_A = 1.5$  while the repaired column, in addition to a significant lateral load increase, was able to maintain a stable response to approximately  $\mu_A = 4$ . C-1/R exhibited slight degradation in the load-displacement response at the end of the testing.

For circular columns with starter bars, C-1 had the poorest lateral load resistance and ultimate displacement, while C-1/R demonstrated performance substantially better than C-1 and almost as good as C-2 and C-3.

After testing was complete, the results of the experimental work described here was compared with the analytical studies (Saadatmanesh, 1992, 1994a, and 1994b) presented in Section 3.5. Results indicate that the analytical model used to generate the moment-curvature response plots for the columns is a reasonable analytical tool for predicting maximum curvature and moment. However, the model seemed to provide better results for the circular column than for rectangular columns. The model consistently under predicted the curvature in areas where the moment-curvature response was an ascending curve. Close agreement of analytical and experimental results was only evident in the horizontal portion of the moment-curvature response where the curvature increases rapidly with little or no increase in moment. Divergence of the analytical and experimental results was greater for rectangular specimens than for circular specimens. The explanation given below is one presented by the authors of this document and is not based on conclusions reached by Jin, Saadatmanesh, and Ehsani (1994) or Saadatmanesh (n.d., 1996a, 1996b).

A possible explanation for the divergence in the ascending portion of the moment-curvature response is that the model is a modified version of that proposed by Mander, Priestley, and Park (1988b), and is based on a constant lateral confining stress equal to the fracture stress in the straps. For the scenario

where passive retrofits are used in particular, the assumption that the straps have a hoop strain or stress equal to that at fracture is not valid in areas of ascending moment. The passive, and even active retrofits, must undergo concrete dilation before the strap reaches its fracture strain; and consequently, the amount of confinement is less than that which is assumed in the model. Smaller amounts of confinement result in less confinement of the lap splice and consequently, bond slip may be occurring before full confinement is mobilized. This could be an explanation for the fact that greater curvatures than predicted were observed before occurrence of nearly constant moment but rapidly ascending curvature.

In general, even with the minor discrepancy in analytical and experimental moment-curvature results in the ascending portion of the moment-curvature diagram, the experimental results clearly demonstrate that composite straps used as a jacketing material are not only an effective means of retrofitting existing deficient columns but also a viable means of repairing damaged columns to perform better in most cases than the original undamaged column.

The use of a prefabricated composite shell can also be employed as a column seismic retrofit. The particular system in question is the Snap-Tite™ Composite Column Reinforcement System. This shell is designed by NCF Industries (n.d.) and manufactured under license by CMI, Inc., Rancho Cordova, California.

The Snap-Tite system consists of a prefabricated E-glass shell constructed with an isophthalic polyester resin. The prefabricated shell is composed of E-glass fibers with an elastic modulus of 49.6 GPa (7,200 ksi) and fracture strain of 0.004 which corresponds to a fracture strength of 199 MPa (28.8 ksi). The layers are approximately 3 mm (1/8 in.) thick. This shell, whose height and diameter are variable, has a vertical slit in the jacket. For installation, an initial epoxy layer is applied to the column, the jacket slit is opened like a clamshell, and snaps shut once in place around the column. Additional layers of epoxy and shells are applied with alternating symmetric seams, until a desired thickness is attained. Then the system is bound together with a series of belts and clamps until it cures. This system has successfully been tested on 1/2-scale specimens in the laboratory of The University of Southern California (USC) (Xiao, Martin, Yin, and Ma, 1995a, 1995b, 1996) and also in the field on full size bridge columns by the Illinois Department of Transportation (Gamble, Hawkins, and Kaspar, 1995), (Lin, Gamble, and Hawkins, 1994), and (Shkurti et al., 1995) with very good results. These field installations are described in Section 3.4 of this report. Like most retrofits, the intent of the retrofit is to provide lateral confinement and a high degree of displacement ductility. The advantage of this system is its speed of installation and high quality. The quality control problems which can occur during hand lay-up, as well as other construction-related concerns, are eliminated with a prefabricated factory-controlled product such as the Snap-Tite system.

Xiao, Martin, Yin, and Ma (1995a), which is summarized in Xiao, Martin, Yin, and Ma (1995b, 1996), discusses the use of this system in a laboratory setting. Three specimens were constructed, one to be tested in the "as-built" condition, and two which were to be retrofit using the aforementioned system. The columns were to be 1/2-scale representations Fairfax-Washington Undercrossing on the I-10 Santa Monica Freeway which collapsed in the 1994, Northridge Earthquake. The specimens were 2,440 mm (8 ft) tall and 610 mm, (2 ft) in diameter. The columns were longitudinally reinforced with twenty, 19 mm (#6) reinforcing bars which constitute a longitudinal reinforcing ratio of 2%. These bars were lap spliced at the column bottom. Transverse reinforcement consisted of smooth 6 mm (#2) reinforcing bars spaced at 125 mm (5 in.) on center. The original columns were constructed with 276 MPa (40 ksi) reinforcing bars which were unavailable at the time of model construction. In lieu of the steel grade mentioned

above, nominal 414 MPa (60 ksi) reinforcing steel was substituted in its place. The actual measured yield and ultimate strengths of the longitudinal reinforcing was 462 MPa (67.0 ksi) and 672 MPa (97.5 ksi), respectively, and for the hoops, 379 MPa (55.0 ksi) and 531 MPa (77.0 ksi). This higher yield point steel will impose higher ductility demands on the column than the more mild steel bars present in actual columns in the field. The concrete strength was 45 MPa (6.5 ksi).

In Xiao, Martin, Yin, and Ma (1995a), the theoretical moment capacity of the "as-built" column was calculated based on the confined concrete model developed by Mander, Priestley, and Park (1988b). The yield moment capacity was reported to be 574 kN-m (5,082 kip-in.) and the ultimate moment capacity to be 755 kN-m (6,684 kip-in.). The lateral force required to produce the yield moment at the base was then calculated to be 3010 kN (69.6 kips). These lateral forces were less than the theoretical shear capacity of the column and thereby indicated that a flexural failure of the "as-built" specimen would be expected. The expected ductility factor for this column was  $\mu_{\Delta} = 2.0$ . These computations are predicated on the assumption that the longitudinal steel is continuous. Since that is not the case in the test specimens, assessment of the amount of transverse reinforcing required to inhibit lap-splice debonding was conducted. The conclusion was that the amount of reinforcing was insufficient to assure adequate force transfer and that the expected failure mode of the column would be a flexural failure characterized by lap-splice debonding.

For the design of the jacketed specimens, the confined concrete model in Mander, Priestley, and Park (1988b) was employed with the assumption that equivalent composite hoops were spaced at a unit distance. Using this confinement model and four layers of 3 mm (0.125 in.) jacketing, only three of which were deemed effective, a first yield moment of 566 kN-m (5,009 kip-in.) was calculated. In addition, the ideal flexural moment was computed to be 823 kN-m (7,286 kip-in.), the ultimate moment to be 1,037 kN-m (9,179 kip-in.), and the ultimate horizontal force to be 425 kN (95.6 kips). The corresponding displacement ductility computed on the basis of moment curvature analysis was 11.

On the basis of these computations, Xiao, Martin, Yin, and Ma decided that the jacket should be placed on the lower 1,220 mm (4 ft) of the column. To determine jacket height, one examines at what height above the column base would the "as-built" specimen have adequate moment capacity assuming that the moment is caused by the ultimate lateral load. Although high displacement ductilities were expected, this 4-layer retrofit was not sufficient to prevent eventual lap splice debonding. The moments and displacement mentioned for the analytical example retrofit were based on continuous longitudinal reinforcing and are overly optimistic for a scenario in which longitudinal debonding occurs.

Three columns were constructed in this research. The first column, the "as-built" specimen, was tested to failure under cyclic push-pull loads and axial loading. The other two columns were tested after the jacket was installed using the same load sequence. In addition, the "as-built" specimen was patched and jacketed for a test to study the effectiveness of the prefabricated system as a repair alternative to damaged columns.

Column C1-A is the "as-built" specimen. Column C2-RT4 is a specimen with four layers of jacketing on the lower 610 mm (24 in.) and three layers on the next 610 mm (24 in.) of height. C3-RT5 is a specimen with five layers of jacketing on the lowest 1,290 mm (48 in.) followed by three layers on the next 990 mm (39 in.) of height. Finally, C4-RP4 is the repaired "as-built" specimen with four layers of jacketing over the lower 1,290 mm (48 in.).

The loading sequence for all of the specimens consisted of (a) application of a 832 kN (187 kip) axial load on the column via two post-tensioning bars, (b) one cycle to 2.5 mm (0.1 in.), (c) five cycles to  $\mu_{\Delta} = 0.5$ , and (d) three complete cycles to  $\mu_{\Delta} = 1, 1.5, 2, 3, 4, 5,$  and  $6$ . For column C1-A, the "as-built" specimen, the maximum lateral force was attained at  $\mu_{\Delta} = 1.0$  and from interpretation of the hysteresis diagrams in Xiao, Martin, Yin, and Ma (1995a), this load is approximately 227 kN (51 kips). This load produced a column displacement somewhat in excess of 13 mm (0.5 in.) and extensive flexural cracking throughout the lap-spliced region. At a displacement of 40 mm (1.6 in.) the lap splices were determined to have failed due to the presence of extensive vertical cracking in the lap-spliced region. At this point, lateral load capacity dropped 25%-30%. The test was finally terminated when the capacity dropped to 50% of the yield capacity at a displacement of 60 mm (2.4 in.),  $\mu_{\Delta} = 3$ . In contrast to the rapid degradation and failure noted in C1-A, columns C2-RT4 and C3-RT5 exhibited stable ductile response to high ductility levels.

Column C2-RT4 developed a stable force displacement response up to  $\mu_{\Delta} = 5.7$  at which point the lateral capacity was approximately equal to 289 kN (65 kips). From examination of the hysteresis diagrams, this load was very close to the ideal flexural capacity shear. Degradation of the lateral force displacement response was noted at this point, and testing continued until three cycles at  $\mu_{\Delta} = 8.0$  were completed. Following the third cycle to  $\mu_{\Delta} = 8$ , the lateral force capacity was reduced to approximately 178 kN (40 kips) or 62% of the ideal flexural capacity.

Column C3-RT5 developed a stable force-displacement response until  $\mu_{\Delta} = 6.0$  at a lateral load capacity of approximately 311 kN (70 kips), very close to the ideal flexural capacity shear. At this point, gradual lap splice debonding led to a degradation of the response; at  $\mu_{\Delta} = 8$ , testing was discontinued. At the time the test was stopped, the lateral load capacity on the third cycle to  $\mu_{\Delta} = 8$ , was approximately 222 kN (50 kips), which was still the approximate load required to cause first yield in the longitudinal reinforcing. Because a higher yield point steel than typically encountered in older columns was used in these retrofit tests, actual displacements on retrofitted columns can be expected to be somewhat higher.

In testing the repaired specimen C4-RP4, the column was able to sustain lateral loads equal to the first yield lateral loads of approximately 222 kN (50 kips) until  $\mu_{\Delta} = 4$ . At this point, gradual response degradation was noted until at  $\mu_{\Delta} = 8$ , and the lateral load resisting capacity was approximately 50% of the first yield lateral force stated above. The jacketed specimens performed very well with no discernable delamination of the jackets and only fine horizontal cracks at  $\mu_{\Delta} = 8$ .

Having identified lap-splice debonding as a possible failure mode for retrofits of this nature, Xiao, Martin, Yin, and Ma also developed an analytical model that can be used to predict that force displacement response of a Snap-Tite™ retrofitted column. The model was found to be in good agreement with experimental data presented by Xiao, Martin, Yin, and Ma as well as others. An example of an existing column which was analyzed and found to have insufficient ductility was presented. A trial number of jacket layers was assumed and the column reanalyzed for displacement ductility. This process of assuming a number of layers and employing the bond slip models to determine overall ductility is repeated until the design criteria is met.

Seible, Hegemier, et al. (1995b) discuss the results of a combined analytical, laboratory, and field demonstration research project for column jacketing which employed an automated fiber winding process using prepreg carbon fiber tows. The project consisted of the development of a design methodology for carbon fiber-jacketed columns, experimental validation of the models, and field testing of the automated

winding technique. The summary paper discusses results found in the following reports: (Seible, Hegemier, et al., 1994a, 1994b, 1995a, 1995c, 1995d, 1995e), (Seible, Priestley, and Innamorato, 1995). Results from these reports are presented in discussions on flexurally and shear deficient columns of both circular and rectangular cross-section throughout this Section. The research is based on the system developed by the XXsys Corporation (XXsys Technologies, 1995a, 1995b).

This jacketing process employs the Robo-Wrapper™ automated column wrapping machine as developed by the Composite Retrofit Corporation (CRC) Division of XXSys Technologies, Inc. The machine is designed to wind large structures with AS4D carbon fiber tows, manufactured by Hercules and preimpregnated with Ciba M10E epoxy resin. The fiber tows, known as 12k tows, consist of 12,000 filaments having a combined cross sectional area of 0.44 mm<sup>2</sup> (6.88x10<sup>-4</sup> in.<sup>2</sup>). The nominal mechanical properties of the unidirectional cured laminate consist of a tensile strength of 1.72 GPa (250 Ksi), tensile modulus of 142 GPa (20,600 Ksi), and ultimate tensile strain of 1.15%.

Jacket installation begins with removal of dust, dirt, and surface irregularities from the column face. Cracks and spalls are then filled with a plastic putty. A thin copper strip is installed along the column height so that eddy current measurements of the overwrap thickness can be made. Prepreg tows are spool fed onto the winding machine, which when set up, can circle a column at 6 rpm while traveling vertically up the column on a 6,100 mm (20 ft) mast at a predetermined speed so as to control jacket thickness. The machine can wrap a 1,370 mm (4.5 ft) diameter column with a 19 mm (3/4 in.) band in a single pass. The jacket winding process follows a program whereby jacket thickness can be changed at different elevations along the column depending on the type of retrofit required. Curing consists of using heat blankets with a 20-minute ramp up to 77° C, a 30-minute dwell at this temperature, a 30-minute ramp to 121° C, and a one-hour dwell at 121° C. Finally, the jacket is sealed with an acrylic emulsion spray coating for protection and architectural purposes.

In the analytical portion of the research program (Seible, Priestley, and Innamorato, 1995), concrete columns were separated into areas where shear retrofits, plastic hinge confinement retrofits, and lap splice clamping force retrofits would be required. Upon identification of these deficiencies as well as expected shear, ductility, and confinement demands on the column during an earthquake, design relationships were established which showed the dependence of jacket thickness on the tensile modulus, ultimate jacket strain, and ultimate jacket stress. The design methodology presented in the aforementioned reference was then subjected to 0.4 scale-model validation studies at the University of California, San Diego, as part of the Advanced Composites Technology Transfer Consortium, Advanced Research Projects Agency, Technology Reinvestment Program (ACTT/ARPA/TRP). The testing was carried out similarly to those previously conducted for Caltrans on "as-built" and steel-jacketed specimens. The retrofit would be deemed acceptable if (a) it met or exceeded the performance of the steel-jacketed specimens, (b) it achieved a displacement ductility level,  $\mu_{\Delta} = 8$ , twice the Caltrans design level, and (c) it more than doubled the ductility of the "as-built" specimens.

In order to determine the validity of the retrofit and its ability to perform to the specifications listed above, seven columns with varying geometries, reinforcement layouts, and deficiencies were constructed. These columns consisted of a circular shear deficient column with 2.5% reinforcement (CS2.5), a circular shear deficient column with 1% reinforcement (CS1), a rectangular shear deficient column with 2.5% reinforcement (RS2.5), two circular flexurally deficient columns with lap splices (CF1, CF2), a rectangular flexurally deficient column with lap splice (RFLS), and a rectangular flexurally deficient column with 5.0% reinforcement (RF5). The test results for four of these columns, CS2.5, CF1, CF2, and

RF5 were described in the summary paper (Seible, Hegemier, et al., 1995b); results for the remaining three tests were presented in tabular form. A summary of the test results from both the summary paper and original reports is presented below as well as in other portions of this section.

Two circular flexurally deficient columns with base region lap splices, CF1 and CF2, (Seible, Hegemier, et al., 1995d) were constructed with a distance to the point of load application measured from the top of footing of 3,660 mm (12 ft) and a clear height from the top of footing of 3,430 mm (11.25 ft). The columns were 610 mm (24 in.) in diameter and were reinforced longitudinally with twenty-six, 19 mm (#6) reinforcing bars and transversely with 6 mm (#2) reinforcing bars at 125 mm (5 in.) on center. The longitudinal bars had an average measured yield stress of 303 MPa (43.9 ksi) and the transverse bars, 403 MPa (58.5 ksi). The compressive strength of the column concrete at the time of testing was 39 MPa (5,610 psi).

The columns were tested with a nearly constant axial load of 1,780 kN (400 kips) and increasing lateral load and displacement. The theoretical yield capacity,  $V_y$ , was 178 kN (40 kips) and the theoretical flexural strength,  $V_{vi}$ , 245 kN (55 kips).

For purposes of comparison, the results of a similarly constructed "as-built" column originally described in Chai, Priestley, and Seible (1991b) and summarized in Section 2.2.1.1 of this report were used as the benchmark. This column was able to exceed the ideal yield capacity but was unable to attain its ideal flexural capacity. Following a peak in load resistance during the first cycle to  $\mu_\Delta = 2$ , the column response rapidly degraded because of brittle lap splice debonding. The steel-jacketed specimen, also described in Chai, Priestley, and Seible (1991b) and Section 2.2.1.1 of this report, was able to maintain ever increasing lateral load resistance well in excess of the ideal flexural capacity until  $\mu_\Delta = 7$  at which point the resistance of the column began to degrade.

Composite retrofit column CF2 is shown in figure 3-1. The total wrap length of 1,065 mm (42 in.) represented the lower 30% of the column height and was intended to prevent the brittle lap splice debonding at the base of the column where a  $20 d_b$  lap splice was located. Two retrofit columns were constructed because following the test of CF1, it was determined that an improper jacket thickness of only 75% of the design thickness was placed on the column. CF2 was then constructed to correct this error. The measured material properties of CF1 are: fiber volume fraction, 50%; ultimate tensile strength, 1,385 MPa (201 ksi); and tensile modulus, 111.5 GPa (16,178 ksi). Similarly for CF2, the properties are: fiber volume fraction, 52%; ultimate tensile strength, 1,572 MPa (228 ksi); and tensile modulus, 127.6 GPa (18,500 ksi).

Column CF1 exhibited a ductile flexural response up to  $\mu_\Delta = 5.3$  ( $\pm 4.8\%$  drift) after which a very gradual decrease in lateral strength capacity from the maximum lateral load of 275 kN (61.8 kips) was observed with increasing levels of ductility. At  $\mu_\Delta = 8.6$  ( $\pm 7.8\%$  drift), the lateral load-resisting capacity was reduced to 75% of the maximum lateral load; and testing was halted. The drop in capacity between maximum lateral load and 75% of the maximum load was not accompanied by a drastic change in behavior but a gradual softening of the response due to lap splice debonding as a consequence of the undersized jacket.

Column CF2 exhibited a stable ductile flexural hysteretic response up to  $\mu_\Delta = 8$  ( $\pm 5.6\%$  drift) with no drop in lateral load capacity from the maximum of approximately 325 kN (73 kips). At a displacement of  $\mu_\Delta = 10$  ( $\pm 6.9\%$  drift), the footing starter bars ruptured due to low-cycle fatigue after being subjected to 24

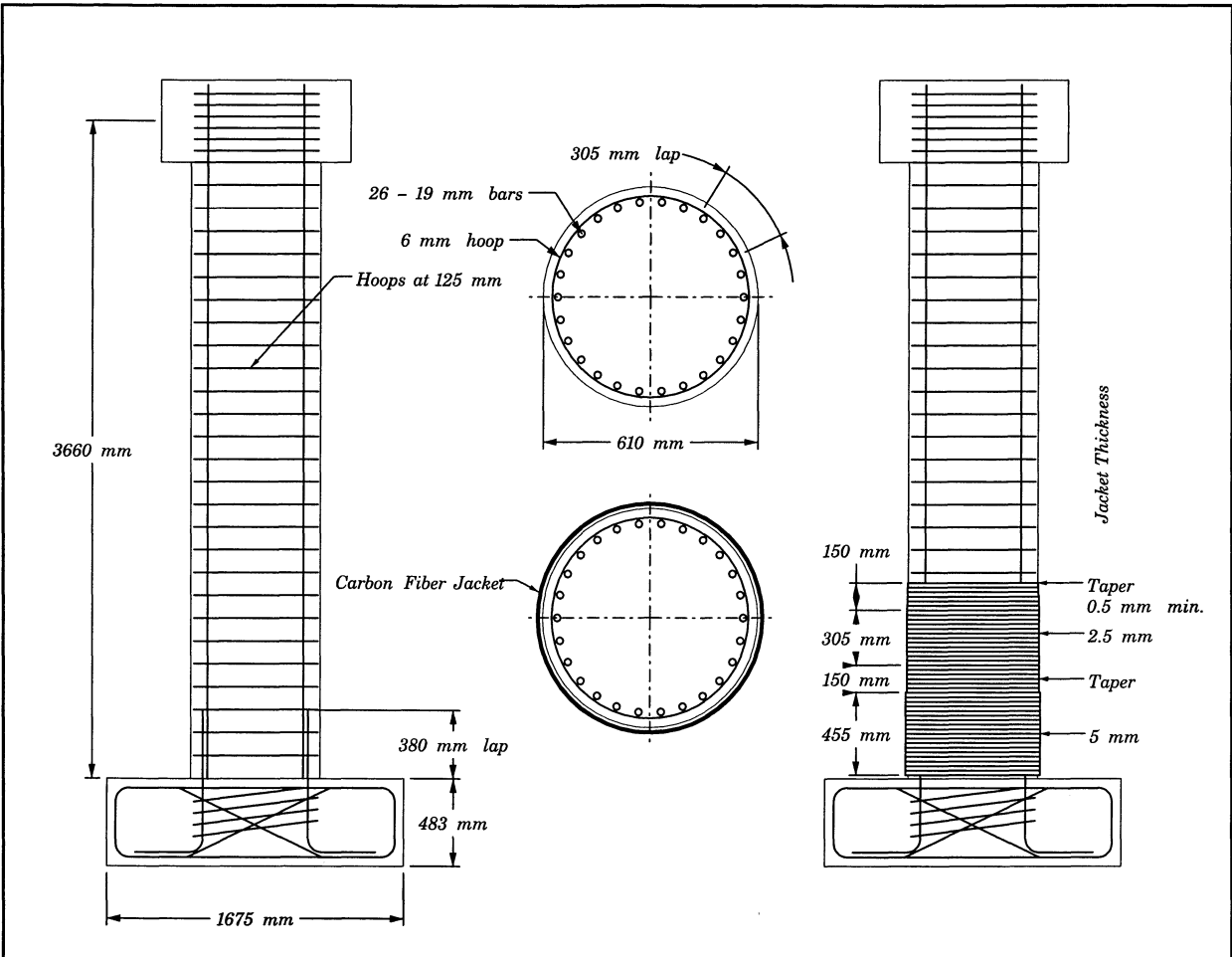


**FIGURE 3-1 Circular Column with Lap Splice, CF2 (Seible, Hegemier, et al., 1995d)**

cycles of loading at increasing displacement ductilities from 1 to 10. At this point the test was discontinued. Rupture of these bars is indicative of the ability to promote force transfer in the lap-spliced region.

The test results of the improperly constructed CF1 and correctly constructed CF2 indicate that the carbon fiber winding process is an effective means of providing lap splice force transfer and inelastic rotation confinement in the areas of maximum moment and curvature. Both columns were able to easily exceed their ideal lateral strength and in the case of CF2, maintain this strength until column steel failure.

Seible, Priestley, and Innamorato (1995) present the guidelines for carbon fiber retrofit of deficient bridge columns. The document discusses both the full-scale field installation of several carbon fiber jackets installed with an automated wrapping machine and the design and construction of a full-size two-column bridge bent in the Powell Laboratory at the University of California at San Diego. This full size model will first be tested with the existing columns wrapped in carbon fiber following the design guidelines developed at UCSD. Following this test, a new link beam, installed below the existing cap beam, will be

installed and the retrofit frame tested once again. As of the writing of Seible, Priestley, and Innamorato (1995), testing of this frame had not been completed.

### 3.3.1.2 Rectangular Flexural Columns

Seible and Priestley (1993a) present the results of a series of tests which studied the effect of E-glass composite jacketing on the strong and weak direction performance of flexurally deficient rectangular reinforced-concrete columns. Additionally, the results are compared to several other retrofit techniques under consideration at the time as viable retrofit alternatives for deficient columns.

In these tests, the use of the composite jackets in an oval configuration is described. The oval retrofit is one in which a rectangular column is first made into an oval shape so that the jacket can function in membrane tension as opposed to lateral bending stiffness. This technique was first employed in the development of steel jacket retrofits where it was observed that even extensively stiffened steel plates placed around rectangular specimens were not as effective as steel jacket retrofits on columns which were first made oval in shape. In this set of tests, the major concern was the performance of the lap splice region at the base of the columns. The lap splices used in these columns were 380 mm (15 in.) long, which corresponds to  $25 d_b$ . Using equations presented in Seible and Priestley (1993a) and developed explicitly for the mechanical properties of the Hexcel Fyfe TYFO S system in the active-passive combination, researchers determined that the retrofits would employ an active thickness of 6 mm (0.24 in.). For columns tested in the weak direction, this jacket extended over the bottom 1,220 mm (4 ft) of the column, was actively pressurized to 1.38 MPa (200 psi), and a 9 mm (0.36 in.) passive layer was placed over the lap splice region only. For the strong direction load tests, a 29 mm (1.15 in.) layer of passive retrofit was applied since the jacket was only actively pressurized to 0.45 MPa (65 psi).

Weak direction testing demonstrated excellent ductile flexural response up to  $\mu_{\Delta} = 8$  at which point the test was discontinued due to equipment limitations. Examination of the load-displacement response of this test indicates that the lateral load kept increasing through progressive levels of ductility until testing ceased, which is indicative of a column that still had not reached its ultimate lateral load resisting capacity. Comparing the response of this column to that of the steel-jacketed specimens indicates that at  $\mu_{\Delta} = 8$ , slight differences in response were noted, with the steel jacket retrofit showing signs of lap splice slip. The composite jacket exhibited slightly higher stiffness and maximum lateral capacity than the steel jacket with the composite jacket providing a 27% increase in strength over the "as-built" case and the steel jacket providing a 19% increase. The slightly higher stiffness in the composite jacket was attributed to extra wraps of composite material above and beyond the design level used for assuring proper anchorage of the layers.

The strong direction test indicates stable hysteretic response to  $\mu_{\Delta} = 8$  where the first signs of lap splice slip were noted. This response is again higher than  $\mu_{\Delta} = 7$  where slip was noted in the steel jacket retrofits. The composite-jacketed specimen once again demonstrated a slight increase in stiffness and resisted a lateral load 7% higher than the steel-jacketed specimen. Both retrofits, however, demonstrated lateral load increases of over 50% as compared to the "as-built" specimen. The composite-jacketed specimen was tested to  $\mu_{\Delta} = 10$  where after three cycles, the lateral resistance was still greater than the shear corresponding to ideal flexural capacity.

The following text concerns column tests conducted by Saadatmanesh, Ehsani, and Jin (n.d.) at the University of Arizona. The general description of the tests and systems employed as the retrofit have

previously been presented on pages 67-71 of this report. These pages should be consulted for all relevant details pertaining to the geometry and loading of the columns described below.

Specimen R-1 exhibited a peak lateral resistance of 92 kN (20.7 kips), essentially the ideal flexural strength shear of 89 kN (20.1 kips). Significant degradation of response began at  $\mu_{\Delta} = 1.5$  and a drop in lateral resistance of nearly 80% was noted by the time cycling progressed to  $\mu_{\Delta} = 4$ . Column R-2 showed a 50% increase in lateral strength over R-1 and had wide and stable hysteresis loops until  $\mu_{\Delta} = 5$ .

In addition to assessment of strength deterioration over the life of the test, stiffness deterioration was examined by comparing the stiffness at each cycle to the initial stiffness. All of the rectangular columns saw their stiffness at the initial cycle reduced considerably through subsequent inelastic displacement cycles as would be expected. However, the retrofit specimens had a slower rate of stiffness deterioration than did the "as-built" specimens.

Moment curvature data were plotted for the columns. For retrofit column R-2, the curvature increased significantly after the longitudinal steel yielded, but the bending moment remained nearly constant. Conversely, the moment curvature response for the "as-built" specimens is characterized by poor performance due to concrete crushing before the onset of steel yielding.

In examining the hysteresis loops of all test specimens, varying degrees of pinching were noticed. Pinching was amplified in columns with lap-spliced bars where the narrowing near the origin is due to longitudinal lap splice slippage.

The repair column, R-1/R, was subjected to the same loading as the original specimen. For comparison, the load-displacement envelope of the repaired column was plotted with the original test results. The average stiffness per cycle was also computed for comparison. Results of the test indicate that R-1/R exhibited a strength increase of 38% over the original R-1; however, such results are not in and of themselves representative of the overall effects of the repair.

For instance, when column R-1 was originally tested, it was only able to attain a stable response to  $\mu_{\Delta} = 1.5$ , while the repaired column was able to maintain a stable response to approximately  $\mu_{\Delta} = 5$  in addition to a significant lateral load increase. R-1/R exhibited slight degradation in the load-displacement response at the end of the testing. In examining the strength envelope for rectangular columns with starter bars, the poor performance of R-1 is evident when compared to the responses for R-1/R and R-2 which are nearly identical.

The carbon fiber retrofit of a flexurally deficient rectangular column, column RFLS, is described in Seible, Hegemier, et al. (1995e). This test, carried out on a 0.4 scale model of prototype columns constructed prior to 1971, involves cyclic lateral load testing of a column with a 20  $d$  lap splice at the base. The column had a distance to the point of load application measured from the top of footing of 3,660 mm (12 ft) and a clear height from the top of footing of 3,430 mm (11.25 ft). The column cross section measures 730 mm x 490 mm (28.75 in. x 19.25 in.). The column longitudinal reinforcing consists of thirty-two, 19 mm (#6) reinforcing bars and similarly sized dowel bars. Lateral ties are 6 mm (#2) reinforcing bars at 125 mm (5 in.) on center. The measured yield stress of the longitudinal reinforcing steel in this column was 293 MPa (42.5 ksi); the measured yield stress of the transverse steel is 403 MPa (58.5 ksi). The measured concrete compressive strength was 41.9 MPa (6,080 psi) at the time of testing.

General information regarding the innovative automated column wrapping process used on this and other columns, can be found beginning on page 73.

This column was tested in single bending under a load control-displacement control test sequence and a constant axial load of 1,780 kN (400 kips). The column had a theoretical lateral yield capacity of 294 kN (66 kips) and an ideal capacity of 365 kN (82 kips).

An "as-built" column specimen used as a benchmark for determining the effectiveness of the retrofit is described in Sun, Seible, and Priestley (1993b) and subsequently in Section 2.2.1.2 of this report. The "as-built" specimen was unable to attain its ideal flexural strength and began to degrade from its maximum lateral capacity at  $\mu_{\Delta} = 1.5$ . Testing was discontinued at  $\mu_{\Delta} = 4$  due to negligible resistance in the column. The remaining lateral resistance was due primarily to the horizontal component of the axial load.

The oval steel jacket retrofit described in Sun, Seible, and Priestley (1993b) and in Section 2.2.1.2 was able to maintain a stable response above the ideal load level until approximately  $\mu_{\Delta} = 7$ . Gradual degradation in lateral strength was noted and testing was discontinued at  $\mu_{\Delta} = 9$ .

The retrofit for column RFLS involved first casting an oval concrete overlay around the flexural hinge region of the column so that the carbon could use its hoop stress capacity as a means of providing lateral confinement to the column. The augmented region was over the bottom 1,015 mm (40 in.) of the column. Following construction of this oval, a carbon jacket was wrapped onto the surface of the newly cast concrete. The retrofit for column RFLS is shown in figure 3-2. The measured material properties of the composite, which had a fiber volume fraction of 52%, were tensile strength, 1,393 MPa (202 ksi); and tensile modulus, 118 GPa (17,044 ksi).

A minor flexural crack was noticed in the jacket of the retrofit column at a ductility of  $\mu_{\Delta} = 1$ . These cracks also developed above the jacket and were seen to generally coincide with the location of the lateral reinforcing. Concrete in the gap between the bottom of the jacket and top of the footing crushed and spalled at  $\mu_{\Delta} = 6$ . At  $\mu_{\Delta} = 8$ , the starter bars on the tension side of the column ruptured and caused a 33% reduction in lateral capacity. This column easily reached and maintained lateral load resistance in excess of the ideal lateral capacity until starter bar rupture.

Comparison with the results of the steel jacket retrofit indicates that the steel jacket provided a higher lateral load capacity. Both columns were able to exceed the ideal lateral capacity for a number of cycles. In both specimens, concentrated displacements in the gap between the bottom of the jacket and top of the footing ultimately resulted in failure.

Column RF5 (Seible, Hegemier, et al., 1995a), shown in figure 3-3, was constructed with a distance to the point of load application measured from the top of footing of 3,660 mm (12 ft) and a clear height from the top of footing of 3,430 mm (11.25 ft). It is a rectangular column whose cross-section measures 730 mm x 490 mm (28.75 in. x 19.25 in.). The column has a longitudinal reinforcing ratio of 5.0%. The longitudinal steel is continuous from the footing, i.e., no lap splice is present. Lateral ties are 6 mm (#2) reinforcing bars at 125 mm (5 in.) on center. The measured yield stress of the longitudinal reinforcing steel in this column varied from 280 MPa (40.6 ksi) to 327 MPa (47.4 ksi); measured yield stress of the transverse steel is 403 MPa (58.5 ksi); measured concrete strength was 40 MPa (5,780 psi) at the time of testing.

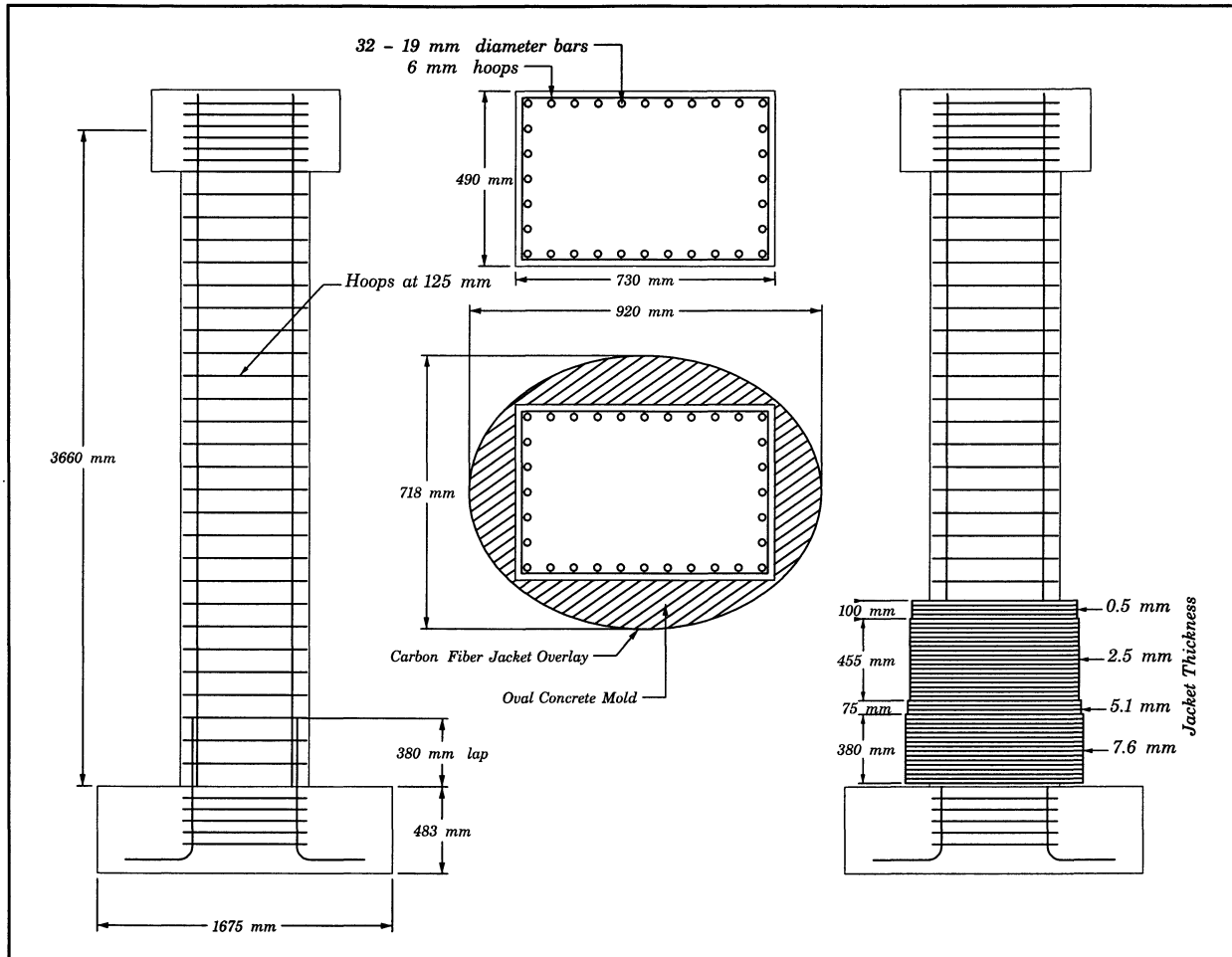


**FIGURE 3-2 Rectangular Flexural Column with Lap Splice, RFLS**  
(Seible, Hegemier, et al., 1995e)

This column was tested in single bending under a load control-displacement control test sequence and a constant axial load of 1,780 kN (400 kips). The unique feature of this test was that the column was not made oval in shape as is commonly done in steel jacket retrofits. The only measure taken to alter the column cross section was placement of 1/4 of a PVC pipe section on all four corners for the full height of the specimen so as to avoid undue stress concentrations at the corners.

The "as-built" column specimen used as a benchmark for determining the effectiveness of the retrofit is described in Sun, Seible, and Priestley (1993b) and in Section 2.2.1.2 of this report. The "as-built" specimen was able to attain its ideal flexural strength of 580 kN (130.5 kips) at  $\mu_h = 3$  prior to suffering rapid failure due to loss of cover concrete in the plastic hinge region. Testing was discontinued at  $\mu_h = 4$  due to negligible resistance in the column. The remaining lateral resistance was due primarily to the horizontal component of the axial load.

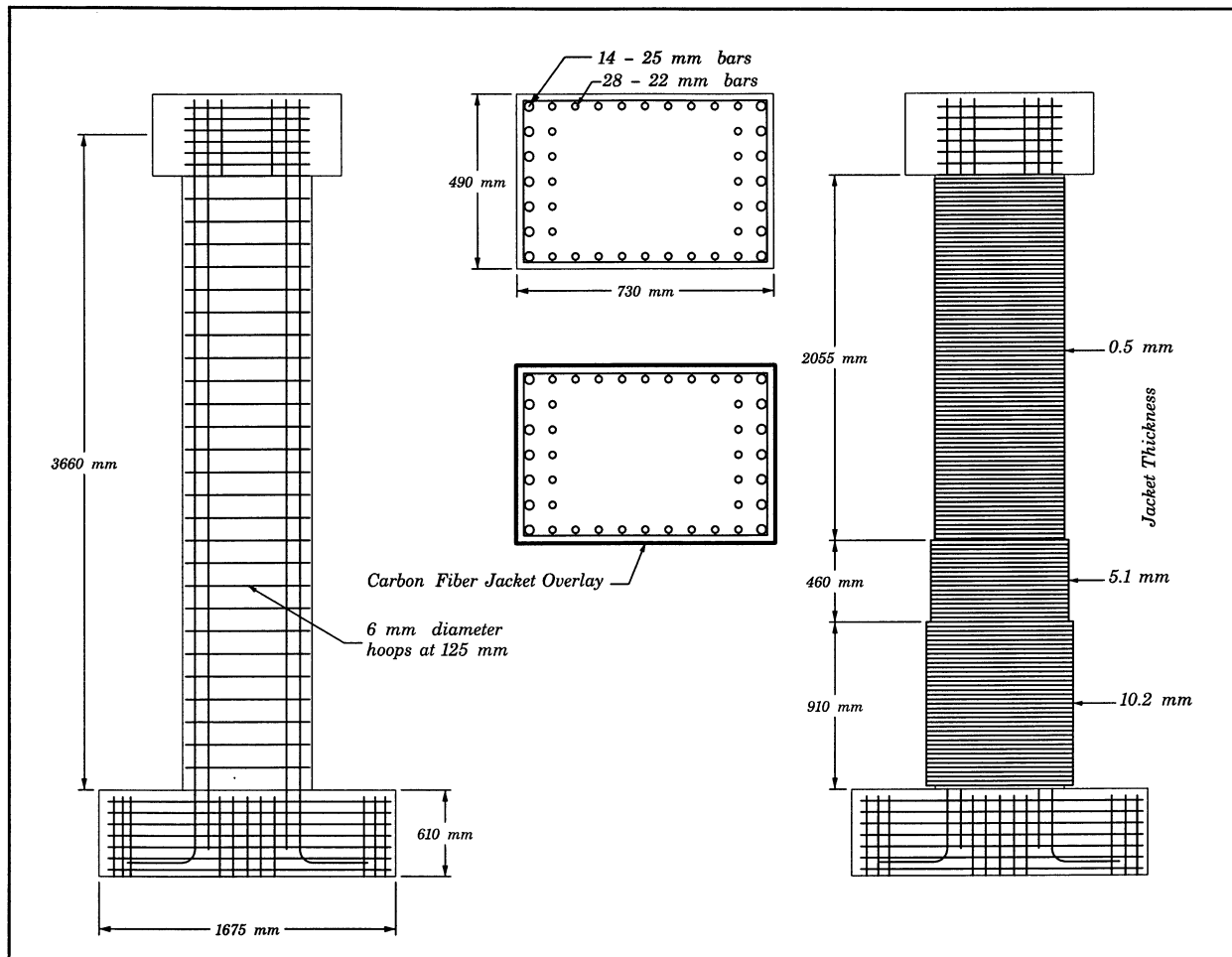


**FIGURE 3-3 Continuous Reinforcing Specimen RF5 (Seible, Hegemier, et al., 1995a)**

The oval steel jacket retrofit described in Sun, Seible, and Priestley (1993b) and in Section 2.2.1.2 was able to maintain a peak lateral load of approximately 700 kN (157 kips) through  $\mu_{\Delta}=6$ . During the first push cycle to  $\mu_{\Delta}=8$  at approximately  $\mu_{\Delta}=7.7$ , rapid degradation of lateral strength was noticed. The test continued with a rapidly decreasing lateral load to  $\mu_{\Delta}=8$ , but suffered a failure on the return cycle. The dependable capacity of this retrofit is likely  $\mu_{\Delta}=6$ .

The measured material properties of the composite retrofit depicted in figure 3-3, which had a fiber volume fraction of 52%, are: tensile strength, 1,572 MPa (228 ksi); and tensile modulus, 128 GPa (18,500 ksi).

This specimen exhibited stable hysteretic response up to  $\mu_{\Delta}=7$  ( $\pm 5.8\%$  drift) without lateral load capacity degradation from a peak of approximately 620 kN (139 kips). At this ductility level, the compression zone at the base of the column began to bulge. At  $\mu_{\Delta}=8$ , the carbon fiber jacket ruptured on the column compression face resulting in termination of the test. Prior to rupture, strains in the fiber were measure as high as 6640  $\mu\epsilon$ . The dependable capacity of this retrofit is  $\mu_{\Delta}=7$ .

Comparison of the "as-built", steel and carbon fiber retrofits shows that the carbon fiber retrofit is capable of attaining the same ductility levels as steel but at a lower lateral load level. Both retrofits exhibited significant ductility enhancement over the "as-built" condition, with the carbon fiber coming closest to the specification of twice the ductility of an "as-built" specimen.

The effect of carbon fiber strengthening on scale-model, rectangular reinforced concrete bridge piers is detailed in Matsuda et al. (1990) along with a number of different retrofit scenarios. The types include flexural strengthening, where retrofit involved the gluing of longitudinally oriented unidirectional (UD) carbon fiber tapes on the column surface; ductility improvement by applying the UD tapes transversely to the column surface; or a combination of the two techniques. Additionally, in some cases, the tapes were further overwrapped with carbon fiber strands composed of monofilament. These two techniques were investigated because of the vulnerability of many bridges in Japan due to longitudinal bar termination near mid-height of the column. The flexural reinforcement scenario relieves some of the load from the main continuing reinforcement in the cut-off region during an earthquake and prevents subsequent shear failure due to section degradation. The ductility retrofit provides the transverse confinement necessary to provide for stable hinge formation. The strengthening techniques described above are similar to those shown previously presented in Figure 1-3.

Six specimens were constructed so that they were approximately one-third the cross-sectional dimension of columns typically found on the Tomei Expressway, 1.2 m x 1.8 m (47 in. x 71 in.) in section and 8 m (26.25 ft) high. The specimens were chosen to be 400 mm x 600 mm (15.8 in. x 23.6 in.) x 2,600 mm (8.53 ft) high from top of footing to the point of lateral load application. Longitudinal reinforcing consists of 16 mm (0.63 in.) diameter longitudinal bars with 6 mm (0.24 in.) transverse bars at 200 mm (7.9 in.) spacing. At 900 mm (35.4 in.) above the top of the footing, 50% of the steel was terminated. This is approximately 1/3 of the way up the column measured from the top of footing.

Specimen 1 was an "as-built" specimen as described above. Specimen 2 was retrofit with an anchored steel jacket retrofit placed along a length of 1.0 D, 400 mm (15.8 in.), above the termination point and 0.5 D, 200 mm (7.9 in.), below the termination point. Specimen 3 had four UD tapes, two layers each placed longitudinally and transversely with the tapes weighing 350 g/m<sup>2</sup> (1.15 oz/ft<sup>2</sup>). They were glued to the column for approximately 450 mm (17.7 in.) above and below the termination point. Specimen 4 was reinforced with two tapes in the longitudinal direction extending 300 mm (11.8 in.) above and 250 mm (9.8 in.) below the termination point. The bottom 1,200 mm (47.2 in.) of the pier was wound with carbon fiber strand of an area equal to 0.46 mm<sup>2</sup> (7.13x10<sup>-4</sup> in.<sup>2</sup>) at a 2.5 mm (0.1 in.) pitch. Specimen 5 had two layers of transverse tape extending 600 mm (23.6 in.) from the base. In addition, this specimen did not have the premature termination of longitudinal steel present in the other specimens. Finally, specimen 6, also constructed without a termination point, was reinforced with carbon fiber strands at a 5 mm (0.2 in.) pitch over the bottom 600 mm (23.6 in.) of the column.

In these tests, load was applied via a hydraulic cylinder with controlled loading until yield and then controlled multiples of the yield displacement thereafter. A constant load of 141.2 kN (14.4 tf, 31.7 kips) was applied throughout the testing. Testing as described above yielded the following results.

For specimen 1, main reinforcement yield above the termination point occurred at  $\mu_{\Delta} = 2$  with rebar buckling above the termination point occurring at  $\mu_{\Delta} = 3$ . In specimen 2, the steel jacket specimen, flexural cracks propagated below the jacket at  $\mu_{\Delta} = 2$  and the plate yielded. For specimen 3, flexural shear cracking occurred below the reinforced section during loading at  $\mu_{\Delta} = 4$  and part of the UD tape was

damaged during crack growth. For specimen 4, the reinforcing yielded below the jacket and near the base simultaneously because of a smaller region of strengthening. Upon loading at  $\mu_{\Delta} = 4$ , the tape became debonded and there was a decrease in load capacity. With further load applied, large flexural cracks developed at the bottom of the wrapped region, and bulging of the specimen was noted at  $\mu_{\Delta} = 6$ . However, at  $\mu_{\Delta} = 7$ , lateral load capacity only slightly decreased and only part of the carbon strands ruptured. For specimen 5, load was sustained with increasing capacity through subsequent ductilities until  $\mu_{\Delta} = 11$ , the maximum capacity of the test equipment. Concrete at the base suffered some damage but in the area of the wrap, there was no damage. Specimen 6 showed yielding at the base as well as cover swell at  $\mu_{\Delta} = 5$ . With further load, many of the strands within D of the base failed.

In summary, vertically oriented tape increased flexural strength and caused the relocation of failure to the column base. Transverse tape specimens exhibited significant increases in ductility. Only minor differences were noted in the transverse tape and filament-wound specimens.

Results from testing similar to that described above can be found in Katsumata et al. (1990) which describes the use of carbon fiber as a structural retrofit for columns in buildings, chimneys, and for existing bridge columns. The use of an automated winding machine for wrapping carbon fiber strands around structural members is shown at the end of this reference in photographs depicting actual retrofit operations. The machine seems to be similar in construction and operation as the one developed by XXSys Technologies (1995a, 1995b) and employed by Seible, Hegemier, et al. (1994a, 1994b, 1995a, 1995b, 1995c, 1995d, 1995e) and Seible, Priestley, and Innamorato (1995).

Ogata et al. (1993) and Ogata, Maeda, and Andoh (1994) discuss the use of carbon fiber retrofit wraps in Japan as a means of reinforcing concrete bridge columns with premature reinforcement termination. A total of five columns were tested under axial load and reversed cyclic loads.

The two main types of columns were rectangular in section, 400 mm x 600 mm (15.7 in. x 23.6 in.) and stood 2,800 mm (110.2 in.) above an 800 mm (31.5 in.) thick footing. The first type, specimens 1, 2, and 5, were typical Japanese construction with longitudinal bar termination at approximately 1/3 of the column height, 900 mm (35.4 in.), from the top of the footing. Prior to bar termination, the column was reinforced with three 10 mm (0.4 in.) diameter bars on each narrow face and thirteen 16 mm (0.6 in.) diameter bars on each long face. After termination, only one bar remained on each short face and the thirteen-bar long faces had been reduced to seven each. The second column type, Specimens 3 and 4, did not have reinforcing termination and were constructed similar to the layout described for the first set of columns prior to termination.

The columns were all subjected to similar test conditions with a constant applied axial stress of 588 kPa (6 kgf/cm<sup>2</sup>, 85 psi). The loading was the common load control-displacement control pattern with load control being employed until longitudinal yielding occurred and displacement control thereafter. The displacement control tests consist of three cycles at  $\mu_{\Delta} = 1, 2, \text{ and } 3$  with one cycle at  $\mu_{\Delta} = 4, 5, 6, \text{ etc.}$ , until failure. Retrofit patterns, similar to those in Figure 1-3, and test results are as follows:

- Column 1 was an "as-built" specimen and had a flexural failure at the cut-off location.
- Column 2 was wrapped in the area of the cut-off region with two transverse and two longitudinal carbon fiber sheets extending 450 mm (17.7 in.) above and below the cut-off location. This column

experienced stable response until the second cycle to  $\mu_{\Delta} = 4$ , when a shear failure occurred at the base due to flexural degradation of the specimen.

- Column 3 was only wrapped for the 600 mm (23.6 in.) near the column base with an amount of carbon fiber strand equivalent to the thickness of one sheet. The column had a stable load displacement response up to  $\mu_{\Delta} = 5$  followed by a significant drop in response through  $\mu_{\Delta} = 6$  and 7. The maximum reliable capacity of this retrofit should be  $\mu_{\Delta} = 5$ .
- Column 4 is similar to 3 except that two sheets of laterally oriented sheets were placed at the column bottom in lieu of the strand. The capacity of this column exceeded the capacity of the loading mechanism with a maximum  $\mu_{\Delta} = 11.1$ . This ductility was accompanied by a lateral load displacement response that showed the maximum lateral load continued to increase as the ductility levels grew higher.
- Column 5 was purposely damaged at the base of the specimen and at the cut-off region and repaired via epoxy injection of cracks and wrapping with fiber sheets to examine the suitability of this technique for use as a repair method following an earthquake. Results of the testing indicate that the failure mode was relocated from the cut-off location to the base of the column and the specimen was able to sustain a stable response to  $\mu_{\Delta} = 5$  with a maximum  $\mu_{\Delta} = 8$  occurring after substantial degradation of the lateral load capacity. This column was able to perform better than an "as-built" specimen even after being damaged and repaired.

### 3.3.2 Composite Jacket Retrofit of Shear Deficient Bridge Columns

#### 3.3.2.1 Circular Shear Columns

Priestley, Seible, and Fyfe (1994) discuss the use of a fiberglass-epoxy jacketing system in the retrofit of shear capacity deficient circular columns. As part of this research, two columns, referred to as columns 4 and 5, were constructed with diameters of 610 mm (24 in.) and clear height to the load point of 3.66 m (12 ft). Reinforcing consisted of twenty-six, 19 mm diameter (#6) reinforcing bars lap spliced 20  $d$  at the base. Transverse reinforcement consisted of 6 mm (#2) hoops lap spliced in the cover concrete and spaced vertically at 125 mm (4.9 in.). The reinforcing strength had a yield strength of 469 MPa (68 ksi) to maximize the shear force required for the column to be loaded to its flexural strength. The nominal concrete strength,  $f'_c$ , was 34.5 MPa (5 ksi). The columns were intended to be 0.4 scale models of columns typically constructed from 1950-1970. The columns were subjected to double bending with an applied axial load of 503 kN (113 kips). The "as-built" column used as a reference for these tests had a brittle shear failure.

For the retrofit, a combination of active and passive fiberglass wraps was applied to the columns. The active wrap, as reported in Fyfe (1994a, 1994b), consists of an elastomeric bladder placed over the region to be retrofit prior to the placement of the wrap. The wrap is placed so that the fibers are orientated in the circumferential direction. Upon initial cure of the "active" layers, the elastomeric bladder is injected with grout and thus induces radial pressure on the wrap and column and strains in the jacket fibers. These radial pressures are required to preserve the integrity of the force-transfer mechanism of the lap splice. Excessive dilation of the cover concrete will prohibit the lap splice from transferring load. The passive layers are placed after the pressure grouting is complete and will only be strained as the concrete dilates under load.

The retrofit for column 4 consisted of three components. First, two 1.15 mm (0.045 in.) layers were placed over the end 610 mm (2 ft) and pressurized with cement grout to 0.69 MPa (100 psi). Secondly, 8 passive layers of 0.4 mm (0.016 in.) high modulus E-Glass were placed over the end 305 mm (1 ft). Lastly, three 1.15 mm (0.045 in.) passive layers were bonded directly to the central 1.2 m (3.94 ft) of the column. The design strain for this retrofit was 4,000  $\mu\epsilon$ .

Column 5 was similar to column 4 except that in the central region of the column previously described, the passive wrap was reduced to two 1.15 mm (0.045 in.) layers. The design strain for this retrofit was 6,000  $\mu\epsilon$ .

Test results for both columns were excellent with stable flexural ductile hysteretic response and drift ratios in excess of 5%, which was due to test limitations and not column failure. The critical column was judged to be column 5 because of the thinner central region jacket. The force displacement response for this column showed stable loops with very little force or stiffness degradation on subsequent cycles to the same ductility level. The maximum ductility measured was 8, corresponding not to failure in the column, but as previously stated, limitations in the stroke of the test jack. The maximum lateral force was also at the level of the maximum displacement, indicating that the column at this level of displacement is not experiencing stability problems.

Seqad Consulting Engineers (1993) details the repair of a circular column previously tested to failure in the "as-built" condition in Verma, Priestley, and Seible (1993). The results from Verma, Priestley, and Seible (1993) have previously reviewed in Section 2.2.2.1 of this report. The column during previous testing had experienced brittle shear failure at the column mid-height and had lost 75% of its maximum lateral load-carrying capacity. The method of repair entailed the use of glass fiber-epoxy wraps as previously described as well as epoxy injection of cracks in the column.

The column was reinforced with 276 MPa (40 ksi) reinforcing bars, a longitudinal reinforcing ratio of 2.5% and transverse ratio of 0.175%. Cover to the main reinforcing bars was 20 mm (0.8 in.). The column had a clear height of 2,440 mm (8 ft), and diameter of 610 mm (24 in.), producing a shear span-depth ratio of 2.0, considering double bending behavior in the test frame. The concrete strength of the specimen, was listed as 34.5 MPa (5 ksi) in Verma, Priestley, and Seible (1993). Likewise, the axial load, reported by Verma, Priestley, and Seible (1993) was 1,779 kN (400 kips), corresponding to an axial load ratio of 0.18  $f'_c A_g$ . The lateral force corresponding to first yield was 525 kN (118 kips), and the lateral force corresponding to the ideal flexural capacity was 672 kN (151 kips).

During testing of the "as-built" specimen (Verma, Priestley, and Seible, 1993), a force control loading was imposed until the level of first yield. After first yield, multiples of the yield displacement were applied in a displacement controlled test. At a ductility level  $\mu_\Delta = 1.5$ , the lateral force was 690 kN (155 kips), slightly in excess of the lateral load noted above corresponding to the ideal flexural capacity. At this ductility level, the column had exceeded its ideal flexural capacity without a shear failure. The maximum lateral shear in the column was 738 kN (166 kips) during the first push cycle to  $\mu_\Delta = 2$ . Lateral force capacity degradation began at the first cycle to  $\mu_\Delta = 2$ , and significant strength degradation of 15% was seen during the first push cycle to  $\mu_\Delta = 3$ . During load reversal, there was a significant strength reduction, followed by a decrease in lateral load capacity of 40% during the second push cycle to  $\mu_\Delta = 3$ . A third cycle to  $\mu_\Delta = 3$  was performed after which the column had lost 75% of its lateral load capacity.

This column was repaired by removing the loose concrete, patching the voids with a cement-sand mortar, installing a full height fiberglass and epoxy jacket, and injecting epoxy in the cracks via ports installed in the cracks prior to placement of the jacket.

The jacket retrofit was based on Hexcel Fyfe's SEH 51 system with individual layer thicknesses of 1.3 mm (0.051 in.) and was consistent with the goal of providing a shear capacity in the repaired column exceeding the shear required to produce moments of 150% of the ideal flexural strength. The fiberglass jacket had a modulus of elasticity of 22 GPa (3,200 ksi) and a design strain of 4,000  $\mu\epsilon$ . This results in a design fiber stress of 88 MPa (12.8 ksi). The concrete column was conservatively assumed to have a shear capacity equal to zero. This left the shear resistance of the column to be dependent on the lateral tie contribution, the shear strength due to the presence of the axial load, and the jacket contribution. Based on the Seqad Consulting Engineers (1993) design equations, a minimum jacket thickness of 3.6 mm (0.143 in.) was required; therefore, three layers of SEH 51 with a total thickness of 3.9 mm (0.153 in.) were used.

During testing, the column was subjected to a lateral load which consisted of force control up to  $\mu_{\Delta} = 1$  and three fully reversed cycles at  $\mu_{\Delta} = 1, 1.5, 2, 3, 4, 6, 8,$  and 10. The first sign of distress was toe crushing during the first cycle to  $\mu_{\Delta} = 6$  with noticeable delamination of the jacket in the vicinity of the compression toe, however, no drop in lateral load was recorded. The first horizontal jacket rupture was at approximately  $\mu_{\Delta} = 8$  on the column tension side near the footing and extended during cycling at this level. Cycling was continued to  $\mu_{\Delta} = 10$  without any degradation in lateral load capacity. Examination of the hysteresis loops indicates that the force required for greater levels of ductility was progressively higher throughout the entire test sequence. Testing was discontinued at  $\mu_{\Delta} = 10$  due to stroke limitations of the horizontal actuator, and at this point no drop in load capacity or narrowing of the hysteresis loops was noticed. The displacement at  $\mu_{\Delta} = 10$  corresponds to a drift angle of 4.9%.

In comparing the force displacement response of the "as-built" and repaired columns, up to  $\mu_{\Delta} = 2$ , the columns have nearly identical responses, including initial stiffness, indicative of the jackets ability to restore the original stiffness of the column. A repair of a similarly damaged "as-built" column was made with a steel jacket and is described in Verma, Priestley, and Seible (1993). Seqad Consulting Engineers (1993) plot the load deflection envelopes of the "as-built" column, the steel jacket retrofitted column, and the composite jacket retrofitted column. Examination of these envelopes illustrated that the steel and composite retrofits had a nearly identical response.

This limited degree of testing indicates that composite jackets can not only repair a damaged column so that it regains its original stiffness but also can greatly exceed the performance characteristics of the virgin "as-built" column. A stable ductile flexural response was demonstrated to a maximum of  $\mu_{\Delta} = 10$ , equal to that of a steel-jacketed repair column.

Results of the carbon fiber retrofit testing of a circular column, CS2.5, are originally presented in Seible, Hegemier, et al. (1994b) and are summarized in Seible, Hegemier, et al. (1995b). General information regarding the innovative automated column wrapping process used on this and other columns, can be found beginning on page 73.

Column CS2.5, as shown in figure 3-4, is a 2,440 mm (8 ft) high column, 610 mm (24 in.) in diameter and reinforced longitudinally with twenty-six, 19 mm (#6) reinforcing bars and transversely with 6 mm (#2) reinforcing bars at 125 mm (5 in.) on center. The bars had a measured yield strength of 315 MPa

(45.7 ksi), and the concrete had a compressive strength of 42 MPa (6.07 ksi) at the time of testing. Double bending tests were conducted on these columns under increasing lateral loads and subsequently ductility increments with a constant axial load of 592 kN (133 kips).

"As-built" CS2.5 suffered a brittle shear failure as expected on the first cycle to  $\mu_{\Delta} = 3$ . The peak lateral load the column sustained was at  $\mu_{\Delta} = 3$  just before failure and is slightly higher than the ideal flexural strength of the column, 531 kN (119.4 kips). As failure commenced on the first cycle to  $\mu_{\Delta} = 3$ , the load dropped rapidly to approximately 178 kN (40 kips) and the column failed in shear. The oval steel-jacketed specimen tested in Verma, Priestley, and Seible (1993), and previously discussed in Section 2.2.2.1, reached an ultimate ductility of 10 with no drop in lateral load capacity from the maximum lateral load of approximately 712 kN (160 kips). This result shows a significant increase over an ideal flexural strength of the steel-jacketed specimen of 565 kN (127 kips).

The composite retrofit design is shown in figure 3-4. The thickness of the five different retrofit zones was measured after testing was complete. The thicknesses of the five levels, from the bottom to top, are 1.80 mm, 1.05 mm, 0.60 mm, 1.05 mm, 2.00 mm (0.072 in., 0.041 in., 0.024 in., 0.041 in., 0.078 in.) respectively. The measured properties of the composite material show that the material used in this test had a fiber volume fraction of 30%, ultimate tensile strength of 1,393 MPa (202 ksi) and a tensile modulus of 117 GPa (17,000 ksi).

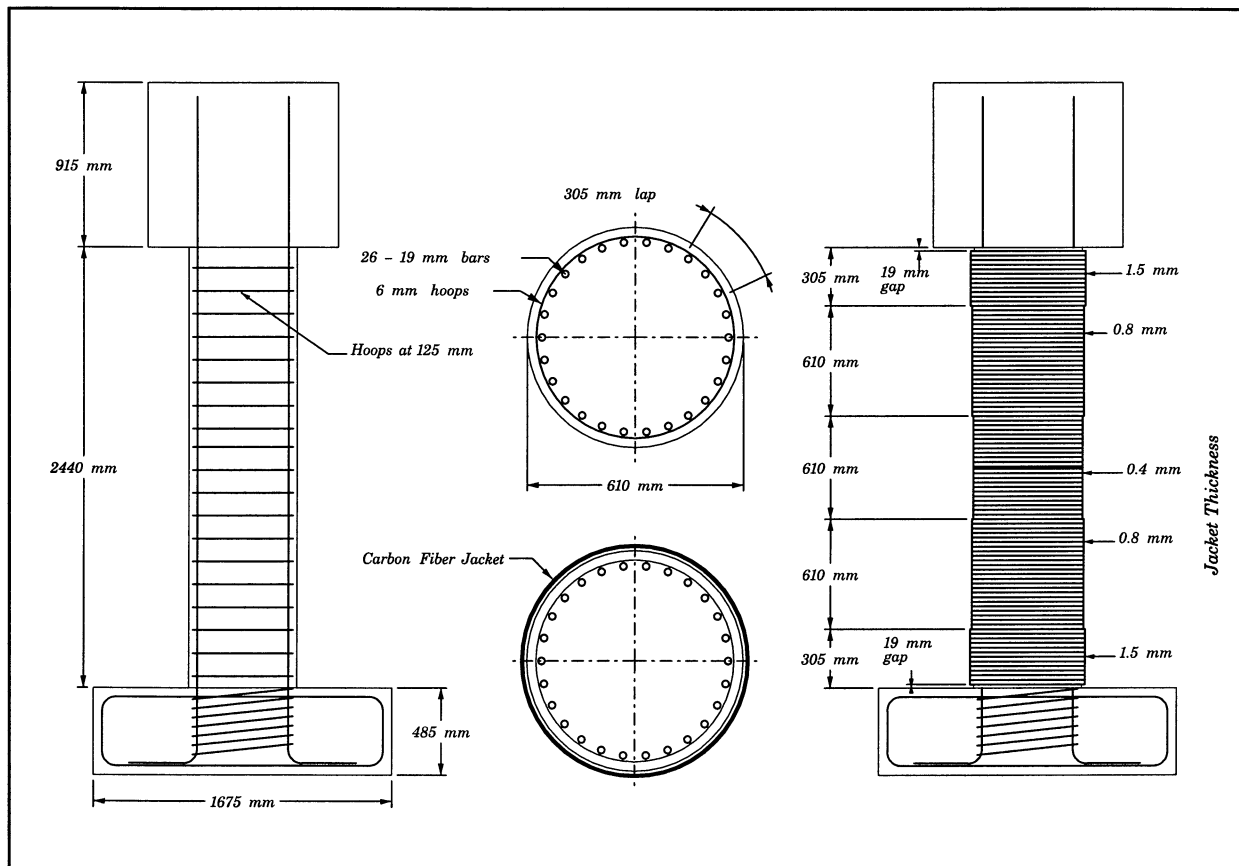


**FIGURE 3-4 Circular Shear Column with 2.5% Reinforcing, CS2.5 (Seible, Hegemier, et al., 1994b)**

This retrofit design allowed the column to sustain an ultimate  $\mu_{\Delta} = 10.5$  ( $\pm 4.5\%$  drift) with no drop in lateral load capacity from a peak of approximately 600 kN (135 kips). The ideal flexural capacity lateral load was 538 kN (121 kips). The significant ductility and loads in excess of the ideal flexural strength capacity are indicative of a conversion in behavior of this column from a brittle shear mode in the "as-built" specimen to a ductile flexural response. Thus, this retrofit met all three of the performance criteria established for judging structural performance, namely, performance on par with a steel jacket retrofit,  $\mu_{\Delta} \geq 8$ , and ductility twice that of the "as-built" column.

Seible, Hegemier, et al. (1994a) describe the testing of a very short circular column with 1% reinforcing and its retrofit, CS1. The columns have a diameter of 610 mm (24 in.) and are reinforced longitudinally with ten, 19 mm (#6) reinforcing bars and transversely with 6 mm (#2) reinforcing bars at 125 mm (5 in.) on center. The longitudinal bars had an average measured yield stress of 293 MPa (42.5 ksi), and the transverse bars, 403 MPa (58.5 ksi). The compressive strength of the "as-built" column concrete at the time of testing was 36.7 MPa (5,330 psi) and for the retrofit column, 37.2 MPa (5,390 psi). Refer to page 73 for general information regarding the innovative automated column wrapping process used on this and other columns.

The columns are subjected to an axial load of 1,780 kN (400 kips) during the test as well as increasing lateral displacements. The "as-built" column had a theoretical yield capacity,  $V_y$ , of 507 kN (114 kips), and an ideal theoretical flexural capacity,  $V_{yi}$ , of 614 kN (138 kips). The "as-built" specimen was able to achieve a ductility,  $\mu_{\Delta} = 8$ , and had a stable lateral load capacity in excess of its theoretical flexural strength capacity until the second push cycle to  $\mu_{\Delta} = 6$ . At this point, lateral load resistance was seen to begin gradual but stable degradation until the third push cycle to  $\mu_{\Delta} = 8$  at which point the testing was discontinued after lateral load resistance dropped to approximately 450 kN (101 kips). Testing was discontinued because the column bars were completely exposed at the base and substantial buckling of the reinforcing was apparent.

The retrofit for column CS1 is illustrated in figure 3-5. The thickness of the five retrofit zones was measured after completion of testing was complete. The thicknesses of the five zones from the bottom to top are 4.30 mm, 2.65 mm, 0.60 mm, 2.55 mm, and 4.35 mm (0.170 in., 0.105 in., 0.024 in., 0.100 in., and 0.171 in.) respectively. The measured properties of the composite material indicate that the material used in this test had a fiber volume fraction of 60%, an ultimate tensile strength of 1,393 MPa (202 ksi), and a tensile modulus of 117 GPa (17,040 ksi).

The retrofit column was able to sustain a ductile flexural response up to three cycles at  $\mu_{\Delta} = 14$  with no degradation in lateral load capacity from a maximum of approximately 752 kN (169 kips). This was the largest displacement ductility ever recorded for a column retrofit in the UCSD laboratory (XXSys Technologies, 1995b). Significant horizontal splitting cracks were present in the jacket at this load level, and yield penetration into the load stub was evident. Rotation of the load stub was noticed, indicating the presence of significant flexural deformation at the top of the column. Testing was discontinued due to limitations of the test setup and the real capacity of this retrofit is unknown.

The results of circular shear deficient column tests conducted by Saadatmanesh, Ehsani, and Jin (n.d.) at the University of Arizona are presented in the following paragraphs. These tests were part of a multifaceted research program described in Section 3. For information related to the retrofit materials used and specimen geometry, the reader is referred to pages 67-71 of this report. These pages should be consulted for all relevant specimen geometry and load details.

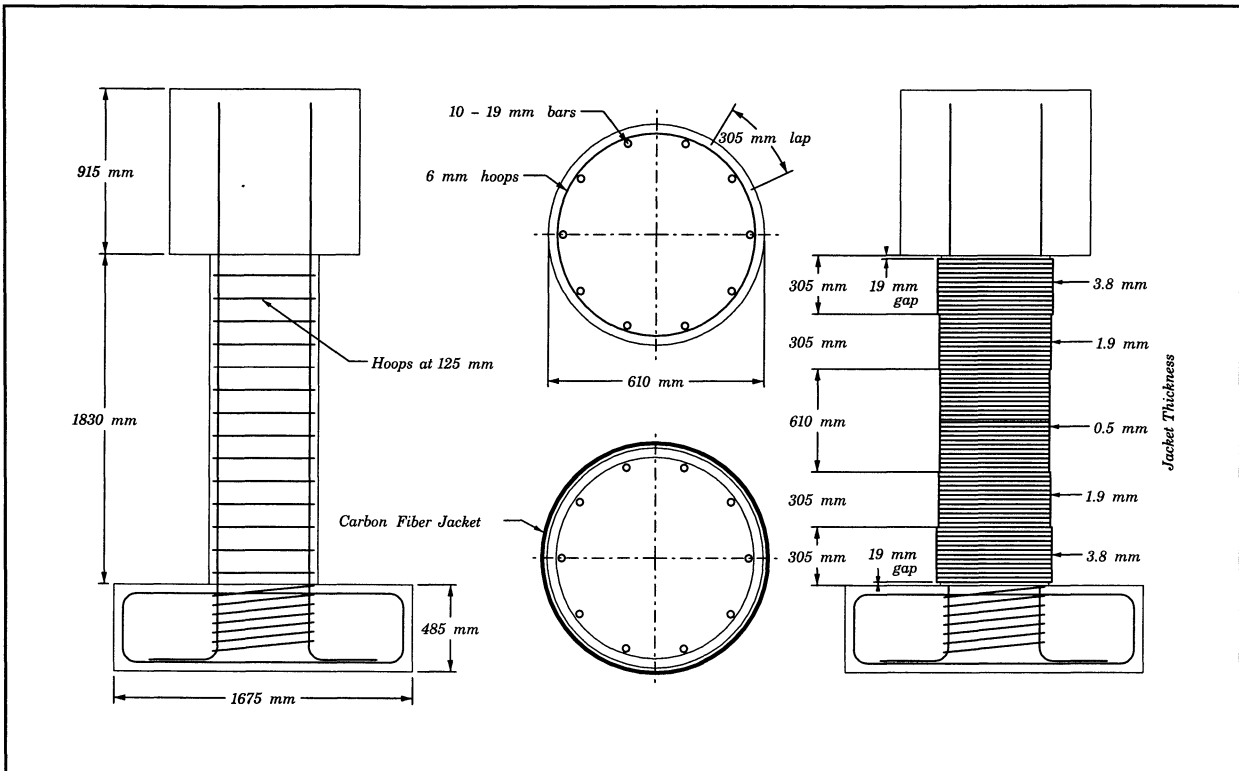


**FIGURE 3-5 Circular Shear Deficient Column with 1% Reinforcing (Seible, Hegemier, et al., 1994a)**

In specimen C-4, the maximum capacity of 72 kN (16.1 kips) was noted on the first push cycle to  $\mu_{\Delta} = 3$ , but rapid degradation of strength was noted at  $\mu_{\Delta} = 5$ . Column C-5 was tested with nearly the same hysteresis results as C-2 and C-3, columns with lap splices, presented on page 69. C-5 exhibited an increase in capacity of 22% over "as-built" C-4.

In addition to assessment of strength deterioration over the life of the test, stiffness deterioration was examined by comparing the stiffness at each cycle to the initial stiffness. As expected, all of the circular and rectangular columns saw their stiffness at the initial cycle reduced considerably through subsequent inelastic displacement cycles. However, the retrofit specimens had a slower rate of stiffness deterioration than did the "as-built" specimens.

Moment curvature data were plotted for the columns. The curve for column C-5 was essentially linear up to the point of steel yield, and a large increase in curvature occurred with increasing bending moment. Conversely, the moment curvature response for the "as-built" specimens was characterized by poor performance due to concrete crushing before the onset of steel yield.

In examination of the hysteresis loops of all test specimens, varying degrees of pinching were noticed. Pinching was amplified in columns with lap-spliced bars where the narrowing near the origin is due to longitudinal lap splice slippage.

As the initial test program progressed, a select number of columns were selected for repair testing. The repair columns were subjected to the same loading as the original specimens. The load-displacement envelope of the repaired column was plotted simultaneously with the original test results for comparison. The average stiffness per cycle was also computed for comparison purposes. Column C-4/R showed no increase in strength over the original C-4. Results of lateral load comparison are not representative of the overall effects of the repair. For instance, the results for C-4 and C-4/R are particularly misleading if lateral resistance is the only parameter by which the results are judged. Both columns attained the same lateral resistance, but while the load-displacement response of the original C-4 began to degrade at  $\mu_{\Delta} = 4$ , the retrofit was able to maintain a stable response to  $\mu_{\Delta} = 6$ . C-4/R demonstrated ever increasing lateral load resistance throughout the test sequence. Results of circular columns with continuous longitudinal bars illustrate that not only did the repaired column C-4/R have significantly improved overall performance as compared to C-4, the response was nearly as good as C-5.

### 3.3.2.2 Rectangular Shear Columns

Seqad Consulting Engineers (1992) present the results of a study in which rectangular columns, known to be deficient in shear capacity from tests conducted in an earlier investigation, were retrofitted with fiberglass-epoxy wraps. The intent of this investigation was to study the effect of retrofitting rectangular columns in their original shape, i.e., without first converting them into oval columns, as is common in steel jacket retrofits. The only modification to the columns was to round over the corners so as to avoid undue stress concentrations.

The columns had a clear height of 2,440 mm (8 ft), and cross-sectional dimensions of 610 mm x 405 mm (24 in. x 16 in.), producing a shear span-depth ratio of 2.0. The two columns to be retrofit were constructed with 19 mm diameter (#6) longitudinal reinforcing bars with a yield strength of 414 MPa (60 ksi) and a reinforcing steel ratio of 0.025. The transverse reinforcement consisted of 6 mm (#2) plain bars with 90° corner hooks lapped in the cover concrete. The two columns were identified by the authors as columns 6 and 7. Column 6 was subjected to an axial load of 507 kN (114 kips) during the test sequence while column 7 was subjected to an axial load of 1,780 kN (400 kips).

The retrofit for the columns was identical. The central 1,220 mm (4 ft) of the column was retrofit with three 1.15 mm (0.045 in.) layers of fiberglass fabric wrapped directly onto the column. The end regions, 600 mm each, were wrapped with an additional three layers, for a total wrap thickness in this region of 6.85 mm (0.27 in.). The layers were placed around the column in a passive state so as to avoid large membrane stresses in the jacket.

The theoretical moment capacity of the columns, 901 kN-m (662.5 kip-ft) and 1026 kN-m (754.3 kip-ft) for columns 6 and 7, respectively, was based on an ultimate compression strain of 0.005, a reinforcing bar yield strength of 462 MPa (67 ksi) and an unconfined concrete compressive strength of 34.5 MPa (5 ksi). These ideal capacities correspond to shears of 737 kN (165.6 kips) and 839 kN (188.6 kips) for columns 6 and 7 respectively. The fiberglass retrofit material was assumed to have a modulus of elasticity of 20.7 GPa (3000 ksi) and a maximum permissible strain of 4000  $\mu\epsilon$ .

The shear strength of the "as-built" and retrofitted columns was computed on the basis of equations developed in Priestley, Fyfe, and Seible (1991) using an angle between the column axis and the principal compression strut,  $\theta$ , of 30° and 45°. On the basis of a flexural overstrength factor of 1.25, corresponding to shears of 921 kN and 1,050 kN (207 kips and 236 kips) for columns 6 and 7,

respectively, column 6 would require a compression strut inclination of approximately  $30^\circ$ , while column 7 would require an angle closer to  $45^\circ$  to sustain these loads. Considering flexural ductility alone and an ultimate compression strain of 0.00864, displacement ductility factors,  $\mu_\Delta$ , of 4.5 and 3.0 were predicted for columns 6 and 7 in the "as-built" condition, predicated on the assumption that shear displacement and failure was prevented. However, column 6 was predicted to have an "as-built" shear strength of 628 kN (141.1 kips) with  $\theta=30^\circ$  and column 7 had a predicted strength of 882 kN (198.3 kips) with  $\theta = 30^\circ$ . When these capacities are compared to the theoretical moment capacity shears of 737 kN (165.6 kips) and 839 kN (188.6 kips) for columns 6 and 7, respectively, column 6 will be unable to attain its flexural capacity while column 7 will have a sudden failure after attaining its flexural capacity.

During full reversal cyclic testing, column 6 developed a stable flexural ductile response up to  $\mu_\Delta = 4.5$  with first signs of plastic hinge area failures, as evidenced by jacket buckling at  $\mu_\Delta = 6$ . At  $\mu_\Delta = 8$ , the jacket corner began to tear and had subsequent strength degradation; but residual strength was still in excess of the theoretical flexural strength, and cycling continued until  $\mu_\Delta=10$  when a complete jacket failure occurred with subsequent loss of confinement. Final failure was through low-cycle fatigue of the longitudinal steel. This column sustained a maximum shear force of 979 kN (220 kips), 32.5% above the nominal flexural strength.

Column 7, with a higher axial load, was expected to be a more critical test scenario. The performance of this column was also excellent. The peak lateral load was 1,168 kN (262.5 kips) at  $\mu_\Delta = 8$ , 39% above the nominal flexural strength. As in column 6, structural distress began at  $\mu_\Delta = 6$ , with final failure of the jacket occurring at  $\mu_\Delta = 8$ . The maximum shear was close to the predicted value using  $\theta = 30^\circ$  for column 7 of 1,181 kN (265.6 kips).

Based on these results, the authors concluded that columns with similar proportions and jacket designs could be safely designed to a displacement ductility of  $\mu_\Delta = 4$  and occasionally 5 or 6. The ability to convert a brittle shear response into a ductile flexural response was demonstrated with these two test columns. The authors tentatively concluded that columns with a more slender aspect ratio would not attain these ductility levels due to confinement failures.

The earliest reference located on composite retrofitting of concrete columns was published in Japan by Katsumata, Kobatake, and Takeda (1988). The objective of their research was to study the effectiveness of directly winding continuous carbon fiber strands onto the surface of rectangular columns to improve their seismic performance. Two types of substrate treatment were performed: (1) unbonding, which consisted of a layer of an isolation film applied between the fibers and column, and (2) direct winding, which consisted of bonding a resin and fibers directly to the surface of the specimen.

Ten rectangular 1/4-scale specimens were constructed. These specimens measured 200 mm (7.87 in.) square in cross-section and were 600 mm (23.6 in.) high. They were capped at the top and bottom with substantial rectangular blocks which fit into a loading frame in order to assure a fixed condition at the top and bottom during the reverse bending tests. The prototype columns had an axial reinforcing ratio of 0.95%, a shear reinforcing ratio of 0.107%, and a shear span ratio of 1.5. A constant axial stress of 4.57 MPa (46.6 kgf/cm<sup>2</sup>, 663 psi) was applied during testing. The carbon fiber material was an HP grade carbon fiber with each tow having an area of 0.23 mm<sup>2</sup> ( $3.57 \times 10^{-4}$  in.<sup>2</sup>) and an ultimate tensile strength of 2.87 GPa (29,300 kgf/cm<sup>2</sup>, 417 ksi).

The prototype column was shown to be dominated by insufficient shear capacity with significant loss of load-carrying capacity after only a few cycles at a drift angle of 1/150.

In two specimens, which were very lightly strengthened, bond cracks along the longitudinal bars grew and concrete crushing began at a drift angle of 1/50. Flexural yield was not attained and ultimate failure was a bond failure.

Finally, in the majority of the retrofit columns, excluding those previously mentioned, the following behavior predominated. Flexural yielding was seen to occur at an angle of 1/80; the beginnings of concrete crushing were evident at 1/50; and the mode of failure was transferred from shear to a ductile flexural response. Ultimate failure of most of the specimens was through eventual carbon fiber fracture. Very substantial increases in ultimate displacement, lateral load capacity, and especially hysteretic energy dissipation capacity were observed in the majority of retrofit specimens. The increase in displacement and energy dissipation was seen to be essentially a linear function of the amount of carbon fiber wrapping because of the enhanced degree of confinement provided by higher volumetric confinement ratios.

The difference in the unbonded and direct winding specimens was small. The direct winding specimens suffered eventual loss of bond with the concrete column, and at later stages of loading the performance of the fibers originally prevented from bonding and intentionally bonded was very similar. It was also found that a conversion of carbon fiber reinforcing to equivalent steel reinforcing was a reasonable approximation for determining the amount of fiber required if the equation below was used.

$$\rho_f \sigma_{cf} v_{cf} = \rho_w \sigma_{wy} \quad (3-1)$$

where

$\rho_f$	=	winding fiber ratio
$\sigma_{cf}$	=	tensile strength of carbon fiber
$v_{cf}$	=	strength effectiveness factor of carbon fiber, assumed to be two-thirds
$\rho_w$	=	transverse reinforcement ratio
$\sigma_{wy}$	=	yield strength of hoop reinforcement

This research was performed at the Technical Research Institute, Tokyo, and supported by the Mitsubishi Kasei Corporation, who provided materials for the experimentation.

The carbon fiber retrofit of a shear deficient rectangular bridge column, column RS2.5, is described in Seible, Hegemier, et al. (1995c). The column in question is a 0.4 scale model of prototypical columns constructed prior to 1971. The plan dimensions of the column are 610 mm x 405 mm (24 in. x 16 in.). The column is reinforced with twenty-two, 19 mm (#6) continuous longitudinal reinforcing bars with a measured yield of 290 MPa (42.1 ksi). This amount of reinforcing constitutes a longitudinal reinforcing ratio of 2.5%. Lateral reinforcing consists of 6 mm (#2) reinforcing bars spaced vertically at 125 mm (5 in.) on center. The measured yield stress of the lateral ties is 403 MPa (58.5 ksi).

The column was loaded with a vertical load of 507 kN (114 kips) and increasing lateral loads and displacements. The column was loaded in double bending so as to produce maximum moment at the column ends and constant shear along the column height. The theoretical yield capacity of the "as-built" specimen is 401 kN (90 kips), and the theoretical ideal capacity, 545 kN (122.5 kips).

The "as-built" and steel jacket specimens used as a reference point for this testing are originally presented in Xiao, Priestley, and Seible (1993) and are presented in Section 2.2.2.2 of this report. The "as-built" specimen failed in a shear mode at  $\mu_{\Delta} = 3$  after a capacity reduction of approximately 25% from the theoretical flexural strength of 545 kN (122.5 kips). The oval steel jacket retrofit was able to exceed the theoretical flexural strength and sustained a lateral load of approximately 650 kN (146 kips) until the column bars ruptured on the first pull cycle at  $\mu_{\Delta} = 12$ .

The retrofit of the rectangular column involved wrapping the whole column in a variable thickness jacket. Rectangular columns are more difficult to retrofit than oval ones because of the inability to develop hoop stresses and the possibility of stress concentrations at the corners. In order to reduce the stress concentrations, the original chamfered corners were ground into more rounded profiles. The "as-built" and retrofit specimens can be seen in figure 3-6.

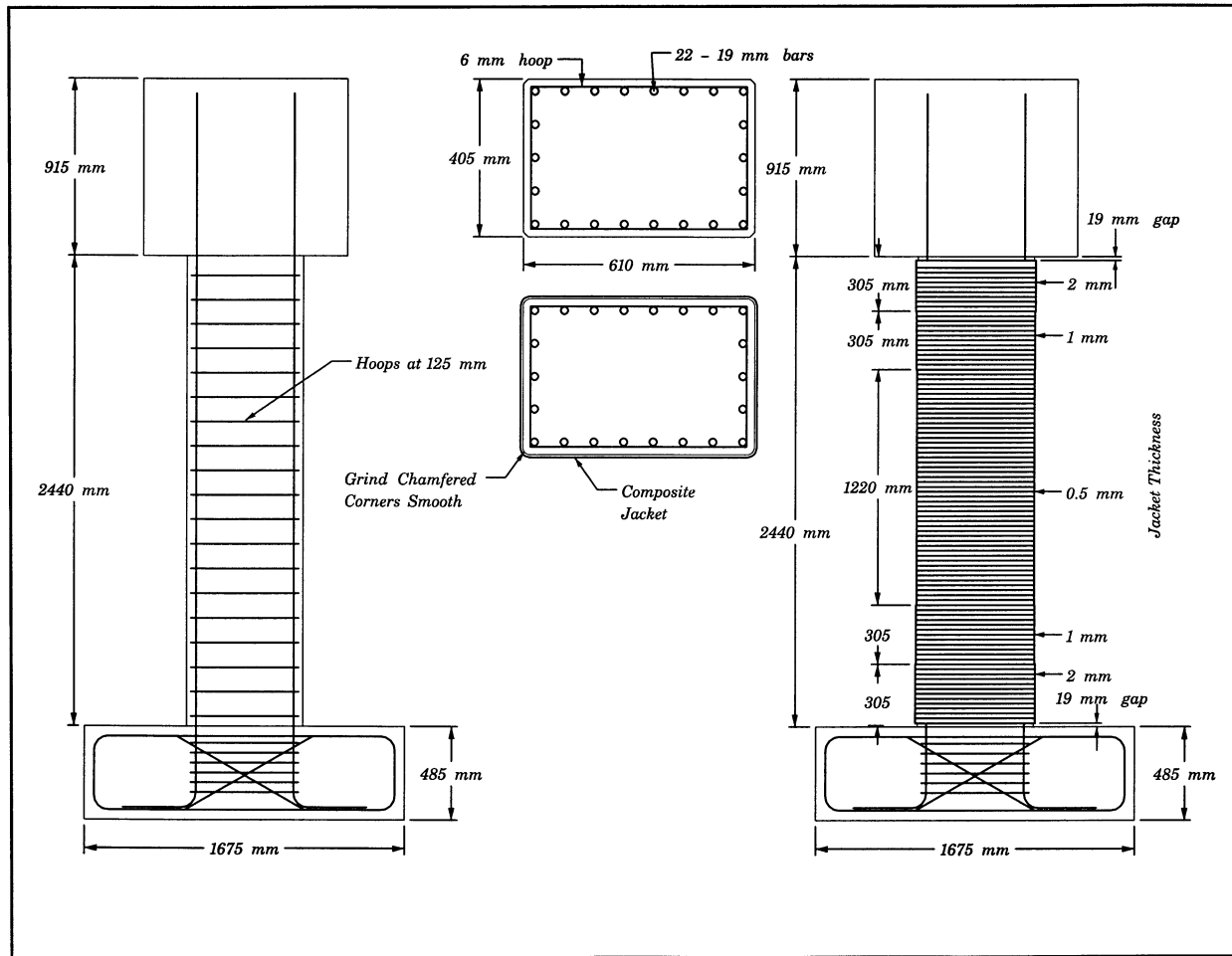


**FIGURE 3-6 Rectangular Shear Deficient Column RS2.5 (Seible, Hegemier, et al., 1995c)**

The carbon fiber jacket was able to maintain its theoretical flexural strength until  $\mu_{\Delta} = 8$ , at which time the lateral load resistance was reduced gradually. At this point, several horizontal cracks in the wrap were present, and the jacket began to bulge at the column ends. The test was stopped after three cycles to  $\mu_{\Delta} =$

12, due to capacity degradation to approximately 75% of the maximum capacity. At the end of the testing, the vertical column reinforcing had significantly buckled and the fibers had begun to fray.

Comparison of the steel and carbon fiber retrofits shows that the oval steel-jacketed column had a slightly higher lateral load capacity than to the carbon fiber retrofit column, but the carbon fiber retrofit column had a higher ultimate ductility.

The results of rectangular shear deficient column tests conducted by Saadatmanesh, Ehsani, and Jin (n.d.) at the University of Arizona are presented in the following paragraphs. These tests were part of a multi-faceted research program described throughout Section 3. For information related to the retrofit materials used and specimen geometry, the reader is referred to pages 67-71 of this report. These pages should be consulted for all relevant geometry and load details for the specimens described herein.

Column R-3 was tested as a reference column for the more highly reinforced rectangular specimens. It was expected that this column would exhibit shear-dominated failure. This column reached its ideal flexural capacity at  $\mu_{\Delta} = 1.5$  and large flexural shear cracks appeared at  $\mu_{\Delta} = 2$ . On the first push cycle to  $\mu_{\Delta} = 3$ , extensive shear cracks over the entire height of the column were noted and the longitudinal bars separated from the column core due to poor transverse confinement. Columns R-4 and R-5 were both tested and behaved in a stable fashion to  $\mu_{\Delta} = 6$  with no drop in capacity. R-4 was retrofit in the original rectangular shape while R-5 was first made oval in shape in order to induce membrane stresses into the jacket material. Columns R-4 and R-5 demonstrated increases in strength of 32% and 39% over "as-built" R-3.

In addition to assessing of strength deterioration over the life of the test, stiffness deterioration was examined by comparing the stiffness at each cycle to the initial stiffness. All of the circular and rectangular columns saw their stiffness at the initial cycle reduced considerably through subsequent inelastic displacement cycles as would be expected. However, the retrofit specimens had a slower rate of stiffness deterioration than did the "as-built" specimens.

Moment curvature loops were plotted for the columns. The curves for columns R-4 and R-5 were practically linear up to the point of steel yield, and a large increase in curvature occurred with increasing bending moment. Conversely, the moment curvature response for the "as-built" specimens is characterized by poor performance due to concrete crushing before the onset of steel yield.

In examining of the hysteresis loops of all test specimens, varying degrees of pinching were noticed. Pinching was amplified in columns with lap-spliced bars where the narrowing near the origin is due to longitudinal lap splice slippage.

During the initial test program, a number of columns were selected for repair testing. Column R-3/R was a repaired version of R-3. The load-displacement envelope of the repaired column was plotted simultaneously with the original test results for comparison. The average stiffness per cycle was also computed for comparison. Results of the test indicate that column R-3/R attained a maximum lateral load 31% greater than that of column R-3 and demonstrated ever increasing lateral load resistance throughout the test sequence.

Test results for rectangular columns with continuous bars show that although the original R-3 failed in shear, specimen R-3/R had an indiscernible response from columns R-4 and R-5. This was the most effective retrofit in comparing the response of the repair to originally tested columns.

### **3.3.3 Environmental Testing and Effects on Composite Performance**

This section presents some of the environmental performance characteristics of composite materials. The information presented here, though not directly related to column retrofitting, is intended to describe some of the possible damage modes in composite retrofit specimens due to freeze-thaw effects, salt water affects, temperature cycling, and other factors. In addition, the evaluation of bond characteristics between composites and concrete specimens is included. This review is not a comprehensive treatment of the subject but is only intended to identify several areas of concern in the use of composite materials.

Environmental tests on 60 small retrofit and "as-built" beam specimens, is reported in Chajes et al. (1994). The retrofit beams had their tension flanges retrofit with either aramid, E-glass, or graphite fabrics. These beams were fabricated in five batches of twelve. Each batch had three beams retrofit on the tension side with aramid, three with E-glass, three with graphite, and three left unwrapped.

Two test procedures were employed. The first test was a freeze-thaw test in general conformity with ASTM C672-84. Two of the five batches of twelve beams were submerged in a calcium chloride solution and kept in airtight containers. The beams were exposed to temperatures of  $-17^{\circ}\text{C}$  ( $1.4^{\circ}\text{F}$ ) for 16 hours and then allowed to rest at room temperature for 8 hours for 50 cycles for one batch and 100 cycles for the other. The beams were then loaded to failure in four-point bending.

The second test procedure involved cycling two batches of beams at room temperature in the same type of calcium chloride solution but alternately submerging the beams for 16 hours and allowing them to dry at room temperature for 8 hours; as previously noted, one batch underwent 50 cycles and the other 100 cycles. The fifth batch was used as a control with neither freeze- thaw nor wet-dry cycling being applied.

In general, test results showed that the wet-dry cycling was found to be more severe. All E-glass beams failed following fabric tearing, while the environmental conditions in some cases affected the failure mode of the graphite and aramid fiber reinforced beams. Examination of the failed beams showed debonding in some instances in the graphite and aramid reinforced beams, while the E-glass reinforced beams showed no debonding.

The graphite beams showed a markedly smaller decrease in strength than the aramid and E-glass-reinforced specimens. For example, the graphite exhibited only a 19% drop in strength after 100 wet-dry cycles, while the aramid and E-glass retrofit specimens exhibited a decrease in flexural strength of 36%. The unwrapped specimens had a 12% reduction in strength for this same cycling as compared to the 0 cycle controls.

After evaluating the effects of all environmental cycling, only the graphite-reinforced specimens maintained their strength advantage over the unwrapped specimens. The strength advantage of the aramid specimens over the unwrapped specimens before 100 cycle wet-dry cycling was 191% and after cycling, 111%. Similarly, the E-glass specimens had a pre-cycling strength advantage of 88% and post-cycling advantage of 37%. In contrast to these results, the graphite-reinforced specimens exhibited a pre-

cycling strength advantage of 139% and maintained a strength advantage of 127% after 100 freeze-thaw cycles and 120% after 100 wet-dry cycles.

The effect of substrate preparation and bond between concrete and composites was documented in Finch et al. (1994). Specimens were constructed to examine the effect of surface preparation, type of adhesive, bond length, and concrete strength on the average bond strength. Results of tests performed with four different two-part epoxy adhesives illustrated that bond strengths much greater than the shear strength of the concrete could be attained.

Three different surface preparation methods were also examined: bonding the composite to the "as-cast" surface, mechanically abrading the surface, and mechanically abrading the surface and subsequently sealing the concrete with a silane primer. Test results indicate that abrasion in conjunction with the primer represented the optimum surface preparation method. The capacity of the interface was determined to vary with the compressive strength of the concrete.

To examine the effect of bond length, a series of specimens with bond lengths varying from 50 mm (2 in.) to 205 mm (8 in.) were tested. Fairly constant shear flow was observed in the specimens and minimum transfer lengths for the joints were determined.

The results of freeze-thaw durability tests on two glass fiber composites are presented in Gomez and Castro (1996). The purpose of the experiments was to explore the effects of cyclic freezing and thawing on the strength and stiffness characteristics of commercially available glass fiber composites. Two matrix materials were selected for the study: (1) a vinyl ester and (2) an isophthalic polyester. The glass fibers were continuous strand mats for multidirectional strength properties and continuous strand rovings in the direction of pultrusion. Testing was conducted on coupons measuring 10 mm (0.375 in.) thick, 305 mm (12 in.) long, and 25 mm (1 in.) wide. Some of the coupons had their edges sealed with an epoxy sealant to restrict moisture infiltration, while others were left uncoated.

The coupons were tested by the same test method used to characterize the freeze-thaw durability of concrete, ASTM C-666, Standard Test Method for Resistance of Concrete to Rapid Freezing and Thawing. Testing consisted of placing the coupons in a 2% NaCl-water solution and a ramp down in temperature from 4.4°C (40°F) to -17.8°C (0°F). The specimens were held at this temperature and then elevated in temperature to 4.4°C (40°F) followed by a subsequent hold at this temperature. A complete cycle took approximately three hours. Every 50 cycles, groups of three coupons were removed for testing. Also tested were three coupons that were placed in solution for an equal amount of time but not cycled. The coupons were tested for dynamic modulus per ASTM C-215, Standard Test Method for Fundamental Transverse, Longitudinal, and Torsional Frequencies of Concrete Specimens. The coupons were then tested to flexural failure using ASTM D-790, Standard Test Methods for Flexural Properties of Unreinforced and Reinforced Plastics and Electrical Insulating Materials. From these series of tests, plots of flexural strength and dynamic modulus versus number of cycles were prepared with normalization of the data to the virgin specimen values. Calculation of Young's Modulus and Modulus of Toughness, expressed as the area under the load-deflection curve, was performed at each cycle on each coupon.

Results from the 300 cycle specimens show degradation of flexural strength and toughness with exaggeration of these effects for the specimens whose edges were not sealed. Back calculation of Young's Modulus illustrated a 24% loss and 22% loss for the isophthalic polyester and vinyl ester composite, respectively.

The unsealed vinyl ester coupons lost 32% of their initial flexural strength after 300 cycles while sealed coupons lost 22%. Both sealed and unsealed coupons lost approximately 3% of their initial dynamic modulus and between 22% and 32% of their initial Modulus of Toughness. Moisture content was judged to be 0.14% for the unsealed coupons and 0.07% for the sealed.

The unsealed isophthalic polyester resin coupons lost 19% of initial flexural strength after 300 cycles while the sealed specimens lost 24%. The unsealed coupons lost 3%-4% of their initial dynamic modulus while sealed specimens lost 2.5%-3%. Modulus of Toughness decreased 20% for the unsealed coupons and 27% for the sealed coupons. The values for the 300 cycle unsealed isophthalic polyester resin did not follow the trend of all of the other test data and were considered to be irregular and not representative of the actual degradation of the specimen properties. Moisture contents at the termination of cycling were found to be 0.15% for the unsealed coupons and 0.14% for the sealed coupons.

Coupons immersed in solution but not subjected to the freeze-thaw cycling were tested with the following results. The sealed isophthalic polyester resin exhibited a 3% loss in flexural strength, 7% reduction in Modulus of Toughness, and 2% reduction in Young's Modulus. The unsealed isophthalic polyester resin specimens had a 5% loss in flexural strength, 9% in Modulus of Toughness, and 5% reduction in Young's Modulus. The sealed vinyl ester resin specimens exhibited a 6% drop in flexural strength, 10% in Modulus of Toughness, and 3% in Young's Modulus. Finally, the unsealed vinyl ester resin specimens suffered a 7% loss of flexural strength, 15% degradation in Modulus of Toughness, and 4% drop on Young's Modulus.

These results show that freeze-thaw cycling has a dramatic impact on the engineering properties of the two glass fiber materials tested. This damage was hypothesized to be due to crack enlargement because of the expansion of ice crystals in the material. Also hypothesized was that the fiber and fiber/matrix interface damage may have occurred during repeated cycling. Significant scatter in the data was reported in both the cycled and virgin test specimens, which is consistent with composite material test results in general. The freeze-thaw cycling was judged to be the direct cause of the difference in test results between the virgin and cycled specimens.

The effect of cold temperatures on the performance of composite wrapped standard concrete cylinders was studied and presented in Karbhari and Eckel (1994). In this test program, ASTM standard test cylinders with a 28-day strength of 51.9 MPa (7522 psi) and a secant modulus of 33.8 GPa ( $4.9 \times 10^6$  psi) were used as the virgin specimens. The wrapped specimens involved the use of a wet layup technique as well as glass, carbon, and aramid fibers. After wrapping, the specimens were vacuum bag cured at room temperature for 36 hours. Following curing, the specimens were divided into two sets, one set maintained at ambient room temperature and referred to as controls, and the second set maintained at  $-17.8^\circ\text{C}$  ( $0^\circ\text{F}$ ) in conjunction with high humidity. This conditioning was carried out for 60 days. This time period was determined to be sufficient for the composites to reach a saturated state. A minimum of three specimens of each conditioning type and material were constructed including controls.

The specimens were tested in axial compression using urethane pads in a steel receiver to insure pure axial load. Axial deformation was measured as was rotation due to uneven crushing of the cylinders. Failure load ratios for the ambient and cold temperature specimens were computed. The maximum failure load increase was in the carbon fiber-wrapped specimens with ambient and cold temperature conditioning exhibiting an increase in strength of 26.15% and 31.70%, respectively, over the unwrapped specimens. All three material types showed an increase in failure load at the  $-17.8^\circ\text{C}$  ( $0^\circ\text{F}$ ) level as

compared to the ambient temperature levels. This result can be traced to the matrix hardening that occurs at low temperatures, increasing the off-axis and transverse composite material strengths. Additionally, comparison of the amount of axial deformation at failure illustrates that the glass fiber-wrapped cylinders showed the highest deformation and aramid fiber wrapped specimens had the smallest deformation at failure. The glass and carbon-wrapped specimens exhibited an increase in stiffness after cold temperature conditioning while the aramid specimens exhibited a decrease in stiffness because the aramid fibers and resin debond at cold temperatures resulting in individual element failure as opposed to failure of a composite material.

The results of this experimentation tend to show that the carbon fiber presents the best means of strengthening a concrete specimen in low temperatures though ultimate failure is sudden and catastrophic. The glass fibers exhibit significant tearing of fibers in the hoop direction but fail in a more gradual fashion. On the basis of their marginal strengthening characteristics, the aramid fibers were envisioned to be used as a protective layer against ice abrasion in cold climates because they are highly abrasion resistant compared to glass and carbon fibers.

### **3.4 Field Installations**

The construction of actual composite retrofits is presented in this section. Information includes composite jacketing in the United States and Japan and discussions of some successful and unsuccessful attempts to retrofit columns in-situ.

Koga et al. (1994) explore various applications of carbon fibers to structural retrofitting. They present a series of field applications in Japan where carbon fiber sheets and strands were used for the strengthening of reinforced concrete structures. In one instance, a solid wall "hammerhead" bridge pier was strengthened at its base with vertically oriented fiber sheets for increasing flexural strength and horizontally oriented fibers to enhance shear strength. The use of an automatic winding machine was illustrated as a means of rapidly winding carbon fiber strand not only onto bridge columns but also chimneys, water tanks, etc. In addition, Koga et al. present the results of experimental testing of two one-third scale rectangular column specimens loaded cyclically about their weak axis under constant axial load.

Typical of many existing columns in Japan, the specimens tested had termination of the longitudinal reinforcement at approximately one-third of the height of the column measured from the footing. Testing of the "as-built" specimen resulted in the longitudinal reinforcing bar buckling at the cut-off point due to shear failure. The retrofit specimen consisted of vertically oriented carbon fiber sheets over-wrapped with 12 K carbon fiber tows wound in the horizontal direction. This column experienced a ductile flexural failure, a maximum lateral force 24% greater than the "as-built" specimen, and a threefold increase in lateral displacement capacity.

The use of the Hexcel Fyfe TYFO S retrofit system, described previously in this section on page 65, is also described in a number of citations (Better Roads, 1993), (Fyfe, 1994a, 1994b), (Hexcel Fyfe, 1995), (McConnell, 1993), (Noori and Saiidi, 1993) with reference to the seismic upgrade of the Sparks viaduct in Sparks, Nevada. The viaduct carries Interstate 80 (I-80) about 18 miles east of the California/Nevada state line. The unique feature of the viaduct is that several of the bridge columns penetrate the roof of a casino under the bridge. Many of the columns are close to gaming tables and three run through a salt

water aquarium in the casino. The casino operates 24 hours a day and was to remain open for the duration of construction.

Seismic evaluation of the structure as described in Noori and Saiidi (1993) indicated that there were major deficiencies in the column to cap beam lap splices and in the confinement of plastic hinge regions. Column shear capacity outside of the hinge regions was deemed adequate. Retrofit was to consist of drop panels at the top of the column and steel casings on the columns immediately below the drop panels. The steel jackets were to be 1,370 mm (4.5 ft) high and 9.5 mm (3/8 in.) thick. This combined retrofit was intended to provide a column displacement ductility of 6. A total of 96 columns were to be retrofit as described above (Better Roads, 1993).

The contractor on the job quickly realized the logistical problems that would be encountered if steel jackets were used. The jackets would need to be lowered onto the roof of the casino and through penetrations in the roof after closing a lane on the freeway above. This was to minimize construction inside the casino. Additionally concerns included welding and grouting the column jacket inside the casino and the potential property damage that could be incurred. Other complications involved the fact that in some locations, clearance around the columns is 19 mm (3/4 in.). Recognizing these problems, the contractor submitted a value engineering proposal, which was approved, that entailed use of the Hexcel Fyfe TYFO S Fibrwrap™ System.

Wraps were passed through a resin bath to saturate the fiberglass and placed upon the upper regions of the column below the drop panels as previously described. Workers were able to wrap three to four columns per day. The actual retrofit of the columns entailed passive retrofit of varying thicknesses and was completed within the original budget.

Hawkins, Patel, and Steckel (1995, 1996) discuss the failure of two composite jackets in the Griffith Park Area of Los Angeles. In this area, fifteen circular reinforced concrete columns were reinforced with the SEH 51/TYFO S retrofit system designed by Hexcel Fyfe. These retrofits, which underwent extensive structural testing at the University of California, San Diego, consist primarily of circumferential E-glass fiber tows with widely spaced vertical tows of E-glass and carbon fiber. The two column failures in question employed the "stressed" TYFO S system. This stressed retrofit process has been described previously in this document in the discussion of a number of references but is presented again herein for clarity.

The stressed jacket construction process consists of cleaning and smoothing the column surface, placing an elastomeric bladder around the column, saturating a composite sheet in an epoxy resin, wrapping the composite sheet around the elastomeric bladder, curing the jacket at ambient conditions, injecting grout into the bladder so as to create a hoop stress condition in the jacket and radial pressure on the column face, letting the grout set, applying passive layers of composite, and finally, applying a coating for architectural and protective purposes. Upon construction of these retrofits, a set of control panels was also constructed measuring 305 mm x 305 mm (12 in. x 12 in.) and three plies thick.

The two columns that ruptured are described as Bent 11 and Bent 12. These columns survived the January 1994 Northridge Earthquake unscathed but unexpectedly failed in routine service about 9 months after the earthquake. Bent 11 extended approximately 4,570 mm (15 ft) above ground and was wrapped with five, 915 mm (3 ft) wide wraps. The location of the rupture is in the second wrap from the top of the column. This rupture extends the full width of the wrap. Bent 12 was somewhat shorter at 3,050 mm (10

ft) above ground and had three visible wraps; fracture occurred in the middle wrap. The fractured portion of the composite jacket was removed from each bent for laboratory analysis. The tests consisted of optical microscopic analysis, fractographic analysis, and fiber content analyses.

In their discussion of the laboratory findings, Hawkins et al. concluded that the wraps failed in tension after a tensile crack reached a length at which the growth of the crack became unstable. This tension crack started in a relatively flat region of the jacket parallel to the column axis and progressed to an irregular region where the crack propagated axially and circumferentially. Wrap distortion was present, which was thought to be indicative of significant residual stress relief at rupture.

There was a significant bulge in the Bent 12 wrap in the area where the flat region and irregular region came together. Hawkins et al. hypothesized that this bulge formed after fracture due to the lack of a bulge in the grout remaining on the column. In the bulge area, all of the vertical Kevlar tows for one ply has a discernable jog in the circumferential direction. A corresponding jog is not found in the matrix, leading Hawkins et al. to conclude that the jog was formed because of nonuniform fabric tension before the matrix cured. This defect would conceivably lead to nonuniform fiber loading during prestressing. This nonuniform loading was hypothesized to be the explanation for the residual stresses and premature failure of these wraps because some of the fibers were at much higher stresses than traditional hoop stress theories would predict.

Parts of the removed wrap samples were analyzed in a resin burn-off test which leaves only the glass fibers as products of the combustion. Hawkins et al. determined from the test that 96% of the glass fibers were oriented circumferentially around the column and that they constituted a volume fraction of 0.35. On the basis of the rule of mixtures for composites which defines the properties of a composite as a function of the volume fraction and properties of the constituent materials, the tensile strength of the glass/epoxy composite was predicted to be 1,207 MPa (175 ksi). However because of the effects of weaving and fiber crimp during manufacture of the woven glass panels, actual strengths are significantly lower. Strengths of 552 MPa (80 ksi) to 586 MPa (85 ksi) for the TYFO S jacketing system have been reported.

The predicted hoop stress state in the composite based on the  $\sigma = pr/t$  formula for thin-walled pressure vessels was 207 MPa (30 ksi) based on a grout pressure,  $p = 0.69$  MPa (100 psi), a column radius,  $r = 914$  mm (36 in.), and a jacket thickness,  $t = 3.05$  mm (0.12 in.). This is much less than the strengths listed above. Testing of a specimen from the "as-built" retrofit produced an *in-situ* tensile strength of only 309 MPa (45 ksi) due to the effects of nonuniform loading, much closer to the predicted stress.

Hawkins et al. reports the results of other researchers indicating that composites suffer from stress corrosion/creep rupture, a phenomenon whereby composite materials held at constant stresses well below their theoretical stress limits failed over time. For instance, Hawkins et al. reports that fiberglass strands held at 33% of their ultimate failed after 10 years, and 38 of 95 specimens held at 50% of ultimate failed after 5 years. In the case of the failed column jackets, the ratio of the predicted uniform hoop stress to the *in-situ* tensile strength is approximately 67% with localized fiber stresses much higher due to the jogged plies. This combination of a high uniform stress ratio and much higher localized stress ratios was hypothesized to be sufficient to have caused the creep rupture in three years. Note that passive retrofits have not experienced similar problems.

In a field demonstration of an automated column wrapping technique, the Robo-Wrapper™ as designed by the XXSys Corporation was taken to I-10 (Santa Monica Viaduct) in Los Angeles, California, for use in wrapping two bridge bents comprised of five columns total (Seible, Priestley, and Innamorato, 1995). The bents have pile cap foundations with bottom mat reinforcing only and 1,220 mm (48 in.) lap splices between the longitudinal column reinforcing and the footing starter bars. The columns have very close transverse reinforcing for the 1956-57 construction period, 13 mm (#4) reinforcing spirals at an 90 mm (3 1/2-in.) pitch. Because of this high degree of confinement, only the lap splice force transfer in the cap beam and footing were of real concern. The bridge had a low seismic vulnerability and was therefore deemed appropriate for a demonstration project to show the application of this new technique and to monitor the long-term performance of the system. The column wrapping was part of an overall retrofit that also includes installation of a link beam below the column cap.

Gamble, Hawkins, and Kaspar (1995), Lin, Gamble, and Hawkins (1994), and Shkurti et al. (1995) present the results of a series of tests on "as-built" and retrofitted bridge columns in East St. Louis, Ill. Nine columns were tested in all: four in the "as-built" condition and five in the retrofitted state. Of the retrofit columns, three involved tensioned steel bands or strands, and two involved fiberglass jackets from different manufacturers. Test results from the steel band/strand retrofits can be found in Section 4.2 of this report while the "as-built" and composite jacket retrofits are described here. Table 3-2 presents information on the test columns, including those described in other parts of this report.

**TABLE 3-2 I-70 Bridge Retrofit Test Columns**

Column Designation	Retrofit Type	Diameter	# of 36 mm (#11) bars
B14S	"As-Built"	1220 mm (48 in.)	18
B18N	Bands	1370 mm (54 in.)	28
B18S	"As-Built"	1370 mm (54 in.)	28
C14N	NCF	1220 mm (48 in.)	18
C14S	RJW	1220 mm (48 in.)	18
C15N	Bands	1220 mm (48 in.)	18
C15S	"As-Built"	1220 mm (48 in.)	18
C17N	DSI	1370 mm (54 in.)	24
C17S	"As-Built"	1370 mm (54 in.)	24

The nine bridge columns described in the three reports mentioned in the previous paragraph formed part of an extensive interchange on the East St. Louis, Ill, side of the Poplar Street Bridge, which was constructed in 1968 and carries I-70 over the Mississippi River. Because of the presence of a lap splice at the column base, a poor crash wall reinforcing anchorage when the column is pushed away from the centerline of the pier, little or no tension capacity in the anchorage between the battered piles and the pile cap, and piles too short to reasonably accommodate the potential liquefaction at the site, it was decided to replace the main structures carrying I-70. However, the ramp structures and feeder roads that connect to

this major interchange were to be preserved by means of external retrofit. Upon removal of the main structures of the interchange, nine columns were then to be tested to assess the "as-built" and retrofit response.

The "as-built" columns were either 1,220 mm (48 in.) or 1,370 mm (54 in.) in diameter, 9 m to 11 m (29.5 ft to 36.1 ft) tall. They formed part of a two column pier connected at the top by a weak link beam. They were all reinforced with 36 mm (#11) longitudinal bars with a yield stress of 276 MPa (40 ksi). The number of bars in the column varied from column to column from 18 to 28. The bars were lap spliced at the base over a length of 1,090 mm (43 in.), equivalent to  $30 d_b$ . Lateral reinforcing consisted of 13 mm (#4) hoops spaced at 305 mm (12 in.) closed with a 380 mm (15 in.) lap. The design strength of the concrete was 24 MPa (3.5 ksi). Actual *in-situ* concrete strength was found to be 1.5 to 2.5 times greater than specified on the basis of field cores and cubes removed from the column concrete. The reinforcing was found to be highly irregular in its spacing and cover. The clear cover to the ties ranged from 2.5 mm (0.1 in.) to 100 mm (4 in.) in the same column. In one of the 1,370 mm (54 in.) columns, very few of the longitudinal bars and dowel bars were in contact with some separations as large as 150 mm (6 in.). The columns with fewer bars tended to be more uniform than those with a larger amount of steel. Remarkably, very little corrosion was found on the main bars of the test columns, in spite of the negligible cover in some instances.

Lin, Gamble, and Hawkins (1994) report the results of the first two "as-built" column tests as well as the first retrofit test. The results of the "as-built" test of specimens B18S and B14S is presented here with retrofit results for retrofit column B18N presented in Section 4.2 this report. Column B14S is a 1,220 mm (48 in.) diameter column reinforced with eighteen, 36 mm (#11) bars while column B18S was a 1,370 mm (54 in.) diameter column with twenty-eight, 36 mm (#11) bars.

An analytical model was developed to apply horizontal loads sufficient to cause plastic hinging in the rigid frame model of the two columns and link beam while the dead load of the roadway above was acting. Analysis showed that hinges in the columns and beam formed almost simultaneously with the column hinges being located 6.71 m (22 ft) above the crash wall. This analysis is based on assumed material properties of  $f'_c=27.6$  MPa (4,000 psi) and  $f_y=276$  MPa (40 ksi). The column load/moment interaction diagram revealed that in a pure moment condition, the column bending capacities were 2,440 kN-m (1800 ft-kips) and 4,202 kN-m (3,100 ft-kips) for the 1,220 mm (48 in.) and 1,370 mm (54 in.) columns, respectively. The nominal lateral loads applied at a distance of 6.71m (22 ft) above the crash wall to produce flexural yielding at the base were computed to be 365 kN (82 kips) and 623 kN (140 kips). These loads were significantly less than the shear capacity of the columns; therefore a flexural failure of the "as-built" specimens was expected.

Moment curvature relationships were developed for the two columns considering zero axial load, an axial load of 890 kN (200 kips), and an axial load of 1,779 kN (400 kips). The 1,779 kN (400 kip) load is the maximum expected service dead plus live load. Because lateral seismic loads would tend to unload one column and more heavily load another column, Lin decided that axial forces could be neglected and that testing of single columns as opposed to the entire bent would be sufficient.

Testing consisted of reversed lateral loading via two horizontally actuated hydraulic jacks with a capacity of 890 kN (100 tons) each. Displacements at the load point as well as limited measurements of column base curvature were recorded. Because testing was conducted in the middle of a construction site in less than desirable conditions, the amount of data collected was limited as previously noted.

Column B18S was first loaded laterally to 356 kN (80 kips) in the north direction, with a resulting displacement of 15 mm (0.6 in.). Upon load reversal using the same load, the displacement was 25 mm (1 in.). The difference in load/displacement response was attributed to extensive cracking on load reversal. Also when loaded in the north direction, the crash wall tends to stiffen the response, while when loaded in the south direction, the column is pulled away from the crash wall. The load was increased to 534 kN (120 kips) in the north and 507 kN (114 kips) in the south with a corresponding decrease in stiffness and development of extensive flexural cracking. Finally, the load was increased to 601 kN (135 kips) north, just below the previously mentioned theoretical flexural yield lateral load of 623 kN (140 kips). At this time, large vertical splits developed along the lap splice on the tension side of the column. Upon load reversal, the load only reached 507 kN (114 kips), less than on the previous load cycle to the south. Additional tensile side vertical splitting was observed. On the final cycle to the north, the capacity dropped to about 267 kN (60 kips); and the displacement was 53 mm (2.1 in.), approximately the same as that which accompanied the flexural yield load on the previous cycle to the north. Additional push to the north was continued with decreasing lateral force resistance until a maximum tip displacement of approximately 152 mm (6 in.) was reached.

Column B14S, a 1,220 mm (48 in.) diameter column, was tested similarly to B18S. Two fully reversed lateral load cycles of 222 kN (50 kips) were conducted with an average displacement of 23 mm (0.9 in.). An "effective" yield displacement of 38 mm (1.48 in.) was established from the testing. In addition, two fully reversed displacement cycles to  $\mu_{\Delta} = \pm 1.2, \pm 1.8, \pm 2.4$ , and one cycle to  $\pm 3.0$  were conducted followed by a half cycle to  $\mu_{\Delta} = 3.6$  and a second half cycle to  $\mu_{\Delta} = 5.5$ . The maximum lateral load was 449 kN (101 kips) for loading in the north direction and 302 kN (72 kips) for loading in the south direction. Flexural yielding would theoretically occur, as previously mentioned, at a lateral load of 365 kN (82 kips). Lateral load capacity degradation was not evident from examination of the hysteresis response diagrams.

In 1994, two additional "as-built" columns were tested and the results reported in detail in Shkurti et al. (1995) and in a briefly summarized fashion in Gamble, Hawkins, and Kaspar (1995). These columns will be referred to as C17S and C15S. Companion columns from these bents were retrofit; results of these tests are reported in Section 4.2.

Column C17S was a 1,370 mm (54 in.) diameter column constructed with twenty-four, 36 mm (#11) reinforcing bars. The column was first loaded with a lateral load of 362 kN (81 kips) in the north direction that tends to load against the crash wall and provides higher column stiffness. The resulting displacement was 22 mm (0.9 in.). The first load in the southerly direction was also 362 kN (81 kips) but displacement increased to 24 mm (nearly 1 in.). This difference was due to extensive cracking upon load reversal and the lack of the barrier wall resistance. The second cycle to 40 mm (1.6 in.) in each direction required a lateral load of 554 kN (124 kips) in the north direction and 520 kN (117 kips) in the south direction. This cycle had an accompanying decrease in stiffness and an increase in flexural cracking. Increasing the load to 520 kN (117 kips) resulted in cracking of the crash wall. Finally, the load in the north direction was increased to 579 kN (130 kips) which corresponded to a deflection of 55 mm (2.17 in.). At this load, vertical cracking along the lap splice region was noticed on the tension side of the column. Upon load reversal, just prior to reaching the same load mentioned above, the load peaked at 576 kN (129.5 kips) at 70 mm (2.75 in.) deflection and dropped 13-18 kN (3-4 kips). The hydraulic pump was turned off but this did not prevent additional vertical cracking. The cracks kept growing as did the displacement by 4 mm (0.15 in.) as the load was decreased. The column was then pushed even further with decreasing load required. At 80 mm (3.15 in.), the lateral load was 437 kN (98 kips) while at

100 mm (4 in.), the load declined to 350 kN (78 kips). This decreasing lateral load-displacement response is indicative of column failure.

C15S was tested in a manner similar to C17S. Column C15S was a 1,220 mm (48 in.) diameter column with eighteen, 36 mm (#11) longitudinal reinforcing bars. The column was first subjected to fully reversed lateral loads of 270 kN (60 kips) with an average displacement of 26 mm (1.02 in.). The "effective" yield displacement was extrapolated to be 44 mm (1.72 in.). Displacement control tests at  $\mu_{\Delta} = \pm 1.0$  required lateral loads of 376 kN and 352 kN (84 kips and 79 kips) respectively. In subsequent cycles to  $\mu_{\Delta} = \pm 2.0$  and 3.0, the lateral load resistance increased to approximately 486 kN (109 kips) and 425 kN (95 kips) for loads towards and away from the crash barrier, respectively. During these cycles, several flexural cracks developed. The first vertical cracks in the column were observed at 470 kN (105 kips) and a displacement of 76 mm (3 in.), coinciding with first cracking of the crash wall. Crushing of the north side of the column where it joined the crash wall was also noticed. It was planned to pull the column to  $\mu_{\Delta} = 4$ , 160 mm (6.3 in.). At a displacement of 134 mm (5.3 in.) and a lateral load of 430 kN (96.7 kips), however, the vertical cracks grew rapidly resulting in column failure. The column was subsequently pushed to 160 mm (6.3 in.) but the load had declined to 345 kN (77 kips). Upon load reversal, at 140 mm (5.5 in.), the load peaked at 398 kN (89 kips) and dropped for increasing deflections. At 160 mm (6.3 in.) the lateral load capacity had dropped to 335 kN (75 kips); and at a final displacement of 180 mm (7.1 in.), the load decreased to 281 kN (63 kips).

Column C14N was retrofit using the NCF Snap-Tite™ E-glass jacket (NCF Industries, n.d.). Each ply of the four-ply jacket was 2,440 mm (8 ft) high. The cylinders, when fit around the column did not completely close leaving approximately a 50 mm (approximately 2 in.) gap. The seams in the jacket were staggered as alternating layers of resin and jacket were applied. The total thickness of the four layer jacket was approximately 25 mm (1 in.).

The first cycle, a load control cycle to  $\pm 270$  kN (60 kips), produced deflections of 28 mm (1.1 in.) and 31 mm (1.2 in.). These deflections indicate a negligible change in stiffness as compared to the "as-built" specimen, B14S. Changing the test to deflection control, one cycle to  $\mu_{\Delta} = \pm 1.0$  required lateral loads of 341 kN (77 kips) and 323 kN (73 kips) while subsequent double cycles to  $\mu_{\Delta} = \pm 2.0$ , 3.0, and 4.0 required lateral loads to 456, 466, 478 kN (103, 105, and 107 kips) for loads in the south direction and 403, 414, and 436 kN (91, 93, and 98 kips) for loads in the north direction on the first cycle to these displacements. During this cycling, cracking noises, hypothesized to be delamination of the layers, were heard. Small vertical cracks at the base of the column were arrested by the radial pressure from the jacket. At  $\mu_{\Delta} = 4$ , a deflection of 160 mm (6.3 in.), 2-3 mm (0.08-0.12 in.) wide cracks in the crash wall were noted on the north side. The next cycle to  $\mu_{\Delta} = \pm 5.0$ , 200 mm (7.9 in.), required lateral loads of 479 and 440 kN (108 and 99 kips) for loading to the south and north, respectively. The crash wall was now severely damaged with cracks in excess of 5 mm and significant spalling. Nine flexural cracks were noticed above the jacket. Instead of unloading the column at the end of these cycles, during which the lateral loads imposed continued to increase over previous ductility levels, the hydraulic cylinder was extended to its full stroke of 260 mm (10.2 in.) at a load of 481 kN (108 kips). The column was then pulled to 331 mm,  $\mu_{\Delta} = 8.3$ , at which time snapping noises of unknown origin were heard. A crack in the jacket was noticed at mid-height as well as several small cracks in the glue at the joint. The load peaked during this testing at 522 kN (117 kips), however, the column did not fail.

The other composite retrofit performed on the Poplar Street Bridge was on column C14S. This column was jacketed with a fiberglass retrofit supplied by R. J. Watson, Inc. The jacket was field installed by

using a wet lay-up procedure and consisted of 5 layers of fiberglass fabric epoxy bonded to the column. The jacket measured a total of 6.4 mm (0.25 in.) thick and extended over the lower 2,790 mm (9.15 ft) of the column.

The first cycle, a load control cycle to  $\pm 270$  kN (60 kips), produced deflections of 30 mm (1.2 in.) and 35 mm (1.4 in.). Minor cracking at the column connection to the crash wall was noticed at this stage. Following this series of cycles, the test was deflection controlled. A single cycle of deflections to 40 mm (1.58 in.), corresponding to  $\mu_{\Delta} = \pm 1.0$ , was followed by two cycles each at  $\mu_{\Delta} = \pm 2.0, 3.0$ , and 4.0. A single cycle to  $\mu_{\Delta} = 5.0$  was applied with a lateral load peak of 504 kN (113 kips) in the north direction and 410 kN (92 kips) in the south. Concrete in the crash wall, already significantly cracked, began to spall. Instead of unloading the column after the south directed load, the hydraulic cylinder was extended to full stroke, 215 mm (8.5 in.) requiring a load of 423 kN (95 kips), the maximum load in the south direction. Full hydraulic cylinder stroke was applied in the north direction with ultimate loads and displacements of 556 kN (125 kips) and 340 mm (13.3 in.) without column failure.

Having not been able to produce failure in either of the composite retrofit columns nor the steel band retrofit columns (see Section 4.2 in this report) it was decided to load the columns in the direction of the roadway as opposed to the lateral load tests that had previously been conducted. The goal was to provide a qualitative assessment of the suspect tension connection between the pile cap and the steel pipe piles. Researchers determined if there were zero tension capacity in the connection between the pile and pile cap, a horizontal load applied at the column top of 180 to 200 kN (40 to 45 kips) would be required to fail the column. In order to provide this load, the contractor secured three heavy duty winch trucks to bent 14 which had the NCF and RJW composite retrofits. Each truck had two cable drums with each line being equipped with a pulley block allowing the drum tension to be doubled up to the truck weight. Three lines were hooked with cable choker to the pier. Close observations of the response were not made due to the potential of cable breaks, but there was no discernable movement of the footing. Although failure of one of the chokers interrupted the test, it was evident that the connection had significant tension capacity.

The lines were rearranged so that a greater portion of the load was applied to the RJW retrofit column, C14S. After significantly loading this column, large deflections and eventual collapse occurred. Interestingly, the failure of the column was due to dowel steel fracture, indicative of the ability of the retrofit to provide lap splice force transfer in even the most extreme conditions.

Although there were some minor differences in the load-deflection response of the NCF and RJW retrofits as well as in the maximum applied load during the tests, it is evident that both retrofits performed well as they greatly exceeded the performance of the comparable “as-built” columns. The performance of the retrofit is also evident in that eventual out-of-plane collapse of the RJW retrofit was due to longitudinal steel fracture and not failure of the jacket, evidence of excellent confinement from the jacket.

### **3.5 Analytical Models and Design Considerations**

This section contains a review of several references which present, in varying degrees of detail, analytical models for composite confined concrete. In Section 3.5.2, a review of the numerous design considerations that must be addressed when using composite materials as a structural retrofit are presented. These considerations are based on the work of Caltrans and a number of academic and industry partners.

### 3.5.1 Analytical Models for Composite Retrofit Column Behavior

A theoretical model is developed in Saadatmanesh, Ehsani, and Li (1992), summarized in Saadatmanesh (1994) and Saadatmanesh, Ehsani, and Li (1994), and used to predict the effects of composite fiber jacketing via straps on the strength and ductility of reinforced concrete columns. The model is an extension of Mander, Priestley, and Park's (1988b) model for confined concrete which was originally developed considering internal steel reinforcing bars as the means of confinement. The equation for concrete stress,  $f_c$ , as a function of strain, unconfined compressive strength, confined compressive strength, initial tangent modulus of concrete, and a secant modulus connecting the stress-strain curve origin and ultimate confined compressive strength was originally developed by Popovics and used by Mander, Priestley, and Park in the formulation shown below.

$$f_c = \frac{f'_{cc} x r}{r-1+x^r} \quad (3-2)$$

where

$$x = \frac{\epsilon_c}{\epsilon_{cc}} \quad (3-3)$$

$$\epsilon_{cc} = \epsilon_{co} \left[ 1 + 5 \left( \frac{f'_{cc}}{f'_{co}} - 1 \right) \right] \quad (3-4)$$

$$r = \frac{E_c}{E_c - E_{sec}} \quad (3-5)$$

$$E_{sec} = \frac{f'_{cc}}{\epsilon_{cc}} \quad (3-6)$$

$$f'_{cc} = f'_{co} \left( -1.254 + 2.254 \sqrt{1 + \frac{7.94 f'_i}{f'_{co}} - 2 \frac{f'_i}{f'_{co}}} \right) \quad (3-7)$$

where

- $\epsilon_c$  = longitudinal compressive concrete strain
- $f'_{cc}$  = confined compressive strength of concrete
- $\epsilon_{cc}$  = strain at maximum confined concrete stress
- $f'_{co}$  = maximum unconfined compressive strength of concrete
- $\epsilon_{co}$  = strain at maximum unconfined stress in concrete, generally taken to be 0.002

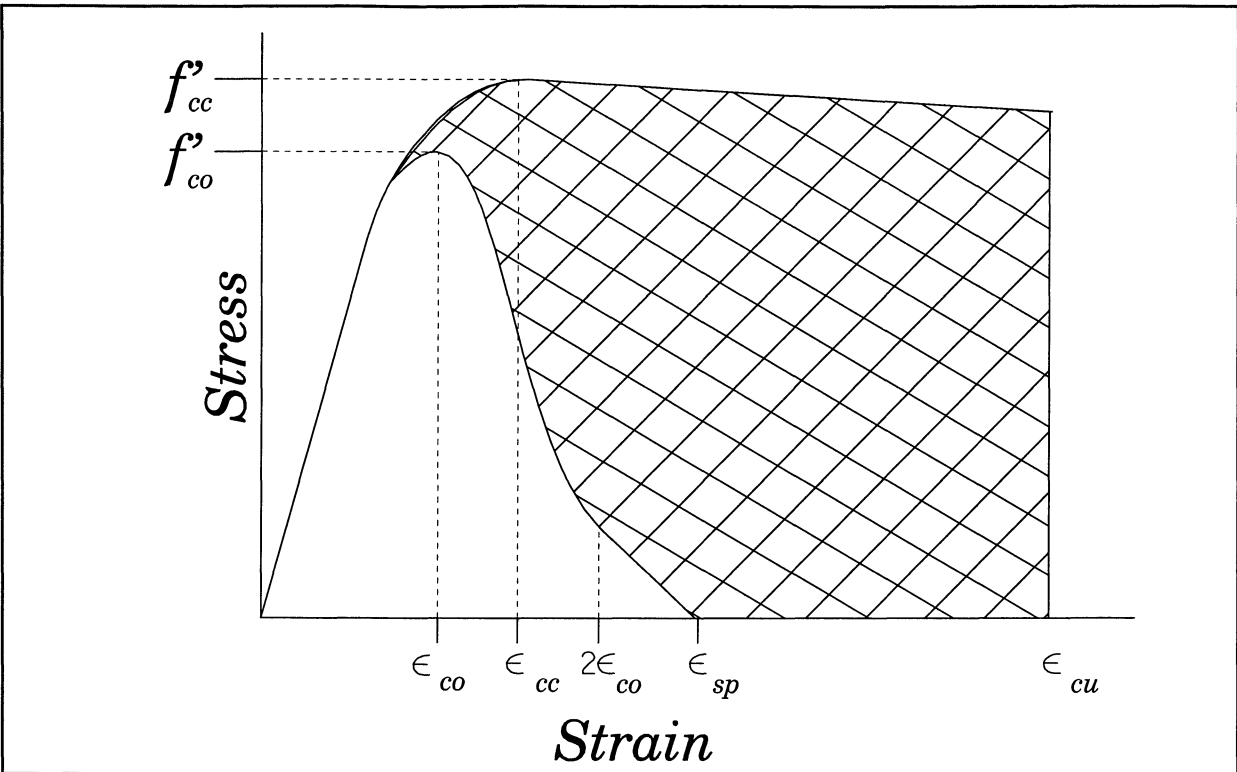


**FIGURE 3-7 Confined and Unconfined Concrete Stress-Strain Diagram**

- |                 |   |  |
|-----------------|---|--|
| $f'_{co}$       | = | maximum unconfined compressive strength of concrete                              |
| $\epsilon_{co}$ | = | strain at maximum unconfined stress in concrete, generally taken to be 0.002     |
| $\epsilon_{cu}$ | = | ultimate concrete compressive strain at strap fracture                           |
| $E_c$           | = | modulus of elasticity of concrete  |
| $E_{sec}$       | = | secant modulus at peak confined stress   |
| $f'_l$          | = | effective lateral confining stress uniformly distributed over the concrete core. |

Figure 3-7 illustrates the stress-strain relationship for confined and unconfined concrete. The effective lateral confining pressure,  $f'_l$ , is based upon a constant lateral confining stress corresponding to the effectiveness of the confinement and the ultimate rupture stress in the composite strap. The effectiveness depends on the center-to-center spacing of the straps,  $s$ , the thickness of the straps,  $t$ , and the clear vertical spacing between the straps,  $s'$ . The assumption of constant lateral stress is predicated on an active state of stress in the strap that is equal to the ultimate stress in the strap regardless of other factors. Therefore, the confined compressive strength of concrete given by equation (3-7) is directly related to the fracture strength of the composite straps. Equations (3-2) through (3-7) are used with equations (3-8) through (3-15) to back solve for the strain in the confined concrete corresponding to first hoop fracture,  $\epsilon_{cu}$ . Based on the energy balance approach proposed by Mander, Priestley, and Park (1988b), the additional compressive strength and energy absorption of the confined specimen is due to the energy stored in the transverse confinement as shown in (3-8).

$$U_{st} = U_{cc} + U_{sc} - U_{co} \quad (3-8)$$

where

$$U_{st} = \rho_s A_c \int_0^{\epsilon_{us}} f_{cs} d\epsilon_{cs} \quad (3-9)$$

$U_{st}$	=	ultimate strain energy per unit volume in the composite strap
$\rho_s$	=	transverse volumetric confinement ratio
$A_c$	=	Area of concrete enclosed by the strap
$f_{cs}$	=	stress in the composite strap
$\epsilon_{cs}$	=	strain in the composite strap
$\epsilon_{us}$	=	ultimate strain of composite strap

Because the composites commonly used in civil engineering applications, namely glass and carbon fibers, are linearly elastic, the area represented by the integral presented in equation (3-9) may be obtained algebraically and may subsequently be rewritten as shown in equation (3-10).

$$U_{st} = \frac{f_{us} \epsilon_{us} \rho_s A_c}{2} \quad (3-10)$$

In addition,

$$U_{cc} = A_c \int_0^{\epsilon_{cu}} f_c d\epsilon_c \quad (3-11)$$

$U_{cc}$  = ultimate strain energy per unit volume for confined concrete

$$U_{sc} = \rho_{cc} A_c \int_0^{\epsilon_{cu}} f_{sl} d\epsilon_c \quad (3-12)$$

$U_{sc}$  = energy required to maintain yield in longitudinal steel in compression

$\rho_{cc}$  = ratio of area of longitudinal steel to area of core

$$U_{co} = A_c \int_0^{2\epsilon_{co}} f_c d\epsilon_c \quad (3-13)$$

$U_{co}$  = ultimate strain energy per unit volume for unconfined concrete

Equation (3-13) has different limits of integration than Mander, Priestley, and Park's original equation in that the upper limit of integration in their original formulation was  $\epsilon_{sp}$ , the spalling strain of the cover concrete. This strain is greater than the value of  $2\epsilon_{co}$ , the upper bound on the strain in the confined core used by Saadatmanesh, Ehsani, and Li (1992). Mander, Priestley, and Park state that the integral for  $U_{co}$  when integrated from 0 to  $\epsilon_{sp}$  equals the following:

$$\begin{aligned}
\int_0^{\epsilon_{sp}} f_c d\epsilon_c &= 0.017 \sqrt{f'_{co}} \left( \frac{MJ}{m^3} \right) \\
&= 0.2046 \sqrt{f'_{co}} \left( \frac{inch-lb}{inch^3} \right)
\end{aligned}
\tag{3-14}$$

Saadatmanesh, Ehsani, and Li use these same values but assert that they are found by integrating to  $2\epsilon_{co}$  and not  $\epsilon_{sp}$  as originally shown by Mander, Priestley, and Park (1988b). This is a reasonable approximation if the strains in question are similar in magnitude and occur at very low stress levels. Under these conditions, this combination of factors will result in no appreciable area under the curve in relation to the significant area under the stress-strain curve measured from 0 to  $2\epsilon_{co}$ . If however, these assumptions are not true, the above redefinition by Saadatmanesh, Ehsani, and Li somewhat overestimates the strain energy absorbed by specimen.

Simplifying and substituting equations (3-9) to (3-14) into equation (3-8) yields the results presented in equation (3-15).

$$\begin{aligned}
\frac{1}{2} \rho_s f_{us} \epsilon_{us} &= \int_0^{\epsilon_{cu}} f_c d\epsilon_c + \rho_{cc} \int_0^{\epsilon_{cu}} f_{sl} d\epsilon_c - 0.017 \sqrt{f'_{co}} \left( \frac{MJ}{m^3} \right) \\
&= \int_0^{\epsilon_{cu}} f_c d\epsilon_c + \rho_{cc} \int_0^{\epsilon_{cu}} f_{sl} d\epsilon_c - 0.2046 \sqrt{f'_{co}} \left( \frac{inch-lb}{inch^3} \right)
\end{aligned}
\tag{3-15}$$

With the knowledge of the variation of concrete stress  $f_c$  from equation (3-2) and  $f_{sl}$  from the assumed perfect elastic-plastic response of the reinforcing steel, the ultimate compressive strain,  $\epsilon_{cu}$ , at composite strap fracture can be numerically isolated from either of the equations shown as (3-15). The entire stress strain curve of the confined specimen can now be defined as can the maximum axial force, moment-axial force interaction curves, and curvature-axial load curves. Saadatmanesh, Ehsani, and Li recommend that at the ultimate point, one should assume that the ultimate strain in the compressive fiber,  $\epsilon_{cf}$ , is equal to  $\epsilon_{cu}$ , and the extreme steel tension strain,  $\epsilon_{sf}$ , should be incremented in order to derive the interaction surfaces. Alternately at the yield point, Saadatmanesh, Ehsani, and Li recommend assuming that  $\epsilon_{cf}$  be assumed with the knowledge that  $\epsilon_{sf}$  is equal to  $\epsilon_y$  for the reinforcing steel. A computer program was developed for this analysis and was applied in the analysis of circular and rectangular specimens in a parametric study.

In the parametric study, the effect of varying concrete compressive strength, strap thickness, clear spacing between straps, center to center strap spacing, strap type and cross section type were chosen as variables. The unconfined concrete compressive strength was assumed to be 20.7 MPa (3 ksi), 27.6 MPa (4 ksi), or 34.5 MPa (5 ksi). Strap thickness was either 5 mm (0.197 in.), 10 mm (0.394 in.) or 15 mm (0.591 in.). Clear spacing between straps,  $s'$ , was chosen as either 0, 150 mm (6.0 in.), 305 mm (12 in.), or 455 mm (18.0 in.). Spacing between strap centers,  $s$ , is used in conjunction with clear spacing to quantify overall strap size and was selected to be 150 mm (6.0 in.), 305 mm (12.0 in.), 455 mm (18.0 in.), 610 mm (24.0 in.) or 915 mm (36.0 in.). Strap type was either E-glass with an ultimate strain of 0.023 and ultimate stress of 1.10 GPa (160 ksi) or carbon fiber with an ultimate strain of 0.017 and ultimate

stress of 2.86 GPa (415 ksi). The area under the stress-strain curve for the carbon fiber is approximately 1.9 times that of E-glass. Column sections were either circular or rectangular.

Considering the various material strengths, strap thicknesses, and strap spacings mentioned in the previous paragraph, a nomenclature was adopted to identify the various analytical cases. The columns are designated as either C or R for geometry; 3, 4, or 5 for concrete strength; T5, T10, or T15 for strap thickness; S'0, S'6, S'12, and S'18 for clear spacing; and S6, S12, S18, S24, and S36 for center-to-center strap spacing.

To investigate the various options for strengthening circular columns, a basic column specimen was selected consistent with those used by Chai, Priestley, and Seible at the University of California, San Diego (Chai, Priestley, and Seible, 1991b, 1991c, 1991d). The column is 1,525 mm (60 in.) in diameter and is reinforced with an area of steel of 46,460 mm<sup>2</sup> (32 - #14 bars). The transverse steel consists of 13 mm (#4) reinforcing bars at 305 mm (12 in.). The results of a number of the analytical investigations are presented below so as to establish trends in the data.

When  $t = 5$  mm (0.197 in.),  $s' = 0$ ,  $s = 150$  mm (6 in.), and concrete strengths,  $f'_{co}$ , of 20.7 MPa (3 ksi), 27.6 MPa (4 ksi) and 34.5 MPa (5 ksi) are chosen, the following is observed. For increasing concrete strength, the ultimate axial load is increased by 103%, 92%, and 82% for the E-glass retrofit, and 171%, 162%, and 151% for the carbon fiber retrofit. The moment capacity increases 53%, 48%, and 45% for E-glass and 87%, 83%, and 79% for the carbon strap. The increase of moment strength being less than in axial load strength was not seen as a shortcoming of this technique because most columns, if deficient in strength, are deficient in shear strength and not moment strength. Flexurally deficient columns generally lack the confinement required to maintain their strength through increasing ductility levels. Examination of the interaction plots involving only a change in unconfined strength illustrates that curvature ductility  $\phi_u/\phi_y$  increases significantly with the presence of the straps but is relatively insensitive to concrete strength.

When the following parameters were held constant,  $f'_{co} = 34.5$  MPa (5 ksi),  $t = 5$  mm (0.197 in.), and clear spacing,  $s'$ , and center to center spacing of straps,  $s$ , varied, as follows;  $s'0$  and  $s6$ ,  $s'6$  and  $s12$ , and  $s'12$  and  $s18$ , the following results were obtained. (Note: all three scenarios assume a 150 mm (6 in.) wide band). The axial load increased by 82%, 44%, and 22% for E-glass and 151%, 92%, and 63% for the carbon fiber retrofit with increasing center-to-center spacing. The increase in moment followed a similar trend with increases of 45%, 25%, and 17% for E-glass and 79%, 47%, and 33% for carbon fiber straps. In the  $s'12$  scenario, the curvature ductility vs. axial load curve was nearly the same as an "as-built" specimen except at very high axial load levels and very low curvature ductilities where the retrofit has some effect in providing for higher axial loads as mentioned previously.

For common parameters of  $f'_{co} = 34.5$  MPa (5 ksi);  $s' = 0$ ;  $s = 150$  mm (6 in.); and thickness  $t$  varied as 5 mm (0.197 in.), 10 mm (0.394 in.), and 15 mm (0.591 in.), the following results were obtained. The ultimate axial load is increased by 92%, 130%, and 163% for E-glass and 151%, 208%, and 235% for carbon fiber straps in order of increasing strap thickness. The maximum moment increase was 45%, 75%, and 98% for E-glass and 70%, 120%, and 148% for carbon fiber straps, which indicates significant influence of strap thickness on retrofit efficiency. For specimens where strap thickness and the volumetric confining ratio were constant but actual strap geometry was different due to different clear and center-to-center spacings, the response was only slightly affected. These observations are indicative of the volumetric confining ratio being an important means of assessing retrofit effectiveness.

The relationship between curvature ductility,  $\phi_u/\phi_y$ , and strap thickness,  $t$ , shows that ductility increases with strap thickness but at a slower rate as strap thickness increases. In addition, when specimens whose only difference is concrete strength are examined, curvature ductility rises slower as the concrete strength increases. Also for specimens where concrete strength and strap thickness are varied, the rate of increase in ductility with increasing strap thickness is slower as unconfined compressive strength increases. The ratio of  $M_u/M_y$ , where  $M_u$  is the ultimate moment capacity of the confined column and  $M_y$  is the yield moment in the unconfined column, increases with increasing strap thickness but at a slightly slower rate for increasing strap thickness. Where specimens are chosen whose only difference is unconfined compressive strength, the moment ratio increases at a slower rate with increasing unconfined concrete compressive strength. In addition, where the ratio of axial load,  $P$ , to the maximum axial load in an unconfined specimen,  $P_o$ , is examined as a parameter along with strap thickness, the following was observed. As the axial load ratio increases, the moment ratio also increases. For a given increase in axial load ratio, the greatest moment ratio increases corresponded to the specimens with the thickest straps. Ductility was found to be constant as long as the volumetric confining ratio of the straps,  $\rho$ , was kept constant.

The effect of column size on the results was also examined. Two alternate columns were examined in this study: a column with a diameter of 1,220 mm (48 in.), cover to the transverse bars of 40 mm (1.6 in.), and longitudinal reinforcing of 29,735 mm<sup>2</sup> (46.09 in.<sup>2</sup>) as well as a column with a 915 mm (36 in.) diameter, 30 mm (1.2 in.) cover, and 16,730 mm<sup>2</sup> (25.93 in.<sup>2</sup>) of longitudinal reinforcing. Results indicate that the axial load ratio, moment ratio, and ductility factor are unaffected by the different column diameters as long as the volumetric confinement ratio is constant throughout the varying scenarios.

The conclusion was that for circular columns confined with composite E-glass and carbon fiber straps, higher compressive strengths reduce curvature ductility; ductility increases linearly with strap thickness; larger clear spacings significantly reduce ductility; constant values of volumetric confinement generate constant values of axial load ratio, moment ratio, and curvature ductility.

Rectangular columns were also studied in this investigation. The primary column had the following dimensions: cross-section of 1,830 mm x 1,220 mm (72 in. x 48 in.) for an h/b ratio of 1.5. Reinforcing was distributed along all four faces and comprised a total of 58,080 mm<sup>2</sup> (90 in.<sup>2</sup>). Cover measured to the face of the transverse reinforcement was 50 mm (2 in.).

For a rectangular column with t5 straps, S'0 and S6, with unconfined compressive strength of concrete varying from 20.7 MPa to 34.5 MPa (3 ksi to 5 ksi), axial load is increased by 102%, 91%, and 82% for columns wrapped with E-glass and 169%, 160%, and 150% for columns wrapped with carbon fiber straps. The corresponding moment capacity increases were 60%, 56%, and 54% for E-glass and 97%, 94%, and 91% for carbon fiber straps, respectively. At small axial loads, flexural capacity is relatively independent of concrete strength. Ductility is significantly impacted by confinement but only slightly by concrete strength.

Comparison of analyses where the configuration is  $f'_{co} = 34.5$  MPa (5 ksi); t5; and s' and s that vary as follows: s'0 and s6; s'6 and s12; s'12 and s18 (Note: all scenarios assume a strap width of 150 mm (6 in.)), the following results were obtained. Ultimate axial load is increased by 82%, 44%, and 28% for sections strengthened with E-glass straps, and by 150%, 91%, and 62% for sections strengthened with carbon fiber corresponding to the spacing scenarios outlined above. Moment increases of 54%, 32%, and 23% were observed for E-glass retrofit specimens and 91%, 55%, and 40% for carbon fiber retrofit specimens.

The larger spacings result in significant decreases in curvature ductility enhancement. In the s'12, s18 scenario, the curvature ductility of the E-glass retrofit specimen was very near the "as-built" condition.

In the scenario where columns were of the R, 5, s'0, s6 type and strap thickness,  $t$ , varied as 5 mm (0.197 in.), 10 mm (0.394 in.) and 15 mm (0.591 in.), the following results were obtained. The ultimate axial load increased by 82%, 129%, and 162% for the E-glass specimens and 150%, 206%, and 231% for the carbon fiber strap retrofit specimens. Maximum moment increases of 54%, 86%, and 110% were predicted for E-glass jacketed specimens and 91%, 135%, and 162% for the carbon strap jacketed specimens. This illustrates the strong dependence of specimen behavior and volumetric confinement ratio. For specimens where clear and center-to-center spacing were varied, but in such a fashion so as to maintain a constant volumetric confinement ratio,  $\rho_s$ , of 0.00685, the percent increase in axial load and the maximum moment were fairly constant though slightly smaller increases in strength and ductility were observed with an increase in spacing even though volumetric ratios were held constant.

The relationship between curvature ductility,  $\phi_u / \phi_y$ , and strap thickness,  $t$ , indicates a linear increase in ductility with increasing strap thickness; and for larger clear spacings,  $s'$ , the rate of increase is smallest. When the only variable is unconfined compressive strength,  $f'_{co}$ , the higher strength concretes have the smallest increase in ductility. When concrete strength and strap thickness are studied simultaneously, the higher the concrete strength, the smaller the rate of ductility increase with increasing strap thickness. When the variables consist of the axial load ratio,  $P/P_o$ , and thickness,  $t$ , the higher the load ratio the slower the ductility factor increases with an increase in strap thickness. The relationship between  $M_u/M_y$ , and thickness,  $t$ , illustrates that the moment ratio increases linearly with strap thickness and that the increase is nearly the same for different clear spacings. The moment ratio increases a lesser amount for higher strength concretes. In addition, where the ratio of axial load,  $P$ , to the maximum axial load in an unconfined specimen,  $P_o$ , is examined as a parameter along with strap thickness, the following was observed. As the axial load ratio increases, the moment ratio also increases. For a given increase in axial load ratio, the greatest moment ratio increases corresponded to the specimens with the thickest straps.

Two other rectangular columns were analyzed to investigate size effects. These columns are a rectangular column with sides of 1,370 mm x 915 mm (54 in. x 36 in.),  $h/b = 1.5$ ; cover equal to 38 mm (1.5 in.); and area of longitudinal steel of 32,670 mm<sup>2</sup> (50.64 in.<sup>2</sup>) as well as a column measuring 915 mm x 610 mm (36 in. x 24 in.),  $h/b = 1.5$ ; cover of 25 mm (1 in.); and longitudinal steel area of 14,520 mm<sup>2</sup> (22.51 in.<sup>2</sup>). Similar to the circular columns, findings indicate that size does not have an effect on column axial load ratio, moment ratio, and curvature ductility as long as the volumetric confining ratio is kept constant among specimens of different geometry.

The results of the rectangular column study are summarized below. Higher strength concrete results in a relatively small increase in ductility; ductility increases linearly with strap thickness; large clear spacing impacts seriously on the ductility of the specimen; constant values of volumetric confinement results in constant values of ductility factor, axial load ratio, and moment ratio regardless of other geometric considerations.

In Mirmiran and Shahawy (1995), a new confinement model for composite wrapped reinforced concrete is proposed. The model, in the form of a cubic polynomial where radial strain in the concrete is related to the axial strain in the specimen, also includes the effects of axial strain level on the Poisson's ratio of the concrete. Once the variation of radial strain as a function of axial strain is determined, the variation of the confining pressure can be found using the thin shell equilibrium equations. When the confining

pressures are established, an incremental use of the Mander, Priestley, and Park (1988b) energy balance model is employed to assure equilibrium of forces, compatibility of strains and energy balance at failure.

Mirmiran et al. (1996) propose a technique intended to replace the existing steel in a reinforced concrete column with a composite shell that acts as the pour form and the reinforcing for the column. Although this development is not directly applicable to this literature review, the paper does include a critique of the extension of Mander, Priestley, and Park's (1988b) model for confined concrete by others to the field of composite jacketing. The paper by Mirmiran et al. does not question the suitability of the model as originally developed, only its extension by others into related areas. The paper discusses the need for a new confinement model for composite-jacketed columns.

The concept of confined concrete, as illustrated through numerous references presented previously in this report, is that due to enhanced confinement, a concrete sample can attain higher stresses and strains before failure than plain samples. This increase in performance is due to the energy absorption of the transverse steel ties in the concrete specimen. The Mander, Priestley, and Park model, originally developed for transverse steel reinforcing, is a uniaxial model which relates the increase in axial load capacity to the level of the lateral confining stress, expressed as the ratio of the confined to unconfined strengths of the concrete,  $f'_{cc}/f'_{co}$ , versus the ratio of the effective lateral confining pressure to the unconfined compressive strength,  $f_r/f'_{co}$ . (Note: The notation of  $f_r$  for the effective lateral confining stress used by Mirmiran et al. is different from the notation of  $f'_1$  originally used in the Mander, Priestley, and Park model). Mirmiran et al. indicates that the Mander, Priestley, and Park model predicts that the maximum increase in axial strength,  $f'_{cc}/f'_{co}$ , of 4.04 is obtained when  $f_r/f'_{co}$  is equal to 2.4. For higher values of  $f_r/f'_{co}$ , The Mander, Priestley, and Park model is a parabolically descending model which predicts lesser gains in axial strength than the peak of 4.04. Mirmiran et al. states that this is an erroneous model for composite fibers such as carbon fibers which have very high uniaxial tensile strengths and can subsequently provide much greater confining pressures. Additionally, the Mander, Priestley, and Park model is predicated upon the assumption that a constant lateral confining pressure is present throughout the loading history. If this is not the case, such as with a passive retrofit where lateral confining pressure is proportional to the dilation of the concrete, the model will provide erroneous results. Mirmiran et al. also state that the model ignores the stress strain behavior of the confining material. This insight is significant as steel jacketing can be idealized as having an elasto-plastic response while composites such as glass an carbon fibers are linearly elastic until failure. Finally, the model assumes that the jacket and concrete reach their ultimate capacities regardless of jacket type or size. Mirmiran et al. also asserts that Saadatmanesh, Ehsani, and Li (1994) illustrates that the failure point as determined by an energy balance approach is less than the peak stress in the concrete. Mirmiran et al. further conclude that the equilibrium and energy balance approaches are not compatible for composite-jacketed columns.

Hoppel et al. (1994) conducted an analytical investigation aimed at characterizing the stress in a composite wrapped specimen up to the point of first concrete failure. The objective was to relate the hydrostatic state of stress in the concrete to the applied axial stress in the concrete column.

Hoppel et al. developed two separate equations based on the circumferential wrap being either perfectly bonded to the concrete or unbonded to the concrete.

$$\frac{Pr}{tE_{\theta w}} + \frac{P}{E_c}(1 - \nu_c) = \frac{\sigma_{con}(P=0) + 3.7(\sigma_{con}(P=0)) \left( \frac{P}{\sigma_{con}(P=0)} \right)^{0.86}}{E_{z \text{ system}}} (\nu_c - \nu_{z\theta}) \quad (3-16)$$

$$P = \frac{\sigma_{con}(P=0)\nu_c t E_{\theta w}}{r E_c} \quad (3-17)$$

where

P	=	radial stress in the concrete
r	=	radius of the specimen
t	=	thickness of the composite
$E_{\theta w}$	=	Young's Modulus of the composite in the cylinder hoop direction
$E_c$	=	Young's Modulus for concrete
$\nu_c$	=	Poisson's ratio for concrete
$\nu_{z\theta}$	=	Poisson's ratio relating axial stress and circumferential strain
$\sigma_{con}(P=0)$	=	unconfined compressive strength
$E_{z \text{ system}}$	=	axial stiffness of the cylinder based on the rule of mixtures

The first equation assumes perfect bond and strain compatibility between the concrete and composite while the second is a simplified version of the first and assumes axial independence of the cylinder and wrap. Very little difference in predicted axial strength at first concrete failure was observed between the two equations lending credence to the assertion that perfectly bonded hoop-oriented wraps have very little effect on the axial stress in a concrete cylinder. Hoppel et al. examined cylinders tested by others in a separate investigation and showed that the bond between the cylinder and composite wraps was excellent even after testing to failure. Thus, they proceeded with this assumption in further analytical studies.

The sensitivity of the axial failure stress to the properties of the composite was investigated for glass fiber-reinforced epoxy and high-modulus graphite fiber-reinforced composites. The stiffer high-modulus graphite wraps lead to much higher predicted increases in axial failure stress than the more compliant glass fiber wraps.

The strength increase is also dependent upon the properties of the concrete. For a specimen not bonded to the composite, the hydrostatic pressure is directly related to the Poisson's ratio of the concrete which can be altered through different aggregate selections. In specimens where the wrap is bonded to the specimen, the hydrostatic stress is proportional to the difference in Poisson's ratio of the concrete and composite. If the difference is zero, the hydrostatic pressure in the concrete will be zero. If Poisson's ratio of the wrap is greater than of the concrete, the wrap will induce radial tension on the interface which may ultimately lead to failure at the interface.

Hoppel et al. were able to identify the dominant variables in determining the axial strengthening efficiency of composite material and concrete cylinder combinations. The results can be used to optimize the combination of composite and concrete type when an axial strength increase is desired. The

analytical results were in close agreement with experimental results conducted by others and cited by Hoppel et al.

Seible, Priestley, and Innamorato (1995) present the guidelines for carbon fiber retrofit of deficient bridge columns. The document also discusses the full-scale field installation of several carbon fiber jackets installed with an automated wrapping machine as well as the design and construction of a full-size two-column bridge bent in the Powell Laboratory at the University of California at San Diego. This full size model will first be tested with the existing columns wrapped in carbon fiber per the design guidelines developed at UCSD. Following this test, a new link beam, installed below the existing cap beam, will be installed and the retrofit frame tested once again. Testing of this frame had not yet begun when Seible, Priestley, and Innamorato (1995) was written.

In the analytical portion of Seible, Priestley, and Innamorato (1995), concrete columns were separated into areas where shear retrofits, plastic hinge confinement retrofits, and lap splice clamping force retrofits would be required. Upon identification of these deficiencies as well as expected shear, ductility, and confinement demands on the column during an earthquake, design relationships were established which showed the dependence of jacket thickness on the tensile modulus, ultimate jacket strain, and ultimate jacket stress. The reader is referred to Seible, Priestley, and Innamorato (1995) for a complete analysis.

### **3.5.2 Design Considerations and Recommendations**

The description of the Caltrans composite materials evaluation program for column retrofits is detailed in Sultan, Hawkins, and Sheng (1995). The original Caltrans composite jacketing research conducted at the University of California at San Diego was aimed at determining the structural performance of composite materials as column retrofits. At that time, however, the research did not adequately address the degradation of structural performance due to environmental effects nor did it address issues related to construction techniques (i.e., hand lay-up or filament winding), and structural performance issues related to the composite itself such as joints and fiber orientation, weave type, voids, resin type, and others. Sultan, Hawkins, and Sheng note that simply comparing the results of steel and composite jacket research tests is inadequate unless other factors as enumerated above are considered. As a result of inconsistent data from manufacturers of composite products who are actively seeking a share of the retrofit market, Caltrans recognized that a standardized means of evaluating the composite systems should be developed to address the following concerns:

1. Strength and performance of the fibers
2. Strength and performance of the resin
3. Strength and performance of the composite laminate
4. Behavior of the system as a structural member
5. The validity of the design approach

Many of these issues were not only a concern to Caltrans but also to the authors of this report who had similar concerns in attempting to develop an overall evaluation technique for the various column retrofit alternatives.

Due to the number of variables in the process, Caltrans determined that only through a partnering effort with private industry, could sufficient guidelines be developed and information collected. Therefore, on November 4, 1994, Caltrans began its program of evaluating composite materials with a meeting attended

by 80 individuals representing approximately 60 different companies, FHWA members, academics, and consulting engineers, where it was decided that Caltrans would focus on two areas: seismic retrofit of bridges and bridge strengthening and rehabilitation methods. In order to conduct an objective and sound technical evaluation, the Society for the Advancement of Material and Process Engineering (SAMPE) has been chosen to facilitate the work on the project. Material testing is to be conducted by the Aerospace Corporation of El Segundo, California, and the U.S. Air Force Advanced Composites Program Office at McClellan Air Force Base (AFB) in Sacramento, California. Structural testing is to be conducted at the University of California at Irvine.

The objectives of the program are to prequalify a group of well-documented composite material systems for infrastructure rehabilitation uses. To accomplish this, the Caltrans program has identified the following objectives:

1. Identify appropriate material testing techniques consistent with the intended use of the material. (This includes environmental and physical factors which will affect strength characteristics).
2. Identify existing, or develop new structural testing methods to verify the shear, confinement, and flexural strength of the composite system. (The goal is to develop simple but reliable test methods).
3. Develop appropriate analysis and design tools for the composite retrofits including interaction between the composite and existing structure.
4. Develop performance criteria for the different techniques.
5. Develop standard specifications and special provisions for the various systems. (The specifications should address material types, manufacturing techniques, mixing and curing, quality control/assurance, and construction methods. ASTM tests will be identified and used when applicable).
6. Develop design guidelines that consider environmental effects when possible.

This program is an aggressive and far-reaching project aimed at developing a standardized evaluation technique for materials used in the composite retrofit of columns. This project was initiated because of the need to objectively evaluate many composite materials with such diverse characteristics as strength, stiffness, cost, and different construction techniques. The reader is referred to California Department of Transportation (1996a, 1996c, and 1996d) for additional information.

The short synopsis presented in the previous pages, related to the first two years of the Caltrans materials standardization and characterization program, is intended to briefly illustrate the amount of consideration given to composites by one member of the transportation community. The Caltrans process may allow composites to gain greater acceptance in the civil engineering community where, to this point, the use of composites has been severely limited because of concerns about material properties, long-term performance, and lack of standardized design processes. However, presentation of the Caltrans process is by no means an endorsement of the process as the correct approach for all scenarios.

The positive aspects of the Caltrans study include the search for reliable material testing techniques and design processes as well as an examination of the impact of environment on system strength. The Caltrans approach has, understandably, limited acceptance of composite systems to those which meet very strict structural and environmental requirements. These requirements are outlined in California Department of Transportation (1996a and 1996d). The requirements on structural performance will, in all likelihood, be too severe for areas of the country with appreciably lower seismic demand. These

requirements will disqualify (i.e., fail to prequalify) a number of systems which may, in fact, be well-suited for areas of lesser demand. It is unreasonable to expect states where seismic retrofit is less of a priority to initiate similar projects to prequalify retrofit systems. A possible consequence is that some states may elect to simply accept the requirements set forth by the State of California and henceforth naturally exclude some systems that are well-suited for their seismic requirements yet fail to appear on the list of qualified alternatives for having failed some of the Caltrans required tests.



## SECTION 4 OTHER COLUMN RETROFIT METHODS

To this point, this report has focused on research in the area of concrete column retrofitting using steel and composite jackets. Although these techniques are the most widely researched, they do not constitute the entire subject matter of column retrofitting. Other techniques developed for the purpose of column retrofitting include concrete jacketing; external post-tensioning and confinement by external reinforcing bars; angle and bar retrofits; and internal repair and strengthening. Due to the limited amount of available information, this section will elaborate on the specific techniques mentioned above in less detail than previous chapters.

### 4.1 Concrete Jacketing and Infill Shear Walls

A review of literature indicates that the field of concrete jacketing is more heavily centered on the field of building structure strengthening than on bridge strengthening. Many references not cited in this report but categorized as pertaining to concrete jacketing are examples. References pertaining to building retrofit were not added to the reference list once it was determined that this would overgeneralize the research through inclusion of nonpertinent information. Although valuable to the field of structural and earthquake engineering, inclusion of building retrofit research was not considered appropriate for this report. For these reasons, only the references that contained concrete jacketing information relating to bridge retrofit are included. Examples of references not summarized include Bett, Klingner, and Jirsa (1988), Ersoy, Tankut, and Suleiman (1993), Rodriguez and Park (1992, 1994), Tankut and Ersoy (1991), and Valluvan, Kreger, and Jirsa (1993).

The implementation of concrete jacket retrofits seems to be more common in Japan than in the United States. Several references pertaining to Japanese projects include Kawashima (1990, 1991), Kawashima and Unjoh (1992), and Kawashima, Unjoh, Iida (1990, 1991, 1992). The use of concrete jackets and infill shear walls is also mentioned in Priestley, Seible, and Chai (1992a), Yashinsky and Hipley (1996), and Yashinsky, Hipley, and Nguyen (1995).

The use of concrete jackets and steel jackets is explored in Amari et al. (1994). The experimental results pertaining to the concrete jacket retrofits will be presented below while results from the steel jacket retrofits can be found in Section 2.2.1, the pertinent section on such retrofits.

The investigation carried out by Amari, et al. focused on the development of strengthening techniques for reinforced concrete column bases. The performance of the column retrofits in enhancing shear and flexural strength was examined. Additionally, a retrofit method where the steel and concrete jacket techniques were combined on the same specimen is also described.

For flexural testing of the concrete-jacketed specimens, an "as-built" specimen and two retrofit specimens were constructed. The cross-sectional dimensions of all of the columns were the same prior to jacketing. The columns measured 500 mm x 500 mm (19.7 in. x 19.7 in.) and were 2.3 m (7.55 ft) tall. The column reinforcing consists of twenty longitudinal bars, 19 mm (0.75 in.) in diameter, and 10 mm (0.39 in.) diameter transverse bars spaced 90 mm (3.54 in.) on center. The jacketed columns, numbered F2 and F4, measured 620 mm x 620 mm (24.4 in. x 24.4 in.) in cross-section after jacketing. The concrete jackets were reinforced with five, 13 mm (0.51 in.) diameter reinforcing bars on each face as well as by 10 mm (0.39 in.) diameter transverse hoops spaced 180 mm (7.1 in.) on center. The difference in the retrofit

specimens is that the jacket in column F2 was long enough, 1.3 m (4.27 ft), to develop the 13 mm (0.51 in.) diameter retrofit bars, while the jacket on specimen F4 was limited to 1 m (3.28 ft) in height and did not have sufficient development length.

Tests on the columns used a constant axial stress of 1.96 MPa (20 kgf/cm<sup>2</sup>, 284 psi) to simulate the effects of dead load. The lateral load was progressively statically applied until yield of the longitudinal steel was noted. Further cycling at  $\mu_{\Delta} = 2, 3, 4,$  and 5 was carried out by applying one static cycle and ten dynamic cycles followed by a change to the next ductility level, if warranted.

The "as-built" specimen achieved a displacement ductility,  $\mu_{\Delta} = 4$ . This was accompanied by concrete spalling, hoop tie loosening and longitudinal bar buckling. Specimens F2 and F4 achieved ductilities of  $\mu_{\Delta} = 5.8$  and  $\mu_{\Delta} = 5$  respectively. Main bar fracture was present in these specimens, and failure along the cold joint between the existing column and retrofit jacket was observed.

Shear retrofits were also tested using concrete jacketing techniques. The cross-sectional dimensions of all of the columns were the same prior to jacketing. The columns measured 500 mm x 500 mm (19.7 in. x 19.7 in.) and were 1.8 m (5.9 ft) tall above the top of the footing. The column height above the top of footing was selected to produce a shear span ratio of approximately 3, ensuring a shear failure before flexural capacity was reached. The column reinforcing consists of twenty longitudinal bars, 19 mm (0.75 in.) in diameter, and 10 mm (0.39 in.) diameter transverse bars. The transverse bars were spaced at 100 mm (4 in.) centers over the lower 500 mm (19.7 in.) of the column, followed by 200 mm (7.9 in.) spaces for the next 1,000 mm (39.4 in.), and three spaces of 38 mm (1.5 in.) at the top of the column. The jacketed columns, numbered S2 and S3, measured 620 mm x 620 mm (24.4 in. x 24.4 in.) in cross-section after jacketing. The concrete jackets were reinforced with five, 13 mm (0.51 in.) diameter reinforcing bars on each face as well as by 10 mm (0.39 in.) diameter transverse hoops spaced 100 mm (4 in.) on center. Tests on the columns used a constant axial stress of 1.96 MPa (20 kgf/cm<sup>2</sup>, 284 psi) to simulate the effects of dead load.

Specimen S2 was retrofit over a height equal to the lateral dimension of the column, 500 mm (19.7 in.), with a concrete jacket, while column S3 employed a 750 mm (29.5 in.) high concrete jacket at the base. The development of extensive diagonal shear cracking was noted during the testing of both the "as-built" and retrofit specimens. The failure zone was pushed upward into the column with the longer retrofit but a shear failure still occurred in the unreinforced region. Strength was insufficient for the shear forces acting on the section. Specimens S1 and S2 failed at  $\mu_{\Delta} = 2$  and 3 respectively. Specimen S3 sustained an applied displacement level of  $\mu_{\Delta} = 6$  prior to failure and as examination of the load displacement envelopes showed, behaved significantly better than the other two column specimens.

The use of a novel combined retrofit was also explored in Amari (1994). The construction of three columns, described as C1, C2, and C3 was the same as the concrete-jacketed specimens described previously, namely, 500 mm (19.7 in.) square column sections jacketed to a lateral dimension of 620 mm (24.4 in.). The shear span ratio for these specimens was 4. The sustained axial load applied in all previous tests was again employed in these tests.

The novelty of this retrofit approach is the use of the mixed jacketing technique. The column is first retrofit over its full height with a square steel jacket placed over the original 500 mm (19.7 in.) column. This jacket is then covered in the area of the column which would be below grade, with a concrete jacket. In column C1, this concrete jacket was simply cast over the steel jacket, while in C2 and C3, the jacket

was mechanically bonded to the steel plates with shear studs. In column C2, two horizontal lines of studs were placed on the four surfaces of the column in the minimum amount dictated by the yield criteria for the studs. Column C3 employed an extra horizontal row, increasing the number of studs used in C2 by 50%.

Test results on the three columns show that in specimen C1, cracks formed at the top of the concrete jacket as soon as loading commenced and the concrete jacket and steel jacket began to separate. Failure eventually occurred at the bottom of the inside steel plate. Column C1 reached  $\mu_{\Delta} = 7$  but this was below the desired level established for this retrofit. Specimens C2 and C3 exhibited concrete jacket cracking in the area of the shear studs that eventually progressed over the full concrete jacket. Final failure was by reinforcing steel fracture in the columns. These columns exhibited slightly higher lateral load capacity than C1 but a smaller displacement at failure. There were no significant differences in these retrofit alternatives.

The use of concrete jacketing is briefly described in Ono et al. (1994). This paper deals with repairs conducted following two earthquakes in Japan: the Kushiro Earthquake of January 1993 and the Hokkaido Earthquake of July 1993.

In the Kushiro earthquake, serious damage to column bases was observed. The Yoda Bridge was constructed with 1.4 m (4.6 ft) diameter columns with thirty-six D19 (0.75 in.) reinforcing bars at the base. One third of these reinforcing bars were terminated 300 mm (11.8 in.) above the footing and another third at 1 m (3.28 ft) above the footing. Longitudinal steel buckling was observed at the 1 m (3.28 ft) location and 6 of the 12 bars that continued past this location were fractured. For repair purposes, 12 additional longitudinal bars were grouted into holes drilled into the footing and extended 3 m (9.84 ft) up the column. These bars, as well as the existing reinforcing, were enclosed in an increased amount of transverse steel to restrain future buckling. The Hatsune and Matsunoe bridges suffered similar damage and were similarly retrofit.

In the Hokkaido earthquake, the Motouriya and Shin-Shiriuchi bridges suffered damage similar to that incurred in bridges during the Kushiro earthquake due to premature termination of longitudinal steel and insufficient lateral confinement. Retrofit measures consisted of installation of new longitudinal steel and transverse ties, and increasing of the column dimensions with a concrete jacket.

Tsubouchi, Ohashi, and Arakawa (1990) report the implementation of earthquake countermeasures on the Tomei Expressway, which runs from Tokyo through Yokohama on the way to Nagoya. This highway is located in a region where earthquakes are expected to be of magnitude 8.0. This road is also an emergency route during an earthquake. Approximately 70%, or 254, of the bridges on this highway required extensive retrofitting operations. The retrofit of two of these bridges is described below.

The Torisaka viaduct is a 218 m (715 ft) long, 13 span bridge with twin column bents. The presence of mid-height longitudinal steel termination points was deemed to be a weak link in the bridge. Of the 12 intermediate bents, the 7 fixed piers needed retrofit due to inadequate moment capacity when loaded in the longitudinal axis of the bridge. Retrofit consisted of concrete jacketing whereby the existing cover concrete was chipped away, and a 150 mm (5.9 in.) thick concrete jacket with 22 mm (0.87 in.) diameter bars within the confines of the jacket was placed. The new bars were also placed into holes drilled into the existing footing.

The Nishiokazu viaduct is a six-span bridge with four double column bents and one frame pier. The frames were examined for longitudinal seismic loading as well as transverse loads. Transverse analysis of the frame pier indicated that first a plastic hinge in the cap beam would form, then a hinge at the column base, and finally a hinge above the base hinge at the column top. Due to the difficulty of retrofitting the beams and columns separately, a shear wall retrofit was constructed. The wall was 300 mm (11.8 in.) thick and was reinforced in both directions with 19 mm (0.75 in.) diameter bars doweled into the existing columns, cap beam, and grade beam.

The use of infill walls to retrofit existing multi-column bents in Japan is discussed in Kawashima, Unjoh, and Mukia (1994). Upon seismic evaluation, a two-column, reinforced concrete bridge pier was found to be deficient in lateral strength in the transverse direction. To remedy this situation, an infill wall was constructed between the columns. The critical issue in this retrofit was the adequacy of the interaction between the wall and the existing columns. To attain reliable integration, 10 mm (0.39 in.) of the existing cover was chipped off of the existing pier members and holes drilled 240 mm (9.45 in.) into the existing columns. Reinforcing bars, 16 mm (0.63 in.) in diameter, were epoxy grouted into the holes and placed 300 mm (11.8 in.) on center both vertically and horizontally through the area where the new wall would be formed. Finally, a 400 mm (15.75 in.) thick wall was poured between the columns, cap beam, and strap footing.

Turkington, Wilson, and Kennedy (1991) describe the retrofit of the Oak Street Bridge in Vancouver, British Columbia, Canada. The bridge is 1,840 m (6034 ft) long and is supported by 83 reinforced concrete piers. The bridge has concrete approach spans, three main steel spans over the Fraser River, and five steel approach spans on the south side. The approach spans are supported on two column piers, while the main river spans are supported on a pier comprised of a solid wall section to above the high water line and twin columns upward to the bridge seat. Results of a seismic analysis indicated that the short approach span piers were shear deficient and that there was inadequate confinement and lap splice length at the column base. Numerous other deficiencies in the structure, such as a shear deficient cap beam and inadequate bridge beam seats, were also noted.

As part of a bridge-widening project, the cap beam was extended and widened to accommodate the additional loads and to provide sufficient seismic capacity. The cap beam was then strong enough to force plastic hinges to develop in the columns. Inadequate shear capacity in the plastic hinge regions following degradation in an earthquake caused concern. The remedy was to place full height steel jackets, although partial height jackets would have been sufficient, on all approach span columns less than approximately 10.5 m (34.4 ft) in height. The main river spans were expected to develop plastic hinges at the location where the twin columns tie into the wall pier and where the wall pier is connected to the unreinforced footings. A rocking response was also expected under longitudinal seismic load. Two piers were retrofit by providing an infill wall above the termination of the existing wall pier and vertically post-tensioning through the infill and existing pier shaft, a combined height of approximately 19.2 m (63 ft), with a 3.66 m (12 ft) anchorage length in the footing.

Serroels (1993) evaluates four retrofit alternatives for the Sutterville Road Overhead in Sacramento, California. The bridge is a low-priority structure carrying local traffic over two surface streets and five rail lines. The structure is 110 m (360 ft) long and is supported by three, two-column bents. Each column is approximately 8.5 m (28 ft) high and measures 1,220 mm x 1,220 mm (4 ft x 4 ft). Transverse reinforcing is inadequate with 12.7 mm (#4) transverse bars spaced vertically at 305 mm (12 in.). The connection between the column and the footing was designed to provide for no moment transfer. The

structure in its "as-built" condition was analyzed using the GTSTRUDL program for an estimate of the ratio of the elastic force demand to the nominal capacity as well as maximum longitudinal and transverse displacements.

Retrofit Strategy 1 involved the placement of shear walls between the columns of two of the three bents with the assumption that the columns in the third bent would pin at the top. For analysis, the walls were assumed to be at bents 2 and 3, minimizing the eccentricity of the transverse stiffness of the bridge and the center of mass and reducing torsional forces on the structure. The wall was intended to resist shear forces and the existing columns were intended to resist overturning axial forces. Also included was a tie at the base of the columns to prevent them from relative movement and possible separation from the wall boundary. This retrofit was one that primarily resisted transverse displacements and did very little in the longitudinal direction due to the negligible out-of-plane stiffness of the wall as compared to its transverse shearing stiffness. The wall was therefore assumed to be pinned at the top and bottom. Computer analysis of this retrofit alternative indicated significant transverse displacement reduction along with forces at the base of the wall strong enough to disconnect it from the footing. This was desirable because the decoupling of the wall from the excitation point, the footing, would effectively result in partial structure isolation.

Retrofit Strategy 2 employed steel jackets as a means of increasing ductility but not strength. The jacket thickness was chosen so that the jackets would develop 2.07 MPa (300 psi) of lateral confining pressure. The circular jacket was placed around a square column and filled with grout with no connection between the grout, jacket, and existing column, a detail that provided a negligible change in column stiffness and therefore little additional load. With a negligible effect on stiffness, the torsional forces are not an issue as with the shear wall retrofit and the structure can be retrofit without concern for this issue. In this strategy, jackets were placed on bents 3 and 4 but not on 2 to avoid construction near the adjoining railroad tracks. The columns of bent 2 were assumed to pin at the top. Analysis of this retrofit was done assuming no change in column section properties for the jacket because no increase in stiffness was expected. Results showed that the two retrofit jacket columns would see flexural demands on the order of 4.0 to 4.5, well within the ductility capacity of steel-jacketed columns.

Retrofit Strategies 3 and 4 did not involve any modifications to the columns and are not presented although they did include modifications at the abutment areas. These modifications were intended to draw load away from the columns to modify the bridge response.

Serroels concludes by stating that options 1, 2, and 4 would be feasible but would require the consideration of factors other than purely structural ones. The cost, the impact of construction on roads and rail lines, and other factors pertaining to expected damage would all need to be considered in determining the most feasible retrofit strategy.

Examination of the "as-built" and retrofit response of a three-column bridge bent typical of construction in the Eastern United States in the 1950's and 1960's is presented in Mander and Chen (1994). In the class of bridge columns investigated in this study, the dominant mode of failure was damage to the joint core. To remedy this problem, the cap beam was retrofit jacketed with high-strength concrete and externally longitudinally post-tensioned to force the failure location into the top of the column.

The "as-built" 1/3 scale bridge model was of a three column bent. The columns were 280 mm (11 in.) in diameter and had a clear height of 1,830 mm (72 in.). Longitudinal reinforcing consists of sixteen, 9.5

mm (#3) reinforcing bars enclosed with "soft wire" transverse hoops at 102 mm (4 in.) centers. Sixteen dowel bars extended from the grade beam spread footing at the base of each column. The grade beam and the cap beam were both 280 mm (11 in.) high.

The "as-built" model was outfitted with load cells placed at mid-height of each column to determine the portion of load carried by each column. Test results indicate that despite inadequate transverse reinforcing, the column was able to sustain drift angles of up to 5% with little distress. Failure was due to inadequate longitudinal steel anchorage into the cap beam. The joints also exhibited shear failure due to inadequate core reinforcing. The failure mode was not properly predicted by the ATC 6-2 provisions, which predicted a brittle shear failure in the column with no ductility. Failure of the spread footing was similar to the cap beam. Mander and Chen determined that a traditional steel jacket retrofit would only exacerbate the problem by inducing higher joint shear force demands. Also, because the columns exhibited a reasonable amount of ductility, they were best left alone. The retrofit, therefore, consisted of the following.

The cap beam was jacketed in concrete and transversely post-tensioned. The footing was also strengthened by casting a wall or foundation beam above the existing footing enclosing the bottom lap splices and prohibiting joint failure. The failure location would then move into the column above the level of the lap splice. Failure finally occurred in shear in the region of the load cells. The retrofit was able to change the failure mode of the frame and also provide lateral strength increases of approximately 40% to 50%.

An alternative retrofit method was devised in which the shear demand is reduced rather than increased by other retrofit methods. The proposed method is to cut the existing longitudinal steel at the base and then encase the region with a concrete collar, providing a rocking response to the column. The size of the collar is proportioned so that the column remains elastic beneath the cap beam hinge. To investigate the method, one column was constructed and tested under increasing cyclic lateral load up to drift angles of 10%. Although this specimen's response was hypothesized to be bilinear elastic, examination of the hysteresis loops indicated significant energy dissipation. The dissipation was credited to Coulomb friction between the lower portion of the severed column and the collar.

On the basis of examination of the foundation beam and concrete collar retrofit scenarios, the summary recommendation is to consider the foundation beam scenario only if the columns have dependable shear capacity at the flexural overstrength level. The rocking base is a viable retrofit alternative because it reduces the shear demand and allows the dissipation of energy through Coulomb damping.

#### **4.2 External Post-Tensioning and Mild Reinforcing Retrofits**

External reinforcing retrofits can be used in several ways. They can provide sufficient lap splice confinement so that flexural strength can be maintained. They can provide external confinement to the plastic hinge region so that stable hinge formation can occur. External ties can be used as shear reinforcing. The other potential use for external reinforcing retrofits is lateral confinement for axial load strengthening. Several examples of these techniques are presented below.

The use of externally post-tensioned reinforcing bars as lateral confinement in plastic hinge regions of columns lacking sufficient confinement is discussed in Coffman, Marsh, and Brown (1991) and summarized in Coffman (1992) and Coffman, Marsh, and Brown (1993). These tests were carried out at

the University of Washington for the Washington State Department of Transportation and involved the construction of four, half-scale models of typical flexurally-deficient bridge columns constructed in Washington State in the 1950's and 1960's.

Test columns were circular columns measuring 455 mm (18 in.) in diameter and 3.05 m (10 ft) in height. They were tested in single bending as vertical cantilevers to represent the lower half of a column twice this height tested in asymmetrical bending. The column was axially loaded to  $0.20f'_cA_g$  because this represents the upper end of sustained dead loads that a column might need to carry after an earthquake. Column reinforcing consists of nine, 19 mm (#6) reinforcing bars on a 170 mm (6.75 in.) radius. Dowels of the same diameter extended from the footing and were lap spliced at a length of  $35d_b$ , the maximum lap length at the time. (This lap is longer than the typical lap used by other researchers,  $20d_b$ , and should be considered when interpreting the results). The dowels were screwed and welded to a steel base plate that the column was post-tensioned to during testing. Lateral ties of 9.5 mm (#3) bars spaced vertically at 305 mm (12 in.) were used with lap splices in the cover concrete of 355 mm (14 in.). As determined from cylinder tests at 84 days, the concrete strength of the columns was 22 MPa (3,200 psi). The longitudinal steel, expected to be 276 MPa (40 ksi) steel, was tested at 379 MPa (55 ksi). The internal ties were also expected to be 276 MPa (40 ksi) steel but were estimated to have a yield point of 434 MPa (63 ksi). The retrofit hoops were to be 414 MPa (60 ksi) steel but were estimated to have a yield strength of between 483 MPa (70 ksi) and 558 MPa (81 ksi) depending on the size of bar used.

The test columns were retrofitted with post-tensioned steel reinforcing bars and mechanical swage couplers. The rebar was nominal 414 MPa (60 ksi) ASTM A615 reinforcing steel with actual strengths as described in the previous paragraph. The bars were bent into two semicircles that were fit into opposite thread swage couplers. A machined stud connecting the couplers was then tightened to induce a significant amount of prestress into the bars. This prestress of 345 MPa (50 ksi) was applied to actively confine the lap splice region and plastic hinge region. The three columns to be retrofit were constructed with differing external reinforcing arrangements. In all columns, the first hoop was placed a distance of 75 mm (3 in.) from the bottom of the column. Column 2 was retrofit with eleven, 13 mm (#4) hoops spaced vertically at 75 mm (3 in.). Column 3 was retrofit with eleven, 9.5 mm (#3) reinforcing hoops spaced vertically at 75 mm (3 in.) centers. Finally, column 4 was retrofit with nine, 9.5 mm (#3) hoops spaced vertically at 100 mm (4 in.).

Column loading consisted of a constant axial load and a cyclic lateral load. The axial load was a constant 703 kN (158 kips) applied via a pretensioned bar placed in a sleeve cast in the center of the column. The lateral load was displacement control led after the first yield occurred in the longitudinal steel. The control column required a displacement at the load point of 27 mm (1.07 in.) to produce yielding. The intended load was one cycle at  $\mu_\Delta = 0.75$ , two cycles at  $\mu_\Delta = 1$  and 2, and continual cycling at  $\mu_\Delta = 4$  until failure.

Results of testing the "as-built" specimen are as follows. At a ductility,  $\mu_h = 2$ , a large flexural crack developed at the top of the splice and concrete crushing began at the toe. The crack then joined with other cracks as cycling began at  $\mu_\Delta = 4$ . At this level, cover concrete began to spall and lap splice slippage occurred. The force required to attain  $\mu_\Delta = 4$  began to decrease on the first return cycle to  $\mu_\Delta = 4$ , the cycle that completed the plastic hinge development at the base. In the final test cycle, the axial load was removed and then reapplied after cycle completion. After the test was completed, the column was still capable of holding the load. A photo taken at the completion of testing shows that the cover concrete

was completely spalled over approximately the lower 760 mm (30 in.), indicating complete cover loss up to the third transverse tie in the "as-built" specimen.

The retrofit columns demonstrated significantly enhanced performance over the "as-built" specimen. Columns 2, 3, and 4 sustained 12, 14, and 16 cycles at  $\mu_{\Delta} = 4$  before failure. Columns 2 and 3 behaved in a very similar fashion; their dowels fractured at the end of cycling at the weld to the steel base plate. Concrete crushing in column 2 extended into the column core. Concrete crushing at the column base occurred before cycling to  $\mu_{\Delta} = 4$  began and damage increased at this ductility. Several cracks opened at the top of the lap splice in these columns but no shear displacements were evident unlike the "as-built" column 1. Most strain gages on the dowels at the base of the columns were rendered inoperable after indicating strains of 1% to 3%. The strain gages at mid-depth of the dowels remained operational and recorded strains 3 to 4 times the yield strain. Column 4 experienced crushing at the base during the initial cycles to  $\mu_{\Delta} = 4$ . The retrofit hoops were most significantly strained near the top and bottom of the longitudinal splice but the external hoops above the splice showed very little effect.

In the cycles up to  $\mu_{\Delta} = 2$ , all columns, retrofit and "as-built", exhibited the same behavior and dissipated similar cumulative amounts of energy. With cycling at  $\mu_{\Delta} = 4$ , the "as-built" specimen sustained only 1 cycle, while the hysteresis loops of all three retrofit columns overlaid one another for 12 cycles. The retrofit columns dissipated approximately 20% more energy in the first cycle to  $\mu_{\Delta} = 4$  than the "as-built" column; subsequent cycling reduced the energy absorbed per cycle to approximately that of the first  $\mu_{\Delta} = 4$  cycle of the "as-built" specimen. The total energy absorbed by the "as-built" column and three retrofits follows. Column 1, the "as-built" specimen, dissipated a total energy of 30.4 kN-m (269 in-kips), column 2 a total of 164.8 kN-m (1,459 in-kips), column 3 a total of 176.9 kN-m (1,565 in-kips) and column 4 a total of 208.2 kN-m (1,842 in-kips). The retrofit columns provided energy dissipation capacity of 542%, 582%, and 685% that of the "as-built" column.

Examination of the load-displacement plots of all four columns indicates that until  $\mu_{\Delta} = 2$ , the stiffness of the four columns was the same. The cycling to  $\mu_{\Delta} = 2$  produced damage in all specimens and softened the response. This somewhat degraded stiffness was then maintained by all columns until failure. The lateral load capacity of the retrofit columns diminished slightly with each cycle to  $\mu_{\Delta} = 4$  until dowel fracture when the lateral strength dropped significantly.

Coffman, Marsh, and Brown (1991) comment that the force transfer mechanism in the splice seems to have been preserved and that most yielding was concentrated at the base of the column adjacent to the foundation. They also indicate that the most desirable response yields a significant portion of the longitudinal steel length, preserving column strength and the energy dissipation characteristics. The fact that column 4, the column with the lowest amount of transverse confinement, sustained the greatest number of cycles is due to the yield of the external hoops in this retrofit and the lack of yield in the other two retrofit columns. Yield of the transverse reinforcing allowed a spread of plasticity to occur in the hinge region.

The very rigid base was not an accurate representation of the footing and column interaction, which tended to soften the column's overall response. Actual footing use was hypothesized to allow for enhanced column performance due to the footing's ability to contribute to the column response via yield penetration.

In summary, the results of this testing indicate the ability of prestressed steel external hoops to provide stable hinge formation in reinforced concrete columns having inadequate transverse confinement. The single cantilever column was selected to represent the bottom of a column bent in asymmetrical bending due to a rigid base and cap beam. The prototype column addressed by this retrofit is one that actually measures 12.2 m (40 ft) in height and 915 mm (36 in.) in diameter. The column dimensions were specifically selected to ensure a flexure-dominated failure. The results of this retrofit are not known if applied to a shear-dominated short column or to columns with more critical lap splice lengths, i.e.,  $20 d$ , but the improvement would be equal to that demonstrated in this research.

The results of an investigation of flexurally deficient bridge columns externally post-tensioned to confine the plastic hinge region are briefly presented in Priestley, Seible, and Chai (1992a). These results have also been summarized and included in Priestley and Seible (1991, 1992), as well as in University of California (1991). The equations and methodology presented in these documents have been incorporated into the FHWA seismic retrofit guidelines (Federal Highway Administration, 1995).

The technique in question involved the active confinement of potential plastic hinge regions with a prestress wire wrap furnished by the VSL Corporation. The response of two columns under reversed inelastic loading was studied.

In the first test, a circular column was wrapped with 4.9 mm (0.192 in.) prestressed wire spaced vertically at 30 mm (1.2 in.). This corresponds to an effective lateral confining pressure of 2.43 MPa (352 psi). The second column was more extensively confined; wire of the same diameter was spaced vertically at 6.6 mm (0.26 in.) centers. This corresponds to a lateral confining pressure of 11.17 MPa (1,620 psi). To create this pressure, the wires were stressed to 1,207 MPa (175 ksi), a stress level equal to  $0.7f_{pu}$ .

Results of the testing indicate that both columns demonstrated a stable response and little degradation up to drift levels of 4% to 5%. The final failure mode in both specimens was low-cycle fatigue of the longitudinal reinforcing. Low-cycle fatigue failure is generally indicative of excellent lap splice force transfer.

The text which follows describes the field testing of several columns in East St. Louis, Illinois. These tests were part of a more comprehensive test program that included "as-built" column tests as well as composite jacket column testing. Refer to the text which begins on page 101 for a description of the "as-built" tests results as well as the composite retrofit test results.

Shortly after construction of the Poplar Street Bridge piers, splitting at the tops of the columns was observed due to forces exerted from the superstructure beams. External hoops were applied to the column tops to arrest this splitting. When the bridge superstructure was demolished, this reinforcement was removed from the column top and reinstalled on the column bottom to determine its ability to prevent lap-splice debonding. The hoops are 19 mm (0.75 in.) square AISI 4140 heat-treated steel bars with threaded ends. The bars were bent into semicircles and placed into a bracket in which they would be anchored. Upon placement in the bracket, washers and nuts were placed on the bars and tightened to 298 N-m (220 lb-ft) of torque to form a continuous ring around the column. A total of six rings at 205 mm (8 in.) spacing were used to confine the entire length of the lap splice.

The first column tested with this retrofit was column B18N in 1993 (Lin, Gamble, and Hawkins, 1994). This column was a 1,370 mm (54 in.) diameter column reinforced with twenty-eight, 36 mm (#11)

longitudinal bars. Initial loading consisted of two cycles to 356 kN (80 kips) in both north and south directions. The column had an enhanced stiffness when being moved toward the crash wall. A 10% increase of displacements for loading toward the crash wall and 25% for loading away from the crash wall was observed from the first to second cycles of the load. An average displacement of 20 mm (0.8 in.) was used for cracked stiffness computations and for definition of an "effective" yield displacement. This "effective" yield displacement was found from extrapolation of the initial test data to be 36 mm (1.4 in.). Additionally, two cycles to  $\mu_{\Delta} = \pm 1.1$ , one cycle to  $\mu_{\Delta} = \pm 1.7$ , one half cycle in the south direction to  $\mu_{\Delta} = +2.3$ , and a final south half cycle to  $\mu_{\Delta} = +3.4$  were conducted. The initial stiffness was similar for this retrofit and its companion "as-built" column, B18S, because the bands do not play any role in increasing column flexural stiffness. The maximum loading attained in this test was 703 kN (158 kips) for loading toward the crash wall and 538 kN (121 kips) for loading directed away from the crash wall. These loads exceeded the lateral load response of the "as-built" column, B18S, although the retrofitted column sustained more inelastic cycles at higher displacement ductility levels. This supports the ability of the steel bands to promote force transfer in the lap splice region.

Column C17N, a 1,370 mm (54 in.) diameter column with twenty-four, 36 mm (#11) reinforcing bars was retrofit using a system developed by Dywidag Systems International (DSI). The retrofit consisted of nine retrofit rings spaced at 205 mm (8 in.) centers along the lap splice region. Each retrofit ring consisted of two, 15 mm (0.6 in.) diameter prestressing strands, each one half of the column circumference, which formed a loop around the column when coupled together. The strands were stressed to 387 kN (87 kips) to provide lateral confinement of the lap splice region.

This column was first subjected to lateral loading to 356 kN (80 kips) in both south and north directions with deflections of 21 mm (0.8 in.) and 24 mm (approximately 1 in.) respectively. No increase in stiffness between the "as-built" and DSI retrofit was noted at this point. Subsequent load cycles were displacement controlled. During the first cycle to 40 mm (1.58 in.), the column cracked at the external hoop 150 mm (6 in.) above the crash wall at a lateral load of 560 kN (126 kips). At the same displacement in the opposite direction, a more flexible response was produced requiring a load of only 502 kN (113 kips). This cycle created several cracks in the crash wall. Subsequent cycling to  $\mu_{\Delta} = \pm 2.0$ ,  $\pm 80$  mm ( $\pm 3.15$  in.) required lateral loads of 702 kN and 642 kN (158 kips and 144 kips) respectively for opposite directions of load. For the second cycle to this displacement, the loads were 8% to 10% smaller due to column deterioration. Two short vertical cracks formed at the column base during these cycles but ended at the first strand. This sequence of two fully reversed cycles was repeated at  $\mu_{\Delta} = \pm 3.0$ , requiring loads on the first of the two cycles of 725 kN and 640 kN (163 kips and 144 kips) as well as another series of two cycles at  $\mu_{\Delta} = \pm 4.0$ , requiring lateral loads of 732 kN and 646 kN (165 kips and 145 kips). The crash wall damage continued to grow noticeably during these cycles. A single cycle to  $\mu_{\Delta} = 5$  was carried out, producing a displacement of 200 mm (8 in.). Significant deterioration of the crash wall continued but the maximum lateral load increased to 770 kN (173 kips) with a south load. Due to hydraulic cylinder stroke limitations, all subsequent displacements were in the pull direction. The column was pulled to the limit of the deflection scale,  $\mu_{\Delta} = 360$  mm (14.15 in.) without failure. There were no vertical cracks indicative of splice failure except those arrested at the column base by the first set of DSI strands. The maximum load applied to this column during this cycle was equal to 801 kN (180 kips), which indicates a column with a stable response past that which could be measured in the field.

The use of a novel external confinement technique is described in Frangou and Pilakoutas (1994) and Frangou, Pilakoutas, and Dristos (1995). The strengthening technique involved the tensioning of discrete metal strips around the outside of a column to provide external confinement. These strips are the same

metal strips used in the packaging industry for securing cargo and loads to pallets. The use of commercially available strapping machines allows an operator to provide significant tension to the strips and also to secure them under tension. The tensioning force used in this experiment was just below the yield level of the straps.

Frangou, Pilakoutas, and Dristos (1995) presented a summary of the results of axial compression tests on 18 cylindrical and 28 rectangular specimens. The cylindrical specimens were 100 mm (3.94 in.) in diameter and the rectangular specimens measured 100 mm (3.94 in.) on a side. All specimens were 200 mm (7.87 in.) in length. The specimens were confined with metal strips of 12.77 mm (1/2 in.) width and 0.5 mm (0.02 in.) thickness. The clear spacing between strips,  $s'$ , varied from 0 mm, 12.7 mm, and 25.4 mm (0 in., 1/2 in., 1 in.) in the cylindrical specimens and 0, 12.7 mm, 25.4 mm, and 38.1 mm (0 in., 1/2 in., 1 in., 1.5 in.) in the prismatic specimens. The strips were of two different materials: Bryten and Extraten. The average ultimate stress of the Bryten strips was 490 MPa (71 ksi) and of Extraten, 767 MPa (111 ksi).

When examined, the results of a cylindrical test stress and strain diagram indicated that an unconfined cylinder had a compressive strength of approximately 30 MPa (4,350 psi), a corresponding peak strain of approximately 0.004, and an ultimate strain of less than 0.01. The specimen with the largest strap spacing, 25.4 mm (1 in.), had an unconfined compressive strength of approximately 37 MPa (5,360 psi), a corresponding peak strain of approximately 0.005, and an ultimate strain of 0.02. The specimen with the strap spacing of 12.7 mm (1.2 in.) had a compressive strength of 40 MPa (5,800 psi), peak strain of approximately 0.0075, and an ultimate strain of 0.0275. Finally, the specimen that was continuously wrapped exhibited a compressive strength of approximately 46 MPa (6,670 psi), a peak strain of approximately 0.01, and an ultimate strain of over 0.02.

General test results indicate that the strength ratio of the confined to unconfined compressive strength of the specimen decreases as the strap spacing increases. Additionally, for a given strap spacing, the cylindrical specimen is more effectively strengthened than a corresponding rectangular specimen.

Test results were compared to the analytical predictions of Eurocode 8, a piecewise linear model relating the confined compressive strength of concrete to the unconfined strength, confinement effectiveness, and the volumetric confinement ratio of the transverse reinforcing. The results were also compared to Mander, Priestley, and Park's (1988b) model for confined concrete. Comparison of the experimental results to the equations mentioned above indicates that the Eurocode 8 model was the most effective in predicting the specimen response and its piecewise nature coincided with the slope change of the experimental data. Mander, Priestley, and Park's model was significantly unconservative at high levels of confinement, predicting as high as 20% more strength than experimentally determined for the cylindrical specimens. For the rectangular specimens, all models were conservative for low levels of confinement, but Mander, Priestley, and Park's model was the least conservative. For high levels of confinement, the Eurocode 8 model was the best predictor, and Mander, Priestley, and Park's model predicted a greater increase in strength than experimentally observed.

This technique was very effective at increasing the axial load strength of confined cylindrical and rectangular concrete specimens. The strapping technique is easy to apply but must be done properly to ensure proper tensioning and anchorage. The Eurocode 8 model for confinement was the best predictor in axial load capacity increase due to its piecewise linear nature. Mander, Priestley, and Park's model was either the least conservative or unconservative depending on the confinement ratio. Additional

experimentation should be carried out in this area with larger scale columns tested with combined axial, shear, and bending forces.

### 4.3 External Angle and Bar Retrofit

The external angle bar retrofit, like concrete jacketing, receives more attention from the building retrofit community. In Section 2.2.2 on steel jacketing, the retrofit of shear-deficient rectangular-reinforced concrete columns was discussed in McLean and Bernards (1992), which was subsequently summarized in Bernards, McLean, and Henley (1992). These references also contain test results documenting the use of angle and bar retrofits.

The angle and bar retrofit consists of four steel angles placed on the corners of the steel column and connected by threaded bars, 6 mm (1/4 in.) in diameter, which act as external hoops to the column. These retrofit hoops, according to the authors, were expected to provide additional confinement as would regularly spaced internal ties. This retrofit would also be easily constructed in the field. The columns tested in this fashion were columns 3 and 5. The "as-built" specimens to which comparisons were made are described below.

Specimens of a 2/5 scale were constructed, employing the shear-deficient details common in prototype columns of the Puget Sound region of Washington State. The prototype columns measured 510 mm x 760 mm (20 in. x 30 in.) and had a longitudinal reinforcing ratio of 2.6% with the reinforcing concentrated on the short faces. A lap splice was not present at the base of the columns. Transverse reinforcing consisted of 9.5 mm (#3) bars spaced at 305 mm (12 in.) with 100 mm (4 in.) hook extensions lapped in the cover concrete. All column reinforcing had a yield strength of 276 MPa (40 ksi), typical for the columns under investigation. The test specimen was 40% of this size, i.e., 205 mm x 305 mm (8 in. x 12 in.), and was 915 mm (36 in.) high above the top of the footing. Test specimens were vertical cantilevers tested in single curvature bending.

Specimen testing followed the same procedure. An axial load was applied to the specimen approximately equal to  $0.09f'_cA_g$ . This load varied by approximately  $\pm 12\%$  during the test. The cyclic lateral load was applied at 760 mm (30 in.) above the footing and consisted of two cycles at  $\mu_\Delta = 1, 2, 4, 6,$  and  $8$ , unless failure occurred before this cycling was completed. The yield displacement was initially computed to be 2.8 mm (0.11 in.) but was modified during testing after this value was recognized as being too low. The refined value of 6.6 mm (0.26 in.) was adopted as  $\Delta_y$ .

The first two columns tested were control columns. Both columns exhibited classic shear failure as demonstrated by pronounced x-cracking. Column 1 was originally tested with the low estimation of yield displacement and its results were, therefore, not useful for computing ductility. After this column's response was assessed, the refined estimate of yield displacement was made and column 2 tested in accordance with the yield displacement of 6.6 mm (0.26 in.). Column 2 exhibited shear cracking and tie yield at  $\mu_\Delta = 1$ . Load carrying capacity dropped significantly at  $\mu_\Delta = 2$  after which very little lateral load could be sustained. The reliable ductility of this column was judged to be  $\mu_\Delta = 1$ .

Column 3 had retrofit hoops spaced at 150 mm (6 in.) on center. The bars were uniformly prestressed to 50% of their yield stress; yield was measured as 448 MPa (65 ksi) before loading began. During testing, internal tie yield occurred at  $\mu_\Delta = 2$  along with inclined cracks at  $45^\circ$  angles. Load capacity dropped significantly during the first cycle to  $\mu_\Delta = 4$  due to brittle fracture at the ends of the threaded rods. The

lowest set of bars failed first and failure progressed upwards. After rod failure, shear cracks opened in the column similar to those observed in the "as-built" specimens. The lateral load increased only 7% over the "as-built" specimen and this retrofitted column was deemed to have a dependable capacity of  $\mu_A = 2$ .

Column 5 had its hoop spacing decreased to 100 mm (4 in.) and the bars were annealed in order to provide a more ductile failure. Internal tie yield was not observed until the first cycle to  $\mu_A = 4$  with a corresponding development of shear cracks at  $45^\circ$  near the angles placed on the column corners. This column maintained its lateral load capacity until  $\mu_A = 6$  when the external bars started to fail the threads. The bars necked down before failure, which started at the middle of the column and progressed toward the base. Following hoop fracture, substantial cracking developed, longitudinal reinforcing buckled, and core degradation occurred. The capacity of this retrofit column was 7% greater than that of an "as-built" specimen. Dependable ductility of this specimen was judged to be  $\mu_A = 4$ .

By providing external confinement at the corners of the column via angles post-tensioned together, shear capacity was expected to increase enough to precipitate a flexural failure. This was not the case due to the limitations in the elongation capacity of the steel bars. The use of upset threads would likely improve this retrofit's performance, but at an increased cost.

#### **4.4 Internal Reinforcing Methods**

The use of internal reinforcing techniques has received very little attention because of the difficulties perceived in maintaining structural integrity while removing portions of the column cover and portions of the transverse reinforcing and core. These difficulties have not stopped investigation into this area, however, but the amount of information is very limited at this point.

The development of a replaceable hinge detail is described in Mander and Cheng (1995) as a summary to the work carried out in Chang and Mander (1994a, 1994b). The replaceable hinge detail is employed as a repair option for damaged columns that were originally constructed with the replaceable bar hardware and whose failure mode is low cycle fatigue of the longitudinal reinforcing. The replaceable hinge is not envisioned as a repair technique for existing columns but as a construction detail for columns of the future which allows for enhanced post-earthquake serviceability and repair. Research into this technique is ongoing as part of a separately funded FHWA research project at the State University of New York at Buffalo.

Following the low-cycle fatigue failure of the longitudinal bars at the base of a column in an earthquake, the structure can be shored, the damaged bars removed, new reinforcing placed via mechanical couplers, additional spiral reinforcing applied, and the column reconstructed with rapid setting, shrinkage-compensating concrete. These specially machined bars, known as fuse bars, are thinned to ensure that yield and final fracture occurs at a predetermined location.

One experimental column was tested and repaired five times using this method with no damage to the foundation or upper portion of the column. The variables included length of the fuse bars, amount of transverse reinforcing in the hinge area, and magnitude of the axial load. A similar specimen was representative of factory-made precast columns and was repaired ten times using the above approach.

Renewable hinge design is based on a comparison of the hysteretic fatigue demand due to ground motion and the hysteretic fatigue capacity of specific fuse bar designs. The rules for the hysteretic damage and

demand models are extensively presented in Chang and Mander (1994a, 1994b) and briefly in Mander and Cheng (1995) and are beyond the scope of this document.

In Adachi, Kosa, and Murayama (1994), the behavior of a 1/3 scale single column pier designed in accordance with the Hanshin Expressway standard design code is evaluated in the "as-built" condition and after subsequent repair. The model measured 1 m (3.28 ft) by 1.167 m (3.83 ft) in plan area and was constructed with a typical Japanese column detail where longitudinal bars are terminated in accordance with the linear decreasing moment diagram as one moves away from the base. The Japanese design code mandated in 1980 that this termination point be where the bars are stressed to 50% of their allowable stress, plus an additional  $20 d_b$  and a distance equal to the effective column depth. This code is significantly different from older versions of the Japanese code, which had only the  $20 d_b$  extension provision and higher allowable shear stresses. To ensure shear failure at the termination point, Adachi, Kosa, and Murayama used the older anchorage provision, which located the termination point closer to the foundation. This premature termination caused significant flexural damage and subsequent shear failure at the cut-off location. Adachi, Kosa, and Murayama also reduced the amount of continuing reinforcement from 70% to 55%. Before bar termination, the column had a reinforcement ratio of 2.28% and after termination, 1.26%. The longitudinal bars were 13 mm (0.51 in.) diameter and had a measured yield of 373 MPa (38 kgf/mm<sup>2</sup>, 54 ksi). The bar cut-off point was 1.233 m (4.05 ft) above the footing and the clear height from the top of the footing to the point of lateral load application was 4.3 m (14.1 ft). The overall column dimensions and shear span ratio were essentially the same as a prototypical column.

The "as-built" column was tested in gradually increasing, fully reversed single curvature bending, six cycles in all, until the load caused first yield in the longitudinal steel. At this point the test became a displacement controlled test with 10 cycles at each of  $\mu_\Delta = 1, 2, 3,$  and  $4$  being the intended sequence. Under this sequence, the flexural cracks that first appeared in the cut-off region at 130 kN (13.3 tf, 29 kips), shifted to diagonal cracks at 737 kN (75.2 tf, 166 kips), which was denoted as the yield strength load. Increased spalling in the cut-off region was noted and the range of spalling increased beginning at the third cycle to  $\mu_\Delta = 3$ . Column reinforcing buckled on the sixth cycle to  $\mu_\Delta = 3$  and hysteretic performance significantly dropped on the first cycle to  $\mu_\Delta = 4$ . At this point, the shear reinforcing had yielded in the cut-off region and fractured. The column was then retrofit as follows.

The concrete was chipped away to expose the second layer of internal longitudinal steel. All main reinforcing and hoop steel in the fracture zone was cut with a gas torch with approximately 10 bars being removed at a time to maintain specimen stability. New bars were weld connected to the existing steel with weld lengths of 150 mm (5.9 in.) and 70 mm (2.75 in.) for the 13 mm (0.51 in.) and 6 mm (0.24 in.) longitudinal and hoop bars respectively. Coarse aggregate was placed into the void, followed by cement paste. After the forms were removed, epoxy grout was applied to any remaining cracks. This specimen was tested under the same criteria established for the "as-built" specimen with the following results. The initial flexural cracks in the specimen changed to diagonal shear cracks at a later load of 696 kN (71.0 tf, 157 kips), followed by an enhanced degree of spalling at  $\mu_\Delta = 3$  and a rapid degradation of the hysteretic response on the first cycle to  $\mu_\Delta = 4$ . The hysteretic response for the "as-built" and repaired column was essentially the same. With this project, Adachi demonstrated an effective means of repairing a damaged bridge pier so that the bridge could be reopened until a more permanent replacement or retrofit solution could be applied.

## SECTION 5 COLUMN PERFORMANCE EVALUATION METHODS

### 5.1 Introduction

Having presented a significant amount of information on very disparate tests in Sections 2 through 4, one is left with the task of trying to objectively assess the performance of the various retrofits. The types of columns, column deficiencies, types of retrofits, test methods, etc., were all described in the preceding sections. Some of the variables to consider when comparing column performance are presented in the following text.

Columns can be circular or rectangular. The literature review indicated that column concrete strength varied from test to test. The columns were of variable dimensional scale factors of different prototype dimensions. The test could either be a vertical cantilever single-bending test or a double-bending test. The columns were tested under varying degrees of axial and lateral load.

The column reinforcing may be lap spliced with the laps differing from test to test or may be continuous. The column steel yield and ultimate strengths varied from test to test.

The columns could have inadequate flexural strength, inadequate flexural ductility, or inadequate shear capacity. The location of the deficiency could be at the top, bottom, or middle of the column, or may include the entire column as a whole.

The retrofit could be a steel jacket, composite jacket, concrete jacket, external post-tensioning retrofit, etc. Within the retrofit types, the column may be retrofit in its original shape or the shape may be altered to facilitate a more effective means of confinement.

Additionally, inconsistent reporting of valuable information required for a comprehensive comparison of all references was a problem.

Noting all of the variables and perceived problems, several different scenarios were still considered as a solution to the evaluation dilemma. The two solutions that were viewed as being most promising include the use of modern design standards as a means of assessing minimum acceptable performance criteria and a ranking technique that would attempt to assign a numerical rank to the different references.

It should be noted that the primary objective of this study was to assess the structural capabilities of the available retrofit techniques. As such, the means of evaluating and ranking retrofit alternatives is biased towards the capacity side of the capacity vs. demand equation. The research reviewed was also strongly biased towards a discussion of structural performance without regard to demand. The goal of most of the laboratory testing discussed in the preceding chapters was to prove that a retrofit was structurally comparable to steel jacket retrofits, the first type of retrofit explored extensively in a laboratory setting. The steel jacket retrofits have been shown to provide a great deal of enhanced performance, i.e., enhanced shear strength, displacement ductility, and lap splice confinement, to a deficient column, even in the most severe of structural tests. Most other retrofit techniques which followed had as their target the structural performance of these very effective steel jacketed columns. This is an appropriate approach if all geographical areas are striving for the same degree of seismic performance. It is a much too conservative approach for areas where the need for seismic retrofit is less critical. An engineer / agency

should keep in mind that when selecting a seismic retrofit technique, the goal is not to install the “best that money can buy”, but rather the most appropriate solution for the demands of the site. The worthiness of a particular retrofit can not and should not be completely established by simply comparing its structural performance relative to that of other methods but should be a function of structural capacity versus seismic demand and the cost of the system.

## 5.2 Minimum Acceptable Performance Criteria

The review of United States, Japanese, New Zealand, and European bridge design codes is carried out in two documents published by the Applied Technology Council (1995a and 1995b). This review presents the various analysis and design philosophies established by each agency for newly constructed bridges and related structures. As part of this review, seismic analysis methods consisting of equivalent static analysis, response spectrum methods, and time history analysis, among others, are presented in the context of the individual agency requirements. As part of the presentation, requirements for detailing and ductility are discussed so as to assure the assumed level of performance of the structure. This is particularly true for structures analyzed with the equivalent static load approach where the level of assumed ductility determines the force reduction factor to be used in design. One must then assure that the type of structure assumed is designed so that forces are on par with the assumed values. The minimum required levels of ductility for certain bridge types are also stipulated in the code documents. One approach for assuring adequate structural performance in new structures is that proposed by New Zealand and is summarized below.

Chapman (1995), in addition to describing the current structural design practices in New Zealand related to earthquake design of new bridges and highway structures, also presents in an appendix, the latest amendment to the Transit New Zealand Bridge Manual (TNZBM). This amendment explains, among other things, the acceptable levels of structural performance for new bridge structures in terms of structural ductility. The important point is made that the overall structural ductility, generally characterized as a displacement ductility, is much different than the localized curvature ductility in the area of a plastic hinge. The document illustrates that to attain a displacement ductility of the structure equal to 6 in columns whose height/lateral dimension ratios range from 2.5 to 10, the curvature ductility,  $\phi_u/\phi_y$ , may vary from 10.3 to 69.5. The basis for relating local curvature ductility to displacements of the center of mass of the superstructure is prescribed in the TNZBM as follows.

$$\frac{\phi_u}{\phi_y} = 1 + \frac{C(\mu - 1)}{3 \left( \frac{L_p}{L} \right) \left( 1 - \frac{0.5L_p}{L} \right)} \quad (5-1)$$

where

$\phi_u$	=	Ultimate curvature of the plastic hinge
$\phi_y$	=	Yield curvature of the plastic hinge
C	=	Coefficient to represent the increase in system flexibility due to foundation and bearings
$\mu$	=	Displacement ductility, $\Delta_u/\Delta_y$
$L_p$	=	Equivalent plastic hinge length
L	=	Distance from the column base to the center of the superstructure mass

Structures in the TNZBM are categorized into a number of different types corresponding to the geometry of the superstructure and substructure. Within these categories, an overall structural design displacement ductility is assumed. This ductility is used to compute the seismic force demands on the structure through the use of an equivalent static force analysis. Structures with higher degrees of displacement ductility are designed for smaller equivalent forces than those closer to a fully elastic response. Of particular interest, is the displacement ductility assumed to exist in certain types of structures and the requirements on the stability of the ductile response.

A ductile structure is one in which a full plastic hinge mechanism develops. This is characterized by increasing displacement ductility with a constant force. The TNZBM stipulates that a ductile structure should be capable of attaining a displacement ductility factor of at least 6, along with four cycles of the maximum design displacement, without more than a 20% decrease in horizontal load resistance. Examples of structures designed to exhibit ductile response are single and multi-column bents on pile footings where the plastic hinge is expected to develop above the ground or normal water level.

A partially ductile structure (Type I and II) is a structure that exhibits only localized plastic hinging. They are designed so that after the first hinge develops, the structure can continue to have an upward sloping force displacement response. These structures are designed to have a maximum ductility capacity of 4 or less. In a Type I structure, partial hinging continues up to the design displacement level while a Type II structure will eventually form a complete mechanism but at unpredictable load levels. Examples of these structures are single or multi-column bents on spread footings with the embedment of the top of the footing less than 2 m (6.56 ft).

Having assumed displacement ductilities from the structure type and computed equivalent static force demands, the elastic ductility can be substituted into the previously supplied equation relating displacement ductility to rotational ductility and the structure detailed to accommodate the required rotations.

This document establishes some minimum acceptable performance criteria for a broad classification of bridge types. Most typical highway bridges in New Zealand and around the world are of the types mentioned in the above classification of substructure type. The performance of a retrofit column could easily be compared to the simple criteria established above for new bridge structures and an assessment of adequacy be made.

There are, however, disagreements with some of the design procedures for new structures. Concerns about the CALTRANS method of computing column capacities is presented below.

The current CALTRANS approach for designing new bridge columns based on maximum ductility and force capacities is criticized in Duan and Cooper (1995). They assert that the current CALTRANS design approach of only considering section failure induced by lateral seismic forces in conjunction with P- $\Delta$  behavior is inadequate except in the case of short columns, which are unconditionally stable until failure. The authors state that the ultimate displacement,  $\Delta_u$ , is the displacement when either the section reaches its ultimate load-carrying capacity, ultimate curvature capacity, or suffers from a stability failure characterized by a 10% to 20% drop in lateral load capacity from the peak lateral load. When this definition, as opposed to the current CALTRANS approach of considering only strength limit states corresponding to confinement failure, was employed in the evaluation of three sample columns, it was found that the current approach overestimated lateral load capacity by 89%, 77%, and 144% while

simultaneously overestimating displacement ductility by 16%, 36%, and 182% for columns with a KL/r of 80, 95.8, and 212 respectively. This overestimation is due to the fact that the current CALTRANS load/displacement curves are constantly ascending curves until the prediction of failure and do not recognize the onset of instability in medium and long columns. This is evident in examining the overestimation of ductility vs. KL/r in which it can be seen from graphs presented in Duan and Cooper (1995) that as the column grows more slender, the CALTRANS values digress further away from the proposed method.

The assessment procedure based on the minimum performance criteria established in code documents and recognized design procedures is adequate as long as the procedures are deemed to be valid. As long as questions are raised about the inherent correctness of the design approaches themselves, questions will remain as to how current design philosophies can be used to assess the performance of retrofit specimens.

### **5.3 Numerical Assessment and Ranking of Alternatives**

One of the first tasks in this research, after collection of literature was substantially complete, was the development of an assessment technique. Although the minimum performance criteria approach was presented first in this section, the equation approach presented below was the first technique considered. This technique was first developed in the Fall of 1995 and was revisited and revised throughout this project.

The concept of a comprehensive assessment formula which would compute a numerical result, indicative of not only the performance of the individual test column, but of the retrofit technique as a whole, was a difficult task. In the end, the evaluation method presented below was abandoned for several reasons. First, most of the information required as input to the formula approach was not available in most research reports, or was completely unavailable. Secondly, there was concern over whether the equation approach would provide a meaningful assessment or just a number subject to interpretation. The equation approach is made more cumbersome in that it combines data that are for the most part unavailable or not easily related and combined. However, the equation approach, although abandoned, will be presented because it represents a valid conceptual framework for comprehensive evaluation of retrofit alternatives. The categories requiring examination as well as the individual variables in a particular equation are all important considerations that should be examined when evaluating the test results of a column retrofit or when considering a retrofit type in general. The significance of the equation approach is not that it is presently a workable solution but that it addresses many of the areas that one should consider when evaluating a retrofit alternative.

In developing an evaluation technique for the various retrofit methods, the following categories will be used in assessing the performance of the retrofit concepts.

- Structural Performance
- System Cost
- Environmental Performance
- Design Process

In addition to identifying the four major categories listed above, a weighting technique will be described so that the importance of structural performance, system cost, environmental performance, and known design processes can be quantified via a ranking equation. The sensitivity of these weights should be

investigated to examine what change in priorities among the four categories would be required to alter the outcome of the ranking equation.

Although the four categories previously listed are theoretically all of practical importance in evaluating the true desirability of a method, the majority of the published information on concrete column retrofit pertains solely to structural performance. For this reason, the structural performance quantification will be explored in greater depth than the other categories. Because of the lack of information in the other three major categories, the goal of a weighted analysis including the four major categories may be an unattainable one at this time.

### 5.3.1 Structural Performance

The criteria that were chosen to define structural performance are as follows.

#### 5.3.1.1 Capacity Increase, CI

$$CI = \frac{V_{retrofit}}{V_{as-built}} \quad (5-2)$$

This relationship quantifies the increase in column lateral load capacity due to the effect of the retrofit. It has been shown, however, that increasing the load-carrying capacity is not always desirable because of the deleterious effects this may have on footings which may be of inadequate capacity to accommodate the increased load capacity of the column. By increasing the capacity of a column section, one can shift the failure mode and failure location into the footing.

#### 5.3.1.2 Displacement Ductility Increase, DDI

$$DDI = \frac{\mu_{retrofit}}{\mu_{as-built}} \quad (5-3)$$

A common measure of column enhancement is through a comparison of the ductility of a retrofitted column with that of an "as-built" condition column. Ductility can theoretically be defined as the maximum attainable displacement divided by the displacement at first yield of the column reinforcing. This measurement should be modified, however, to a measurement known as the maximum usable ductility, to reflect the fact that at the maximum ductility level, the capacity of the retrofitted member may have been so degraded that it would no longer be capable of supporting the service dead and live loads.

#### 5.3.1.3 Number of Cycles to Failure, NC

The number of cycles to failure is a key measure of the survivability of a column during an earthquake. However, the following scenario should be considered in illustrating the fact that the number of cycles alone is inadequate in describing survivability and adequacy of a retrofitted column.

Scenario A: A reinforced concrete column is strengthened so that in a displacement controlled test to failure the column undergoes twelve cycles at a ductility level of 2.0 before failure.

Scenario B: A similar column is also tested in a displacement control fashion with two cycles at every increment of ductility from 1 through 6, i.e., two cycles at ductility = 1, 2, ..6.

A simple comparison would reveal that both columns underwent twelve cycles of loading before failure. The second column did so, however, under increasingly greater demands without failure. This disparity in the test conditions would seem to indicate a much higher performance level in the second test specimen. It is proposed that the number of cycles be adjusted so that this number actually represents the sum of the products of displacement times the number of cycles at a given displacement. For instance, the column discussed in scenario A would be rated as having undergone 6 cycles of ductility equal to 2 for a numerical rating of  $6(2) = 12$ . The column in scenario B would rate as  $2(1+2+3+4+5+6) = 42$ . Quantification of the adjusted number of cycles to failure can be incorporated into the term, NC.

#### 5.3.1.4 Hysteretic Energy Absorption, HEA

A key parameter in assessing the performance of a retrofit is the hysteretic energy absorption of the retrofit as compared to the "as-built" specimen. However, very few research reports and articles contain this information. In several steel jacket retrofit reports generated at UCSD and discussed in Section 2, a comparison of energy absorbed in the retrofit specimens and "as-built" specimens was made. Comparison was also made between the energy absorbed during the actual test cycle and in an equivalent elastic-plastic loop. Similar information comparing the energy absorption capacity of retrofit versus "as-built" specimens is presented in Coffman, Marsh, and Brown (1991), Coffman (1992), and Coffman, Marsh, and Brown (1993) in Section 4.2. This information is valuable but infrequently cited.

Caution against just using energy comparisons is presented in Taylor et al. (1996). He also analyzed damage characteristics in reinforced concrete bridge columns. In this document, the results of experimental testing of reinforced concrete bridge columns, designed to current California Department of Transportation requirements and subjected to traditional push-pull increasing ductility tests and random displacement tests, are compared. The results will be used to develop and refine damage models for bridge columns.

During the research, twelve 1/4 scale cantilever circular columns were constructed with an h/d ratio of 6,  $kl/r = 48$ , to ensure flexural failure. Columns were tested with a constant axial load simulating the effects of superstructure dead load. The main variable examined in the testing was the effect of the displacement pattern applied at the top of the column. In the first six tests, one pushover test was conducted, one standard cyclic increasing displacement test was conducted, and four tests of constant amplitudes of  $\mu_{\Delta} = \pm 2, 3, 4, \text{ and } 5$  were applied. In the other six columns, random inelastic displacements were applied to the columns with the displacement history being calculated through use of the computer program IDARC. A series of four or five events of varying magnitude were applied to each column. For example, in one column, two minor events were followed by a major event and then a severe event while another column was subjected to a major event, two minor events, and then a severe event.

In constant cycling of specimen 3 to  $\mu_{\Delta} = \pm 2$  for 150 cycles, no real damage or degradation of response was noted and the test was discontinued because no more useful information could be realized from this specimen. Specimen 6 was subjected to cycling at  $\mu_{\Delta} = \pm 5$  and lost nearly all strength and stiffness after only five cycles. Specimen 5, cycled to  $\mu_{\Delta} = \pm 4$ , had a gradual decrease in stiffness and strength during the nine cycles imposed during testing, but not as drastically and abruptly as specimen 6. Examination of the controlled displacement tests seemed to indicate that a threshold ductility of approximately  $\mu_{\Delta} = \pm 4$

served as the demarcation between long duration, stable, behavior, and very rapid failure. Subsequent examination of the random input tests confirmed this observation. A series of minor events with few cycles in excess of  $\mu_{\Delta} = \pm 2$  caused little to no damage, while a single earthquake with several cycles in excess of  $\mu_{\Delta} = \pm 4$  caused extensive damage. The threshold of  $\mu_{\Delta} = \pm 4$  was determined to apply only to columns tested in this program but it was surmised that similarly well detailed columns would have a threshold level which divides long and stable response from short, catastrophic response although it may not be  $\mu_{\Delta} = \pm 4$ .

Additional results from the simulated earthquake loading are as follows. Minor events seemed to have no real effect on the capacity of the columns. It was irrelevant whether a minor event occurred before or after a major event as the damage was essentially the same and attributable for the most part to the major event. Secondly, failure could be classified as belonging to two major categories: low cycle fatigue failure or confinement failure. Confinement failures were more common than low cycle fatigue failures. Because the displacement history was the only variable from test to test, it is, therefore, the reason for the different damage modes. Because the input motion so significantly impacts the failure mode and durability of the column, the need to conduct inelastic dynamic analysis using a variety of feasible input motions was emphasized for design purposes as opposed to use of a common input record. Preliminary analysis of the results indicates that cumulative fatigue damage models were accurate in describing the response of columns whose failure mode was due to low cycle fatigue. The columns that exhibit confinement failure were not well predicted and alternative models for confinement failure are being investigated.

Examination of the column test results indicated that cumulative dissipated energy, defined as the area enclosed by the hysteresis loops, is not a good predictor of failure. It was shown that the cumulative energy at failure as a function of the number of half cycles is dependant on the amplitude of the sawtooth wave of the cumulative energy plot. The standard displacement history test demonstrated a parabolically ascending cumulative energy dissipation due to the increasing nature of the applied ductility and was able to dissipate 79,000 J (58,267 lb-ft) of energy. Constant amplitude tests to  $\mu_{\Delta} = \pm 3$ , 4, and 5 dissipated 126,000 J (92,933 lb-ft), 85,000 J (62,693 lb-ft), and 57,000 J (42,041 lb-ft) of energy respectively. Because of the variable nature of earthquake-induced displacements, the use of cumulative energy alone was discouraged as a tool for assessing damage.

The results of these tests are only valid for circular columns of similar design dominated by flexure. Columns of other geometries or failure mode, i.e., shear, were not considered in the above study.

#### **5.3.1.5 Response Degradation, RD**

Response degradation can be addressed in conjunction with the ductility requirements listed above. As a column and column jacket undergo progressive damage through an increasing number of cycles and ductilities, theoretically, the force required to produce the second, third, etc., cycles to a given ductility become less. This lessening of the force required is a measure of the degradation of the column. As an alternate means of quantifying the RD for a column, one can compare the drop in lateral resistance from the peak resistance and the ductility that accompanies this resistance, to the maximum reduced resistance one will allow in a column and the corresponding ductility.

### 5.3.1.6 Comparison to Modern Designs, CMD

In addition to comparing the performance of a retrofitted column to one constructed thirty years ago, the retrofitted column should be at least on par with what is deemed to be acceptable performance using current codes and standards. The comparison between a retrofitted column and a recently designed column could be based on any of the criteria described in 5.3.1.1 through 5.3.1.5. This is a similar approach to the minimum performance method described in Section 5.2. For instance, some of the articles reviewed in this study have made reference to the New Zealand Building Code statements that a new column will be deemed adequate for design purposes if it can attain a ductility equal to 4 with no more than a 20% loss of axial load capacity. The TNZBM approach mentioned in Section 5.2 would also be an adequate benchmark for performance comparison.

### 5.3.1.7 Post-Earthquake Assessment, PEA

An important consideration in assessing the worthiness of a retrofit method is the ability to determine the condition of the retrofit and underlying column after an earthquake. Additionally, the ability to repair a retrofit versus replace the system entirely after an earthquake is a desirable characteristic. Limited information obtained during the literature review has suggested that upon removal of steel jackets from laboratory test specimens, the columns were found to be in good overall condition. Visual signs of distress were not uncommon in reviewing the test results. These outward signs of bulging in steel and composite jackets, horizontal splitting in composite jackets, etc., can be used as a visual indicator of columns that would have been damaged. Additionally, inspection of 114 jacketed columns following the Northridge earthquake revealed that the jackets and underlying columns were in good condition.

Combination of the terms presented in 5.3.1.1 through 5.3.1.6 into an equation is as shown below.

$$SP = \gamma_{CI}CI + \gamma_{DDI}DDI + \gamma_{NC}NC + \gamma_{HEA}HEA + \gamma_{RD}RD + \gamma_{CMD}CMD + \gamma_{PEA}PEA \quad (5-4)$$

The  $\gamma$  terms can be used to weight the individual terms so that they do not excessively influence the magnitude of SP. For instance, the CI and DDI terms will likely be numbers whose magnitude is less than 10, but the NC and HEA terms can be very large in magnitude and would significantly skew the results.

In addition to structural performance, other considerations enter into the decision to select one type of retrofit over another. The considerations are presented in subsections 5.3.2 to 5.3.4.

## 5.3.2 System Cost, SC

The system cost is composed of the following parameters.

### 5.3.2.1 Material Cost, MC

The initial cost of the retrofit material will be an important consideration for practicing engineers in determining the suitability of a given retrofit technique, or material type within a technique, to the column strengthening problem at hand. Some cost data has been supplied at this point via the questionnaire sent

to state bridge engineers, manufacturers, and others allied to the industry but is limited and applies to different retrofit types.

### **5.3.2.2 Labor and Equipment Cost, LEC**

The cost of the labor and equipment required to implement a given solution is important. Some of the techniques require heavy equipment and specially skilled personnel for proper installation. Other techniques, specifically the concrete jacketing and fusible hinge techniques, seem to necessitate closure of the bridge during rehabilitation, a system cost not measurable in dollars but in the inconvenience to a large number of motorists if the bridge is in or around a major city.

### **5.3.2.3 Long-Term Maintenance and Inspection Costs, MIC**

These costs may be the most difficult to estimate because there is no historical cost data available to judge the actual long-term expenditures associated with the various retrofit solutions.

### **5.3.2.4 Life-Cycle Cost, LCC**

The ultimate criteria for assessing the true cost of an option is to look at its life-cycle cost. The life-cycle cost should include, but is not limited to, the three major cost categories outlined above. Unfortunately, due to the newness of these retrofit techniques, this data will not exist for many years.

Combining the economic factors into a single equation leads to the following.

$$SC = \gamma_{MC}MC + \gamma_{LEC}LEC + \gamma_{MIC}MIC + \gamma_{LCC}LCC \quad (5-5)$$

The terms shown in the equation above refer to the major cost categories mentioned previously. The modifiers are there so that an individual or agency could use this type of equation to establish its own economic priorities. For instance, one might decide to weight materials, labor, and long-term maintenance and inspection cost equally, each with a weight of 1/3, while another agency might neglect these terms altogether and place the entire burden of economic evaluations on the life-cycle cost of the alternative. These cost categories will be difficult to quantify due to limited data.

## **5.3.3 Environmental Performance, EP**

The environmental performance of the retrofit techniques is a factor that must be taken into account. The performance of the techniques through environmental changes such as freeze and thaw cycles, alkali attacks, ultraviolet exposure, salt air exposure, industrial environment exposure, and other environmental exposures, is an important quantity in determining the overall merits of each system.

### **5.3.3.1 Ultraviolet Effect, UE**

The effect of ultraviolet radiation on a given retrofit method should be considered. It would likely only be a concern for the composite material methods.

### 5.3.3.2 Salt-Air Effect, SAE

The effect of long-term exposure of the retrofit methods to salt air should be considered. This is particularly important in coastal areas of the United States.

### 5.3.3.3 Freeze and Thaw Effect, FTE

The durability of the individual retrofit methods during numerous seasons of freeze and thaw cycling should be addressed during the assessment process.

### 5.3.3.4 Pollution Effect, PE

This category would represent the deleterious effect of common airborne pollutants found in major metropolitan areas on the performance and long-term viability of a particular technique.

### 5.3.3.5 Alkali Effect, AE

The susceptibility of the individual retrofit methods to alkali attack and other chemical attacks due to the use of deicing salts, reactive aggregates, etc., should be considered.

The combination of all of these components into an equation takes the following form.

$$EP = \gamma_{UE}UE + \gamma_{SAE}SAE + \gamma_{FTE}FTE + \gamma_{PE}PE + \gamma_{AE}AE \quad (5-6)$$

The environmental performance parameters listed in the above equation, along with their adjustable weighting factors, are not a comprehensive list of modifiers. Additionally, they apply to given geographic locations. The FTE term would not be a concern in Southern California but would certainly impact the design of a retrofit in Alaska more than the pollution effect. How one would actually quantify these effects is an issue and a shortcoming to their numerical evaluation.

## 5.3.4 Design Process, DP

The most important concept to a design engineer is confidence in their ability to design a retrofit technique using a clear design procedure. If a design engineer is to employ a particular retrofit technique, they will need to determine the amount and orientation of the retrofit material and also the predicted response of the newly strengthened column. Design methods have been proposed for both steel jacket and composite jacketed columns. These methods are based primarily on equations derived from test results and theoretical models of column behavior. However, some of the less frequently encountered retrofits have no method for predicting the response of a retrofitted column. If a design engineer has only the original research reports and papers as a reference, the engineer will likely disregard the method in question as a viable technique.

### 5.3.4.1 Process Knowledge, PK

The existence of a design procedure for implementing a particular strengthening technique will be key in determining whether the technique is given ample consideration by practitioners in the process of evaluating alternatives.

### 5.3.4.2 Quality of Information, QI

In addition to the existence of design information, researchers, more so than practitioners, need to critically evaluate the methodology employed in developing design equations, charts, and graphs for use by design engineers. If a procedure is based on limited information, that may be a consideration in not rating the procedure as highly as if it was the product of years of development by numerous independent sources.

The theoretical combination of these terms takes the following form.

$$DP = \gamma_{PK}PK + \gamma_{QI}QI \quad (5-7)$$

This equation takes into account the process knowledge and quality of information related to each individual technique. The weighting factors allow one to tailor the result to their judgment as to the importance of a standardized process or the quality of information used to develop the standardized design procedure.

### 5.3.5 Overall Rating

Finally, the overall rating of a technique is expressed as follows.

$$Rating = \beta_{SP}SP + \beta_{SC}SC + \beta_{EP}EP + \beta_{DP}DP \quad (5-8)$$

This equation should be tested for sensitivity. For instance, one may decide that the four areas considered by the equation should be equally weighted at 25%. Under these conditions retrofit A may be more favorable than retrofit B. It should be a topic of investigation to determine what change in the weights would be required to make B seem more favorable than A. This would be indicative of the change in priorities required to cause a change in the retrofit method given the highest ranking.

In this numerical approach, questions still exist about whether the actual computed quantities are meaningful. Additionally, authorities on the subject of seismic retrofit disagree on what defines some very basic concepts such as ultimate displacement, maximum load, and stability of response. If these definitions are still in flux, it seems short-sighted to base evaluation techniques on them.

## 5.4 Analytical Hierarchy Process Evaluation Technique

The development of a decision-making model based on the Analytical Hierarchy Process (AHP) technique is presented in El-Mikawi (1996). The reference demonstrates the use of a model that enhances an engineer's ability to make decisions and select retrofit alternatives on the basis of a number of criteria and weighing techniques. It specifically focused on composite retrofit materials and their application to infrastructure rehabilitation. The reference was published after much of the development work related to the derivation of a comprehensive evaluation technique presented in Section 5.3 was completed. The general format and categorization of important evaluation criteria is, however, very similar to the proposed model and provides additional justification that the format and goals of this proposed evaluation model are appropriate.

In the AHP approach, a problem is hierarchically structured so that the overall goal is subdivided into criteria, which are then divided into subcriteria, etc., until the most basic input information exists. Expert judgments are required of the user regarding many aspects of the decision process. Numerical input and subjective input are readily input into the process. Relative weights and priorities can be established and a measure on inconsistency is developed so that errors in model formulation can be established. The mathematical approach that the model uses is one that employs pairwise comparisons of multiple subcriteria with the criteria in the next highest level. The development of the computer models and hierarchies was carried out with the aid of Expert Choice software.

The goal of any AHP study is user defined. In El-Mikawi's study, the goal is the selection of an optimal technique for the repair of deteriorated bridge columns. Assessment criteria on which the AHP model was built are very similar to the comprehensive evaluation criteria presented in this report. The main criteria consist of structural performance indicators, economic indicators, environmental aspects, codes and regulations, material availability, and architectural aspects. Structural performance was divided into two subcriteria, corrosion resistance properties and seismic loading upgrade. These were further subdivided into ductility, strength, and stiffness.

Economic performance was divided into primary cost and secondary cost. Primary cost was further subdivided into initial cost, life expectancy, and maintenance requirements, while secondary cost was subdivided into availability of the structure and construction implementation and social impacts.

Environmental aspects consists of corrosion resistance properties, electro-magnetic and lightning properties, and fire retardancy and coefficient of thermal expansion.

Codes and regulations was divided into two subcriteria consisting of building code requirements and permit requirements.

Material availability focused on the two subcriteria that characterize whether the retrofit employs special materials not readily available or can be constructed with "off-the-shelf" construction materials.

Finally, architectural aspects focuses on whether it is important to preserve and retain the original shape of the member and whether confined construction areas will affect the selection of a retrofit technique.

Testing of the proposed method was based on a case study that endeavored to develop repair techniques for deteriorated and damaged bridge columns. The two retrofit alternatives were carbon fiber composite jackets and steel jackets. The study was based on ten reinforced concrete columns in the Washington, D.C., area with extensive cracking due to moisture, de-icing salts, exhaust fumes, and poor maintenance. The columns were 13.7 m (45 ft) tall and 1.5 m (4.9 ft) in diameter. The objective of the repair was to stop deterioration, protect the longitudinal steel, and provide additional vertical load capacity to the structure.

To conduct the economic analysis, the expected repair life was assumed to be 12 years for steel and 20 for the composite; the initial cost ratio was 1 for steel and 1.3 for carbon fiber; the maintenance cost ratio was 1 for steel and 0.25 for carbon; and construction duration was 6 months for steel and 3 months (2 for fabrication, 1 for construction) for carbon.

Five different structural engineering experts were selected for the study. The first expert had twenty years of experience in bridge repairs but limited knowledge of composites. The second expert, like the first, was experienced in bridge repair but had little experience in composite retrofit. The third expert was a university professor with 15 years of experience in structural engineering and was a pioneer in the use of composite material in civil engineering. Two other experts who work for the State of Virginia and Fairfax County were selected; they had 15 years of experience in bridge engineering with no prior knowledge in composites. All experts received approximately three hours of training on the model and the software. They were also provided a portable computer for model testing, which lasted approximately one hour.

Pairwise comparison of the six main criteria used in the study and examination of their influence on the goal resulted in the assignment of weights. The computer assigned weights were structural indicators, 34.7%; economic indicators, 36.0%; environmental aspects, 15.6%; codes and regulations, 8.2%; material availability, 3.3%; and architectural aspects, 2.1%. Most evaluators used these numbers along with experience and intuition to enter actual weights. The model generated an inconsistency ratio of 11% with 10% or lower being the preferred outcome. Having assigned relative weights to the main criteria, weighting of the subcriteria is carried out in a similar fashion. Results of the analysis indicates that the preference of composites over steel is approximately 2:1 with composites having a preference ranking of 63.9% and steel of 36.1%. The alternative with the highest ranking is the preferred alternative.

A sensitivity analysis of the results indicates the following. A change in the economic weight by  $\pm 10\%$  has no noticeable effect on outcome. A change in the structural weight by  $\pm 10\%$  has almost no effect. An increase in the environmental weight to 25% slightly enhances the favorability of composites, while decreasing the weight to 5% reduces the preference ranking of composites to 57%. The codes and regulations criteria weight was increased from 8.2% to 35% to achieve an equal ranking of composites and steel. The material availability weight was adjusted to 43% to achieve an equal ranking. The architectural aspects weight was increased by 10% with no real impact.

The final analysis of data indicates that the overall preference ranking of composites ranged from 56% to 74%, in all cases exceeding that of steel. Composites were consistently preferred over steel except in the individual criteria of codes and standards and material availability where steel would logically have an advantage. The model developed by El-Mikawi and the AHP process in general are a significant tool to compare multi-criteria problems in a manner that facilitates a sensitive investigation. This technique may provide the mathematical tool that allows the logical extension of the detailed evaluation criteria presented in Section 5.3 of this document from its present state as an ideal concept to a working analytical tool.



## SECTION 6 SUMMARY AND ISSUES FOR FURTHER STUDY

### 6.1 Task Summary

This report has presented the history of column retrofitting and presented a comprehensive review of the state-of-the-art in concrete column retrofitting. Three major sections were presented which reviewed numerous retrofit types as detailed in the literature. Another section detailed the problems encountered in trying to develop a comprehensive evaluation technique. Appendix A contains nearly 200 references compiled and summarized by type of information. A cross-reference list is also provided in Appendix A. The purpose of the cross-reference list is to allow the reader to find where in this document a particular bibliography entry is listed. Appendix B presents results of a survey sent to members of the transportation community to obtain information on current retrofit programs, state-supported research programs, design criteria, and systems being employed.

The general results of this literature review indicate that numerous retrofit techniques have been investigated in the laboratory. The results of these tests have been almost uniformly promising. There is very little to differentiate the performance of most of the retrofit techniques, especially when comparing the steel and composite jacket retrofits. They are equally adept at strengthening shear and flexurally deficient columns as well as providing confinement in plastic hinge regions so that stable ductile behavior can be obtained.

The most commonly applied retrofit in the field to date is steel jacketing. Disparities in United States and Japanese practice were noted with the Japanese seemingly constructing many more concrete jacket retrofits and composite retrofits than the United States. In addition, steel jackets in Japan are more likely to be rectangular in plan when applied to rectangular columns whereas in the United States, the columns are first made into oval shapes through field casting of a concrete overlay. With the exception of several journal articles of minor value, no useful information was obtained from Europe though numerous individuals and organizations were contacted.

The major contribution of this research has been the collection and review of pertinent literature and the presentation of an overview of a vast amount of information related to column retrofit. New information was catalogued and reviewed to within weeks of writing the final report. The only shortcoming was the inability to develop a comprehensive evaluation technique, although the conceptual framework for one was established. The use of the analytical hierarchy process discussed in Section 5.4 should be considered as a viable alternative in considering comprehensive evaluation tools.

### 6.2 Issues for Further Study

#### 6.2.1 Scale Effects

The vast majority of research on reinforced concrete bridge column in "as-built" and retrofit conditions applies to scale laboratory models. These models have typically been on the order of 10% to 40% of the prototype dimensions. It is not readily apparent that the "exact" same retrofit has been constructed on columns of varying dimensions to study the effects of scale. Of particular interest in the area of result scaling are a number of studies on composite wrap architecture and strengthening effectiveness as based on the results of compression tests on standard 150 mm x 305 mm (6 in. x 12 in.) concrete cylinders. The

literature shows that the effectiveness of the retrofit decreases as cylinder size increases and can logically be extrapolated to imply that the results of column tests would be much less promising than the cylinder test results.

### **6.2.2 Dynamic Effects**

Only a few references from Japan and Macrae, Priestley, and Seible (1994) incorporated actual dynamic input as the lateral load via hydraulic actuators. Most column retrofit tests have been conducted on specimens where the load is very gradually applied in a controlled fashion. The use of dynamic loads via shake tables or high-speed actuators would allow for the examination of dynamic response characteristics. These characteristics include not only force displacement responses but also damping properties inherent to "as-built" and retrofit specimens.

### **6.2.3 Standardized Testing**

Many researchers have conducted experiments in the area of column retrofitting both in the United States and abroad. Examination of the test results indicates that a great deal of variability exists in specimen design, load history, etc. For objective structural comparisons, the test results need to be placed on similar basis. Simple similitude relationships, such as post yield deformation in bridge columns, are generally considered inadequate for nonlinear behavior, and would therefore rule out this approach. A standardized test column and test procedure could be developed so that the results of the test could be used to evaluate the effect of the retrofit. However, such a scheme so that the results of the tests could be used to simply judge the effect of the retrofit, does not imply that this column would be representative of all local design differences. These standard tests should incorporate columns which are flexurally deficient due to inadequate seismic design forces, ductility deficient due to inadequate confinement and lap splice placement, and shear deficient due to improper design approaches (elastic behavior) and detailing practices.

### **6.2.4 Standardized Reporting**

The development of standardized methods of data acquisition and reporting of results should be considered along with the development of standardized tests. One of the great difficulties encountered in this research was deciding how to objectively rank the retrofit techniques. It was concluded that there was no feasible way to assign numerical rankings to even broad categories of retrofit techniques let alone each individual reference. This is partly due to inconsistent and incomplete data reporting. A desirable means of conducting a structural comparison of retrofits would include an assessment of the degree of strengthening provided, enhancement in ductility over "as-built" specimens, hysteretic energy dissipation, response degradation, and a comparison to the expected performance of a column designed by modern standards. Unfortunately, sporadic data presentation in many references, such as lack of data related to hysteretic energy dissipation during testing, renders ineffective the use of a comprehensive, formula-based comparison approach. In addition, even if two columns were shown to dissipate equivalent amounts of energy, for instance, the effects of scale, load history required to "fail" the column, and a number of other factors complicate even the interpretation of this individual term.

Additional inconsistencies lie in the reporting of ductility. Most references report ductility of columns based on ratios of the ultimate displacement and yield displacement at the load point. However, some references report curvature ductility of the plastic hinge region in lieu of displacement ductility. From a

design standpoint, the curvature ductility is the more meaningful term because it represents the true ductility demands on the hinge regions of the column. These rotational demands are issues that can be addressed through design. However, the more commonly reported displacement ductility represents not only the effects of column elastic bending and inelastic hinge rotation but also includes the influence of footing displacements and rotations.

### **6.2.5 Definition of Critical Parameters and Limit States**

In order to employ any standardized means of evaluation to all column retrofit reports, one must not only assure that the same type of information is reported in each test report but also must determine what the required information should be. Minimum performance criteria and limit states that differentiate between acceptable and unacceptable behavior should be defined. Examine, for instance, the seemingly simple matter of displacement ductility.

A complicating factor in determining ductility increase over an "as-built" specimen is what limit states should control the reporting of maximum ductility in the retrofit and "as-built" columns. In the case of the retrofit columns, use of a maximum ductility criteria that relates the maximum usable ductility capacity to some function of lateral load resistance degradation seems incomplete. For instance, a common approach to defining "failure" of a retrofit specimen is to define the ductility level where the column lateral strength has decreased to 80% of the maximum lateral strength,  $V_{max}$ , as the point where the retrofit is deemed to have failed. However, if all subsequent cycles require less resistance than the residual resistance of  $0.8V_{max}$ , the column may not fail unless the degradation continues regardless of load or ductility demands.

Further testing of columns could essentially duplicate the above scenario by loading a column to a predetermined ductility level rather than constantly increasing displacement levels until substantial lateral resistance decreases occur. At this point, smaller increments of displacement would be applied and testing of the column continued until a predetermined point. This may provide better insight into the performance of the retrofit in "real" earthquakes where the maximum displacement does not constantly increase. Information presented in Taylor et al. (1996), described previously in Section 5.3.1.4, is similar to this concept.

The definition of characterizing parameters and limit states for comparing retrofits is by no means limited to ductility but extends to all areas of performance where appropriate definition of what information to report and how to report it are key issues. Determining the necessary information to report and in what form will not be an easy undertaking, but is important as a decision-making tool for engineers and researchers trying to compare the effectiveness of disparate alternatives objectively.



## BIBLIOGRAPHY

- Aboutaha, Riyad Said, (1994), "Seismic Retrofit of Non-Ductile Reinforced Concrete Columns Using Rectangular Steel Jackets", Ph.D. Dissertation, University of Texas at Austin, 1994.
- Aboutaha, R.S., M. D. Engelhardt, James O. Jirsa and M. E. Kreger, (1994a), "Seismic Retrofit of R/C Columns Using Steel Jackets", ACI Symposium of Seismic Rehabilitation, 1994.
- Aboutaha, R.S., M. D. Engelhardt, James O. Jirsa and M. E. Kreger, (1994b), "Seismic Retrofit of R/C Columns with Inadequate Lap Splices", Structures Congress XII: Proceedings Structures Congress 94 in Atlanta, Georgia, by the American Society of Civil Engineers, 1994, pp. 1502-1507.
- Aboutaha, R.S., M. D. Engelhardt, James O. Jirsa and M. E. Kreger, (1994c), "Seismic Shear Strengthening of R/C Columns Using Rectangular Steel Jackets", Proceedings of the Fifth U. S. National Conference on Earthquake Engineering, Earthquake Engineering Research Institute, Oakland, CA, vol. 5, 1994, pp. 799-808.
- Adachi, Yukio, Kenji Kosa and Yasuo Murayama, (1994), "An Experimental Study on the Behavior of a Large Model Pier After Behavior", Second U.S.-Japan Workshop on Seismic Retrofit of Bridges by Public Works Research Institute (Japan) and Federal Highway Administration, January 20-21, 1994.
- Agarwal, Bhagwan A. and Lawrence J. Broutman, (1990), "Analysis and Performance of Fiber Composites", John Wiley and Sons, 1990.
- Akimoto, Taisuke, Hiraku Hakajima and Fukashi Kogure, (1990), "Seismic Strengthening of Reinforced Concrete Bridge Piers on Metropolitan Expressway", Proceedings of the First U.S.-Japan Workshop on Seismic Retrofit of Bridges, Tsukuba Science City, Japan, December 17-18, 1990, pp. 280-298.
- Alameddine, Fadel, (1996), "U.C.S.D. Tests of Columns with Carbon Fiber Jackets", What's Shakin'?, An Informal Information Memo by the Office of Earthquake Engineering, California Department of Transportation, March, 1996.
- Amari, Kenichi, Hisamitsu Hanno, Keizo Otsuka and Yoshiichi Fujimoto, (1994), "Seismic Reinforcement of Existing Reinforced Concrete Piers", Second U.S.-Japan Workshop on Seismic Retrofit of Bridges, by Public Works Research Institute (Japan) and Federal Highway Administration, January 20-21, 1994.
- Applied Technology Council, (1995a), "ATC-18 - Seismic Design Criteria for Bridges Current and Future", Applied Technology Council, 1995.
- Applied Technology Council, (1995b), "Draft for Comment - Seismic Design Criteria for Bridges and Other Highway Structures Current and Future", Applied Technology Council, 1995.
- Asnaashari, Ali, (1993), "Real World Challenges Experienced During Seismic Retrofit of the Santa Monica Viaduct", Proceedings of the Second Annual Seismic Research Workshop, California Department of Transportation, Division of Structures, Sacramento, CA, 1993.

Bavarian, Behzad, Jon Shively, Richard Ehgott and Roger Di Julio, (1996), "External Support of Concrete Structures Using Composite Materials", Fiber Composites in Infrastructure, Proceedings of the First International Conference on Composites in Infrastructure, Tucson, AZ, edited by M. R. Ehsani and H. Saadatmanesh, Department of Civil Engineering and Engineering Mechanics, University of Arizona, 15-17 January 1996, pp. 917-928.

Bernards, Laura L., David I. McLean and Edward H. Henley Jr, (1992), "Seismic Retrofitting of Rectangular Bridge Columns for Shear", Transportation Research Record 1371, Transportation Research Board, 1992, pp. 119-128.

Bett, B. John, Richard E. Klingner and James O. Jirsa, (1988), "Lateral Load Response of Strengthened and Repaired Reinforced Concrete Columns", ACI Structural Journal, September-October 1988, pp. 499-508.

Better Roads, (1993), "Seismic Retrofit Cuts Installation Costs", Better Roads, May 1993, p. 20.

Brown, Ski, (1992), "Fiber / Epoxy Composites Strengthen Bridge Columns", Materials: Performance and Prevention of Deficiencies and Failures, Proceedings of the Materials Engineering Congress, Atlanta, GA, edited by Thomas D. White, Materials Engineering Division of the American Society of Civil Engineers, August 10-12, 1992, pp. 691-695.

Buckland, Peter, (1995), "State-of-the-Art Seismic Design and Retrofit of Bridges in Canada", Proceedings, National Seismic Conference on Bridges and Highways, San Diego, CA, by Federal Highway Administration and California Department of Transportation, December 1995.

California Department of Transportation, (1990), "Seismic Design References", California Department of Transportation, 1990.

California Department of Transportation, (1995a), "CALTRANS' Seismic Retrofit Program Fact Sheet", California Department of Transportation, 1995.

California Department of Transportation, (1995b), "Construction Statistics 1995", California Department of Transportation, 1995.

California Department of Transportation, (1995c), "Memo to Designers 20-4, Earthquake Retrofit Guidelines for Bridges", California Department of Transportation, 1995.

California Department of Transportation, (1996a), "Pre-Qualification Requirements for Alternative Column Casings for Seismic Retrofit", California Department of Transportation, 1996.

California Department of Transportation, (1996b), "Seismic Safety Retrofit Program Chronology of Events", California Department of Transportation, 1996.

California Department of Transportation, (1996c), "Specification dated 3/6/1996 on Alternative Column Casing", California Department of Transportation, 1996.

California Department of Transportation, (1996d), "Standard Drawing Sheet XS-12-75, Composite Column Casing, dated 4/96", California Department of Transportation, 1996.

Casey, John, John Pohle, Kent Cordtz and Robert Jones, (1994), "Seismic Bridge Retrofit in California: A Case Study", Proceedings of the Fifth U. S. National Conference on Earthquake Engineering, Earthquake Engineering Research Institute, Oakland, CA, 1994, vol. 5, pp. 457-466.

Chai, Yuk Hon, M. J. Nigel Priestley and Frieder Seible, (1990), "Retrofit of Bridge Columns for Enhanced Seismic Performance", Proceedings of the First U.S.-Japan Workshop on Seismic Retrofit of Bridges, Tsukuba Science City, Japan, December 17-18, 1990, pp. 321-340.

Chai, Yuk Hon, M. J. Nigel Priestley and Frieder Seible, (1991a), "Flexural Retrofit of Circular Reinforced Bridge Columns by Steel Jacketing - COLRET - A Computer Program for Strength and Ductility Calculations. Report No. SSRP-91/05", Department of Applied Mechanics and Engineering Sciences, University of California, San Diego, 1991.

Chai, Yuk Hon, M. J. Nigel Priestley and Frieder Seible, (1991b), "Flexural Retrofit of Circular Reinforced Bridge Columns by Steel Jacketing - Experimental Studies. Report No. SSRP - 91/06", Department of Applied Mechanics and Engineering Sciences, University of California, San Diego, 1991.

Chai, Yuk Hon, M. J. Nigel Priestley and Frieder Seible, (1991c), "Seismic Retrofit of Bridge Columns by Steel Jacketing", Third Bridge Engineering Conference, Report: Transportation Research Record, 1290, vol. 2., Washington, D. C., 1991, pp. 95-103.

Chai, Yuk Hon, M. J. Nigel Priestley and Frieder Seible, (1991d), "Seismic Retrofit of Circular Bridge Columns for Enhanced Flexural Performance", ACI Structural Journal, vol 88, no. 5, September-October, 1991, pp. 572-584.

Chai, Yuk Hon, M. J. Nigel Priestley and Frieder Seible, (1994), "Analytical Model for Steel-Jacketed RC Circular Bridge Columns", Journal of Structural Engineering, vol. 120, no. 8, August, 1994, pp. 2358-2376.

Chajes, Michael J., Dennis R. Mertz, Theodore A. Thomson, Jr. and Cory A. Farschmann, (1994), "Durability of Composite Material Reinforcement", Infrastructure: New Materials and Methods of Repair, Proceedings of the Third Materials Engineering Conference, San Diego, California, Materials Engineering Division of the American Society of Civil Engineers, November 13-16, 1994, pp. 599-605.

Chang, G.A. and J. B. Mander, (1994a), "Seismic Energy Based Fatigue Damage Analysis of Bridge Columns: Part I - Evaluation of Seismic Capacity. Technical Report NCEER-94-0006", National Center for Earthquake Engineering Research, State University of New York at Buffalo, 1994.

Chang, G.A. and J. B. Mander, (1994b), "Seismic Energy Based Fatigue Damage Analysis of Bridge Columns: Part II - Evaluation of Seismic Demand. Technical Report NCEER-94-0013", National Center for Earthquake Engineering Research, State University of New York at Buffalo, 1994.

Chapman, Howard E, (1995), "Earthquake Resistant Bridges and Associated Highway Structures: Current New Zealand Practice", Proceedings, National Seismic Conference on Bridges and Highways,

San Diego, CA, Federal Highway Administration and California Department of Transportation, December 1995.

Civil Engineering, (1994), "Fiber Wraps Migrate East", Civil Engineering, July 1994.

Coffman, Harvey L., M. Lee Marsh and Collin B. Brown, (1991), "Seismic Durability of Retrofitted R.C. Columns", Washington State Department of Transportation, 1991.

Coffman, Harvey L, (1992), "Retrofitting of Reinforced Concrete Bridge Columns", Transportation Research Record 1371, Transportation Research Board.

Coffman, Harvey L., M. Lee Marsh and Collin B. Brown, (1993), "Seismic Durability of Retrofitted Reinforced-Concrete Columns", Journal of Structural Engineering, vol. 119, no. 5, May, 1993, pp. 1643-1661.

Concrete Reinforcing Steel Institute, (1994), "Performance of Reinforced Concrete Bridges in the Northridge Earthquake", Concrete Reinforcing Steel Institute, 1994.

Cooper, James D., Ian M. Friedland, Ian G. Buckle, Roland B. Nimis and Nancy McMullin Bobb, (1994), "The Northridge Earthquake: Progress Made, Lessons Learned in Seismic-Resistant Bridge Design", Public Roads, Summer, 1994, pp. 26-36.

Daily Journal of Commerce, Seattle, Washington, (1995), "New Process used for Seismic Upgrade", Daily Journal of Commerce, Seattle, Washington, 6 July 1995.

Darwish, I., M. Saiidi and D. Sanders, (1995a), "Experimental Study of Seismic Susceptibility of Tapered Bridge Column-Footing Connections. Report Number CCEER-95-5", Center for Civil Engineering Earthquake Research, University of Nevada, Reno, 1995.

Darwish, I., M. Saiidi and D. Sanders, (1995b), "Seismic Retrofit of R/C Bridge Columns with Inadequate Bar Anchorage in Footings", Proceedings, National Seismic Conference on Bridges and Highways, San Diego, CA, Federal Highway Administration and California Department of Transportation, December 1995.

Darwish, I., M. Saiidi and D. Sanders, (1996), "Seismic Retrofit of RC Oblong Tapered Bridge Columns with Inadequate Bar Anchorage in Columns and Footings. Report Number CCEER-96-3", Center for Civil Engineering Earthquake Research, University of Nevada, Reno, 1996.

Dokken, Richard A, (1995), "An Overview of Characteristics of 65 Seismically Retrofitted Highway Bridges in California", Proceedings, National Seismic Conference on Bridges and Highways, San Diego, CA, Federal Highway Administration and California Department of Transportation, December 1995.

Dristos, S. and K. Pilakoutas, (1994), "Repair/Strengthening Techniques for Structurally Damaged RC Columns", Proceedings of the Fifth U. S. National Conference on Earthquake Engineering, Earthquake Engineering Research Institute, Oakland, CA, 1994, vol. 5, pp. 667-676.

Duan, Lin and Thomas R. Cooper, (1995), "Displacement Ductility Capacity of Reinforced Concrete Columns", *Concrete International*, November, 1995, pp. 61-65.

El-Mikawi, Mohammed, (1996), "A Decision Making Model for Evaluation of the Use of Composite Materials in Bridge Repair Applications", *Fiber Composites in Infrastructure*, Proceedings of the First International Conference on Composites in Infrastructure, Tuscon, AZ, edited by M. R. Ehsani and H. Saadatmanesh, Department of Civil Engineering and Engineering Mechanics, University of Arizona, 15-17 January 1996, pp. 341-355.

Ersoy, Ugur, A. Tugrul Tankut and Ramadan Suleiman, (1993), "Behavior of Jacketed Columns", *ACI Structural Journal*, vol. 90, no. 3, May-June, 1993, pp. 288-293.

Faza, Salem S. and Hota V. S. GangaRao, (1994), "Fiber Composite Wrap for Rehabilitation of Concrete Structures", *Infrastructure: New Materials and Methods of Repair*, Proceedings of the Third Materials Engineering Conference, San Diego, California, Materials Engineering Division of the American Society of Civil Engineers, November 13-16, 1994, pp. 1135-1139.

Federal Highway Administration, (1995), "Seismic Retrofitting Manual for Highway Bridges", U.S. Department of Transportation, Federal Highway Administration, May, 1995.

Finch, William W., Michael J. Chajes, Dennis R. Mertz, Victor N. Kaliakin and Ahmad Faqiri, (1994), "Bridge Rehabilitation Using Composite Materials", *Infrastructure: New Materials and Methods of Repair*, Proceedings of the Third Materials Engineering Conference, San Diego, California, Materials Engineering Division of the American Society of Civil Engineers, November 13-16, 1994, pp. 1140-1147.

Fish, Bob and George L. Rowe, (1994), "Earthquake Retrofit of a California Bridge, Route 242/680 Separation", Proceedings of the Fifth U. S. National Conference on Earthquake Engineering, Earthquake Engineering Research Institute, Oakland, CA, 1994, vol. 5, pp. 901-910.

Frangou, M. and K. Pilakoutas, (1994), "Novel Technique for the Repair and Strengthening of RC Columns", Proceedings of the Fifth U. S. National Conference on Earthquake Engineering, Earthquake Engineering Research Institute, Oakland, CA, 1994, vol. 5, pp. 637-646.

Frangou, M., K. Pilakoutas and S. Dristos, (1995), "Structural Repair/Strengthening of RC Columns", *Construction and Building Materials*, 1995, vol. 9, no. 5, pp. 259-266.

Fuse, T., K. Okuta, K. Hiramatsu, T. Ozawa and N. Hara, (1992), "Cyclic Loading Tests of Reinforced Concrete Column Strengthened with Steel Tube", Proceedings of the Tenth World Conference on Earthquake Engineering, Rotterdam, ed. A. A. Balkema, 1992, vol. 9, pp. 5227-5233.

Fyfe, Edward R, (1994a), "New Concept for Wrapping Columns with a High Strength Fiber/Epoxy System", *Infrastructure: New Materials and Methods of Repair*, Proceedings of the Third Materials Engineering Conference, San Diego, California, Materials Engineering Division of the American Society of Civil Engineers, November 13-16, 1994, pp. 1156-1162.

Fyfe, Edward R, (1994b), "The High Strength FIBRWRAP System for Retrofitting Bridge and other Structure Columns", Proceedings of the Third Annual Seismic Research Workshop, California Department of Transportation, Division of Structures, 1994.

Fyfe, Edward R., (1995), "Testing and Field Performance of the High Strength Fiber Wrapping System", Structures Congress XIII: Proceedings Structures 95 in Boston, Massachusetts, by the American Society of Civil Engineers, 1995, pp. 603-606.

Fyfe, Edward R. and Santosh J. Kuruvilla, (1993), "Column Seismic Retrofit Using High Strength Fiber/Epoxy Jackets", Proceedings, Symposium on Practical Solutions for Bridge Strengthening and Rehabilitation, Des Moines, Iowa, April 5-6, 1993, pp. 117-122.

Fyfe, Edward R., Ronald J. Watson and Stewart C. Watson, (1996), "Long Term Durability of Composites Based on Field Performance and Laboratory Testing", Fiber Composites in Infrastructure, Proceedings of the First International Conference on Composites in Infrastructure, Tuscon, AZ, edited by M. R. Ehsani and H. Saadatmanesh, Department of Civil Engineering and Engineering Mechanics, University of Arizona, 15-17 January 1996, 982-995.

Gamble, W. L., N. M. Hawkins and I. I. Kaspar, (1995), "Seismic Retrofitting of Bridge Pier Columns", Proceedings, National Seismic Conference on Bridges and Highways, San Diego, CA, Federal Highway Administration and California Department of Transportation, December 1995.

Gamble, William L., Neil M. Hawkins and Iraj I. Kaspar, (1996), "Seismic Retrofitting Experience and Experiments in Illinois", Proceedings of the Fourth National Workshop on Bridge Research in Progress, Sponsored by the National Science Foundation, State University of New York, and National Center for Earthquake Engineering Research, 1996, pp. 247-250.

Gomez, Jose and Brian Casto, (1996), "Freeze-Thaw Durability of Composite Materials", Fiber Composites in Infrastructure, Proceedings of the First International Conference on Composites in Infrastructure, Tuscon, AZ, edited by M. R. Ehsani and H. Saadatmanesh, Department of Civil Engineering and Engineering Mechanics, University of Arizona, 15-17 January 1996, 947-955.

Haroun, Medhat A., Gererd C. Pardoen and Robin Shepherd, (1994), "Seismic Strengthening of Reinforced Concrete Bridge Pier Walls Designed to Old Standards", Second U.S.-Japan Workshop on Seismic Retrofit of Bridges, Public Works Research Institute (Japan) and Federal Highway Administration, January 20-21, 1994.

Hawkins, G. F., N. R. Patel and G. L. Steckel, (1995), "Failure Analysis of Highway Bridge Column Composite Overwraps", Proceedings, National Seismic Conference on Bridges and Highways, San Diego, CA, Federal Highway Administration and California Department of Transportation, December 1995.

Hawkins, G. F., N. R. Patel and G. L. Steckel, (1996), "Failure Analysis of Highway Bridge Column Composite Overwraps", Fiber Composites in Infrastructure, Proceedings of the First International Conference on Composites in Infrastructure, Tuscon, AZ, edited by M. R. Ehsani and H. Saadatmanesh, Department of Civil Engineering and Engineering Mechanics, University of Arizona, 15-17 January 1996, 1126-1140.

Hexcel Fyfe Co, (1995), "Tyfo S Fibrwrap System", San Diego, Hexcel Fyfe Co, 1995.

Hipley, Pat, (1996), "CALTRANS Composite Column Casing Design Assumptions to be used in Conjunction with Memo 20-4", What's Shakin'?, An Informal Information Memo by the Office of Earthquake Engineering, California Department of Transportation, March, 1996.

Hoppel, Christopher P. R., Travis A. Bogetti, John W. Gillespie Jr., I. Howie and Vistasp M. Karbhari, (1994), "Analysis of a Concrete Cylinder with a Composite Hoop Wrap", Infrastructure: New Materials and Methods of Repair, Proceedings of the Third Materials Engineering Conference, San Diego, California, Materials Engineering Division of the American Society of Civil Engineers, November 13-16, 1994, pp. 191-199.

Howie, I. and V. M. Karbhari, (1994), "Effect of Materials Architecture on Strengthening Efficiency of Composite Wraps for Deteriorating Columns in the North-East", Infrastructure: New Materials and Methods of Repair, Proceedings of the Third Materials Engineering Conference, San Diego, California, Materials Engineering Division of the American Society of Civil Engineers, November 13-16, 1994, pp. 199-206.

Imbsen and Associates, (1994), "Retrofit Details, FHWA Project 106", Imbsen and Associates, 1994.

Izuno, K. and T. Ohkawa, (1992), "Quantification of Repair Effect for RC Members Using Inelastic Earthquake Response Analysis", Proceedings of the Tenth World Conference on Earthquake Engineering, Rotterdam, ed. A. A. Balkema, 1992, vol. 9, pp. 5221-5226.

Japan Road Association, (1990), "Specifications for Highway Bridges, Part V: Seismic Design", 1990.

Japan Society of Civil Engineers, (1995), "Preliminary Report on The Great Hanshin Earthquake", Japan Society of Civil Engineers, 1995.

Jaradat, Omar A., David I. McLean and M. Lee Marsh, (1996), "Strength Degradation of Existing Bridge Columns", Proceedings of the Fourth National Workshop on Bridge Research in Progress, Sponsored by the National Science Foundation, State University of New York, and National Center for Earthquake Engineering Research, 1996, pp. 253-256.

Jin, L., H. Saadatmanesh and M. R. Ehsani, (1994), "Seismic Retrofit of Existing Reinforced Concrete Columns by Glass-Fiber Composites", Infrastructure: New Materials and Methods of Repair, Proceedings of the Third Materials Engineering Conference, San Diego, California, Materials Engineering Division of the American Society of Civil Engineers, November 13-16, 1994, pp. 758-763.

Karbhari, V. M., and D. A. Eckel II, (1994), "Effect of Cold Regions Climate on Composite Jacketed Concrete Columns", Journal of Cold Regions Engineering, vol. 8, no. 3, September, 1994, pp. 73-86.

Karbhari, V. M., D. A. Eckel II and G. C. Tunis III, (1993), "Strengthening of Concrete Column Stubs through Resin Infused Composite Wraps", Journal of Thermoplastic Composite Materials, vol. 6, April, 1993, pp. 92-107.

Karbhari, V. M. and D. J. Wilkins, (1993), "Development of Composite Materials and Technology for Use in Bridge Structures", Proceedings, Symposium on Practical Solutions for Bridge Strengthening and Rehabilitation, Des Moines, Iowa, April 5-6, 1993, pp. 211-220.

Katsumata, Hideo, Koza Kimura, Kensuke Yagi, Tsuneo Tanaka, Yoshiro Kobatake and Takeo Sawanobori, (1990), "Applications of Retrofit Method with Carbon Fiber for Existing Reinforced Concrete Structures", Proceedings of a Workshop on Evaluation, Repair, and Retrofit of Structures - U.S.-Japan Panel on Wind and Seismic Effects, UJNR, Gaithersburg, MD, U.S. Department of Commerce, ed. by James O. Jirsa, May 12-14, 1990, pp. 3.11.1 - 3.11.27.

Katsumata, Hideo, Yoshirou Kobatake and Toshikazu Takeda, (1988), "A Study on the Strengthening with Carbon Fiber for Earthquake Resistant Capacity of Existing Reinforced Concrete Columns", Proceedings of the Ninth World Conference on Earthquake Engineering, Tokyo-Kyoto, Japan, August 2-9, 1988, Vol. VII, pp. 517-522.

Kawashima, Kazuhiko, (1990), "Seismic Design, Seismic Strengthening and Repair of Highway Bridges In Japan", Proceedings of the First U.S.-Japan Workshop on Seismic Retrofit of Bridges, Tsukuba Science City, Japan, December 17-18, 1990, pp. 3-61.

Kawashima, Kazuhiko, (1991), "Present Earthquake Engineering Efforts to Mitigate Earthquake Hazards of Road Transportation Facilities in Japan", Public Works Research Institute, in "Recent Selected Publications at Earthquake Engineering Division, Public Works Research Institute", Tsukuba Science City, Japan, 1991, pp. 121-179.

Kawashima, Kazuhiko, (1995), "Impact of the Hanshin/Awaji, Japan, Earthquake on Seismic Design and Seismic Strengthening of Highway Bridges", Proceedings, National Seismic Conference on Bridges and Highways, San Diego, CA, Federal Highway Administration and California Department of Transportation, December 1995.

Kawashima, Kazuhiko and Shigeki Unjoh, (1992), "Seismic Strengthening and Retrofitting of Highway Bridges in Japan", Public Works Research Institute, in "Recent Selected Publications at Earthquake Engineering Division, Public Works Research Institute (No. 2)", Tsukuba Science City, Japan, 1992, pp. 93-113.

Kawashima, Kazuhiko, Shigeki Unjoh and Hiroyuki Iida, (1990), "Seismic Inspection and Seismic Strengthening of Reinforced Concrete Bridge Piers with Termination of Main Reinforcement at Mid-Height", Proceedings of the First U.S.-Japan Workshop on Seismic Retrofit of Bridges, Tsukuba Science City, Japan, December 17-18, 1990, pp. 251-279.

Kawashima, Kazuhiko, Shigeki Unjoh and Hiroyuki Iida, (1991), "Seismic Inspection and Seismic Strengthening of Highway Bridges in Japan", Public Works Research Institute, in "Recent Selected Publications at Earthquake Engineering Division, Public Works Research Institute", Tsukuba Science City, Japan, 1991, pp. 285-318.

Kawashima, Kazuhiko, Shigeki Unjoh and Hiroyuki Iida, (1992), "Seismic Inspection and Seismic Strengthening of Highway Bridges in Japan", NIST Special Publication 840, Proceedings of the 4th

U.S.-Japan Workshop on Earthquake Disaster Prevention for Lifeline Systems, Los Angeles, California, edited by Ronald T. Equchi, August 19-21, 1991, pp. 91-123.

Kawashima, Kazuhiko, Shigeki Unjoh and Hidetoshi Mukai, (1994), "Seismic Strengthening of Highway Bridges", Second U.S.-Japan Workshop on Seismic Retrofit of Bridges, Public Works Research Institute (Japan) and Federal Highway Administration, January 20-21, 1994.

Koga, Masajiro, Hiroshi Uragami, Masahiko Uemura and Tokitaro Hoshijima, (1994), "Rehabilitation and Strengthening of Concrete Structures with Carbon Fiber", Proceedings - 10th U.S. - Japan Bridge Engineering Workshop. Design, Modeling, Experimentation, and Performance. UJNR, U.S. - Japan Panel on Wind and Seismic Effects, Lake Tahoe, Nevada, ed. Bruce M. Douglas and E. "Manos" Maragakis, Sponsored by: National Science Foundation, Federal Highway Administration, National Institute of Standards and Technology and University of Nevada, Reno, May 10-11, 1994, pp. 305-319.

Li, M. W., H. Saadatmanesh and M. R. Ehsani, (1992), "Behavior of Externally Confined Concrete Columns", Materials: Performance and Prevention of Deficiencies and Failures, Proceedings of the Materials Engineering Congress, Atlanta, GA, edited by Thomas D. White, Materials Engineering Division of the American Society of Civil Engineers, August 10-12, 1992, pp. 677-690.

Lin, Yongqian, William L. Gamble and Neil M. Hawkins, (1994), "Report to ILLDOT for Testing of Bridge Piers, Poplar Street Bridge Approaches, East St. Louis, IL", Department of Civil Engineering, University of Illinois at Urbana-Champaign, 1994.

Lwin, M. M. and E. H. Henley, Jr., (1993), "Bridge Seismic Retrofit Program Report", Washington State Department of Transportation, 1993.

Macrae, Gregory A., M. J. Nigel Priestley and Frieder Seible, (1994), "Shake Table Tests of Twin-Column Bridge Bents", Proceedings of the Third Annual Seismic Research Workshop, California Department of Transportation, Division of Structures, 1994.

Maffei, Joe, (1996), "The Seismic Evaluation and Retrofitting of Bridges", Department of Civil Engineering, University of Canterbury, Christchurch, New Zealand, 1996.

Mahin, Stephen A, (1991), "Overview of Berkeley Research and Proof Tests of Double Deck Viaduct Retrofits; Column Retrofit Tests", Proceedings of the First Annual Seismic Research Workshop, California Department of Transportation, Division of Structures, December 3-4, 1991, pp. 167-176.

Mander, J. B. and S. S. Chen, (1994), "Seismic Retrofit Procedures for Reinforced Concrete Bridge Piers in the Eastern United States", Second U.S.-Japan Workshop on Seismic Retrofit of Bridges, Public Works Research Institute (Japan) and Federal Highway Administration, January 20-21, 1994.

Mander, J. B. and C-T. Cheng, (1995), "Replaceable Hinge Detailing for Bridge Columns", Proceedings, National Seismic Conference on Bridges and Highways, San Diego, CA, Federal Highway Administration and California Department of Transportation, December 1995.

Mander, J. B., M. J. N. Priestley and R. Park, (1988a), "Observed Stress-Strain Behavior of Confined Concrete", Journal of Structural Engineering, vol 114, no. 8, August, 1988, pp. 1827-1849.

Mander, J. B., M. J. N. Priestley and R. Park, (1988b), "Theoretical Stress-Strain Model for Confined Concrete", *Journal of Structural Engineering*, vol 114, no. 8, August, 1988, pp. 1804-1826.

Matsuda, Tetsuo, Hiroshi Fujiwara and Yorimasa Higashida, (n.d.), "Aseismic Strengthening of Reinforced Concrete Bridge Piers Using Carbon Fibers - Analysis Based on Loading Tests Results", *Institute of Japan Highway Public Corporation*, vol. 28, (n.d.).

Matsuda, Tetsuo, Takashi Sato, Hiroshi Fujiwara, Norimasa Higashida, (1990), "Effect of Carbon Fiber Reinforcement as a Strengthening Measure for Reinforced Concrete Bridge Piers", *Proceedings of the First U.S.-Japan Workshop on Seismic Retrofit of Bridges*, Tsukuba Science City, Japan, December 17-18, 1990, pp. 356-374.

Matsuura, Yasuo, Ippei Nakamura and Hiroshi Sekimoto, (1990), "Seismic Strengthening Method for Reinforced Concrete Bridge Piers on Hanshin Expressway", *Proceedings of the First U.S.-Japan Workshop on Seismic Retrofit of Bridges*, Tsukuba Science City, Japan, December 17-18, 1990, pp. 299-317.

McConnell, Vicki P, (1993), "Bridge column retrofit, Hybrid woven unifabric", *High-Performance Composites*, September/October 1993, p. 62.

McLean, David I. and Laura L. Bernards, (1992), "Seismic Retrofitting of Rectangular Bridge Column for Shear", WA-RD 255.1, Washington State Department of Transportation, 1992.

Mirmiran, Amir, Moshen Kargahi, Michael Samaan and Moshen Shahway, (1996), "Composite FRP-Concrete Column with Bi-Directional External Reinforcement", *Fiber Composites in Infrastructure*, *Proceedings of the First International Conference on Composites in Infrastructure*, Tuscon, AZ, edited by M. R. Ehsani and H. Saadatmanesh, Department of Civil Engineering and Engineering Mechanics, University of Arizona, 15-17 January 1996, pp. 888-903.

Mirmiran, Amir, and Moshen Shahawy, (1995), "A Novel FRP-Concrete Composite Construction for the Infrastructure", *Structures Congress XIII: Proceedings Structures 95 in Boston, Massachusetts*, by the American Society of Civil Engineers, 1995, pp. 1663-1666.

Mitchell, Dennis, Robert Sexsmith and René Tinawi, (1994), "Seismic Retrofitting Techniques for Bridges - a State-of-the Art Report", *Canadian Journal of Civil Engineering*, vol. 21, October, 1994, pp. 823-835.

Mitsubishi Chemical Corporation, (n.d.), "Examples of Reinforcement and Repair Work Using REPLARK", Mitsubishi Chemical Corporation, Tokyo, n.d.

Nanni, Antonio and Michael S. Norris, (1995), "FRP Jacketed Concrete under Flexure and Combined Flexure-Compression", *Construction and Building Materials*, vol. 9, no. 5, 1995, pp. 273-281.

NCF Industries, (n.d.), "SnapTite Composite Column Reinforcement System", Long Beach, NCF Industries, Inc.

Noori, P. and M. Saiidi, (1993), "Seismic Retrofit of a Viaduct in Sparks, Nevada", Proceedings, Symposium on Practical Solutions for Bridge Strengthening and Rehabilitation, Des Moines, Iowa, April 5-6, 1993, pp. 275-283.

Ogata, Norio, Yoshifumi Maeda and Hirofumi Andoh, (1994), "Tests and Research on Carbon Fiber Strengthening of Existing Bridges", Second U.S.-Japan Workshop on Seismic Retrofit of Bridges, Public Works Research Institute (Japan) and Federal Highway Administration, January 20-21, 1994.

Ogata, Norio, Yoshifumi Maeda, Akira Murayama, Hirofumi Andoh, Yoshirou Kobatake and Satoru Ohno, (1993), "Earthquake Resistant Capacity of RC Pier Retrofitted with Carbon Fibre", Proceedings of the Ninth U.S. - Japan Bridge Engineering Workshop, Technical Memorandum of PWRI no. 3230, Public Works Research Institute, Tsukuba Science City, Japan, May 10-11, 1993, pp. 385-399.

Ohuchi, H., S. Ohno, H. Katsumata, Y. Kobatake, T. Meta, K. Yamagata, Y. Inokuma and N. Ogata, (n.d.), "Seismic Strengthening Technique for Existing Bridge Columns with CFRP", Technical Research Institute, Obayashi Corporation, Tokyo and Japan Highway Public Corporation, n.d., pp. 495-514.

Okamoto, Tadashi, Masaharu Tanigaki, Minoru Oda and Akira Asakuru, (1994), "Shear Strengthening of Existing Reinforced Concrete Column by Winding with Aramid Fiber", Second U.S.-Japan Workshop on Seismic Retrofit of Bridges, Public Works Research Institute (Japan) and Federal Highway Administration, January 20-21, 1994.

Ono, Yuji, Manabu Kaneko, Tadayuki Shirono, Masashi Sato and Toshio Yamauchi, (1994), "Methods of Restoring Bridges Damaged in the Kushiro Offshore Earthquake of January 1993 and the Southwest Hokkaido Offshore Earthquake of July 1993", Second U.S.-Japan Workshop on Seismic Retrofit of Bridges, Public Works Research Institute (Japan) and Federal Highway Administration, January 20-21, 1994.

Picher, F., P. Rochette and P. Labossière, (1996), "Confinement of Concrete Cylinders with GFRP", Fiber Composites in Infrastructure, Proceedings of the First International Conference on Composites in Infrastructure, Tuscon, AZ, edited by M. R. Ehsani and H. Saadatmanesh, Department of Civil Engineering and Engineering Mechanics, University of Arizona, 15-17 January 1996, pp. 829-841.

Priestley, M. J. Nigel, Ed Fyfe and Frieder Seible, (1991), "Column Retrofit Using Fiberglass/Epoxy Jackets", Proceedings of the First Annual Seismic Research Workshop, California Department of Transportation, Division of Structures, December 3-4, 1991, pp. 217-224.

Priestley, M. J. N and Frieder Seible, (1991), "Research into Seismic Retrofit of Reinforced Concrete Bridge Columns", Pacific Conference on Earthquake Engineering, New Zealand, 20-23 November, 1991, pp. 335-346.

Priestley, M. J. N and Frieder Seible, (1992), "Research into Seismic Retrofit of Reinforced Concrete Bridge Columns", Bulletin of the New Zealand National Society for Earthquake Engineering, vol. 25, no. 3, September, 1992, pp. 203-210.

Priestley, M. J. N and Frieder Seible, (1995), "Design of Seismic Retrofit Measures for Concrete and Masonry Structures", Construction and Building Materials, vol. 9, no. 6, 1995, pp. 365-377.

Priestley, M. J. N., F. Seible and G. M. Calvi, (1996) "Seismic Design and Retrofit of Bridges", John Wiley and Sons, 1996.

Priestley, M. J. Nigel, Frieder Seible and Y. H. Chai, (1992a), "Design Guidelines for Assessment Retrofit and Repair of Bridges for Seismic Performance. Report No. SSRP - 92/01", Department of Applied Mechanics and Engineering Sciences, University of California, San Diego, 1992.

Priestley, M. J. Nigel, Frieder Seible and Y. H. Chai, (1992b), "Seismic Retrofit of Bridge Columns Using Steel Jackets", Proceedings of the Tenth World Conference on Earthquake Engineering, Rotterdam, ed. A. A. Balkema, 1992, vol. 9, pp. 5285-5290.

Priestley, M. J. Nigel, Frieder Seible, Y. H. Chai and Z. L. Sun, (1991), "Flexural Retrofit of Bridge Columns by Steel Jacketing", Proceedings of the First Annual Seismic Research Workshop, California Department of Transportation, Division of Structures, December 3-4, 1991, pp. 203-208.

Priestley, M. J. Nigel, Frieder Seible and Ed Fyfe, (1994), "Column Seismic Retrofit Using Fiberglass/Epoxy Jackets", San Diego, Hexcel Fyfe Co, 1994.

Priestley, M. J. Nigel, Frieder Sieble, R. Verma and Y. Xiao, (1993), "Seismic Shear Strength for Reinforced Concrete Columns. Report No. SSRP - 93/06", Department of Applied Mechanics and Engineering Sciences, University of California, San Diego, 1993.

Priestley, M. J. Nigel, Frieder Sieble, Y. Xiao and R. Verma, (1991), "Shear Retrofit of Bridge Columns by Steel Jacketing", Proceedings of the First Annual Seismic Research Workshop, California Department of Transportation, Division of Structures, December 3-4, 1991, pp. 209-216.

Priestley, M. J. Nigel, Frieder Seible, Yan Xiao, and Ravindra Verma, (1994a), "Steel Jacket Retrofitting of Reinforced Concrete Columns for Enhanced Shear Strength - Part 1: Theoretical Considerations and Test Design", ACI Structural Journal, vol. 91, no. 4, July-August, 1994, pp. 394-405.

Priestley, M. J. Nigel, Frieder Seible, Yan Xiao, and Ravindra Verma, (1994b), "Steel Jacket Retrofitting of Reinforced Concrete Columns for Enhanced Shear Strength - Part 2: Test Results and Comparison with Theory", ACI Structural Journal, vol. 91, no. 5 (September-October): 537-551.

Priestley, M. J. Nigel, Ravindra Verma and Yan Xiao, (1993), "Shear Strength of Reinforced Concrete Bridge Columns", Proceedings of the Second Annual Seismic Research Workshop, California Department of Transportation, 1993.

Public Works Research Institute, (1991), "Recent Selected Publications at Earthquake Engineering Division, Public Works Research Institute", Tsukuba Science City, Japan, Public Works Research Institute, 1991.

Public Works Research Institute, (1993), "Recent Selected Publications at Earthquake Engineering Division, Public Works Research Institute (No. 2)", Public Works Research Institute, Japan, 1993.

Ricles, James, Yueh-Shiun Yang and M. J. Nigel Priestley, (1994), "Seismic Response and Retrofitting of Non-Ductile Reinforced Concrete Bridges", Structures Congress XII: Proceedings Structures Congress 94 in Atlanta, Georgia, by the American Society of Civil Engineers, 1994, pp. 1226-1231.

Roberts, James E, (1991), "Recent Advances in Seismic Design and Retrofit of Bridges", Third Bridge Engineering Conference, Report: Transportation Research Record, 1290, vol. 2., 1991, pp. 75-79.

Rodriguez, Mario and Robert Park, (1992), "Seismic Load Tests on Reinforced Concrete Columns Strengthened by Jacketing", University of Canterbury, New Zealand, Department of Civil Engineering, 1992.

Rodriguez, Mario and Robert Park, (1994), "Seismic Load Tests on Reinforced Concrete Columns Strengthened by Jacketing", ACI Structural Journal, vol. 91, no. 2 March-April, 1994, pp. 150-159.

Saadatmanesh, Hamid, (1994), "Fiber Composites for New and Existing Structures", ACI Structural Journal, vol. 91, no. 3, May-June, 1994, pp. 346-354.

Saadatmanesh, Hamid, Mohammad R. Ehsani and Limin Jin, (n.d.), "Seismic Strengthening of Reinforced Concrete Bridge Columns", Department of Civil Engineering and Engineering Mechanics, The University of Arizona, n.d..

Saadatmanesh, Hamid, Mohammad R. Ehsani and Limin Jin, (1996a), "Behavior of Concrete Columns Retrofitted with Fiber Composite Straps under Cyclic Loading", Fiber Composites in Infrastructure, Proceedings of the First International Conference on Composites in Infrastructure, Tuscon, AZ, edited by M. R. Ehsani and H. Saadatmanesh, Department of Civil Engineering and Engineering Mechanics, University of Arizona, 15-17 January 1996, pp. 842-857.

Saadatmanesh, H., Mohammad R. Ehsani and Limin Jin, (1996b), "Seismic Strengthening of Circular Bridge Pier Models with Fiber Composites", ACI Structural Journal, November-December, 1996, pp. 639-647.

Saadatmanesh, Hamid, Mohammad R. Ehsani and Mu-Wen Li, (1992), "Strengthening of Concrete Columns with Fiber Composites", Department of Civil Engineering and Engineering Mechanics, The University of Arizona, 1992.

Saadatmanesh, Hamid, Mohammad R. Ehsani and Mu-Wen Li, (1994), "Strength and Ductility of Concrete Columns Externally Reinforced with Fiber Composite Straps", ACI Structural Journal, vol. 91, no. 4, July-August, 1994, pp. 434-447.

Sanders, David H., Bruce M. Douglas and Kurt Cornell, (1993), "Retrofitting of Reinforced Concrete Beam-Column Joints in Moderately Active Seismic Regions", Proceedings, Symposium on Practical Solutions for Bridge Strengthening and Rehabilitation, Des Moines, Iowa, April 5-6, 1993, pp. 313-321.

Seible, F., G. A. Hegemier, M. J. N. Priestley and D. Innamorato, (1994a), "Seismic Retrofitting of Squat Circular Bridge Piers with Carbon Fiber Jackets", Advanced Composites Technology Transfer Consortium Report No. ACTT-94/04, University of California, San Diego, November 1994.

Seible, F., G. A. Hegemier, M. J. N. Priestley, D. Innamorato, D. Weeks and F. Policelli, (1994b), "Carbon Fiber Jacket Retrofit Test of Circular Shear Bridge Column, CRC-2", Advanced Composites Technology Transfer Consortium Report No. ACTT-94/02, University of California, San Diego, September 1994.

Seible, F., G. A. Hegemier, M. J. N. Priestley, F. Ho and D. Innamorato, (1995a), "Rectangular Carbon Jacket Retrofit of Flexural Column with 5% Continuous Reinforcement", Advanced Composites Technology Transfer Consortium Report No. ACTT-95/03, University of California, San Diego, April 1995.

Seible, F., G. A. Hegemier, M. J. N. Priestley and D. Innamorato, (1995b), "Developments in Bridge Column Jacketing using Advanced Composites", Proceedings, National Seismic Conference on Bridges and Highways, San Diego, CA, Federal Highway Administration and California Department of Transportation, December 1995.

Seible, F., G. A. Hegemier, M. J. N. Priestley and D. Innamorato, (1995c), "Rectangular Carbon Fiber Jacket Retrofit Test of a Shear Column with 2.5% Reinforcement", Advanced Composites Technology Transfer Consortium Report No. ACTT-95/05, University of California, San Diego, July 1995.

Seible, F., G. A. Hegemier, M. J. N. Priestley, D. Innamorato, and F. Ho, (1995d), "Carbon Fiber Jacket Retrofit Test of Circular Flexural Columns with Lap Spliced Reinforcement", Advanced Composites Technology Transfer Consortium Report No. ACTT-95/04, University of California, San Diego, June 1995.

Seible, F., G. A. Hegemier, M. J. N. Priestley, D. Innamorato, and F. Ho, (1995e), "Carbon Fiber Jacket Retrofit Test of Rectangular Flexural Column with Lap Spliced Reinforcement", Advanced Composites Technology Transfer Consortium Report No. ACTT-95/02, University of California, San Diego, March 1995.

Seible, Frieder and M. J. N. Priestley, (1993a), "Retrofit of Rectangular Flexural Columns with Composite Fiber Jackets", Proceedings of the Second Annual Seismic Research Workshop, California Department of Transportation, Division of Structures, 1993.

Seible, Frieder and M. J. N. Priestley, (1993b), "Strengthening of Rectangular Bridge Columns for Increased Ductility", Proceedings, Symposium on Practical Solutions for Bridge Strengthening and Rehabilitation, Des Moines, Iowa, April 5-6, 1993, pp. 239-248.

Seible, F., M. J. N. Priestley, and D. Innamorato, (1995), "Earthquake Retrofit of Bridge Columns with Continuous Carbon Fiber Jackets - Volume II, Design Guidelines", Advanced Composites Technology Transfer Consortium Report No. ACTT-95/08, University of California, San Diego, August 1995.

Seqad Consulting Engineers, (1992), "Rectangular Shear Column Tests, Preliminary Report Prepared for Fyfe Associates, Inc.", Seqad Consulting Engineers, 1992.

Seqad Consulting Engineers, (1993), "Repair of Shear Column Using Fiberglass/Epoxy Jacket and Epoxy Injection, Final Report Prepared for Hexcel Fyfe, Co.", Seqad Consulting Engineers, 1993.

Serroels, Christopher J., (1993), "Seismic Retrofit of the Sutterville Road Overhead", Proceedings Symposium on Practical Solutions for Bridge Strengthening and Rehabilitation, Des Moines, Iowa, April 5-6, 1993, pp. 153-161.

Shirolé, A. M. and A. H. Halik, (1993), "Seismic Retrofitting of Bridges in New York State", Proceedings Symposium on Practical Solutions for Bridge Strengthening and Rehabilitation, Des Moines, Iowa, April 5-6, 1993, pp. 123-131.

Shkurti, Fatjon P., Yongqian Lin, William L. Gamble and Neil M. Hawkins, (1995), "Testing of Bridge Piers, Poplar Street Bridge Approach, East St. Louis, IL. A Report to Illinois Department of Transportation, Revised November 1995", Department of Civil Engineering, University of Illinois at Urbana-Champaign, 1995.

Stanton, Gregory A. MacRae and Kirk J. Nosh, (1996), "Carbon Fiber Retrofit of Poorly Confined Square Reinforced Concrete Columns Subjected to Large Axial Forces", Proceedings of the Fourth National Workshop on Bridge Research in Progress, Sponsored by the National Science Foundation, State University of New York, and National Center for Earthquake Engineering Research, 1996, pp. 265-268.

Sultan, Moshen, Gary Hawkins and Li-Hong Sheng, (1995), "Caltrans Program for the Evaluation of Fiber Reinforced Plastics for Seismic Retrofit and Rehabilitation of Structures", Proceedings, National Seismic Conference on Bridges and Highways, San Diego, CA, Federal Highway Administration and California Department of Transportation, December 1995.

Sun, Y. P. and K. Sakino, (1992), "Flexural Behavior of Reinforced Concrete Columns in Square Steel Tube", Proceedings of the Tenth World Conference on Earthquake Engineering, Rotterdam, ed. A. A. Balkema, 1992, vol. 8, pp. 4365-4370.

Sun, Z., Frieder Seible and M. J. Nigel Priestley, (1993a), "Diagnostics and Retrofit of Rectangular Bridge Columns for Seismic Loads - Theoretical Studies. Report No. SSRP - 93-07", Department of Applied Mechanics and Engineering Sciences, University of California, San Diego, 1993.

Sun, Z., Frieder Seible and M. J. Nigel Priestley, (1993b), "Flexural Retrofit of Rectangular Reinforced Concrete Bridge Columns by Steel Jacketing. Report No. SSRP - 93/01", Department of Applied Mechanics and Engineering Sciences, University of California, San Diego, 1993.

Tankut, A. T. and U. Ersoy, (1991), "Behaviour of Repaired/Strengthened Reinforced Concrete Structural Members", Evaluation and Rehabilitation of Concrete Structures and Innovations in Design, Proceedings ACI International Conference, Hong Kong, ACI SP-128, vol. II, 1991, pp. 1257-1276.

Taylor, Andrew W. and William C. Stone, (1993), "Jacket Thickness Requirements for Seismic Retrofitting of Circular Bridge Columns", Proceedings Symposium on Practical Solutions for Bridge Strengthening and Rehabilitation, Des Moines, Iowa, April 5-6, 1993, pp. 249-258.

Taylor, Andrew, Ashraf El-Bahy, Sashi Kunnath and William Stone, (1996), "Modeling Seismic Demand of Circular Reinforced Concrete Bridge Columns", Proceedings of the Fourth National Workshop on

Bridge Research in Progress, Sponsored by the National Science Foundation, State University of New York, and National Center for Earthquake Engineering Research, 1996, pp. 115-118.

Tsubouchi, Toshikazu, Kenji Ohashi and Kazushige Arakawa, (1990), "Large Earthquake Countermeasures for Bridge Substructures of the Tomei Expressway", Proceedings of the First U.S.-Japan Workshop on Seismic Retrofit of Bridges, Tsukuba Science City, Japan, December 17-18, 1990, pp. 223-247.

Turkington, D. H., J. C. Wilson and D. W. Kennedy, (1991), "Seismic Assessment and Retrofit Design for the Vancouver Oak Street Bridge", Pacific Conference on Earthquake Engineering, New Zealand, 20-23 November, 1991, pp. 311-322.

Uji, Kimitaka, (n.d.), "The Earthquake Resisting Performance of Existing Reinforced Concrete Members with Sheet Type Carbon Fiber Reinforcement", n.p., n.d.

University of California, San Diego, (UCSD), (1991), "Seismic Assessment and Retrofit of Bridges", edited by M. J. Nigel Priestley and Frieder Seible, Department of Applied Mechanics and Engineering Sciences, University of California, San Diego, 1991.

Unjoh, S. and K. Kawashima, (1992), "Seismic Inspection and Seismic Strengthening Method of Reinforced Concrete Bridge Piers", Proceedings of the Tenth World Conference on Earthquake Engineering, Rotterdam, ed. A. A. Balkema, 1992, vol. 9, pp. 5279-5284.

Valluvan, Raj, Michael E. Kreger and James O. Jirsa, (1993), "Strengthening of Column Splices for Seismic Retrofit of Nonductile Reinforced Concrete Frames", ACI Structural Journal, vol. 90, no. 4, July-August, pp. 432-440.

Verma, Ravindra, M. J. Nigel Priestley and Frieder Seible, (1993), "Assessment of Seismic Response and Steel Jacket Retrofit of Squat Circular Reinforced Concrete Bridge Columns - Final Report. Report No. SSRP - 92/05", Department of Applied Mechanics and Engineering Sciences, University of California, San Diego, 148.

Verma, Ravindra, M. J. Nigel Priestley and Frieder Seible, (1994), "Seismic Response of "As-Built" and Retrofitted Squat Circular RC Bridge Columns", Proceedings of the Fifth U. S. National Conference on Earthquake Engineering, Earthquake Engineering Research Institute, Oakland, CA, 1994, vol. 5, pp. 477-486.

Wallenberger, Frederick T, (1994), "High Modulus Glass-Ceramic Fiber Reinforced Composites for Currently Emerging Infrastructure Applications", Infrastructure: New Materials and Methods of Repair, Proceedings of the Third Materials Engineering Conference, San Diego, California, Materials Engineering Division of the American Society of Civil Engineers, November 13-16, 1994, pp. 272-279.

Watson, S. and R. Park, (1994), "Simulated Seismic Load Tests on Reinforced Concrete Columns", Journal of Structural Engineering, vol. 120, no. 6, June, 1994, pp. 1825-1849.

Watson, S., F. A. Zahn and R. Park, (1994), "Confining Reinforcement for Concrete Columns", Journal of Structural Engineering, vol. 120, no. 6, June, 1994, pp. 1798-1824.

Wehbe, Nadim, M. Saiid Saiidi, David Sanders, and Bruce Douglas, (1994), "Ductility of Rectangular Reinforced Concrete Bridge Columns with Moderate Confinement", Department of Civil Engineering, University of Nevada, Reno, 1994.

Xiao, Yan and Rui Ma, (1996), "Analysis and Design of Bridge Columns with Lap-Spliced Longitudinal Reinforcement", Proceedings of the Fourth National Workshop on Bridge Research in Progress, Sponsored by the National Science Foundation, State University of New York, and National Center for Earthquake Engineering Research, 1996, pp. 259-262.

Xiao, Yan, Geoffrey R. Martin, Zemin Yin and Rui Ma, (1995a), "Bridge Column Retrofit Using Snap-Tite Composite Jacketing for Improved Seismic Performance. Structural Engineering Research Report No. USC-SERR 95/02", Department of Civil Engineering, University of Southern California, 1995.

Xiao, Yan, Geoffrey R. Martin, Zemin Yin and Rui Ma, (1995b), "Retrofit Design of Existing Reinforced Concrete Bridge Columns Using Prefabricated Composite Jacketing", Proceedings, National Seismic Conference on Bridges and Highways, San Diego, CA, Federal Highway Administration and California Department of Transportation, December 1995.

Xiao, Yan, Geoffrey R. Martin, Zemin Yin and Rui Ma, (1996), "Seismic Retrofit of Existing Reinforced Concrete Bridge Columns using a Prefabricated Composite Wrapping System", Fiber Composites in Infrastructure, Proceedings of the First International Conference on Composites in Infrastructure, Tuscon, AZ, edited by M. R. Ehsani and H. Saadatmanesh, Department of Civil Engineering and Engineering Mechanics, University of Arizona, 15-17 January 1996, pp. 903-917.

Xiao, Yan, M. J. Nigel Priestley and Frieder Seible, (1993), "Steel Jacket Retrofit for Enhancing Shear Strength of Short Rectangular Reinforced Concrete Columns. Report No. SSRP - 92/07", Department of Applied Mechanics and Engineering Sciences, University of California, San Diego, 1993.

XXSys Technologies, Inc, (1995a), Corporate Brochure, San Diego: XXSys Technologies, Inc, 1995.

XXSys Technologies, Inc, (1995b), "XXSys Update 12/95", 12 min. 20 sec. Videocassette, XXSys Technologies, Inc, 1995.

Yashinsky, Mark, (1995), "Seismic Design and Retrofit Procedures for Highway Bridges in Japan", np, 1995.

Yashinsky, Mark and Pat Hipley, (1996), "Performance of Bridge Seismic Retrofits During the Northridge Earthquake", What's Shakin'?, An Informal Information Memo by the Office of Earthquake Engineering, California Department of Transportation, March, 1996.

Yashinsky, Mark, Pat Hipley and Quang Nguyen, (1995), "The Performance of Bridge Seismic Retrofits During the Northridge Earthquake", CALTRANS Office of Earthquake Engineering, June 1995.

Zayati, F., S. Mahin and S. Mazzoni, (1993), "Evaluation of a Seismic Retrofit Concept for Double Deck Viaduct", Proceedings of the Second Annual Seismic Research Workshop, California Department of Transportation, 1993.

Zelinski, Ray, (1996), "Northridge Earthquake Influence on Bridge Design Code", What's Shakin'?, An Informal Information Memo by the Office of Earthquake Engineering, California Department of Transportation, March, 1996.

**APPENDIX A**  
**REFERENCE CLASSIFICATION CHART AND CROSS-REFERENCE LIST**

A Reference Classification Chart was prepared to assist the reader in identifying a particular type of reference or in identifying the type of material in a given reference. This chart, presented as Table A-1 in this appendix, alphabetically lists all of the references cited in the bibliography of this document. Table A-1 presents the following information, when available, for all references: author; year of publication; column type; strengthening objective; type of retrofit; nature of research; number of specimens; and scale.

An "X" placed in a particular column indicates that the reference contains information in this area. An "X" followed by a number indicates references which may discuss a number of different column types or retrofit techniques, the relative distribution of the information. For example, a reference which contains test results of five rectangular columns and three circular columns would have a mark of "X,5" under Column Type, Rectangular; "X,3" in the column marked Column Type, Circular; and the number 8 in the column marked Number of Specimens.

In the column marked "Type of Retrofit, Other" a letter coding system has been adopted to identify the variety of retrofits that fall under this broad categorization. An explanation of the coding for this table column is presented at the bottom of the last page of table A-1.

In the column marked "Scale, Reduced Scale" several references are marked "X (cylinder)". These references discuss tests of retrofit concepts on either standard rectangular prisms or cylinders.

Table A-2, Cross-Reference List, can be used to find citations of a particular article. The reference author(s), year of publication, and page(s) on which the reference is cited are presented. If a reference is listed as NR under the column Page in Table A-2, this indicates that the reference is not specifically mentioned in this report.

TABLE A-1 Reference Classification Chart

Author	Year	Column Type		Strengthening Objective			Type of Retrofit			Nature of Research			Scale					
		Circular	Rectangular	Flexure	Shear	Axial	Steel Jacket	Concrete Jacket	Composite Jacket	Other	Laboratory Test(s)	Field Test(s)	Analytical Model(s)	Retrofit Description	Earthquake Performance	Design Document	Number of Specimens	Full Scale
Aboutaha	1994		X	X, 17	X, 11		X									28		X
Aboutaha et al.	1994a		X	X, 3	X, 4		X											X
Aboutaha et al.	1994b		X	X	X		X											X
Aboutaha et al.	1994c		X	X	X		X											X
Adachi, Kosa, and Murayama	1994		X	X	X				E									X
Agarwal and Broome	1990			X	X		X	X	X				X, 36					X, 4
Aklmoo, Hakajima, and Kogure	1990	X	X	X	X		X	X										X
Alameddine	1996	X	X	X, 8	X, 3		X, 5	X, 8										X
Amari et al.	1994	X	X	X	X		X											X
Asnashari	1993	X	X	X	X		X											X
Applied Technology Council	1995a														X			X (cylinders)
Applied Technology Council	1995b														X			X
Bavarian et al.	1996				X		X, 4		B, 2									X
Bernards, McLean, and Henley	1992		X		X													X
Bett, Klingner, and Jirsa	1988		X		X													X
Better Roads	1993		X		X													X
Brown	1992		X		X													X
Buckland	1993		X		X													X
California Department of Transportation	1990		X		X													X
California Department of Transportation	1990		X		X													X
California Department of Transportation	1995a		X		X													X
California Department of Transportation	1995b		X		X													X
California Department of Transportation	1995c		X		X													X
California Department of Transportation	1995d		X		X													X
California Department of Transportation	1996a		X		X													X
California Department of Transportation	1996b		X		X													X
California Department of Transportation	1996c		X		X													X
California Department of Transportation	1996d		X		X													X
Casey et al.	1994		X		X		X											X
Chai, Priestley, and Seible	1990		X, 12	X, 12	X, 12		X											X
Chai, Priestley, and Seible	1991a		X		X		X											X
Chai, Priestley, and Seible	1991b		X		X		X											X
Chai, Priestley, and Seible	1991c		X		X		X											X
Chai, Priestley, and Seible	1991d		X		X		X											X
Chai, Priestley, and Seible	1994		X		X		X											X
Chajes et al.	1994								F									X
Chang and Mander	1994a								E									X
Chang and Mander	1994b								E									X
Chapman	1995																	X
Civil Engineering	1994		X		X				C				X, 96	X, 15				X
Coffman, Marsh, and Brown	1991		X		X				C									X
Coffman	1992		X		X				C									X
Coffman Marsh and Brown	1993		X		X													X
Cooper et al.	1994						X	X										X
Concrete Reinforcing Steel Institute	1994						X	X										X
Daily Journal of Commerce	1995		X															X
Darwish, Saidi, and Sanders	1995a		X				X											X
Darwish, Saidi, and Sanders	1995b		X				X											X
Darwish, Saidi, and Sanders	1996		X				X											X
Dokken	1996																	X
Dristos and Pilakoutas	1994		X		X				B									X
Duan and Cooper	1995		X															X
El-Mikawi	1996		X															X
Essoy, Tankut, and Sulciman	1993		X															X
Faza and GangaRao	1994		X					X										X
Federal Highway Administration	1995		X						C									X
Finch et al.	1994		X						F									X

TABLE A-1 Reference Classification Chart (Cont'd)

Author	Year	Column Type		Strengthening Objective			Type of Retrofit				Nature of Research			Scale					
		Circular	Rectangular	Flexure	Shear	Axial	Steel Jacket	Concrete Jacket	Composite Jacket	Other	Laboratory Test(s)	Field Test(s)	Analytical Model(s)	Retrofit Description	Earthquake Performance	Design Document	Number of Specimens	Full Scale	Reduced Scale
Fish and Rowe	1994	X		X		X	X										46	X	X (cylinder)
Frangou and Prilakoutas	1994	X,18				X			C	X							5		X
Frangou and Dritos	1995	X	X,28			X			C	X							13		X
Fuse	1992		X														13		X
Fyfe	1994a	X,7	X,6	X,9	X,4												13		X
Fyfe	1994b	X,7	X,6	X,9	X,4												13		X
Fyfe	1995	X	X	X	X													X	X
Fyfe	1995	X	X	X	X													X	X
Fyfe and Kuruvilla	1996	X	X	X	X												9		X
Fyfe, Watson, and Kaspar	1995	X		X					C,D	X	X						15		X
Gamble, Hawkins, and Kaspar	1996	X		X					C,D	X,6	X,9							X	X (cylinder)
Gomez and Castro	1996	X		X		X			C,D	X							13		X
Haroun, Parden, and Shepherd	1994	X	X	X						X							2		X
Hawkins, Patel, and Stockel	1995	X		X						X							2		X
Hawkins, Patel, and Stockel	1996	X		X						X							2		X
Hoxed Fyfe	1995	X	X	X,1	X,2					X							3		X
Hippley	1996	X		X													27		X (cylinder)
Hoppel et al.	1994	X		X		X				X							1		X (cylinder)
Howie and Karbhari	1994	X		X		X			A	X							1		X (cylinder)
Imben and Associates	1994	X	X	X	X													X	X
Izuno and Ohkawa	1992	X		X														X	X
Japan Road Association	1990																	X	X
Japan Society of Civil Engineers	1995	X		X,5	X,3													X	X
Jarudat, McLean, and Marsh	1996	X		X,5	X					X,2							8		X
Jin, Saadmanesh, and Ehsani	1994	X,5	X,5	X	X												10		X
Karbhari and Eckel	1994	X		X		X												X	X
Karbhari, Eckel, and Tunis	1993a	X		X		X												X	X (cylinder)
Karbhari and Wilkins	1993b	X		X		X												X	X (cylinder)
Katsumata et al.	1990	X		X	X													X	X
Katsumata, Kobatake, and Takeda	1988	X		X	X													X	X
Kawashima	1990	X		X	X				A	X								X	X
Kawashima	1991	X		X	X				A	X								X	X
Kawashima	1995	X		X	X				A	X								X	X
Kawashima and Unjoh	1992	X		X	X				A	X								X	X
Kawashima, Unjoh, and Iida	1990	X		X	X				A	X								X	X
Kawashima, Unjoh, and Iida	1991	X		X	X				A	X								X	X
Kawashima, Unjoh, and Iida	1992	X		X	X				A	X								X	X
Kawashima, Unjoh, and Iida	1994	X		X	X				A	X								X	X
Kawashima, Unjoh, and Mukai	1994	X		X	X				A	X								X	X
Koga et al.	1994	X		X	X				A	X								X	X
Li, Shaddameh, and Ehsani	1992	X	X	X														X	X
Lin, Gamble, and Hawkins	1994	X		X					D		X							X	X
Lwin and Henley	1993	X		X					E		X							X	X
Macrae, Priestley, and Scible	1994	X		X	X				A	X								X	X
Maffei	1996	X		X	X				A	X								X	X
Mahin	1991	X		X	X				A	X								X	X
Mander and Chen	1994	X		X	X				E	X								X	X
Mander and Cheng	1995	X		X	X				E	X								X	X
Mander, Priestley, and Park	1988a	X		X	X				E	X								X	X
Mander, Priestley, and Park	1988b	X		X	X				E	X								X	X
Matsuda, Fujiwara, and Higashida	1990	X		X	X				E	X								X	X
Matsuda et al.	n.d.	X		X	X				E	X								X	X
Matsura, Nakamura, and Sekimoto	1990	X		X	X					X,4								X,1	X,4
McConnell	1993	X		X	X					X								X	X
McLean and Bernards	1992	X		X	X				B,2	X								X	X

TABLE A-1 Reference Classification Chart (Cont'd)

Year	Author	Column Type		Strengthening Objective			Type of Retrofit			Nature of Research				Number of Specimens		Scale	
		Circular	Rectangular	Flexure	Shear	Axial	Steel Jacket	Concrete Jacket	Composite Jacket	Other	Laboratory Test(s)	Field Test(s)	Analytical Model(s)	Retrofit Description	Earthquake Performance	Design Document	Full Scale
1996	Mimiran et al.	X		X				X		X						X	
1995	Mimiran and Shahawy	X		X				X		X						X	
1994	Mitchell, Sexsmith, and Tinawi	X	X	X	X			X		X						X	
n.d.	Mitsubishi Chemical Corporation	X	X	X	X			X		X						X	
1995	Naani and Norris	X	X	X	X			X		X						X	
n.d.	NCF Industries	X		X				X		X						X	
1993	Noori and Saidi	X		X				X		X						X	
1994	Ogata, Naeda, and Andoh	X	X	X	X			X		X						X	
1993	Ogata et al.	X	X	X	X			X		X						X	
n.d.	Ohuchi et al.	X		X				X		X						X	
1994	Okamoto et al.	X		X				X		X						X	
1994	Owo et al.	X		X				X		X						X	
1996	Picher, Rochette, and Labossiere	X		X				X		X						X	
1991	Priestley, Fyfe, and Seible	X, 3	X, 3	X, 3	X, 3			X		X						X	
1991	Priestley and Seible	X	X	X	X			X		X						X	
1992	Priestley and Seible	X	X	X	X			X		X						X	
1995	Priestley and Seible	X	X	X	X			X		X						X	
1996	Priestley, Seible, and Calvi	X	X	X	X			X		X						X	
1992a	Priestley, Seible, and Chai	X	X	X	X			X		X						X	
1992b	Priestley, Seible, and Chai	X	X	X	X			X		X						X	
1991	Priestley, Seible, Chai, and Sun	X, 4	X, 1	X				X		X						X	
1994	Priestley, Seible, and Fyfe	X, 5	X, 2	X, 3	X, 4			X		X						X	
1993	Priestley, Seible, Verma, and Xiao	X, 6	X, 6	X	X			X		X						X	
1991	Priestley, Seible, Xiao, and Verma	X, 6	X, 6	X	X			X		X						X	
1994a	Priestley, Seible, Xiao, and Verma	X, 8	X, 6	X	X			X		X						X	
1994b	Priestley, Seible, Xiao, and Verma	X, 8	X, 6	X	X			X		X						X	
1993	Priestley, Verma, and Xiao	X	X	X	X			X		X						X	
1991	Public Works Research Institute	X	X	X	X			X		X						X	
1993	Public Works Research Institute	X	X	X	X			X		X						X	
1991	Roberts	X	X	X	X			X		X						X	
1992	Rodriguez and Park	X	X	X	X			X		X						X	
1994	Rodriguez and Park	X	X	X	X			X		X						X	
1994	Saadmanesh	X		X				X		X						X	
n.d.	Saadmanesh, Ehsani, and Jin	X, 5	X, 5	X	X			X		X						X	
1996a	Saadmanesh, Ehsani, and Jin	X, 5	X, 5	X	X			X		X						X	
1996b	Saadmanesh, Ehsani, and Jin	X, 5	X, 5	X	X			X		X						X	
1992	Saadmanesh, Ehsani, and Li	X	X	X	X			X		X						X	
1994	Saadmanesh, Ehsani, and Li	X	X	X	X			X		X						X	
1993	Sanders, Douglas, and Cornell	X	X	X	X			X		X						X	
1994a	Seible, Hegemier, Priestley, et al.	X	X	X	X			X		X						X	
1994b	Seible, Hegemier, Priestley, et al.	X	X	X	X			X		X						X	
1995a	Seible, Hegemier, Priestley, et al.	X	X	X	X			X		X						X	
1995b	Seible, Hegemier, Priestley, et al.	X, 4	X, 3	X, 3	X, 4			X		X						X	
1995c	Seible, Hegemier, Priestley, et al.	X	X	X	X			X		X						X	
1995d	Seible, Hegemier, Priestley, et al.	X	X	X	X			X		X						X	
1995e	Seible, Hegemier, Priestley, et al.	X	X	X	X			X		X						X	
1993a	Seible and Priestley	X	X	X	X			X		X						X	
1993b	Seible and Priestley	X	X	X	X			X		X						X	
1995f	Seible, Priestley, and Inamamoto	X	X	X	X			X		X						X	
1992	Seqad Consulting Engineers	X	X	X	X			X		X						X	
1993	Seqad Consulting Engineers	X	X	X	X			X		X						X	

TABLE A-1 Reference Classification Chart (Cont'd)

Author	Year	Column Type		Strengthening Objective			Type of Retrofit			Other	Laboratory Test(s)	Field Test(s)	Nature of Research		Earthquake Performance	Design Document	Number of Specimens	Scale	
		Circular	Rectangular	Flexure	Shear	Axial	Steel Jacket	Concrete Jacket	Composite Jacket				Analytical Model(s)	Retrofit Description				Full Scale	Reduced Scale
Seroussi	1993		X		X								X				6	X	
Shirole and Halik	1993	X		X	X				A	X			X				4	X	
Shkurti et al.	1995	X		X	X				C, D	X									
Stanton, MacRae, and Nosho	1996		X		X														
Sultan, Hawkins, and Sheng	1995			X	X														
Sun and Sakino	1992		X		X														
Sun, Scible, and Priestley	1993a		X		X														
Sun, Scible, and Priestley	1993b		X		X														
Fankai and Ersoy	1991		X		X			X											
Taylor and Stone	1993		X		X														
Taylor et al.	1996		X		X														
Tsubouchi, Ohashi, and Amakawa	1990		X		X			X	A										
Turkington, Wilson, and Kennedy	1991		X		X				A										
Uji	n.d.		X		X			X											
University of California	1991	X		X	X			X	B, C										
Unjoh and Kawashima	1992	X		X	X			X											
Valluvan, Kregger, and Jirsa	1993	X		X	X			X	B, D, E, F										
Verma, Priestley, and Scible	1993	X		X	X			X											
Verma, Priestley, and Scible	1994	X		X	X			X											
Waltenberger	1994																		
Watson and Park	1994	X		X	X				E										
Watson, Zahn, and Park	1994	X		X	X				E										
Wehbe	1995		X		X				E										
Xiao and Ma	1996	X		X	X														
Xiao, Martin, Yin, and Ma	1995a	X		X	X														
Xiao, Martin, Yin, and Ma	1995b	X		X	X														
Xiao, Martin, Yin, and Ma	1996	X		X	X														
Xiao, Priestley, and Scible	1993		X		X														
XXSYS Technologies	1995a	X		X	X														
XXSYS Technologies	1995b	X		X	X														
Yashinsky	1995		X		X														
Yashinsky and Hipley	1996	X		X	X			X											
Yashinsky, Hipley, and Nguyen	1995	X		X	X			X											
Zayani and Mazzoni	1993	X		X	X			X											
Zelinski	1996	X		X	X			X											

Key to "Type of Retrofit, Other"

- A. Infill Walls
- B. Angle/Bar
- C. External Post-Tensioning
- D. External Rebar
- E. Internal Reinforcing
- F. Environmental Study



**TABLE A-2 Cross-Reference List**

<b>REFERENCE</b>	<b>PAGE</b>
Aboutaha, (1994)	NR
Aboutaha et al., (1994a)	NR
Aboutaha et al., (1994b)	NR
Aboutaha et al., (1994c)	NR
Adachi, Kosa, and Murayama, (1994)	132
Agarwal and Broutman, (1990)	59
Akimoto, Hakajima, and Kogure, (1990)	39, 48, 49
Alameddine, (1996)	NR
Amari et al., (1994)	29, 119
Applied Technology Council, (1995a)	134
Applied Technology Council, (1995b)	134
Asnaashari, (1993)	NR
Bavarian et al., (1996)	62
Bernards, McLean, and Henley, (1992)	45, 130
Bett, Klingner, and Jirsa, (1988)	119
Better Roads, (1993)	98
Brown, (1992)	60, 65
Buckland, (1995)	NR
California Department of Transportation, (1990)	8, 10
California Department of Transportation, (1995a)	1
California Department of Transportation, (1995b)	NR
California Department of Transportation, (1995c)	8, 10
California Department of Transportation, (1996a)	116
California Department of Transportation, (1996b)	1
California Department of Transportation, (1996c)	116
California Department of Transportation, (1996d)	116
Casey et al., (1994)	51
Chai, Priestley, and Seible, (1990)	NR
Chai, Priestley, and Seible, (1991a)	14, 52, 54, 55, 56
Chai, Priestley, and Seible, (1991b)	14, 17, 19, 52, 55, 75, 110
Chai, Priestley, and Seible, (1991c)	14, 25, 27, 110
Chai, Priestley, and Seible, (1991d)	14, 67, 110
Chai, Priestley, and Seible, (1994)	14, 52, 56
Chajes et al., (1994)	95
Chang and Mander, (1994a)	131, 132
Chang and Mander, (1994b)	131, 132
Chapman, (1995)	134
Civil Engineering, (1994)	65
Coffman, (1992)	124, 138
Coffman, Marsh, and Brown, (1991)	124, 126, 138
Coffman, Marsh, and Brown, (1993)	124, 138

**TABLE A-2 Cross-reference List (Cont'd)**

<b>REFERENCE</b>	<b>PAGE</b>
Concrete Reinforcing Steel Institute, (1994)	2
Cooper et al., (1994)	NR
Daily Journal of Commerce, (1995)	65
Darwish, Saiidi, and Sanders, (1995a)	29
Darwish, Saiidi, and Sanders, (1995b)	29
Darwish, Saiidi, and Sanders, (1996)	29
Dokken, (1995)	3
Dristos and Pilakoutas, (1994)	NR
Duan and Cooper, (1995)	135, 136
El-Mikawi, (1996)	143
Ersoy, Tankut, and Suleiman, (1993)	119
Faza and GangaRao, (1994)	NR
Federal Highway Administration, (1995)	21, 35, 40, 65, 127
Finch et al., (1994)	96
Fish and Rowe, (1994)	51
Frangou and Pilakoutas, (1994)	128, 129
Frangou, Pilakoutas, and Dristos, (1995)	128, 129
Fuse et al., (1992)	NR
Fyfe, (1994a)	65, 66, 84, 98
Fyfe, (1994b)	65, 66, 84, 98
Fyfe, (1995)	65, 66
Fyfe and Kuruvilla, (1993)	65, 66
Fyfe, Watson, and Watson, (1996)	65
Gamble, Hawkins, and Kaspar, (1995)	71, 101, 103
Gamble, Hawkins, and Kaspar, (1996)	NR
Gomez and Castro, (1996)	96
Haroun, Pardoen, and Shepherd, (1994)	33
Hawkins, Patel, and Steckel, (1995)	65, 99
Hawkins, Patel, and Steckel, (1996)	65, 99
Hexcel Fyfe, (1995)	65, 98
Hipley, (1996)	11
Hoppel et al., (1994)	113
Howie and Karbhari, (1994)	61
Imbsen and Associates, (1994)	4
Izuno and Ohkawa, (1992)	NR
Japan Road Association, (1990)	NR
Japan Society of Civil Engineers, (1995)	NR
Jaradat, McLean, and Marsh, (1996)	21, 38
Jin, Saadatmanesh, and Ehsani, (1994)	67, 70
Karbhari and Eckel, (1994)	97
Karbhari, Eckel, and Tunis, (1993)	64
Karbhari and Wilkins, (1993)	NR
Katsumata et al., (1990)	83

**TABLE A-2 Cross-reference List (Cont'd)**

<b>REFERENCE</b>	<b>PAGE</b>
Katsumata, Kobatake, and Takeda, (1988)	59, 91
Kawashima, (1990)	3, 119
Kawashima, (1991)	3, 119
Kawashima, (1995)	NR
Kawashima and Unjoh, (1992)	3, 119
Kawashima, Unjoh, Iida, (1990)	119
Kawashima, Unjoh, Iida, (1991)	3, 119
Kawashima, Unjoh, Iida, (1992)	3, 119
Kawashima, Unjoh, Mukai, (1994)	122
Koga et al., (1994)	98
Li, Saadatmanesh, and Ehsani, (1992)	NR
Lin, Gamble, and Hawkins, (1994)	71, 101, 102, 127
Lwin and Henley, (1993)	NR
Macrae, Priestley, and Seible, (1994)	31, 148
Maffei, (1996)	NR
Mahin, (1991)	NR
Mander and Chen, (1994)	123
Mander and Cheng, (1995)	131, 132
Mander, Priestley, and Park, (1988a)	NR
Mander, Priestley, and Park, (1988b)	14, 22, 43, 52, 67, 70, 72, 106, 113, 129
Matsuda, Fujiwara, and Higashida, (n.d.)	NR
Matsuda et al., (1990)	82
Matsuura, Nakamura, and Sekimoto, (1990)	48
McConnell, (1993)	65, 98
McLean and Bernards, (1992)	45, 130
Mirmiran et al. (1996)	113
Mirmiran and Shahawy, (1995)	112
Mitchell, Sexsmith, and Tinawi, (1994)	NR
Mitsubishi Chemical Corporation, (n.d.)	NR
Nanni and Norris, (1995)	NR
NCF Industries, (n.d.)	71, 104
Noori and Saiidi, (1993)	98, 99
Ogata, Maeda, and Andoh, (1994)	83
Ogata et al., (1993)	83
Ohuchi et al., (n.d.)	NR
Okamoto et al., (1994)	NR
Ono et al., (1994)	121
Picher, Rochette, and Labossière, (1996)	NR
Priestley, Fyfe, and Seible, (1991)	65, 66, 90
Priestley and Seible, (1991)	14, 21, 35, 127
Priestley and Seible, (1992)	14, 21, 127
Priestley and Seible, (1995)	65, 66
Priestley, Seible, and Calvi, (1996)	65, 66

**TABLE A-2 Cross-reference List (Cont'd)**

<b>REFERENCE</b>	<b>PAGE</b>
Priestley, Seible, and Chai, (1992a)	21, 22, 25, 35, 65, 66, 119, 127
Priestley, Seible, and Chai, (1992b)	14, 21, 35
Priestley, Seible, Chai, and Sun, (1991)	14, 21, 40
Priestley, Seible, and Fyfe, (1994)	65, 66, 84
Priestley, Seible, Verma, and Xiao, (1993)	44
Priestley, Seible, Xiao, and Verma, (1991)	35
Priestley, Seible, Xiao, and Verma, (1994a)	35, 40
Priestley, Seible, Xiao, and Verma, (1994b)	35, 40
Priestley, Verma, and Xiao, (1993)	21, 44
Public Works Research Institute, (1991)	NR
Public Works Research Institute, (1993)	NR
Ricles, Yang, and Priestley, (1994)	NR
Roberts, (1991)	NR
Rodriguez and Park, (1992)	119
Rodriguez and Park, (1994)	119
Saadatmanesh, (1994)	67, 70, 106
Saadatmanesh, Ehsani, and Jin, (n.d.)	67, 70, 77, 88, 94
Saadatmanesh, Ehsani, and Jin, (1996a)	67, 70
Saadatmanesh, Ehsani, and Jin, (1996b)	67, 70
Saadatmanesh, Ehsani, and Li, (1992)	67, 70, 106
Saadatmanesh, Ehsani, and Li, (1994)	67, 70, 106, 113
Sanders, Douglas, and Cornell, (1993)	NR
Seible, Hegemier, et al., (1994a)	74, 83, 88
Seible, Hegemier, et al., (1994b)	74, 83, 86
Seible, Hegemier, et al., (1995a)	74, 79, 83
Seible, Hegemier, et al., (1995b)	73, 75, 83, 86
Seible, Hegemier, et al., (1995c)	74, 83, 92
Seible, Hegemier, et al., (1995d)	74, 75, 83
Seible, Hegemier, et al., (1995e)	74, 78, 83
Seible and Priestley, (1993a)	65, 77
Seible and Priestley, (1993b)	NR
Seible, Priestley, and Innamorato, (1995)	74, 76, 83, 101, 115
Seqad Consulting Engineers, (1992)	65, 90
Seqad Consulting Engineers, (1993)	65, 85, 86
Serroels, (1993)	49, 122
Shirolé and Halik, (1993)	50
Shkurti et al., (1995)	71, 101, 103
Stanton, MacRae, and Nosho, (1996)	NR
Sultan, Hawkins, and Sheng, (1995)	115
Sun and Sakino, (1992)	NR
Sun, Seible, and Priestley, (1993a)	28
Sun, Seible, and Priestley, (1993b)	21, 25, 28, 79, 80
Tankut and Ersoy, (1991)	119

**TABLE A-2 Cross-reference List (Cont'd)**

<b>REFERENCE</b>	<b>PAGE</b>
Taylor et al., (1996)	138, 149
Taylor and Stone, (1993)	56, 57
Tsubouchi, Ohashi, and Arakawa, (1990)	121
Turkington, Wilson, and Kennedy, (1991)	50, 122
Uji, (n.d).	NR
University of California, San Diego, (UCSD), 1991	14, 21, 22, 35, 40, 43, 65, 66, 127
Unjoh and Kawashima, (1992)	47
Valluvan, Kreger, and Jirsa, (1993)	119
Verma, Priestley, and Seible, (1993)	34, 38, 85, 86
Verma, Priestley, and Seible, (1994)	35
Wallenberger, (1994)	60
Watson and Park, (1994)	NR
Watson, Zahn, and Park, (1994)	NR
Wehbe et al., (1994)	NR
Xiao and Ma, (1996)	NR
Xiao, Martin, Yin, and Ma, (1995a)	71, 73
Xiao, Martin, Yin, and Ma, (1995b)	71
Xiao, Martin, Yin, and Ma, (1996)	71
Xiao, Priestley, and Seible, (1993)	40, 44, 93
XXSys Technologies, Inc., (1995a)	74, 83
XXSys Technologies, Inc., (1995b)	74, 83, 88
Yashinsky, (1995)	NR
Yashinsky and Hipley, (1996)	2, 119
Yashinsky, Hipley, and Nguyen, (1995)	2, 119
Zayati, Mahin, and Mazzoni, (1993)	NR
Zelinski, (1996)	NR



**APPENDIX B**  
**INDUSTRY SURVEY**

To obtain unpublished information on concrete column seismic retrofitting, a questionnaire was prepared and sent to members of industry so that their input on several questions could be obtained. The individuals contacted consisted of at least one Department of Transportation representative from all fifty states, a representative from the Canadian provinces, individuals associated with the Federal Highway Administration, the Army Corps of Engineers, the District of Columbia, private toll agencies such as the New Jersey Turnpike Authority, and Puerto Rico. A favorable response to the questionnaire was received with many agencies responding and some enclosing retrofit details, cost information, and relevant research reports. The questionnaire originally distributed is shown in the following text.

---

National Center for Earthquake Engineering Research  
Task 106-F-2.2

"Evaluation of Seismic Retrofit Methods for  
Reinforced Concrete Bridge Columns"

---

Please answer all of the questions. If you wish to comment on any of the questions or qualify your answers, please use margins or separate sheets of paper

Questionnaire completed by:

Title:

Address

City:

State:

Phone:

Fax:

E-mail:

Please return the completed questionnaire using the enclosed envelope by Dec. 15, 1995 to:

Prof. F. Wayne Klaiber  
Town Engineering Building  
Iowa State University  
Ames, Iowa 50011  
(Fax: 515-294-8216)

Q-1 Does your state currently have, or anticipate initiation of, a seismic assessment and retrofit program for concrete bridge columns?

1.) Yes                      2.) No

If you answered yes, please describe the system(s) you are using (or anticipate employing). Please provide drawings, specifications, etc. of the system(s) if they are available.

Q-2 If you answered yes to Q-1, what design criteria were used to design the retrofit system(s)?

Q-3 If you have retrofit system(s) in place, do you have a maintenance program that evaluates the performance of the system(s)?

- 1.) Yes                      2.) No

If you answered yes, please describe the system employed.

Q-4 If you have employed retrofit system(s), please provide information on the constructability of the system and its (their) cost.

Q-5 Has your agency funded research in the area of seismic retrofitting of columns?

- 1.) Yes                      2.) No

If yes, please describe the research that was funded.

If no, do you plan on funding such research in the near future?

- 1.) Yes                      2.) No

If yes, please describe the research being initiated.

Q-6 In an effort to collect as much information on column seismic retrofitting as possible, do you know of anyone outside your agency who has been involved in column seismic retrofitting?

Name, etc.

Q-7 Have you been contacted by any vendors, with products, or specialty contractors, with procedures, for seismic retrofitting columns?

- 1.) Yes                      2.) No

If yes, please provide sufficient information so that we may contact them.

The results of this questionnaire are presented in Table B-1, Industry Survey Response Summary.

**TABLE B-1 Industry Survey Response Summary**

Agency	Q-1	Q-2	Q-3	Q-4	Q-5
Alberta, Canada	No		No		No, No
Arkansas <sup>1</sup>	No, decision on project basis	Designed by Roy Imbsen	No		No, No
Army Corps of Engineers	No				
California	Yes <sup>2</sup>	Caltrans Ductility Displacement Criteria	No, inspection only in vicinity of large earthquakes.	see footnote <sup>3</sup>	Yes <sup>4</sup>
Colorado	No		No		No, No
Connecticut	No				No, No
Delaware	No		No		No, No
District of Columbia	No				
Florida	No		No		No, No
Georgia	No				No, No
Idaho	Yes <sup>5</sup>		No		No, No

<sup>1</sup> Provided details / specifications.

<sup>2</sup> Have an ongoing retrofit program which includes seismic improvements for the entire bridge, including columns. Total, 3,000 bridges.

<sup>3</sup> Constructability has not been an issue. Contractors have developed solutions to all designs. Our designers have construction experience and avoid non-constructible details. Typical costs, pile foundation, \$75,000, column casing, \$15,000.

<sup>4</sup> Column casings, superstructure and footing joint shear, knee joints, pier walls.

<sup>5</sup> No system has been selected

**TABLE B-1 Industry Survey Response Summary (Cont'd)**

Agency	Q-1	Q-2	Q-3	Q-4	Q-5
Illinois	Yes <sup>6</sup>	see footnote <sup>7</sup>	Yes <sup>8</sup>	see footnote <sup>9</sup>	Yes <sup>10</sup> , Yes <sup>11</sup>
Indiana	No		No		No, No
Iowa	No				
Kentucky	No		No		No, No
Louisiana	No		No		No, No
Maine	No				Yes <sup>12</sup> , No
Manitoba, Canada	No		No		No, No

<sup>6</sup> Have evaluated the effectiveness of four different retrofit systems for strengthening the deficient splices of main reinforcement on several as-built circular columns. Cyclic testing of the as-built columns were conducted with 3/4" steel bands, 0.6" G-270 strands, rigid fiberglass wraps by NCF of California, and fiber wraps marketed by R. J. Watson. Have used post-tensioned strands in retrofitting of some bridges in the past.

<sup>7</sup> University of Il at Urbana-Champaign is developing design criteria. For some urgent projects we relied on field test results and provided 0.6" diameter strand ties at 7" center to center post-tensioned to 45 kips. Ties were applied along the splice location of main reinforcement and post-tensioning force was applied at two locations in each tie 180 degrees apart.

<sup>8</sup> Research Center of the Northwestern University Civil Engineering Dept. has installed a measurement device on two retrofitted columns to measure cracking of the retrofitted columns. The system is expected to measure elongation of a coaxial wire embedded in concrete and expected to show occurrence of transverse cracks in the future.

<sup>9</sup> The contract plans called for post-tensioned bands with mechanical couplers or post-tensioned strands as an option. The contractor found it more practical and economical to use post-tensioned strands. The post-tensioning was conducted by Dywidag Systems International, St. Louis, MO.

<sup>10</sup> IL DOT has funded column testing to evaluate as-built column strengths also lab tests to evaluate effect of various retrofit measures. Contact Dr. William Gamble of U. of Illinois for test results.

<sup>11</sup> IL DOT is in the process of funding additional research to establish design criteria for various retrofit measures such as steel bands, strand ties, and fiberglass jackets. The research will be conducted by Drs. Gamble and Hawkins of U. of Illinois, Urbana.

<sup>12</sup> A general seismic design of Maine bridges was done in 1992 by the University of Maine at Orono. Seven of Maine's most seismically vulnerable bridges were evaluated for their seismic performance. All bridges met the strength requirements for SPC-B and the study's conclusion was no retrofitting is required for existing bridges.

**TABLE B-1 Industry Survey Response Summary (Cont'd)**

Agency	Q-1	Q-2	Q-3	Q-4	Q-5
Massachusetts	Yes <sup>13</sup>	AASHTO Standard Specifications	No	see footnote <sup>14</sup>	No, No
Michigan	No				No, No
Minnesota	No				No, No
Mississippi	No				No, No
Missouri <sup>1</sup>	Yes, steel jackets	FHWA Manual	No	MHTD provisions	No, No
Montana	Yes, Caltrans Memo 20-4	Collapse prevention	No		No, No
Nebraska	No				No, No
Nevada	see footnote <sup>15</sup>		No, fiber wraps inspected as part of routine inspection	see footnote <sup>16</sup>	Yes <sup>17</sup>
New Brunswick, Canada	No		No		No, No
New Hampshire	No			will soon advertise a composite wrap project	No, ?

<sup>13</sup> Policy is to retrofit bridges for which major rehabilitation work is planned. The intent is to have the retrofitted bridges be the functional equivalent of new construction.

<sup>14</sup> Construction drawings and photos were enclosed as well as cost information indicating a contracted price of \$6400 per column base retrofit.

<sup>15</sup> General assessment by U. of Nevada Risk Method. Detailed assessment per FHWA RD-83-007 and RD-94-052. Retrofit methods include steel casings per Caltrans standards, infill shear walls, and pedestals encasing bar laps at column base.

<sup>16</sup> Steel column casings, \$5/lb. Fiber column casings (special cases only) - cost comparable to steel, used where access is limited only, easily constructed passive wrap. Note - steel casings easily constructed where there is adequate access for cranes to install.

<sup>17</sup> Research at UNR Center for Earthquake Engineering Research on column casings for flared rectangular columns not meeting Caltrans tables and on effects of column flares in architectural columns.

**TABLE B-1 Industry Survey Response Summary (Cont'd)**

Agency	Q-1	Q-2	Q-3	Q-4	Q-5
New Jersey <sup>1</sup>	Yes <sup>18</sup>	AASHTO & NJDOT Bridge Design Manual	Yes, part of regular bi-ennial inspections.		No, No
New Jersey Turnpike Authority	Yes <sup>19</sup>	AASHTO Standard Specifications			No, No
New Mexico	No				No, No
New York	No, decision on project basis		No		No, No
Nova Scotia	No				No, No
North Dakota	No		No		No, No
Ohio	No				
Oklahoma	No		No		No, No
Ontario, Canada	Yes <sup>20</sup>	see footnote <sup>21</sup>	No		No, No
Oregon	No		No		No, No
Pennsylvania	No, decision on project basis	AASHTO & FHWA research	Yes <sup>22</sup>	Seismic wrap and steel shells, both \$12,000 per column.	No, No

<sup>18</sup> The state has recently begun the NJDOT Bridge Seismic Retrofit Program (SRP). The program will retrofit entire structures not just single components.

<sup>19</sup> The Authority is currently implementing Phase I of its seismic retrofit program. This involves the preliminary screening and prioritization of the bridge population for seismic vulnerability. Phase II will address detailed evaluation and design of retrofit systems. Anticipated to begin Phase II in late 1997. Drawings and specifications are not available at this time.

<sup>20</sup> We have just begun preliminary screening of our bridges to determine their susceptibility to earthquakes. We are using a modified version of the screening process described in Chapter 2 of the FHWA Seismic Retrofitting Manual for Highway Bridges.

<sup>21</sup> We have not gone this far yet. Once preliminary screening is complete, detailed evaluations will be done on the highest priority bridges. Once this is done, retrofit solutions will be chosen.

<sup>22</sup> We have a product evaluation program that evaluates every new retrofit product we use.

**TABLE B-1 Industry Survey Response Summary (Cont'd)**

Agency	Q-1	Q-2	Q-3	Q-4	Q-5
Puerto Rico	No		No		No, No
South Carolina	Yes <sup>23</sup>		see footnote <sup>24</sup>		Yes, on bridge systems as a whole.
South Dakota	No				No, No
Tennessee	No		No	Steel shells, \$100/linear ft. for 36" to 40" dia. columns	No, No
Texas	No				
U. S. Coast Guard	No		No		No, No
Virginia	No		No		No, No
Washington	Yes <sup>25</sup>		Routine inspection only.		Yes
West Virginia	No		No		No, No
Wyoming	No				No, No

<sup>23</sup> SCDOT's seismic assessment and retrofit program has not yet been completed / finalized. Anticipate using many different types of retrofit measures including dynamic isolation, jointless structures, integral abutments and steel jacketing for columns.

<sup>24</sup> We do not currently have retrofit systems in place but we do feel strongly, however, towards the need for a well devised maintenance program.

<sup>25</sup> Program has focused on superstructure retrofit to date. First construction contracts for column retrofit will be advertised later this year (1996). Use of 3/8" thick steel jackets full height is planned (elliptical shape for rectangular columns).

The survey was sent to 64 different agencies / individuals. Of these 64 recipients, 49 responded which is a 77% response rate. Of the 50 states, 39 responded, a 78% response rate. The responses are summarized in the following paragraphs.

Question 1 inquired as to whether a seismic retrofit program for concrete columns was in place or was anticipated to be in place in the future. Of the 49 responses, 12 responded that they did have, or intended to have, such a program. Additionally, three other states, Arkansas, New York, and Pennsylvania, indicated that a decision is made only on an as needed basis. The states responding yes are in various parts of the country and are in active seismic areas as well as areas of low seismic risk.

Question 2 asked what design method was employed in retrofitting the columns. This question could only be answered by the 15 agencies that responded yes to question 1. The design methods cited by these agencies varied. They mentioned the use of AASHTO and FHWA design procedures, as well as the California Department of Transportation methodology and systems designed by a consulting firm.

Question 3 was designed to assess what type of maintenance and inspection requirements existed for these retrofits. The most common answer was that no special inspection procedures are in place. The retrofit is examined along with the rest of the bridge as part of routine inspections.

Question 4 was intended to collect cost information related to the construction of column retrofits. The costs reported were very limited and variable and consisted of both lump sum prices and price per lineal foot of retrofit column.

Question 5 inquired as to whether an agency had or intended to fund research in the area of concrete column seismic retrofitting. Of the 49 responses, six agencies indicated that they had previously funded research of this kind. Only Illinois specifically indicated that it intended to fund such research in the future.

Questions 6 and 7 were intended to assist the researchers in the collection of information. The companies and individuals listed in the survey responses were contacted and their information included in the report if deemed appropriate.

**NATIONAL CENTER FOR EARTHQUAKE ENGINEERING RESEARCH  
LIST OF TECHNICAL REPORTS**

The National Center for Earthquake Engineering Research (NCEER) publishes technical reports on a variety of subjects related to earthquake engineering written by authors funded through NCEER. These reports are available from both NCEER Publications and the National Technical Information Service (NTIS). Requests for reports should be directed to NCEER Publications, National Center for Earthquake Engineering Research, State University of New York at Buffalo, Red Jacket Quadrangle, Buffalo, New York 14261. Reports can also be requested through NTIS, 5285 Port Royal Road, Springfield, Virginia 22161. NTIS accession numbers are shown in parenthesis, if available.

- NCEER-87-0001 "First-Year Program in Research, Education and Technology Transfer," 3/5/87, (PB88-134275, A04, MF-A01).
- NCEER-87-0002 "Experimental Evaluation of Instantaneous Optimal Algorithms for Structural Control," by R.C. Lin, T.T. Soong and A.M. Reinhorn, 4/20/87, (PB88-134341, A04, MF-A01).
- NCEER-87-0003 "Experimentation Using the Earthquake Simulation Facilities at University at Buffalo," by A.M. Reinhorn and R.L. Ketter, to be published.
- NCEER-87-0004 "The System Characteristics and Performance of a Shaking Table," by J.S. Hwang, K.C. Chang and G.C. Lee, 6/1/87, (PB88-134259, A03, MF-A01). This report is available only through NTIS (see address given above).
- NCEER-87-0005 "A Finite Element Formulation for Nonlinear Viscoplastic Material Using a Q Model," by O. Gyebi and G. Dasgupta, 11/2/87, (PB88-213764, A08, MF-A01).
- NCEER-87-0006 "Symbolic Manipulation Program (SMP) - Algebraic Codes for Two and Three Dimensional Finite Element Formulations," by X. Lee and G. Dasgupta, 11/9/87, (PB88-218522, A05, MF-A01).
- NCEER-87-0007 "Instantaneous Optimal Control Laws for Tall Buildings Under Seismic Excitations," by J.N. Yang, A. Akbarpour and P. Ghaemmaghami, 6/10/87, (PB88-134333, A06, MF-A01). This report is only available through NTIS (see address given above).
- NCEER-87-0008 "IDARC: Inelastic Damage Analysis of Reinforced Concrete Frame - Shear-Wall Structures," by Y.J. Park, A.M. Reinhorn and S.K. Kunnath, 7/20/87, (PB88-134325, A09, MF-A01). This report is only available through NTIS (see address given above).
- NCEER-87-0009 "Liquefaction Potential for New York State: A Preliminary Report on Sites in Manhattan and Buffalo," by M. Budhu, V. Vijayakumar, R.F. Giese and L. Baumgras, 8/31/87, (PB88-163704, A03, MF-A01). This report is available only through NTIS (see address given above).
- NCEER-87-0010 "Vertical and Torsional Vibration of Foundations in Inhomogeneous Media," by A.S. Veletsos and K.W. Dotson, 6/1/87, (PB88-134291, A03, MF-A01). This report is only available through NTIS (see address given above).
- NCEER-87-0011 "Seismic Probabilistic Risk Assessment and Seismic Margins Studies for Nuclear Power Plants," by Howard H.M. Hwang, 6/15/87, (PB88-134267, A03, MF-A01). This report is only available through NTIS (see address given above).
- NCEER-87-0012 "Parametric Studies of Frequency Response of Secondary Systems Under Ground-Acceleration Excitations," by Y. Yong and Y.K. Lin, 6/10/87, (PB88-134309, A03, MF-A01). This report is only available through NTIS (see address given above).
- NCEER-87-0013 "Frequency Response of Secondary Systems Under Seismic Excitation," by J.A. HoLung, J. Cai and Y.K. Lin, 7/31/87, (PB88-134317, A05, MF-A01). This report is only available through NTIS (see address given above).

- NCEER-87-0014 "Modelling Earthquake Ground Motions in Seismically Active Regions Using Parametric Time Series Methods," by G.W. Ellis and A.S. Cakmak, 8/25/87, (PB88-134283, A08, MF-A01). This report is only available through NTIS (see address given above).
- NCEER-87-0015 "Detection and Assessment of Seismic Structural Damage," by E. DiPasquale and A.S. Cakmak, 8/25/87, (PB88-163712, A05, MF-A01). This report is only available through NTIS (see address given above).
- NCEER-87-0016 "Pipeline Experiment at Parkfield, California," by J. Isenberg and E. Richardson, 9/15/87, (PB88-163720, A03, MF-A01). This report is available only through NTIS (see address given above).
- NCEER-87-0017 "Digital Simulation of Seismic Ground Motion," by M. Shinozuka, G. Deodatis and T. Harada, 8/31/87, (PB88-155197, A04, MF-A01). This report is available only through NTIS (see address given above).
- NCEER-87-0018 "Practical Considerations for Structural Control: System Uncertainty, System Time Delay and Truncation of Small Control Forces," J.N. Yang and A. Akbarpour, 8/10/87, (PB88-163738, A08, MF-A01). This report is only available through NTIS (see address given above).
- NCEER-87-0019 "Modal Analysis of Nonclassically Damped Structural Systems Using Canonical Transformation," by J.N. Yang, S. Sarkani and F.X. Long, 9/27/87, (PB88-187851, A04, MF-A01).
- NCEER-87-0020 "A Nonstationary Solution in Random Vibration Theory," by J.R. Red-Horse and P.D. Spanos, 11/3/87, (PB88-163746, A03, MF-A01).
- NCEER-87-0021 "Horizontal Impedances for Radially Inhomogeneous Viscoelastic Soil Layers," by A.S. Veletsos and K.W. Dotson, 10/15/87, (PB88-150859, A04, MF-A01).
- NCEER-87-0022 "Seismic Damage Assessment of Reinforced Concrete Members," by Y.S. Chung, C. Meyer and M. Shinozuka, 10/9/87, (PB88-150867, A05, MF-A01). This report is available only through NTIS (see address given above).
- NCEER-87-0023 "Active Structural Control in Civil Engineering," by T.T. Soong, 11/11/87, (PB88-187778, A03, MF-A01).
- NCEER-87-0024 "Vertical and Torsional Impedances for Radially Inhomogeneous Viscoelastic Soil Layers," by K.W. Dotson and A.S. Veletsos, 12/87, (PB88-187786, A03, MF-A01).
- NCEER-87-0025 "Proceedings from the Symposium on Seismic Hazards, Ground Motions, Soil-Liquefaction and Engineering Practice in Eastern North America," October 20-22, 1987, edited by K.H. Jacob, 12/87, (PB88-188115, A23, MF-A01).
- NCEER-87-0026 "Report on the Whittier-Narrows, California, Earthquake of October 1, 1987," by J. Pantelic and A. Reinhorn, 11/87, (PB88-187752, A03, MF-A01). This report is available only through NTIS (see address given above).
- NCEER-87-0027 "Design of a Modular Program for Transient Nonlinear Analysis of Large 3-D Building Structures," by S. Srivastav and J.F. Abel, 12/30/87, (PB88-187950, A05, MF-A01). This report is only available through NTIS (see address given above).
- NCEER-87-0028 "Second-Year Program in Research, Education and Technology Transfer," 3/8/88, (PB88-219480, A04, MF-A01).
- NCEER-88-0001 "Workshop on Seismic Computer Analysis and Design of Buildings With Interactive Graphics," by W. McGuire, J.F. Abel and C.H. Conley, 1/18/88, (PB88-187760, A03, MF-A01). This report is only available through NTIS (see address given above).
- NCEER-88-0002 "Optimal Control of Nonlinear Flexible Structures," by J.N. Yang, F.X. Long and D. Wong, 1/22/88, (PB88-213772, A06, MF-A01).

- NCEER-88-0003 "Substructuring Techniques in the Time Domain for Primary-Secondary Structural Systems," by G.D. Manolis and G. Juhn, 2/10/88, (PB88-213780, A04, MF-A01).
- NCEER-88-0004 "Iterative Seismic Analysis of Primary-Secondary Systems," by A. Singhal, L.D. Lutes and P.D. Spanos, 2/23/88, (PB88-213798, A04, MF-A01).
- NCEER-88-0005 "Stochastic Finite Element Expansion for Random Media," by P.D. Spanos and R. Ghanem, 3/14/88, (PB88-213806, A03, MF-A01).
- NCEER-88-0006 "Combining Structural Optimization and Structural Control," by F.Y. Cheng and C.P. Pantelides, 1/10/88, (PB88-213814, A05, MF-A01).
- NCEER-88-0007 "Seismic Performance Assessment of Code-Designed Structures," by H.H-M. Hwang, J-W. Jaw and H-J. Shau, 3/20/88, (PB88-219423, A04, MF-A01). This report is only available through NTIS (see address given above).
- NCEER-88-0008 "Reliability Analysis of Code-Designed Structures Under Natural Hazards," by H.H-M. Hwang, H. Ushiba and M. Shinozuka, 2/29/88, (PB88-229471, A07, MF-A01). This report is only available through NTIS (see address given above).
- NCEER-88-0009 "Seismic Fragility Analysis of Shear Wall Structures," by J-W Jaw and H.H-M. Hwang, 4/30/88, (PB89-102867, A04, MF-A01).
- NCEER-88-0010 "Base Isolation of a Multi-Story Building Under a Harmonic Ground Motion - A Comparison of Performances of Various Systems," by F-G Fan, G. Ahmadi and I.G. Tadjbakhsh, 5/18/88, (PB89-122238, A06, MF-A01). This report is only available through NTIS (see address given above).
- NCEER-88-0011 "Seismic Floor Response Spectra for a Combined System by Green's Functions," by F.M. Lavelle, L.A. Bergman and P.D. Spanos, 5/1/88, (PB89-102875, A03, MF-A01).
- NCEER-88-0012 "A New Solution Technique for Randomly Excited Hysteretic Structures," by G.Q. Cai and Y.K. Lin, 5/16/88, (PB89-102883, A03, MF-A01).
- NCEER-88-0013 "A Study of Radiation Damping and Soil-Structure Interaction Effects in the Centrifuge," by K. Weissman, supervised by J.H. Prevost, 5/24/88, (PB89-144703, A06, MF-A01).
- NCEER-88-0014 "Parameter Identification and Implementation of a Kinematic Plasticity Model for Frictional Soils," by J.H. Prevost and D.V. Griffiths, to be published.
- NCEER-88-0015 "Two- and Three- Dimensional Dynamic Finite Element Analyses of the Long Valley Dam," by D.V. Griffiths and J.H. Prevost, 6/17/88, (PB89-144711, A04, MF-A01).
- NCEER-88-0016 "Damage Assessment of Reinforced Concrete Structures in Eastern United States," by A.M. Reinhorn, M.J. Seidel, S.K. Kunnath and Y.J. Park, 6/15/88, (PB89-122220, A04, MF-A01). This report is only available through NTIS (see address given above).
- NCEER-88-0017 "Dynamic Compliance of Vertically Loaded Strip Foundations in Multilayered Viscoelastic Soils," by S. Ahmad and A.S.M. Israil, 6/17/88, (PB89-102891, A04, MF-A01).
- NCEER-88-0018 "An Experimental Study of Seismic Structural Response With Added Viscoelastic Dampers," by R.C. Lin, Z. Liang, T.T. Soong and R.H. Zhang, 6/30/88, (PB89-122212, A05, MF-A01). This report is available only through NTIS (see address given above).
- NCEER-88-0019 "Experimental Investigation of Primary - Secondary System Interaction," by G.D. Manolis, G. Juhn and A.M. Reinhorn, 5/27/88, (PB89-122204, A04, MF-A01).
- NCEER-88-0020 "A Response Spectrum Approach For Analysis of Nonclassically Damped Structures," by J.N. Yang, S. Sarkani and F.X. Long, 4/22/88, (PB89-102909, A04, MF-A01).

- NCEER-88-0021 "Seismic Interaction of Structures and Soils: Stochastic Approach," by A.S. Veletsos and A.M. Prasad, 7/21/88, (PB89-122196, A04, MF-A01). This report is only available through NTIS (see address given above).
- NCEER-88-0022 "Identification of the Serviceability Limit State and Detection of Seismic Structural Damage," by E. DiPasquale and A.S. Cakmak, 6/15/88, (PB89-122188, A05, MF-A01). This report is available only through NTIS (see address given above).
- NCEER-88-0023 "Multi-Hazard Risk Analysis: Case of a Simple Offshore Structure," by B.K. Bhartia and E.H. Vanmarcke, 7/21/88, (PB89-145213, A05, MF-A01).
- NCEER-88-0024 "Automated Seismic Design of Reinforced Concrete Buildings," by Y.S. Chung, C. Meyer and M. Shinozuka, 7/5/88, (PB89-122170, A06, MF-A01). This report is available only through NTIS (see address given above).
- NCEER-88-0025 "Experimental Study of Active Control of MDOF Structures Under Seismic Excitations," by L.L. Chung, R.C. Lin, T.T. Soong and A.M. Reinhorn, 7/10/88, (PB89-122600, A04, MF-A01).
- NCEER-88-0026 "Earthquake Simulation Tests of a Low-Rise Metal Structure," by J.S. Hwang, K.C. Chang, G.C. Lee and R.L. Ketter, 8/1/88, (PB89-102917, A04, MF-A01).
- NCEER-88-0027 "Systems Study of Urban Response and Reconstruction Due to Catastrophic Earthquakes," by F. Kozin and H.K. Zhou, 9/22/88, (PB90-162348, A04, MF-A01).
- NCEER-88-0028 "Seismic Fragility Analysis of Plane Frame Structures," by H.H-M. Hwang and Y.K. Low, 7/31/88, (PB89-131445, A06, MF-A01).
- NCEER-88-0029 "Response Analysis of Stochastic Structures," by A. Kardara, C. Bucher and M. Shinozuka, 9/22/88, (PB89-174429, A04, MF-A01).
- NCEER-88-0030 "Nonnormal Accelerations Due to Yielding in a Primary Structure," by D.C.K. Chen and L.D. Lutes, 9/19/88, (PB89-131437, A04, MF-A01).
- NCEER-88-0031 "Design Approaches for Soil-Structure Interaction," by A.S. Veletsos, A.M. Prasad and Y. Tang, 12/30/88, (PB89-174437, A03, MF-A01). This report is available only through NTIS (see address given above).
- NCEER-88-0032 "A Re-evaluation of Design Spectra for Seismic Damage Control," by C.J. Turkstra and A.G. Tallin, 11/7/88, (PB89-145221, A05, MF-A01).
- NCEER-88-0033 "The Behavior and Design of Noncontact Lap Splices Subjected to Repeated Inelastic Tensile Loading," by V.E. Sagan, P. Gergely and R.N. White, 12/8/88, (PB89-163737, A08, MF-A01).
- NCEER-88-0034 "Seismic Response of Pile Foundations," by S.M. Mamoon, P.K. Banerjee and S. Ahmad, 11/1/88, (PB89-145239, A04, MF-A01).
- NCEER-88-0035 "Modeling of R/C Building Structures With Flexible Floor Diaphragms (IDARC2)," by A.M. Reinhorn, S.K. Kunnath and N. Panahshahi, 9/7/88, (PB89-207153, A07, MF-A01).
- NCEER-88-0036 "Solution of the Dam-Reservoir Interaction Problem Using a Combination of FEM, BEM with Particular Integrals, Modal Analysis, and Substructuring," by C-S. Tsai, G.C. Lee and R.L. Ketter, 12/31/88, (PB89-207146, A04, MF-A01).
- NCEER-88-0037 "Optimal Placement of Actuators for Structural Control," by F.Y. Cheng and C.P. Pantelides, 8/15/88, (PB89-162846, A05, MF-A01).

- NCEER-88-0038 "Teflon Bearings in Aseismic Base Isolation: Experimental Studies and Mathematical Modeling," by A. Mokha, M.C. Constantinou and A.M. Reinhorn, 12/5/88, (PB89-218457, A10, MF-A01). This report is available only through NTIS (see address given above).
- NCEER-88-0039 "Seismic Behavior of Flat Slab High-Rise Buildings in the New York City Area," by P. Weidlinger and M. Ettouney, 10/15/88, (PB90-145681, A04, MF-A01).
- NCEER-88-0040 "Evaluation of the Earthquake Resistance of Existing Buildings in New York City," by P. Weidlinger and M. Ettouney, 10/15/88, to be published.
- NCEER-88-0041 "Small-Scale Modeling Techniques for Reinforced Concrete Structures Subjected to Seismic Loads," by W. Kim, A. El-Attar and R.N. White, 11/22/88, (PB89-189625, A05, MF-A01).
- NCEER-88-0042 "Modeling Strong Ground Motion from Multiple Event Earthquakes," by G.W. Ellis and A.S. Cakmak, 10/15/88, (PB89-174445, A03, MF-A01).
- NCEER-88-0043 "Nonstationary Models of Seismic Ground Acceleration," by M. Grigoriu, S.E. Ruiz and E. Rosenblueth, 7/15/88, (PB89-189617, A04, MF-A01).
- NCEER-88-0044 "SARCF User's Guide: Seismic Analysis of Reinforced Concrete Frames," by Y.S. Chung, C. Meyer and M. Shinozuka, 11/9/88, (PB89-174452, A08, MF-A01).
- NCEER-88-0045 "First Expert Panel Meeting on Disaster Research and Planning," edited by J. Pantelic and J. Stoyke, 9/15/88, (PB89-174460, A05, MF-A01). This report is only available through NTIS (see address given above).
- NCEER-88-0046 "Preliminary Studies of the Effect of Degrading Infill Walls on the Nonlinear Seismic Response of Steel Frames," by C.Z. Chrysostomou, P. Gergely and J.F. Abel, 12/19/88, (PB89-208383, A05, MF-A01).
- NCEER-88-0047 "Reinforced Concrete Frame Component Testing Facility - Design, Construction, Instrumentation and Operation," by S.P. Pessiki, C. Conley, T. Bond, P. Gergely and R.N. White, 12/16/88, (PB89-174478, A04, MF-A01).
- NCEER-89-0001 "Effects of Protective Cushion and Soil Compliancy on the Response of Equipment Within a Seismically Excited Building," by J.A. HoLung, 2/16/89, (PB89-207179, A04, MF-A01).
- NCEER-89-0002 "Statistical Evaluation of Response Modification Factors for Reinforced Concrete Structures," by H.H-M. Hwang and J-W. Jaw, 2/17/89, (PB89-207187, A05, MF-A01).
- NCEER-89-0003 "Hysteretic Columns Under Random Excitation," by G-Q. Cai and Y.K. Lin, 1/9/89, (PB89-196513, A03, MF-A01).
- NCEER-89-0004 "Experimental Study of 'Elephant Foot Bulge' Instability of Thin-Walled Metal Tanks," by Z-H. Jia and R.L. Ketter, 2/22/89, (PB89-207195, A03, MF-A01).
- NCEER-89-0005 "Experiment on Performance of Buried Pipelines Across San Andreas Fault," by J. Isenberg, E. Richardson and T.D. O'Rourke, 3/10/89, (PB89-218440, A04, MF-A01). This report is available only through NTIS (see address given above).
- NCEER-89-0006 "A Knowledge-Based Approach to Structural Design of Earthquake-Resistant Buildings," by M. Subramani, P. Gergely, C.H. Conley, J.F. Abel and A.H. Zaghaw, 1/15/89, (PB89-218465, A06, MF-A01).
- NCEER-89-0007 "Liquefaction Hazards and Their Effects on Buried Pipelines," by T.D. O'Rourke and P.A. Lane, 2/1/89, (PB89-218481, A09, MF-A01).
- NCEER-89-0008 "Fundamentals of System Identification in Structural Dynamics," by H. Imai, C-B. Yun, O. Maruyama and M. Shinozuka, 1/26/89, (PB89-207211, A04, MF-A01).

- NCEER-89-0009 "Effects of the 1985 Michoacan Earthquake on Water Systems and Other Buried Lifelines in Mexico," by A.G. Ayala and M.J. O'Rourke, 3/8/89, (PB89-207229, A06, MF-A01).
- NCEER-89-R010 "NCEER Bibliography of Earthquake Education Materials," by K.E.K. Ross, Second Revision, 9/1/89, (PB90-125352, A05, MF-A01). This report is replaced by NCEER-92-0018.
- NCEER-89-0011 "Inelastic Three-Dimensional Response Analysis of Reinforced Concrete Building Structures (IDARC-3D), Part I - Modeling," by S.K. Kunnath and A.M. Reinhorn, 4/17/89, (PB90-114612, A07, MF-A01).
- NCEER-89-0012 "Recommended Modifications to ATC-14," by C.D. Poland and J.O. Malley, 4/12/89, (PB90-108648, A15, MF-A01).
- NCEER-89-0013 "Repair and Strengthening of Beam-to-Column Connections Subjected to Earthquake Loading," by M. Corazao and A.J. Durrani, 2/28/89, (PB90-109885, A06, MF-A01).
- NCEER-89-0014 "Program EXKAL2 for Identification of Structural Dynamic Systems," by O. Maruyama, C-B. Yun, M. Hoshiya and M. Shinozuka, 5/19/89, (PB90-109877, A09, MF-A01).
- NCEER-89-0015 "Response of Frames With Bolted Semi-Rigid Connections, Part I - Experimental Study and Analytical Predictions," by P.J. DiCorso, A.M. Reinhorn, J.R. Dickerson, J.B. Radzinski and W.L. Harper, 6/1/89, to be published.
- NCEER-89-0016 "ARMA Monte Carlo Simulation in Probabilistic Structural Analysis," by P.D. Spanos and M.P. Mignolet, 7/10/89, (PB90-109893, A03, MF-A01).
- NCEER-89-P017 "Preliminary Proceedings from the Conference on Disaster Preparedness - The Place of Earthquake Education in Our Schools," Edited by K.E.K. Ross, 6/23/89, (PB90-108606, A03, MF-A01).
- NCEER-89-0017 "Proceedings from the Conference on Disaster Preparedness - The Place of Earthquake Education in Our Schools," Edited by K.E.K. Ross, 12/31/89, (PB90-207895, A012, MF-A02). This report is available only through NTIS (see address given above).
- NCEER-89-0018 "Multidimensional Models of Hysteretic Material Behavior for Vibration Analysis of Shape Memory Energy Absorbing Devices, by E.J. Graesser and F.A. Cozzarelli, 6/7/89, (PB90-164146, A04, MF-A01).
- NCEER-89-0019 "Nonlinear Dynamic Analysis of Three-Dimensional Base Isolated Structures (3D-BASIS)," by S. Nagarajaiah, A.M. Reinhorn and M.C. Constantinou, 8/3/89, (PB90-161936, A06, MF-A01). This report has been replaced by NCEER-93-0011.
- NCEER-89-0020 "Structural Control Considering Time-Rate of Control Forces and Control Rate Constraints," by F.Y. Cheng and C.P. Pantelides, 8/3/89, (PB90-120445, A04, MF-A01).
- NCEER-89-0021 "Subsurface Conditions of Memphis and Shelby County," by K.W. Ng, T-S. Chang and H-H.M. Hwang, 7/26/89, (PB90-120437, A03, MF-A01).
- NCEER-89-0022 "Seismic Wave Propagation Effects on Straight Jointed Buried Pipelines," by K. Elhmedi and M.J. O'Rourke, 8/24/89, (PB90-162322, A10, MF-A02).
- NCEER-89-0023 "Workshop on Serviceability Analysis of Water Delivery Systems," edited by M. Grigoriu, 3/6/89, (PB90-127424, A03, MF-A01).
- NCEER-89-0024 "Shaking Table Study of a 1/5 Scale Steel Frame Composed of Tapered Members," by K.C. Chang, J.S. Hwang and G.C. Lee, 9/18/89, (PB90-160169, A04, MF-A01).
- NCEER-89-0025 "DYNA1D: A Computer Program for Nonlinear Seismic Site Response Analysis - Technical Documentation," by Jean H. Prevost, 9/14/89, (PB90-161944, A07, MF-A01). This report is available only through NTIS (see address given above).

- NCEER-89-0026 "1:4 Scale Model Studies of Active Tendon Systems and Active Mass Dampers for Aseismic Protection," by A.M. Reinhorn, T.T. Soong, R.C. Lin, Y.P. Yang, Y. Fukao, H. Abe and M. Nakai, 9/15/89, (PB90-173246, A10, MF-A02).
- NCEER-89-0027 "Scattering of Waves by Inclusions in a Nonhomogeneous Elastic Half Space Solved by Boundary Element Methods," by P.K. Hadley, A. Askar and A.S. Cakmak, 6/15/89, (PB90-145699, A07, MF-A01).
- NCEER-89-0028 "Statistical Evaluation of Deflection Amplification Factors for Reinforced Concrete Structures," by H.H.M. Hwang, J-W. Jaw and A.L. Ch'ng, 8/31/89, (PB90-164633, A05, MF-A01).
- NCEER-89-0029 "Bedrock Accelerations in Memphis Area Due to Large New Madrid Earthquakes," by H.H.M. Hwang, C.H.S. Chen and G. Yu, 11/7/89, (PB90-162330, A04, MF-A01).
- NCEER-89-0030 "Seismic Behavior and Response Sensitivity of Secondary Structural Systems," by Y.Q. Chen and T.T. Soong, 10/23/89, (PB90-164658, A08, MF-A01).
- NCEER-89-0031 "Random Vibration and Reliability Analysis of Primary-Secondary Structural Systems," by Y. Ibrahim, M. Grigoriu and T.T. Soong, 11/10/89, (PB90-161951, A04, MF-A01).
- NCEER-89-0032 "Proceedings from the Second U.S. - Japan Workshop on Liquefaction, Large Ground Deformation and Their Effects on Lifelines, September 26-29, 1989," Edited by T.D. O'Rourke and M. Hamada, 12/1/89, (PB90-209388, A22, MF-A03).
- NCEER-89-0033 "Deterministic Model for Seismic Damage Evaluation of Reinforced Concrete Structures," by J.M. Bracci, A.M. Reinhorn, J.B. Mander and S.K. Kunnath, 9/27/89, (PB91-108803, A06, MF-A01).
- NCEER-89-0034 "On the Relation Between Local and Global Damage Indices," by E. DiPasquale and A.S. Cakmak, 8/15/89, (PB90-173865, A05, MF-A01).
- NCEER-89-0035 "Cyclic Undrained Behavior of Nonplastic and Low Plasticity Silts," by A.J. Walker and H.E. Stewart, 7/26/89, (PB90-183518, A10, MF-A01).
- NCEER-89-0036 "Liquefaction Potential of Surficial Deposits in the City of Buffalo, New York," by M. Budhu, R. Giese and L. Baumgrass, 1/17/89, (PB90-208455, A04, MF-A01).
- NCEER-89-0037 "A Deterministic Assessment of Effects of Ground Motion Incoherence," by A.S. Veletsos and Y. Tang, 7/15/89, (PB90-164294, A03, MF-A01).
- NCEER-89-0038 "Workshop on Ground Motion Parameters for Seismic Hazard Mapping," July 17-18, 1989, edited by R.V. Whitman, 12/1/89, (PB90-173923, A04, MF-A01).
- NCEER-89-0039 "Seismic Effects on Elevated Transit Lines of the New York City Transit Authority," by C.J. Costantino, C.A. Miller and E. Heymsfield, 12/26/89, (PB90-207887, A06, MF-A01).
- NCEER-89-0040 "Centrifugal Modeling of Dynamic Soil-Structure Interaction," by K. Weissman, Supervised by J.H. Prevost, 5/10/89, (PB90-207879, A07, MF-A01).
- NCEER-89-0041 "Linearized Identification of Buildings With Cores for Seismic Vulnerability Assessment," by I-K. Ho and A.E. Aktan, 11/1/89, (PB90-251943, A07, MF-A01).
- NCEER-90-0001 "Geotechnical and Lifeline Aspects of the October 17, 1989 Loma Prieta Earthquake in San Francisco," by T.D. O'Rourke, H.E. Stewart, F.T. Blackburn and T.S. Dickerman, 1/90, (PB90-208596, A05, MF-A01).
- NCEER-90-0002 "Nonnormal Secondary Response Due to Yielding in a Primary Structure," by D.C.K. Chen and L.D. Lutes, 2/28/90, (PB90-251976, A07, MF-A01).

- NCEER-90-0003 "Earthquake Education Materials for Grades K-12," by K.E.K. Ross, 4/16/90, (PB91-251984, A05, MF-A05). This report has been replaced by NCEER-92-0018.
- NCEER-90-0004 "Catalog of Strong Motion Stations in Eastern North America," by R.W. Busby, 4/3/90, (PB90-251984, A05, MF-A01).
- NCEER-90-0005 "NCEER Strong-Motion Data Base: A User Manual for the GeoBase Release (Version 1.0 for the Sun3)," by P. Friberg and K. Jacob, 3/31/90 (PB90-258062, A04, MF-A01).
- NCEER-90-0006 "Seismic Hazard Along a Crude Oil Pipeline in the Event of an 1811-1812 Type New Madrid Earthquake," by H.H.M. Hwang and C-H.S. Chen, 4/16/90, (PB90-258054, A04, MF-A01).
- NCEER-90-0007 "Site-Specific Response Spectra for Memphis Sheahan Pumping Station," by H.H.M. Hwang and C.S. Lee, 5/15/90, (PB91-108811, A05, MF-A01).
- NCEER-90-0008 "Pilot Study on Seismic Vulnerability of Crude Oil Transmission Systems," by T. Ariman, R. Dobry, M. Grigoriu, F. Kozin, M. O'Rourke, T. O'Rourke and M. Shinozuka, 5/25/90, (PB91-108837, A06, MF-A01).
- NCEER-90-0009 "A Program to Generate Site Dependent Time Histories: EQGEN," by G.W. Ellis, M. Srinivasan and A.S. Cakmak, 1/30/90, (PB91-108829, A04, MF-A01).
- NCEER-90-0010 "Active Isolation for Seismic Protection of Operating Rooms," by M.E. Talbott, Supervised by M. Shinozuka, 6/8/9, (PB91-110205, A05, MF-A01).
- NCEER-90-0011 "Program LINEARID for Identification of Linear Structural Dynamic Systems," by C-B. Yun and M. Shinozuka, 6/25/90, (PB91-110312, A08, MF-A01).
- NCEER-90-0012 "Two-Dimensional Two-Phase Elasto-Plastic Seismic Response of Earth Dams," by A.N. Yiagos, Supervised by J.H. Prevost, 6/20/90, (PB91-110197, A13, MF-A02).
- NCEER-90-0013 "Secondary Systems in Base-Isolated Structures: Experimental Investigation, Stochastic Response and Stochastic Sensitivity," by G.D. Manolis, G. Juhn, M.C. Constantinou and A.M. Reinhorn, 7/1/90, (PB91-110320, A08, MF-A01).
- NCEER-90-0014 "Seismic Behavior of Lightly-Reinforced Concrete Column and Beam-Column Joint Details," by S.P. Pessiki, C.H. Conley, P. Gergely and R.N. White, 8/22/90, (PB91-108795, A11, MF-A02).
- NCEER-90-0015 "Two Hybrid Control Systems for Building Structures Under Strong Earthquakes," by J.N. Yang and A. Danielians, 6/29/90, (PB91-125393, A04, MF-A01).
- NCEER-90-0016 "Instantaneous Optimal Control with Acceleration and Velocity Feedback," by J.N. Yang and Z. Li, 6/29/90, (PB91-125401, A03, MF-A01).
- NCEER-90-0017 "Reconnaissance Report on the Northern Iran Earthquake of June 21, 1990," by M. Mehrain, 10/4/90, (PB91-125377, A03, MF-A01).
- NCEER-90-0018 "Evaluation of Liquefaction Potential in Memphis and Shelby County," by T.S. Chang, P.S. Tang, C.S. Lee and H. Hwang, 8/10/90, (PB91-125427, A09, MF-A01).
- NCEER-90-0019 "Experimental and Analytical Study of a Combined Sliding Disc Bearing and Helical Steel Spring Isolation System," by M.C. Constantinou, A.S. Mokha and A.M. Reinhorn, 10/4/90, (PB91-125385, A06, MF-A01). This report is available only through NTIS (see address given above).
- NCEER-90-0020 "Experimental Study and Analytical Prediction of Earthquake Response of a Sliding Isolation System with a Spherical Surface," by A.S. Mokha, M.C. Constantinou and A.M. Reinhorn, 10/11/90, (PB91-125419, A05, MF-A01).

- NCEER-90-0021 "Dynamic Interaction Factors for Floating Pile Groups," by G. Gazetas, K. Fan, A. Kaynia and E. Kausel, 9/10/90, (PB91-170381, A05, MF-A01).
- NCEER-90-0022 "Evaluation of Seismic Damage Indices for Reinforced Concrete Structures," by S. Rodriguez-Gomez and A.S. Cakmak, 9/30/90, PB91-171322, A06, MF-A01).
- NCEER-90-0023 "Study of Site Response at a Selected Memphis Site," by H. Desai, S. Ahmad, E.S. Gazetas and M.R. Oh, 10/11/90, (PB91-196857, A03, MF-A01).
- NCEER-90-0024 "A User's Guide to Strongmo: Version 1.0 of NCEER's Strong-Motion Data Access Tool for PCs and Terminals," by P.A. Friberg and C.A.T. Susch, 11/15/90, (PB91-171272, A03, MF-A01).
- NCEER-90-0025 "A Three-Dimensional Analytical Study of Spatial Variability of Seismic Ground Motions," by L-L. Hong and A.H.-S. Ang, 10/30/90, (PB91-170399, A09, MF-A01).
- NCEER-90-0026 "MUMOID User's Guide - A Program for the Identification of Modal Parameters," by S. Rodriguez-Gomez and E. DiPasquale, 9/30/90, (PB91-171298, A04, MF-A01).
- NCEER-90-0027 "SARCF-II User's Guide - Seismic Analysis of Reinforced Concrete Frames," by S. Rodriguez-Gomez, Y.S. Chung and C. Meyer, 9/30/90, (PB91-171280, A05, MF-A01).
- NCEER-90-0028 "Viscous Dampers: Testing, Modeling and Application in Vibration and Seismic Isolation," by N. Makris and M.C. Constantinou, 12/20/90 (PB91-190561, A06, MF-A01).
- NCEER-90-0029 "Soil Effects on Earthquake Ground Motions in the Memphis Area," by H. Hwang, C.S. Lee, K.W. Ng and T.S. Chang, 8/2/90, (PB91-190751, A05, MF-A01).
- NCEER-91-0001 "Proceedings from the Third Japan-U.S. Workshop on Earthquake Resistant Design of Lifeline Facilities and Countermeasures for Soil Liquefaction, December 17-19, 1990," edited by T.D. O'Rourke and M. Hamada, 2/1/91, (PB91-179259, A99, MF-A04).
- NCEER-91-0002 "Physical Space Solutions of Non-Proportionally Damped Systems," by M. Tong, Z. Liang and G.C. Lee, 1/15/91, (PB91-179242, A04, MF-A01).
- NCEER-91-0003 "Seismic Response of Single Piles and Pile Groups," by K. Fan and G. Gazetas, 1/10/91, (PB92-174994, A04, MF-A01).
- NCEER-91-0004 "Damping of Structures: Part 1 - Theory of Complex Damping," by Z. Liang and G. Lee, 10/10/91, (PB92-197235, A12, MF-A03).
- NCEER-91-0005 "3D-BASIS - Nonlinear Dynamic Analysis of Three Dimensional Base Isolated Structures: Part II," by S. Nagarajaiah, A.M. Reinhorn and M.C. Constantinou, 2/28/91, (PB91-190553, A07, MF-A01). This report has been replaced by NCEER-93-0011.
- NCEER-91-0006 "A Multidimensional Hysteretic Model for Plasticity Deforming Metals in Energy Absorbing Devices," by E.J. Graesser and F.A. Cozzarelli, 4/9/91, (PB92-108364, A04, MF-A01).
- NCEER-91-0007 "A Framework for Customizable Knowledge-Based Expert Systems with an Application to a KBES for Evaluating the Seismic Resistance of Existing Buildings," by E.G. Ibarra-Anaya and S.J. Fenves, 4/9/91, (PB91-210930, A08, MF-A01).
- NCEER-91-0008 "Nonlinear Analysis of Steel Frames with Semi-Rigid Connections Using the Capacity Spectrum Method," by G.G. Deierlein, S-H. Hsieh, Y-J. Shen and J.F. Abel, 7/2/91, (PB92-113828, A05, MF-A01).
- NCEER-91-0009 "Earthquake Education Materials for Grades K-12," by K.E.K. Ross, 4/30/91, (PB91-212142, A06, MF-A01). This report has been replaced by NCEER-92-0018.

- NCEER-91-0010 "Phase Wave Velocities and Displacement Phase Differences in a Harmonically Oscillating Pile," by N. Makris and G. Gazetas, 7/8/91, (PB92-108356, A04, MF-A01).
- NCEER-91-0011 "Dynamic Characteristics of a Full-Size Five-Story Steel Structure and a 2/5 Scale Model," by K.C. Chang, G.C. Yao, G.C. Lee, D.S. Hao and Y.C. Yeh," 7/2/91, (PB93-116648, A06, MF-A02).
- NCEER-91-0012 "Seismic Response of a 2/5 Scale Steel Structure with Added Viscoelastic Dampers," by K.C. Chang, T.T. Soong, S-T. Oh and M.L. Lai, 5/17/91, (PB92-110816, A05, MF-A01).
- NCEER-91-0013 "Earthquake Response of Retaining Walls; Full-Scale Testing and Computational Modeling," by S. Alampalli and A-W.M. Elgamal, 6/20/91, to be published.
- NCEER-91-0014 "3D-BASIS-M: Nonlinear Dynamic Analysis of Multiple Building Base Isolated Structures," by P.C. Tsopelas, S. Nagarajaiah, M.C. Constantinou and A.M. Reinhorn, 5/28/91, (PB92-113885, A09, MF-A02).
- NCEER-91-0015 "Evaluation of SEAOC Design Requirements for Sliding Isolated Structures," by D. Theodossiou and M.C. Constantinou, 6/10/91, (PB92-114602, A11, MF-A03).
- NCEER-91-0016 "Closed-Loop Modal Testing of a 27-Story Reinforced Concrete Flat Plate-Core Building," by H.R. Somaprasad, T. Toksoy, H. Yoshizuki and A.E. Aktan, 7/15/91, (PB92-129980, A07, MF-A02).
- NCEER-91-0017 "Shake Table Test of a 1/6 Scale Two-Story Lightly Reinforced Concrete Building," by A.G. El-Attar, R.N. White and P. Gergely, 2/28/91, (PB92-222447, A06, MF-A02).
- NCEER-91-0018 "Shake Table Test of a 1/8 Scale Three-Story Lightly Reinforced Concrete Building," by A.G. El-Attar, R.N. White and P. Gergely, 2/28/91, (PB93-116630, A08, MF-A02).
- NCEER-91-0019 "Transfer Functions for Rigid Rectangular Foundations," by A.S. Veletsos, A.M. Prasad and W.H. Wu, 7/31/91, to be published.
- NCEER-91-0020 "Hybrid Control of Seismic-Excited Nonlinear and Inelastic Structural Systems," by J.N. Yang, Z. Li and A. Danielians, 8/1/91, (PB92-143171, A06, MF-A02).
- NCEER-91-0021 "The NCEER-91 Earthquake Catalog: Improved Intensity-Based Magnitudes and Recurrence Relations for U.S. Earthquakes East of New Madrid," by L. Seeber and J.G. Armbruster, 8/28/91, (PB92-176742, A06, MF-A02).
- NCEER-91-0022 "Proceedings from the Implementation of Earthquake Planning and Education in Schools: The Need for Change - The Roles of the Changemakers," by K.E.K. Ross and F. Winslow, 7/23/91, (PB92-129998, A12, MF-A03).
- NCEER-91-0023 "A Study of Reliability-Based Criteria for Seismic Design of Reinforced Concrete Frame Buildings," by H.H.M. Hwang and H-M. Hsu, 8/10/91, (PB92-140235, A09, MF-A02).
- NCEER-91-0024 "Experimental Verification of a Number of Structural System Identification Algorithms," by R.G. Ghanem, H. Gavin and M. Shinozuka, 9/18/91, (PB92-176577, A18, MF-A04).
- NCEER-91-0025 "Probabilistic Evaluation of Liquefaction Potential," by H.H.M. Hwang and C.S. Lee," 11/25/91, (PB92-143429, A05, MF-A01).
- NCEER-91-0026 "Instantaneous Optimal Control for Linear, Nonlinear and Hysteretic Structures - Stable Controllers," by J.N. Yang and Z. Li, 11/15/91, (PB92-163807, A04, MF-A01).
- NCEER-91-0027 "Experimental and Theoretical Study of a Sliding Isolation System for Bridges," by M.C. Constantinou, A. Kartoum, A.M. Reinhorn and P. Bradford, 11/15/91, (PB92-176973, A10, MF-A03).
- NCEER-92-0001 "Case Studies of Liquefaction and Lifeline Performance During Past Earthquakes, Volume 1: Japanese Case Studies," Edited by M. Hamada and T. O'Rourke, 2/17/92, (PB92-197243, A18, MF-A04).

- NCEER-92-0002 "Case Studies of Liquefaction and Lifeline Performance During Past Earthquakes, Volume 2: United States Case Studies," Edited by T. O'Rourke and M. Hamada, 2/17/92, (PB92-197250, A20, MF-A04).
- NCEER-92-0003 "Issues in Earthquake Education," Edited by K. Ross, 2/3/92, (PB92-222389, A07, MF-A02).
- NCEER-92-0004 "Proceedings from the First U.S. - Japan Workshop on Earthquake Protective Systems for Bridges," Edited by I.G. Buckle, 2/4/92, (PB94-142239, A99, MF-A06).
- NCEER-92-0005 "Seismic Ground Motion from a Haskell-Type Source in a Multiple-Layered Half-Space," A.P. Theoharis, G. Deodatis and M. Shinozuka, 1/2/92, to be published.
- NCEER-92-0006 "Proceedings from the Site Effects Workshop," Edited by R. Whitman, 2/29/92, (PB92-197201, A04, MF-A01).
- NCEER-92-0007 "Engineering Evaluation of Permanent Ground Deformations Due to Seismically-Induced Liquefaction," by M.H. Baziar, R. Dobry and A-W.M. Elgamal, 3/24/92, (PB92-222421, A13, MF-A03).
- NCEER-92-0008 "A Procedure for the Seismic Evaluation of Buildings in the Central and Eastern United States," by C.D. Poland and J.O. Malley, 4/2/92, (PB92-222439, A20, MF-A04).
- NCEER-92-0009 "Experimental and Analytical Study of a Hybrid Isolation System Using Friction Controllable Sliding Bearings," by M.Q. Feng, S. Fujii and M. Shinozuka, 5/15/92, (PB93-150282, A06, MF-A02).
- NCEER-92-0010 "Seismic Resistance of Slab-Column Connections in Existing Non-Ductile Flat-Plate Buildings," by A.J. Durrani and Y. Du, 5/18/92, (PB93-116812, A06, MF-A02).
- NCEER-92-0011 "The Hysteretic and Dynamic Behavior of Brick Masonry Walls Upgraded by Ferrocement Coatings Under Cyclic Loading and Strong Simulated Ground Motion," by H. Lee and S.P. Prawel, 5/11/92, to be published.
- NCEER-92-0012 "Study of Wire Rope Systems for Seismic Protection of Equipment in Buildings," by G.F. Demetriades, M.C. Constantinou and A.M. Reinhorn, 5/20/92, (PB93-116655, A08, MF-A02).
- NCEER-92-0013 "Shape Memory Structural Dampers: Material Properties, Design and Seismic Testing," by P.R. Witting and F.A. Cozzarelli, 5/26/92, (PB93-116663, A05, MF-A01).
- NCEER-92-0014 "Longitudinal Permanent Ground Deformation Effects on Buried Continuous Pipelines," by M.J. O'Rourke, and C. Nordberg, 6/15/92, (PB93-116671, A08, MF-A02).
- NCEER-92-0015 "A Simulation Method for Stationary Gaussian Random Functions Based on the Sampling Theorem," by M. Grigoriu and S. Balopoulou, 6/11/92, (PB93-127496, A05, MF-A01).
- NCEER-92-0016 "Gravity-Load-Designed Reinforced Concrete Buildings: Seismic Evaluation of Existing Construction and Detailing Strategies for Improved Seismic Resistance," by G.W. Hoffmann, S.K. Kunnath, A.M. Reinhorn and J.B. Mander, 7/15/92, (PB94-142007, A08, MF-A02).
- NCEER-92-0017 "Observations on Water System and Pipeline Performance in the Limón Area of Costa Rica Due to the April 22, 1991 Earthquake," by M. O'Rourke and D. Ballantyne, 6/30/92, (PB93-126811, A06, MF-A02).
- NCEER-92-0018 "Fourth Edition of Earthquake Education Materials for Grades K-12," Edited by K.E.K. Ross, 8/10/92, (PB93-114023, A07, MF-A02).
- NCEER-92-0019 "Proceedings from the Fourth Japan-U.S. Workshop on Earthquake Resistant Design of Lifeline Facilities and Countermeasures for Soil Liquefaction," Edited by M. Hamada and T.D. O'Rourke, 8/12/92, (PB93-163939, A99, MF-E11).
- NCEER-92-0020 "Active Bracing System: A Full Scale Implementation of Active Control," by A.M. Reinhorn, T.T. Soong, R.C. Lin, M.A. Riley, Y.P. Wang, S. Aizawa and M. Higashino, 8/14/92, (PB93-127512, A06, MF-A02).

- NCEER-92-0021 "Empirical Analysis of Horizontal Ground Displacement Generated by Liquefaction-Induced Lateral Spreads," by S.F. Bartlett and T.L. Youd, 8/17/92, (PB93-188241, A06, MF-A02).
- NCEER-92-0022 "IDARC Version 3.0: Inelastic Damage Analysis of Reinforced Concrete Structures," by S.K. Kunnath, A.M. Reinhorn and R.F. Lobo, 8/31/92, (PB93-227502, A07, MF-A02).
- NCEER-92-0023 "A Semi-Empirical Analysis of Strong-Motion Peaks in Terms of Seismic Source, Propagation Path and Local Site Conditions, by M. Kamiyama, M.J. O'Rourke and R. Flores-Berrones, 9/9/92, (PB93-150266, A08, MF-A02).
- NCEER-92-0024 "Seismic Behavior of Reinforced Concrete Frame Structures with Nonductile Details, Part I: Summary of Experimental Findings of Full Scale Beam-Column Joint Tests," by A. Beres, R.N. White and P. Gergely, 9/30/92, (PB93-227783, A05, MF-A01).
- NCEER-92-0025 "Experimental Results of Repaired and Retrofitted Beam-Column Joint Tests in Lightly Reinforced Concrete Frame Buildings," by A. Beres, S. El-Borgi, R.N. White and P. Gergely, 10/29/92, (PB93-227791, A05, MF-A01).
- NCEER-92-0026 "A Generalization of Optimal Control Theory: Linear and Nonlinear Structures," by J.N. Yang, Z. Li and S. Vongchavalitkul, 11/2/92, (PB93-188621, A05, MF-A01).
- NCEER-92-0027 "Seismic Resistance of Reinforced Concrete Frame Structures Designed Only for Gravity Loads: Part I - Design and Properties of a One-Third Scale Model Structure," by J.M. Bracci, A.M. Reinhorn and J.B. Mander, 12/1/92, (PB94-104502, A08, MF-A02).
- NCEER-92-0028 "Seismic Resistance of Reinforced Concrete Frame Structures Designed Only for Gravity Loads: Part II - Experimental Performance of Subassemblages," by L.E. Aycardi, J.B. Mander and A.M. Reinhorn, 12/1/92, (PB94-104510, A08, MF-A02).
- NCEER-92-0029 "Seismic Resistance of Reinforced Concrete Frame Structures Designed Only for Gravity Loads: Part III - Experimental Performance and Analytical Study of a Structural Model," by J.M. Bracci, A.M. Reinhorn and J.B. Mander, 12/1/92, (PB93-227528, A09, MF-A01).
- NCEER-92-0030 "Evaluation of Seismic Retrofit of Reinforced Concrete Frame Structures: Part I - Experimental Performance of Retrofitted Subassemblages," by D. Choudhuri, J.B. Mander and A.M. Reinhorn, 12/8/92, (PB93-198307, A07, MF-A02).
- NCEER-92-0031 "Evaluation of Seismic Retrofit of Reinforced Concrete Frame Structures: Part II - Experimental Performance and Analytical Study of a Retrofitted Structural Model," by J.M. Bracci, A.M. Reinhorn and J.B. Mander, 12/8/92, (PB93-198315, A09, MF-A03).
- NCEER-92-0032 "Experimental and Analytical Investigation of Seismic Response of Structures with Supplemental Fluid Viscous Dampers," by M.C. Constantinou and M.D. Symans, 12/21/92, (PB93-191435, A10, MF-A03).
- NCEER-92-0033 "Reconnaissance Report on the Cairo, Egypt Earthquake of October 12, 1992," by M. Khater, 12/23/92, (PB93-188621, A03, MF-A01).
- NCEER-92-0034 "Low-Level Dynamic Characteristics of Four Tall Flat-Plate Buildings in New York City," by H. Gavin, S. Yuan, J. Grossman, E. Pekelis and K. Jacob, 12/28/92, (PB93-188217, A07, MF-A02).
- NCEER-93-0001 "An Experimental Study on the Seismic Performance of Brick-Infilled Steel Frames With and Without Retrofit," by J.B. Mander, B. Nair, K. Wojtkowski and J. Ma, 1/29/93, (PB93-227510, A07, MF-A02).
- NCEER-93-0002 "Social Accounting for Disaster Preparedness and Recovery Planning," by S. Cole, E. Pantoja and V. Razak, 2/22/93, (PB94-142114, A12, MF-A03).

- NCEER-93-0003 "Assessment of 1991 NEHRP Provisions for Nonstructural Components and Recommended Revisions," by T.T. Soong, G. Chen, Z. Wu, R-H. Zhang and M. Grigoriu, 3/1/93, (PB93-188639, A06, MF-A02).
- NCEER-93-0004 "Evaluation of Static and Response Spectrum Analysis Procedures of SEAOC/UBC for Seismic Isolated Structures," by C.W. Winters and M.C. Constantinou, 3/23/93, (PB93-198299, A10, MF-A03).
- NCEER-93-0005 "Earthquakes in the Northeast - Are We Ignoring the Hazard? A Workshop on Earthquake Science and Safety for Educators," edited by K.E.K. Ross, 4/2/93, (PB94-103066, A09, MF-A02).
- NCEER-93-0006 "Inelastic Response of Reinforced Concrete Structures with Viscoelastic Braces," by R.F. Lobo, J.M. Bracci, K.L. Shen, A.M. Reinhorn and T.T. Soong, 4/5/93, (PB93-227486, A05, MF-A02).
- NCEER-93-0007 "Seismic Testing of Installation Methods for Computers and Data Processing Equipment," by K. Kosar, T.T. Soong, K.L. Shen, J.A. HoLung and Y.K. Lin, 4/12/93, (PB93-198299, A07, MF-A02).
- NCEER-93-0008 "Retrofit of Reinforced Concrete Frames Using Added Dampers," by A. Reinhorn, M. Constantinou and C. Li, to be published.
- NCEER-93-0009 "Seismic Behavior and Design Guidelines for Steel Frame Structures with Added Viscoelastic Dampers," by K.C. Chang, M.L. Lai, T.T. Soong, D.S. Hao and Y.C. Yeh, 5/1/93, (PB94-141959, A07, MF-A02).
- NCEER-93-0010 "Seismic Performance of Shear-Critical Reinforced Concrete Bridge Piers," by J.B. Mander, S.M. Waheed, M.T.A. Chaudhary and S.S. Chen, 5/12/93, (PB93-227494, A08, MF-A02).
- NCEER-93-0011 "3D-BASIS-TABS: Computer Program for Nonlinear Dynamic Analysis of Three Dimensional Base Isolated Structures," by S. Nagarajaiah, C. Li, A.M. Reinhorn and M.C. Constantinou, 8/2/93, (PB94-141819, A09, MF-A02).
- NCEER-93-0012 "Effects of Hydrocarbon Spills from an Oil Pipeline Break on Ground Water," by O.J. Helweg and H.H.M. Hwang, 8/3/93, (PB94-141942, A06, MF-A02).
- NCEER-93-0013 "Simplified Procedures for Seismic Design of Nonstructural Components and Assessment of Current Code Provisions," by M.P. Singh, L.E. Suarez, E.E. Matheu and G.O. Maldonado, 8/4/93, (PB94-141827, A09, MF-A02).
- NCEER-93-0014 "An Energy Approach to Seismic Analysis and Design of Secondary Systems," by G. Chen and T.T. Soong, 8/6/93, (PB94-142767, A11, MF-A03).
- NCEER-93-0015 "Proceedings from School Sites: Becoming Prepared for Earthquakes - Commemorating the Third Anniversary of the Loma Prieta Earthquake," Edited by F.E. Winslow and K.E.K. Ross, 8/16/93, (PB94-154275, A16, MF-A02).
- NCEER-93-0016 "Reconnaissance Report of Damage to Historic Monuments in Cairo, Egypt Following the October 12, 1992 Dahshur Earthquake," by D. Sykora, D. Look, G. Croci, E. Karaesmen and E. Karaesmen, 8/19/93, (PB94-142221, A08, MF-A02).
- NCEER-93-0017 "The Island of Guam Earthquake of August 8, 1993," by S.W. Swan and S.K. Harris, 9/30/93, (PB94-141843, A04, MF-A01).
- NCEER-93-0018 "Engineering Aspects of the October 12, 1992 Egyptian Earthquake," by A.W. Elgamal, M. Amer, K. Adalier and A. Abul-Fadl, 10/7/93, (PB94-141983, A05, MF-A01).
- NCEER-93-0019 "Development of an Earthquake Motion Simulator and its Application in Dynamic Centrifuge Testing," by I. Krstelj, Supervised by J.H. Prevost, 10/23/93, (PB94-181773, A-10, MF-A03).
- NCEER-93-0020 "NCEER-Taisei Corporation Research Program on Sliding Seismic Isolation Systems for Bridges: Experimental and Analytical Study of a Friction Pendulum System (FPS)," by M.C. Constantinou, P. Tsopelas, Y-S. Kim and S. Okamoto, 11/1/93, (PB94-142775, A08, MF-A02).

- NCEER-93-0021 "Finite Element Modeling of Elastomeric Seismic Isolation Bearings," by L.J. Billings, Supervised by R. Shepherd, 11/8/93, to be published.
- NCEER-93-0022 "Seismic Vulnerability of Equipment in Critical Facilities: Life-Safety and Operational Consequences," by K. Porter, G.S. Johnson, M.M. Zadeh, C. Scawthorn and S. Eder, 11/24/93, (PB94-181765, A16, MF-A03).
- NCEER-93-0023 "Hokkaido Nansei-oki, Japan Earthquake of July 12, 1993, by P.I. Yanev and C.R. Scawthorn, 12/23/93, (PB94-181500, A07, MF-A01).
- NCEER-94-0001 "An Evaluation of Seismic Serviceability of Water Supply Networks with Application to the San Francisco Auxiliary Water Supply System," by I. Markov, Supervised by M. Grigoriu and T. O'Rourke, 1/21/94, (PB94-204013, A07, MF-A02).
- NCEER-94-0002 "NCEER-Taisei Corporation Research Program on Sliding Seismic Isolation Systems for Bridges: Experimental and Analytical Study of Systems Consisting of Sliding Bearings, Rubber Restoring Force Devices and Fluid Dampers," Volumes I and II, by P. Tsopelas, S. Okamoto, M.C. Constantinou, D. Ozaki and S. Fujii, 2/4/94, (PB94-181740, A09, MF-A02 and PB94-181757, A12, MF-A03).
- NCEER-94-0003 "A Markov Model for Local and Global Damage Indices in Seismic Analysis," by S. Rahman and M. Grigoriu, 2/18/94, (PB94-206000, A12, MF-A03).
- NCEER-94-0004 "Proceedings from the NCEER Workshop on Seismic Response of Masonry Infills," edited by D.P. Abrams, 3/1/94, (PB94-180783, A07, MF-A02).
- NCEER-94-0005 "The Northridge, California Earthquake of January 17, 1994: General Reconnaissance Report," edited by J.D. Goltz, 3/11/94, (PB193943, A10, MF-A03).
- NCEER-94-0006 "Seismic Energy Based Fatigue Damage Analysis of Bridge Columns: Part I - Evaluation of Seismic Capacity," by G.A. Chang and J.B. Mander, 3/14/94, (PB94-219185, A11, MF-A03).
- NCEER-94-0007 "Seismic Isolation of Multi-Story Frame Structures Using Spherical Sliding Isolation Systems," by T.M. Al-Hussaini, V.A. Zayas and M.C. Constantinou, 3/17/94, (PB193745, A09, MF-A02).
- NCEER-94-0008 "The Northridge, California Earthquake of January 17, 1994: Performance of Highway Bridges," edited by I.G. Buckle, 3/24/94, (PB94-193851, A06, MF-A02).
- NCEER-94-0009 "Proceedings of the Third U.S.-Japan Workshop on Earthquake Protective Systems for Bridges," edited by I.G. Buckle and I. Friedland, 3/31/94, (PB94-195815, A99, MF-A06).
- NCEER-94-0010 "3D-BASIS-ME: Computer Program for Nonlinear Dynamic Analysis of Seismically Isolated Single and Multiple Structures and Liquid Storage Tanks," by P.C. Tsopelas, M.C. Constantinou and A.M. Reinhorn, 4/12/94, (PB94-204922, A09, MF-A02).
- NCEER-94-0011 "The Northridge, California Earthquake of January 17, 1994: Performance of Gas Transmission Pipelines," by T.D. O'Rourke and M.C. Palmer, 5/16/94, (PB94-204989, A05, MF-A01).
- NCEER-94-0012 "Feasibility Study of Replacement Procedures and Earthquake Performance Related to Gas Transmission Pipelines," by T.D. O'Rourke and M.C. Palmer, 5/25/94, (PB94-206638, A09, MF-A02).
- NCEER-94-0013 "Seismic Energy Based Fatigue Damage Analysis of Bridge Columns: Part II - Evaluation of Seismic Demand," by G.A. Chang and J.B. Mander, 6/1/94, (PB95-18106, A08, MF-A02).
- NCEER-94-0014 "NCEER-Taisei Corporation Research Program on Sliding Seismic Isolation Systems for Bridges: Experimental and Analytical Study of a System Consisting of Sliding Bearings and Fluid Restoring Force/Damping Devices," by P. Tsopelas and M.C. Constantinou, 6/13/94, (PB94-219144, A10, MF-A03).

- NCEER-94-0015 "Generation of Hazard-Consistent Fragility Curves for Seismic Loss Estimation Studies," by H. Hwang and J.-R. Huo, 6/14/94, (PB95-181996, A09, MF-A02).
- NCEER-94-0016 "Seismic Study of Building Frames with Added Energy-Absorbing Devices," by W.S. Pong, C.S. Tsai and G.C. Lee, 6/20/94, (PB94-219136, A10, A03).
- NCEER-94-0017 "Sliding Mode Control for Seismic-Excited Linear and Nonlinear Civil Engineering Structures," by J. Yang, J. Wu, A. Agrawal and Z. Li, 6/21/94, (PB95-138483, A06, MF-A02).
- NCEER-94-0018 "3D-BASIS-TABS Version 2.0: Computer Program for Nonlinear Dynamic Analysis of Three Dimensional Base Isolated Structures," by A.M. Reinhorn, S. Nagarajaiah, M.C. Constantinou, P. Tsopelas and R. Li, 6/22/94, (PB95-182176, A08, MF-A02).
- NCEER-94-0019 "Proceedings of the International Workshop on Civil Infrastructure Systems: Application of Intelligent Systems and Advanced Materials on Bridge Systems," Edited by G.C. Lee and K.C. Chang, 7/18/94, (PB95-252474, A20, MF-A04).
- NCEER-94-0020 "Study of Seismic Isolation Systems for Computer Floors," by V. Lambrou and M.C. Constantinou, 7/19/94, (PB95-138533, A10, MF-A03).
- NCEER-94-0021 "Proceedings of the U.S.-Italian Workshop on Guidelines for Seismic Evaluation and Rehabilitation of Unreinforced Masonry Buildings," Edited by D.P. Abrams and G.M. Calvi, 7/20/94, (PB95-138749, A13, MF-A03).
- NCEER-94-0022 "NCEER-Taisei Corporation Research Program on Sliding Seismic Isolation Systems for Bridges: Experimental and Analytical Study of a System Consisting of Lubricated PTFE Sliding Bearings and Mild Steel Dampers," by P. Tsopelas and M.C. Constantinou, 7/22/94, (PB95-182184, A08, MF-A02).
- NCEER-94-0023 "Development of Reliability-Based Design Criteria for Buildings Under Seismic Load," by Y.K. Wen, H. Hwang and M. Shinozuka, 8/1/94, (PB95-211934, A08, MF-A02).
- NCEER-94-0024 "Experimental Verification of Acceleration Feedback Control Strategies for an Active Tendon System," by S.J. Dyke, B.F. Spencer, Jr., P. Quast, M.K. Sain, D.C. Kaspari, Jr. and T.T. Soong, 8/29/94, (PB95-212320, A05, MF-A01).
- NCEER-94-0025 "Seismic Retrofitting Manual for Highway Bridges," Edited by I.G. Buckle and I.F. Friedland, published by the Federal Highway Administration (PB95-212676, A15, MF-A03).
- NCEER-94-0026 "Proceedings from the Fifth U.S.-Japan Workshop on Earthquake Resistant Design of Lifeline Facilities and Countermeasures Against Soil Liquefaction," Edited by T.D. O'Rourke and M. Hamada, 11/7/94, (PB95-220802, A99, MF-E08).
- NCEER-95-0001 "Experimental and Analytical Investigation of Seismic Retrofit of Structures with Supplemental Damping: Part 1 - Fluid Viscous Damping Devices," by A.M. Reinhorn, C. Li and M.C. Constantinou, 1/3/95, (PB95-266599, A09, MF-A02).
- NCEER-95-0002 "Experimental and Analytical Study of Low-Cycle Fatigue Behavior of Semi-Rigid Top-And-Seat Angle Connections," by G. Pekcan, J.B. Mander and S.S. Chen, 1/5/95, (PB95-220042, A07, MF-A02).
- NCEER-95-0003 "NCEER-ATC Joint Study on Fragility of Buildings," by T. Anagnos, C. Rojahn and A.S. Kiremidjian, 1/20/95, (PB95-220026, A06, MF-A02).
- NCEER-95-0004 "Nonlinear Control Algorithms for Peak Response Reduction," by Z. Wu, T.T. Soong, V. Gattulli and R.C. Lin, 2/16/95, (PB95-220349, A05, MF-A01).

- NCEER-95-0005 "Pipeline Replacement Feasibility Study: A Methodology for Minimizing Seismic and Corrosion Risks to Underground Natural Gas Pipelines," by R.T. Eguchi, H.A. Seligson and D.G. Honegger, 3/2/95, (PB95-252326, A06, MF-A02).
- NCEER-95-0006 "Evaluation of Seismic Performance of an 11-Story Frame Building During the 1994 Northridge Earthquake," by F. Naeim, R. DiSulio, K. Benuska, A. Reinhorn and C. Li, to be published.
- NCEER-95-0007 "Prioritization of Bridges for Seismic Retrofitting," by N. Basöz and A.S. Kiremidjian, 4/24/95, (PB95-252300, A08, MF-A02).
- NCEER-95-0008 "Method for Developing Motion Damage Relationships for Reinforced Concrete Frames," by A. Singhal and A.S. Kiremidjian, 5/11/95, (PB95-266607, A06, MF-A02).
- NCEER-95-0009 "Experimental and Analytical Investigation of Seismic Retrofit of Structures with Supplemental Damping: Part II - Friction Devices," by C. Li and A.M. Reinhorn, 7/6/95, (PB96-128087, A11, MF-A03).
- NCEER-95-0010 "Experimental Performance and Analytical Study of a Non-Ductile Reinforced Concrete Frame Structure Retrofitted with Elastomeric Spring Dampers," by G. Pekcan, J.B. Mander and S.S. Chen, 7/14/95, (PB96-137161, A08, MF-A02).
- NCEER-95-0011 "Development and Experimental Study of Semi-Active Fluid Damping Devices for Seismic Protection of Structures," by M.D. Symans and M.C. Constantinou, 8/3/95, (PB96-136940, A23, MF-A04).
- NCEER-95-0012 "Real-Time Structural Parameter Modification (RSPM): Development of Innervated Structures," by Z. Liang, M. Tong and G.C. Lee, 4/11/95, (PB96-137153, A06, MF-A01).
- NCEER-95-0013 "Experimental and Analytical Investigation of Seismic Retrofit of Structures with Supplemental Damping: Part III - Viscous Damping Walls," by A.M. Reinhorn and C. Li, 10/1/95, (PB96-176409, A11, MF-A03).
- NCEER-95-0014 "Seismic Fragility Analysis of Equipment and Structures in a Memphis Electric Substation," by J-R. Huo and H.H.M. Hwang, (PB96-128087, A09, MF-A02), 8/10/95.
- NCEER-95-0015 "The Hanshin-Awaji Earthquake of January 17, 1995: Performance of Lifelines," Edited by M. Shinozuka, 11/3/95, (PB96-176383, A15, MF-A03).
- NCEER-95-0016 "Highway Culvert Performance During Earthquakes," by T.L. Youd and C.J. Beckman, available as NCEER-96-0015.
- NCEER-95-0017 "The Hanshin-Awaji Earthquake of January 17, 1995: Performance of Highway Bridges," Edited by I.G. Buckle, 12/1/95, to be published.
- NCEER-95-0018 "Modeling of Masonry Infill Panels for Structural Analysis," by A.M. Reinhorn, A. Madan, R.E. Valles, Y. Reichmann and J.B. Mander, 12/8/95.
- NCEER-95-0019 "Optimal Polynomial Control for Linear and Nonlinear Structures," by A.K. Agrawal and J.N. Yang, 12/11/95, (PB96-168737, A07, MF-A02).
- NCEER-95-0020 "Retrofit of Non-Ductile Reinforced Concrete Frames Using Friction Dampers," by R.S. Rao, P. Gergely and R.N. White, 12/22/95, (PB97-133508, A10, MF-A02).
- NCEER-95-0021 "Parametric Results for Seismic Response of Pile-Supported Bridge Bents," by G. Mylonakis, A. Nikolaou and G. Gazetas, 12/22/95, (PB97-100242, A12, MF-A03).
- NCEER-95-0022 "Kinematic Bending Moments in Seismically Stressed Piles," by A. Nikolaou, G. Mylonakis and G. Gazetas, 12/23/95.

- NCEER-96-0001 "Dynamic Response of Unreinforced Masonry Buildings with Flexible Diaphragms," by A.C. Costley and D.P. Abrams, 10/10/96.
- NCEER-96-0002 "State of the Art Review: Foundations and Retaining Structures," by I. Po Lam, to be published.
- NCEER-96-0003 "Ductility of Rectangular Reinforced Concrete Bridge Columns with Moderate Confinement," by N. Wehbe, M. Saiidi, D. Sanders and B. Douglas, 11/7/96, (PB97-133557, A06, MF-A02).
- NCEER-96-0004 "Proceedings of the Long-Span Bridge Seismic Research Workshop," edited by I.G. Buckle and I.M. Friedland, to be published.
- NCEER-96-0005 "Establish Representative Pier Types for Comprehensive Study: Eastern United States," by J. Kulicki and Z. Prucz, 5/28/96.
- NCEER-96-0006 "Establish Representative Pier Types for Comprehensive Study: Western United States," by R. Imbsen, R.A. Schamber and T.A. Osterkamp, 5/28/96.
- NCEER-96-0007 "Nonlinear Control Techniques for Dynamical Systems with Uncertain Parameters," by R.G. Ghanem and M.I. Bujakov, 5/27/96, (PB97-100259, A17, MF-A03).
- NCEER-96-0008 "Seismic Evaluation of a 30-Year Old Non-Ductile Highway Bridge Pier and Its Retrofit," by J.B. Mander, B. Mahmoodzadegan, S. Bhadra and S.S. Chen, 5/31/96.
- NCEER-96-0009 "Seismic Performance of a Model Reinforced Concrete Bridge Pier Before and After Retrofit," by J.B. Mander, J.H. Kim and C.A. Ligozio, 5/31/96.
- NCEER-96-0010 "IDARC2D Version 4.0: A Computer Program for the Inelastic Damage Analysis of Buildings," by R.E. Valles, A.M. Reinhorn, S.K. Kunnath, C. Li and A. Madan, 6/3/96, (PB97-100234, A17, MF-A03).
- NCEER-96-0011 "Estimation of the Economic Impact of Multiple Lifeline Disruption: Memphis Light, Gas and Water Division Case Study," by S.E. Chang, H.A. Seligson and R.T. Eguchi, 8/16/96, (PB97-133490, A11, MF-A03).
- NCEER-96-0012 "Proceedings from the Sixth Japan-U.S. Workshop on Earthquake Resistant Design of Lifeline Facilities and Countermeasures Against Soil Liquefaction, Edited by M. Hamada and T. O'Rourke, 9/11/96, (PB97-133581, A99, MF-A06).
- NCEER-96-0013 "Chemical Hazards, Mitigation and Preparedness in Areas of High Seismic Risk: A Methodology for Estimating the Risk of Post-Earthquake Hazardous Materials Release," by H.A. Seligson, R.T. Eguchi, K.J. Tierney and K. Richmond, 11/7/96.
- NCEER-96-0014 "Response of Steel Bridge Bearings to Reversed Cyclic Loading," by J.B. Mander, D-K. Kim, S.S. Chen and G.J. Premus, 11/13/96, (PB97-140735, A12, MF-A03).
- NCEER-96-0015 "Highway Culvert Performance During Past Earthquakes," by T.L. Youd and C.J. Beckman, 11/25/96, (PB97-133532, A06, MF-A01).
- NCEER-97-0001 "Evaluation, Prevention and Mitigation of Pounding Effects in Building Structures," by R.E. Valles and A.M. Reinhorn, 2/20/97, (PB97-159552, A14, MF-A03).
- NCEER-97-0002 "Seismic Design Criteria for Bridges and Other Highway Structures," by C. Rojahn, R. Mayes, D.G. Anderson, J. Clark, J.H. Hom, R.V. Nutt and M.J. O'Rourke, 4/30/97, (PB97-194658, A06, MF-A03).
- NCEER-97-0003 "Proceedings of the U.S.-Italian Workshop on Seismic Evaluation and Retrofit," Edited by D.P. Abrams and G.M. Calvi, 3/19/97, (PB97-194666, A13, MF-A03).

- NCEER-97-0004 "Investigation of Seismic Response of Buildings with Linear and Nonlinear Fluid Viscous Dampers," by A.A. Seleemah and M.C. Constantinou, 5/21/97, (PB98-109002, A15, MF-A03).
- NCEER-97-0005 "Proceedings of the Workshop on Earthquake Engineering Frontiers in Transportation Facilities," edited by G.C. Lee and I.M. Friedland, 8/29/97.
- NCEER-97-0006 "Cumulative Seismic Damage of Reinforced Concrete Bridge Piers," by S.K. Kunnath, A. El-Bahy, A. Taylor and W. Stone, 9/2/97, (PB98-108814, A11, MF-A03).
- NCEER-97-0007 "Structural Details to Accommodate Seismic Movements of Highway Bridges and Retaining Walls," by R.A. Imbsen, R.A. Schamber, E. Thorkildsen, A. Kartoum, B.T. Martin, T.N. Rosser and J.M. Kulicki, 9/3/97.
- NCEER-97-0008 "A Method for Earthquake Motion-Damage Relationships with Application to Reinforced Concrete Frames," by A. Singhal and A.S. Kiremidjian, 9/10/97, (PB98-108988, A13, MF-A03).
- NCEER-97-0009 "Seismic Analysis and Design of Bridge Abutments Considering Sliding and Rotation," by K. Fishman and R. Richards, Jr., 9/15/97, (PB98-108897, A06, MF-A02).
- NCEER-97-0010 "Proceedings of the FHWA/NCEER Workshop on the National Representation of Seismic Ground Motion for New and Existing Highway Facilities," edited by I.M. Friedland, M.S. Power and R.L. Mayes, 9/22/97.
- NCEER-97-0011 "Seismic Analysis for Design or Retrofit of Gravity Bridge Abutments," by K.L. Fishman, R. Richards, Jr. and R.C. Divito, 10/2/97.
- NCEER-97-0012 "Evaluation of Simplified Methods of Analysis for Yielding Structures," by P. Tsopelas, M.C. Constantinou, C.A. Kircher and A.S. Whittaker, 10/31/97.
- NCEER-97-0013 "Seismic Design of Bridge Columns Based on Control and Repairability of Damage," by C-T. Cheng and J.B. Mander, 12/8/97.
- NCEER-97-0014 "Seismic Resistance of Bridge Piers Based on Damage Avoidance Design," by J.B. Mander and C-T. Cheng, 12/10/97.
- NCEER-97-0015 "Seismic Response of Nominally Symmetric Systems with Strength Uncertainty," by S. Balopoulou and M. Grigoriu, 12/23/97.
- NCEER-97-0016 "Evaluation of Seismic Retrofit Methods for Reinforced Concrete Bridge Columns," by T.J. Wipf, F.W. Klaiber and F.M. Russo, 12/28/97.





*Headquartered at the State University of New York at Buffalo*

State University of New York at Buffalo  
Red Jacket Quadrangle  
Buffalo, New York 14261  
Telephone: 716/645-3391  
FAX: 716/645-3399

ISSN 1088-3800